Molecular Pharmacology of a Series of Nitrogen Mustard Containing- and AT- and GC-Recognising Minor Groove Binding Agents Related to Distamycin.

Submitted by Michael Dunton Wyatt for the
PhD degree at University of London

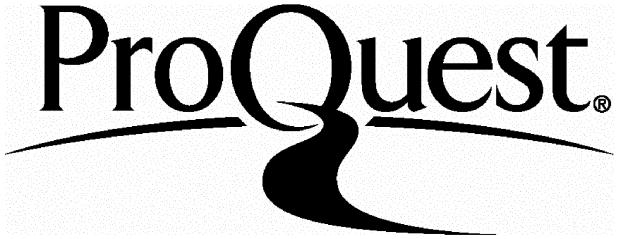

ABSTRACT

The determination of a structure-activity relationship for a series of minor groove binding agents based on the framework of distamycin and which conjugate an aromatic nitrogen mustard is presented. The nitrogen mustard was either benzoic acid mustard (BAM) or chlorambucil (CHL), and was located on the N-terminus of the lexitropsin. The heterocyclic units for the lexitropsin in each family were either AT-recognising pyrroles or GC-recognising imidazoles. Each family contains conjugates of one, two, and three heterocyclic units. The cytotoxicity, DNA interstrand crosslinking, and DNA sequence specificity of alkylation were determined for the series. With one exception, each conjugate was more cytotoxic than the respective parent nitrogen mustard and the cytotoxicity increased for each increase in the number of heterocyclic units. The BAM conjugates cross-linked isolated DNA poorly, while the CHL conjugates cross-linked DNA more efficiently than CHL. Cross-linking efficiency was not affected by the increase in the number of heterocyclic units. Interstrand cross-link formation in cells agreed with the studies in isolated DNA. The sequence specificity of alkylation for the conjugates was determined using modified sequencing techniques. The CHL conjugates were found to alkylate DNA with a similar sequence specificity to that seen for CHL. The monoheterocyclic-BAM conjugates retained the alkylation pattern of BAM, but additional minor groove sites were alkylated. The di- and triheterocyclic-BAM conjugates only alkylated selected sites in the minor groove and the triheterocyclic-BAM conjugates alkylated a subset of those sites alkylated by the mono- and diheterocyclic conjugates, namely the sequence 5'-TTTTGPu. The BAM conjugates showed the greater increase in cytotoxicity and enhancement in alkylation specificity compared to the parent nitrogen mustard, indicating that the less reactive nitrogen mustard was targeted by the lexitropsin more efficiently. The findings have implications for the design of minor groove agents that conjugate reactive groups.

INDEX

LIST OF FIGURES AND TABLES

Figures

Chapter 1

Chapter 2

Chapter 3

Tables

ABBREVIATIONS

Å	Angstrom
A	Adenine
ATP	Adenosine triphosphate
APS	Ammonium persulfate
BAM	Benzoic acid mustard
BCNU	*N,N'*-bis-(2-chloroethyl)-*N*-nitrosourea
C	Cytosine
CD	Circular dichroism
CHL	Chlorambucil
CPI	Cycloproplypyrroloindole
DMS	Dimethyl sulfate
DMSO	Dimethyl sulfoxide
DNA	Deoxyribonucleic acid
dNTP	Deoxynucleoside triphosphates
DTIC	dacarbazine
DTT	Dithiothreitol
EDTA	Ethylenediamine teteracetic acid
FCS	Foetal calf serum
G	Guanine
HPLC	High performance liquid chromatography
Im	Imidazole-2-carboxamide unit
LMP	Low melting point
M	Molar
mM	Millimolar
MPE	Methidiumpropyl-EDTA
MTT	3-[4,5-dimethylthiazol-2-yl]-2,5-diphenyl-tetrazolium bromide

NMR	Nuclear magnetic resonance
ng	nanogram
PBS	Phosphate buffered saline
PCR	Polymerase chain reaction
Pu	Adenine or guanine
Py	Pyrrole-2-carboxamide unit
T	Thymine
TAE	Tris-acetic acid EDTA buffer
TEOA	Triethanolamine EDTA buffer
TBE	Tris-boric acid EDTA buffer
TEMED	*N, N, N, N*-Tetramethyl-ethylenediamine
µg	Microgram
µl	Microlitre
µM	Micromolar

PUBLICATIONS CONTAINING DATA PRESENTED IN THIS THESIS

Broggini, M., Coley, H., Mongelli, N., Grandi, M., Wyatt, M. D., Hartley, J. A., & D'Incalci, M. (1995). DNA sequence specific adenine alkylation by the novel antitumor drug tallimustine (FCE 24517), a benzoyl nitrogen mustard derivative of distamycin, *Nucleic Acids Res.*, **23**, 81-87.

Hartley, J. A., Wyatt, M. D., Garbiras, B. G., Richter, C., & Lee, M. (1994). Probing the importance of the second chloroethyl arm of a benzoic acid mustard derivative of an imidazole-containing analogue of distamycin, *Bioorg. Med. Chem. Lett.*, **4**, 2421-2424.

Lee, M., Rhodes, A. L., Wyatt, M. D., Forrow, S., & Hartley, J. A. (1993). Design, synthesis, and biological evaluation of DNA sequence and minor groove selective alkylating agents, *Anticancer Drug Des.*, **8**, 173-192.

Wyatt, M. D., Garbiras, B. J., Haskell, M. K., Lee, M., Souhami, R. L., & Hartley, J. A. (1994). Structure activity relationship of a series of nitrogen mustard and pyrrole containing minor groove binding agents related to distamycin, *Anticancer Drug Des.*, **9**, 511-525.

Wyatt, M. D., Lee, M., Garbiras, B. J., Souhami, R. L., & Hartley, J. A. (1995). Sequence specificity of alkylation for a series of nitrogen mustard-containing analogues of distamycin of increasing binding site size: evidence for increased cytotoxicity with enhanced sequence specificity, *Biochemistry*, **34**, 13034-13041.

Wyatt, M. D., Lee, M., Hartley, J. A. Alkylation specificity for a series of distamycin analogues that tether chlorambucil: Nitrogen mustard reactivity. (In preparation).

Wyatt, M. D., Lee, M. Hartley, J. A. Sequence specificity of alkylation for a series of benzoic acid mustard and imidazole-containing analogues of distamycin. The importance of local DNA sequence conformation. (In preparation).

ACKNOWLEDGEMENTS

I would like to thank the Dean of University College London Medical School for providing the funds that have supported me throughout my research. I would also like to thank Professor Bob Souhami for allowing me the opportunity to carry out this research in the department, and for his advice and input during the work. Sincere gratitude goes to John Hartley for the support, advice, and direction in all phases of the work. Special thanks also goes to Moses Lee, teacher turned collaborator. And then there's my labmates and friends.....

CHAPTER ONE: INTRODUCTION

1.1 Cancer and Chemotherapy

A cancer represents a population of cells within the body that has escaped from the normal control mechanisms and continues to proliferate until it leads to the death of the host (Priestman, 1989). In a mature adult, there is an intricate homeostasis whereby cell division only occurs to replace lost cells. In recent years numerous and complex mechanisms that control progression through the cell cycle have been discovered. It is a cell or cells that escape the normal mechanisms of control that eventually lead to a tumour burden. The two important characteristics that distinguish a malignant growth from a benign growth are the invasion and destruction of nearby normal tissue, and the ability of some cancerous cells to metastasise. Metastasis is defined as the process whereby cancer cells detach from the primary tumour mass and migrate to distal parts of the body, attach and subsequently divide to produce secondary tumour growths. It is the phenomenon of metastasis to which chemotherapy owes its importance in the treatment of cancer. The timely detection of primary solid tumours allows for efficacious treatment through surgical removal of the tumour and/or local radiation treatment, but the presence of clinically undetectable micro-metastases limits the effectiveness of these treatments. Chemotherapy offers the only chance of a cure once metastasis has occurred. When cancer treatment fails, metastasis is the primary cause of death (Liotta, 1992).

Chemotherapy is defined as the utilisation of drugs that broadly interfere with cell division. Although the five-year survival rate for all cancers combined has only modestly increased in the past 50 years, dramatic increases in the cure-rate of some of the less common tumours have been achieved with chemotherapy (Pratt, *et al.*, 1994). The threat of metastases being present upon detection of a primary tumour introduced the idea of

adjuvant therapy, or chemotherapy used in combination with surgery or radiotherapy. Chemotherapeutic drugs are generally most useful against those tumours with a high proportion of dividing cells, but some normal tissues also have a high proportion of dividing cells. Differentiated cells are mostly unaffected by chemotherapy, but some organs and the stem cell population can be severely damaged. Dose limiting toxicity is the potentially lethal effect of cytotoxic drugs on normal tissues and organs. All cytotoxic drugs share the two common properties of being able to interfere with cell division and being unable to discern between normal dividing cells and malignant cells. Dose limiting toxicity and drug resistance are the two problems that have prevented a more successful application of chemotherapy. Drug resistance is defined as the ability of a sub population of the malignant cells to circumvent the effects of cytotoxic drugs and this can occur by a variety of mechanisms. Drug resistance can be inherent or acquired, such that after an initial response to treatment, a relapse occurs and a tumour reappears which is refractory to the treatment. Acquired resistance is the most common reason for the failure of drug treatment in cancer patients with initially sensitive tumours (Pratt, *et al.*, 1994). The phenomenon of resistance underlies a fundamental question in our knowledge of cancer that remains unanswered, and that is why do different tumour types respond differently to chemotherapy. Some tumour types are extremely sensitive to, and even curable with, chemotherapy alone, while some tumour types may initially be sensitive before resistance occurs, and some essentially do not respond to chemotherapy. The first step in approaching this question requires an introduction to the currently used chemotherapeutic agents.

1.2 The Agents of Chemotherapy

The currently used clinical chemotherapeutic drugs can be grouped into four broad categories; the alkylating agents (classical and non-classical),

the antimitotic antibiotics, the antimetabolites, and plant alkaloids. The classification is primarily biochemical and in some cases implies a common mechanism of action within a group. Elucidating the mechanism of action for an agent is critical for several reasons. Knowledge of the mechanism of action for each agent allows for classification and discovery of novel agents with unique mechanisms of action. An agent with a unique mechanism of action may have a different spectrum of activity against various types of tumours. Agents that possess different mechanisms of action may also have different associated side effects, which has important clinical implications. The clinical utilisation of combination chemotherapy, using several agents simultaneously, allows for the treatment of cancer with several agents at their individual maximum dose while avoiding an additive effect on the dose related side effects. The introduction of combination chemotherapy was a turning point in cancer chemotherapy (Liotta, 1992).

1.2.1 Alkylating Agents (Classical and Non-Classical)

The first category, the alkylating agents, are historically interesting because one of the group, mechlorethamine (HN2, nitrogen mustard), represents the first attempt at chemotherapy in the treatment of cancer (Gilman & Phillips, 1946). Studies of the victims of mustard gas (Figure 1.1) attacks during World War I and subsequent animal studies revealed 'the vulnerability of the blood-forming organs and intestinal tract' and that 'marked effects on hematopoiesis can be obtained with sublethal doses' (Gilman & Phillips, 1946). The pathological progress in leukaemia and the lymphomas is excessive white blood cell formation in the marrow or lymphatic system. There were suggestions as early as 1928 that mustard gas might offer benefit to the sufferers of the disease, but the severely toxic effects of the agent precluded further study (Colvin & Chabner, 1990). A renewed military interest in toxic gases sparked by the second World War

brought about the synthesis of mustard gas analogues, including nitrogen-containing agents such as mechlorethamine. After military declassification of the work in 1946, the first studies of cytotoxic therapy for lymphoma, leukaemia and Hodgkin's disease using mechlorethamine were reported with encouraging results, particularly against Hodgkin's disease (Gilman & Phillips, 1946). With the initial results of this first alkylating agent many thousands have subsequently been prepared for evaluation in cancer treatment. Although fewer than a dozen are currently being used, this class of compound is still the mainstay in the treatment of cancer due to their broad spectrum of activity.

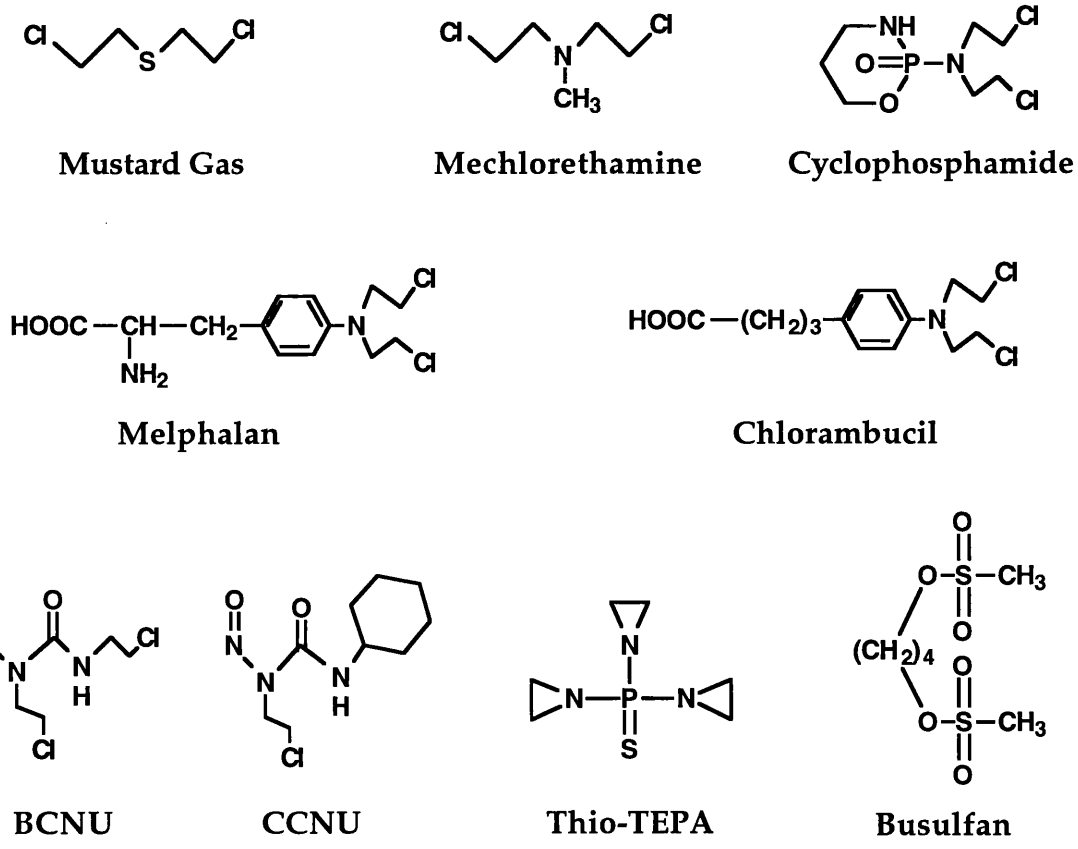

Figure 1.1. Mustard gas and the classical alkylating agents.

Mechlorethamine is part of the family of alkylating agents called the nitrogen mustards, discernible by the bis-(chloroethyl)amino functionality (Figure 1.1). Mechlorethamine is still used clinically, but it causes severe

vomiting and bone marrow suppression, which is its dose limiting toxicity and which is characteristic of alkylating agents (Lewin, 1986). Subsequent agents in this family now utilised clinically retain the bis-(chloroethyl)amino functionality while the methyl group has been substituted for more elaborate chemical groups. An example of this is the agent cyclophosphamide, developed following the observation that tumour tissue contains relatively high concentrations of phosphoramidases (Priestman, 1989). Cyclophosphamide and its analogue, ifosfamide, have proven very valuable clinically in spite of the fact that the drugs are ineffective against tumour cells *in vitro*, and the mechanism of action first requires an enzymatic activation in the liver (Pratt, *et al.*, 1994).

In the publication reporting the synthesis of chlorambucil (CHL, Figure 1.1) the authors stated that "it is hoped to obtain compounds of a more selective action on neoplasms by incorporating the di-2-chloroethylamino-group into molecules which have anionic, cationic, lipophilic, or hydrophilic character (Evertt, *et al.*, 1953)." The study reports the preparation of a series p-bis-(chloroethyl)amino aniline derivatives with the alkyl side chain varying from zero to four methylene groups. Biological evaluation found that the n=3 derivative (CHL) was "outstanding" in inhibiting the growth of transplanted Walker rat carcinoma (Evertt, *et al.*, 1953).

Melphalan (L-phenylalanine-mustard, Figure 1.1) followed soon after (Bergel & Stock, 1954). The authors in this publication stated a growing interest in α-amino acid derivatives due to "the occurrence of such units in the molecules of antibiotics and to the discovery of antimetabolite effects with analogues of essential amino acids." The L-isomer proved the most active of the analogues prepared. There is no evidence that the presence of the phenylalanine group alters the distribution of the drug, although the drug enters cells via amino acid transport mechanisms (Goldenberg & Begleiter, 1980). Melphalan and chlorambucil have several clinical

applications and one distinct advantage these have over mechlorethamine is their oral availability due to their reduced reactivity (Colvin & Chabner, 1990). The DNA interactions of the nitrogen mustards will be discussed in section 1.5.

The nitrosoureas comprise a second family of alkylating agents. This family arose out of a United States government directive for a national co-operative cancer drug research program run by the newly formed National Cancer Institute. The first of the nitrosoureas, *N,N'*-bis-(2-chloroethyl)-*N*-nitrosourea (BCNU, Figure 1.1), was synthesised by Montgomery and coworkers at the Southern Research Institute (Montgomery, 1986). The nitrosoureas have found clinical application, especially in the management of brain tumours due to their lipophilicity. Unfortunately, they can induce a delayed bone marrow toxicity (Priestman, 1989). The nitrosoureas' mechanism of action will be briefly discussed in section 1.5.5.

Busulfan (Figure 1.1) is the only major clinical representative of the alkyl alkane sulfonate family of alkylating agents, and is primarily used against chronic myelogenous leukaemia (Colvin & Chabner, 1990). Thio-TEPA (Figure 1.1) is the major clinical representative of the aziridine family of alkylating agents and has been used in the treatment of breast and ovarian carcinomas (Colvin & Chabner, 1990).

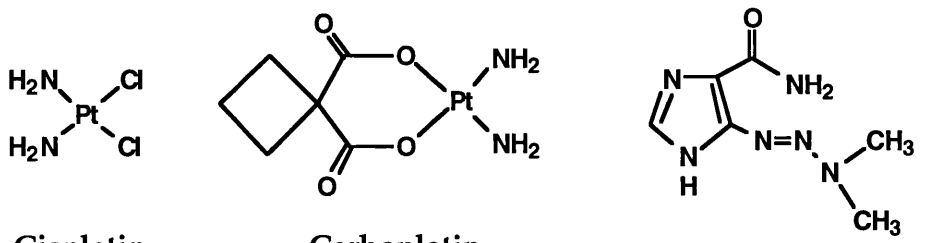

Cisplatin **Carboplatin** **Dacarbazine (DTIC)**

Figure 1.2. Non-classical alkylating agents.

Under the heading of non-classical alkylating agent would fall cisplatin, a square planar platinum coordination complex with two amino

and two chloride ligands in a *cis* configuration (Figure 1.2). The agent was serendipitously discovered when it was noticed that use of a platinum electrode impeded the cell division of bacteria but not their growth (Rosenberg, *et al.*, 1965). Cisplatin has found clinical application, particularly against testicular cancer, but it can severely affect renal function (Lewin, 1986). Many platinum analogues have been prepared and studied in attempt to retain the activity without the side effects, but the only analogue thus far to be utilised clinically is carboplatin (Figure 1.2).

The purine analogue dacarbazine (DTIC) is also considered a non-classical alkylating agent. Although it was originally designed as an antimetabolite, it first requires metabolic activation and is presumed to interact directly with DNA (Montgomery, 1986). It still has a limited clinical application and its dose limiting cytotoxicity is bone marrow suppression (Priestman, 1989). The term 'prodrug' generally applies to an agent that requires activation in order to exhibit its biological properties and there have been successful attempts to develop related agents which are better prodrugs (Stevens & Newlands, 1993). These will briefly discussed in section 1.5.7.

For each of the alkylating agents, their interaction with DNA is presumed to be their mechanism of action. Each agent is capable of producing various types of DNA damage and, with the exception of DTIC, each agent mentioned is capable of cross-linking DNA. Bifunctional alkylating agents can undergo two separate reactions and it is this property that offers the potential for cross-link formation. There are three types of cross-links that can be produced; DNA interstrand cross-links, DNA intrastrand cross-links, and DNA-protein cross-links. DNA interstrand cross-links chemically connects the two DNA strands together, preventing the strands from separating during replication. Reaction with two sites on the same strand represents an intrastrand cross-link, and reaction with a site on DNA and a site on a protein creates a DNA-protein cross-link. Because

each of the alkylating agents are capable of producing a variety of DNA damage, determination of the specific lesions formed is important in assigning mechanism of action and this will be discussed in section 1.5.

1.2.2 Antimitotic Antibiotics

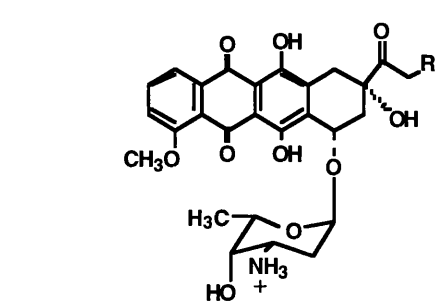

Daunorubicin, R=H; Doxorubicin, R=OH

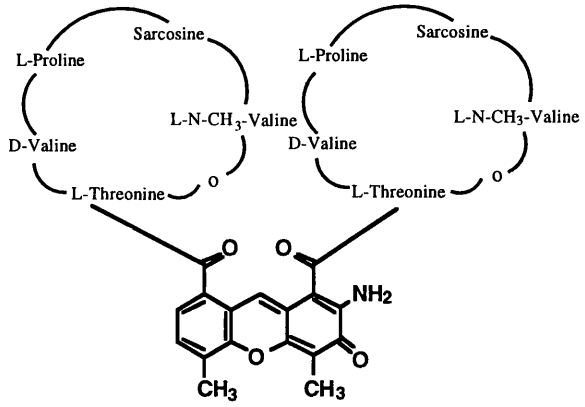

Actinomycin D

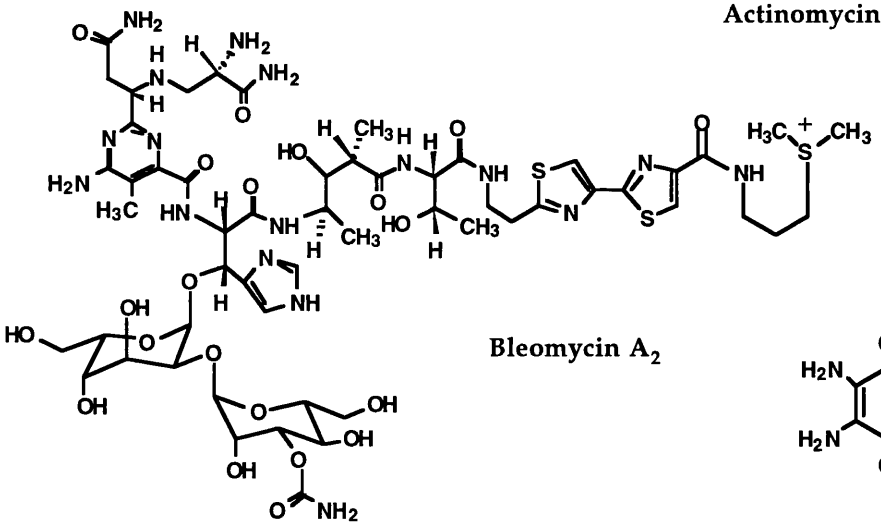

Bleomycin A_2

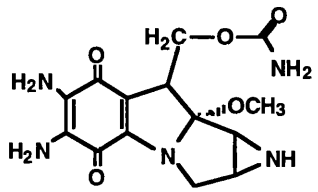

Mitomycin C

Figure 1.3. Antimitotic antibiotics.

The antimitotic antibiotics arose out of the search for novel antibiotics in the 1940's. It was observed that some of these new, naturally occurring antibiotics isolated also had inhibitory effects on tumour cells. All of the clinically useful antibiotics are produced by different strains of the soil fungus *Streptomyces*. The first to be introduced into the clinic was

actinomycin D (Figure 1.3), for the treatment of Wilm's tumour in children (Pratt, *et al.*, 1994). The demonstration of the clinical effectiveness of this agent led to the development of many other agents of this category. The lead compound of the anthracycline family was daunomycin (daunorubicin), which showed good activity against leukaemia. Adriamycin (doxorubicin) only differs from daunomycin by an extra hydroxyl group on the aglycone ring (Figure 1.3), and yet it has a different spectrum of activity, particularly against a range of solid tumours. These compounds possess a potentially serious cardiotoxicity, however (Olson & Mushlin, 1990), which has prompted the search for analogues that retain the activity while displaying a reduced toxicity. A variety of biochemical activities have been demonstrated for this family, some or all of which may contribute to their mechanism of action. In most cases the interaction with DNA is central.

The bleomycins (Figure 1.3) are a family of glycopeptide antibiotics isolated from *Streptomyces verticillus* (Natrajan & Hecht, 1994). There are several variants of bleomycin with minor chemical differences and the clinical preparation is, in fact, a mixture. Bleomycin is used in the treatment of malignant lymphomas and some squamous cell carcinomas and while it has little if any myelosuppressive effect it has a severe pulmonary toxicity with accumulative dosage (Chabner, 1990). The mechanism of action for the bleomycins is presumed to be a DNA damaging event.

The mitomycins were isolated from the fermentation broth of *Streptomyces caespitosus* in the 1950's (Tomasz, 1994) and were found to possess significant antitumour activity. Mitomycin C (Figure 1.3) is used clinically against a range of solid tumours, but has a severe myelosuppression (Lewin, 1986). Mitomycin C, as pictured in Figure 1.3, is unreactive towards DNA and first requires chemical or enzymatic activation. Because of this property, it represents a class of agents known as

'bioreductive' agents. It is well known that hypoxic cells, those that lack sufficient blood supply, are a common feature of solid tumours (Brown & Giaccia, 1994). Hypoxic activation is a possible explanation as to why mitomycin C has proven useful in the management of solid tumours. Bioreductive agents and the specific DNA interactions of mitomycin C will be discussed in section 1.6.4 and 1.6.3.

1.2.3 Antimetabolites

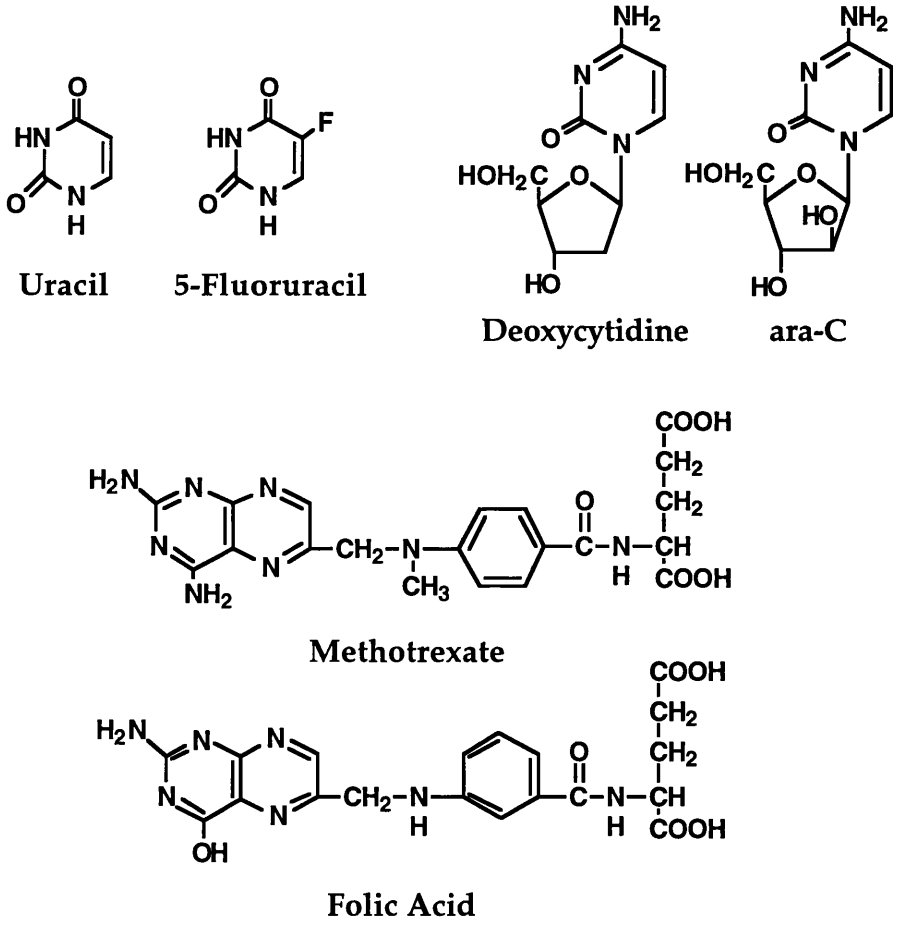

Figure 1.4. Antimetabolites.

The antimetabolites were developed from observations that, before mitosis can occur, a cell must build up large reserves of amino acids, nucleic acids, and other important metabolites (Priestman, 1989). The antimetabolites are simple chemical analogues of normal metabolites and

can act either by the inhibition of critical enzymes in the synthetic pathways of nucleic acids or by incorporation into macromolecules, consequently disrupting normal function. Because these agents do not directly interact with DNA to exert their mechanism of action, this class will only be represented with three specific and exhaustively studied examples.

Antifolates were the first antimetabolites to be introduced into the clinic, when it was shown that aminopterin, an analogue of folic acid, could produce remissions in childhood acute leukaemia (Allegra, 1990). Methotrexate is structurally similar to folic acid (Figure 1.4), but has a much greater binding affinity for the enzyme dihydrofolate reductase than dihydrofolate, the reductase's natural substrate. Folic acid is essential in the synthesis of purines and pyrimidines, and the enzymatic reduction step performed by dihydrofolate reductase is critical to this pathway (Benkovic, 1980).

Fluorouracil was one of a series of fluorinated pyrimidine analogues reported that were developed on the premise that "uracil may be utilised preferentially for nucleic acid biosynthesis in tumours" (Heidelberger, *et al.*, 1957) . Fluorouracil is a uracil analogue (Figure 1.4) that has an affinity a hundred times greater than uracil for the enzyme thymidylate synthetase (TS). Fluorouracil covalently binds to the enzyme, forming a ternary complex, and is an example of suicide substrate inhibition. The conversion of uracil to thymidylate by the TS enzyme is the *de novo* synthesis of thymine and the consequence of this inhibition is referred to as 'thymineless death' (Benkovic, 1980).

Cytosine arabinoside (ara-C, Figure 1.4) is simply an analogue of the nucleoside deoxycytidine, but an arabinose has been substituted for the deoxyribose sugar. Cytosine arabinoside is an competitive inhibitor of DNA polymerases and can be incorporated into DNA during replication. It is incorporation into DNA that has been closely correlated with its cytotoxicity (Kufe, *et al.*, 1980).

1.2.4 Plant Derivatives

The plant alkaloids are agents derived from various plant species and will be briefly mentioned here because the mechanisms of action are different from the previous categories. The vinca alkaloid family, isolated from the root of the periwinkle plant, were the earliest of this category to be employed clinically. The target for the vinca alkaloids is tubulin, to which it binds tightly. Tubulin polymerises to form microtubules and these play a key role in cell division by forming the cell spindle on which the chromatids are arranged during metaphase. Inhibition of microtubule formation leads to metaphase arrest. It is interesting to note that, although they have quite similar structures, vincristine and vinblastine have a different spectrum of clinical activity and different dose limiting toxicities (Priestman, 1989).

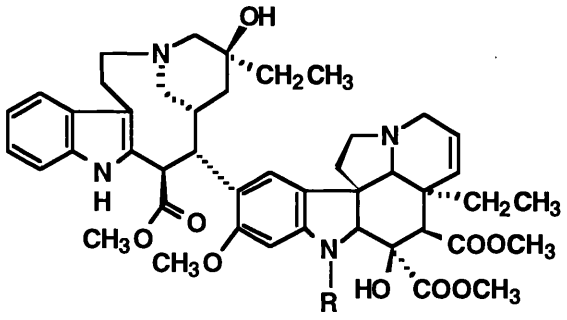

Vincristine, R=CHO; Vinblastine, R=CH_3

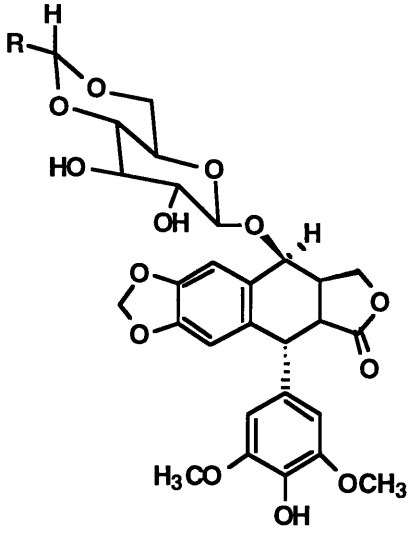

Etoposide, R= CH_3

Teniposide, R=

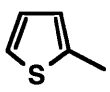

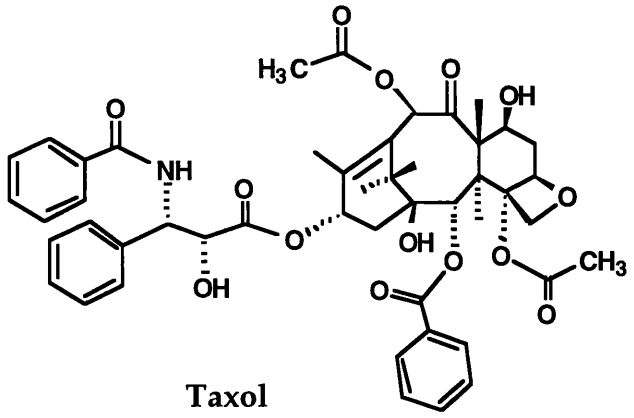

Taxol

Figure 1.5. Plant derivatives.

Taxol is a plant alkaloid that was isolated from the bark of the Pacific Yew tree and was identified as a promising new agent in the NCI sponsored program in which extracts of over 35,000 plant species were tested for anti-cancer activity between 1958 and 1980 (Borman, 1991). Its mechanism of action differs from the vinca alkaloids in that it appears to bind to tubulin in a manner that stabilises microtubule formation, preventing their depolymerization in anaphase. Taxol and taxotere, a closely related semi-synthetic analogue, have shown promise in clinical trials against ovarian and breast cancer (Workman, *et al.*, 1992; Long, 1994).

The epipodophyllotoxins are semi-synthetic derivatives of the plant alkaloid podophyllotoxin. While podophyllotoxin was found to interfere with microtubule formation, the epipodophyllotoxins are thought to act in a different manner. Two have recently found clinical application, etoposide (VP-16) and teniposide (VM-26). These agents have been shown to interfere and inhibit the function of the topoisomerase II enzyme. Topoisomerase II is an important enzyme in the maintenance of chromosomal integrity. It essentially allows one section of DNA to "pass through" another by nicking and then resealing both strands of one section. The epipodophyllotoxins bind to the topo II: DNA complex, stabilising the cleavage complex. This leads to the production of double strand breaks in DNA. Drugs that interfere with the function of topo I, which nicks and reseals one strand only, or topo II have recently emerged as a distinct family and represents the ongoing discovery of new agents with novel mechanisms of action. In addition to the epipodophyllotoxins, the synthetic compounds m-AMSA and mitozantrone, camptothecin, and also the above mentioned anthracyclines have been shown to interfere with the topoisomerases (Ralph, *et al.*, 1994).

1.3 Resistance Mechanisms and Sources of Agents

The above summary is certainly not meant to be exhaustive. It serves to introduce the spectrum and background of the currently employed chemotherapeutics. The simple problem with the chemotherapeutics described above is that these are also cytotoxic to normal proliferating cells. These agents indiscriminately interfere with mitosis and hence can have adverse effects on the healthy tissues and organs. The clinical application of these drugs is, in effect, trying to differently poison the tumour before poisoning the patient. As mentioned earlier, drug resistance is an important problem in the successful application of chemotherapy. When a patient treated with a regimen of chemotherapy has relapsed, that tumour will most likely be resistant to the original regimen. Tumour types which are inherently resistant to chemotherapy usually have very poor prognosis (Pratt, *et al.*, 1994). Knowledge of resistance mechanisms is important in the evaluation of an agent.

1.3.1 Drug Resistance

There are a variety of mechanisms by which malignant cells become more resistant to the killing effects of cytotoxic agents and these usually involve up-regulation or alteration of normal cellular functions. Cells that develop multi-drug resistance (MDR) seem to undergo three major changes; decreased accumulation of cytotoxic drugs, changes in activity or expression of certain cellular proteins, and changes in the cellular physiology (Simon & Schindler, 1994). Up-regulation of the enzyme dihydrofolate reductase has been well-documented as one of several mechanisms in methotrexate resistance. Overproduction of the enzyme thymidylate synthetase and production of an altered form that fluorouracil binds with a weaker affinity has been clearly documented in resistance to fluorouracil (Pratt, *et al.*, 1994). In both cases, overproduction or alteration of the enzyme targeted by the

chemotherapy leads to an increased tolerance of the drug and an increased resistance to its cytotoxic effects.

There are several mechanisms of drug resistance to the alkylating agents. These include alterations in drug uptake or transport, increased repair of drug-induced DNA damage, failure to activate those drugs which require activation, increased scavenging of drug species by non-essential cellular nucleophiles, and increased enzymatic detoxification of the drugs (Clapper & Tew, 1989). One example of a DNA damage repair pathway is the protein O6-alkyl guanine transferase (O6-AGT), which acts by a unique mechanism. The protein catalyses the transfer of an alkyl group from the guanine-O6 position onto an internal cysteine residue in a process that is irreversible (Pegg, 1990). This protein has been found to be overexpressed in some tumours. The lesions produced by methylating and ethylating agents such as DTIC and the nitrosoureas appear to be susceptible to this type of repair and alkyl-transferase activity protects cells from the lethal effects of the nitrosoureas (Pegg, 1990).

Agents such as mitomycin C or cyclophosphamide require activation and a lack of activation results in little or no cytotoxic effect. Glutathione is a ubiquitous cellular nucleophile that can react with and inactivate the alkylating agents and overproduction of glutathione has been well documented in some cell lines resistant to alkylating agents (Tew, 1994). The glutathione-S-transferase enzyme family also acts to inactivate both hydrophobic and electrophilic drugs by conjugating them with glutathione (Clapper & Tew, 1989). It is known that these enzymes are overproduced in many types of tumours (Tew, 1994).

A variety of seemingly unrelated agents are susceptible to the activity of a protein that acts as a cellular pump. The membrane protein, named p-glycoprotein, acts as an 'efflux pump' that transports drugs out of the cell cytoplasm and is the cause of MDR (Kartner & Ling, 1989). Agents which are known substrates for this protein include the anthracyclines, the vinca

alkaloids, etoposide, actinomycin D, mitomycin C and methotrexate (Kartner & Ling, 1989). Each of the examples lend further emphasis to the need to develop novel agents which may not be susceptible to resistance mechanisms. In addition to overcoming inherently resistant cell subtypes, an arsenal of agents with different mechanisms of action is useful in order to combat the onset of acquired resistance if a relapse occurs.

1.3.2 Sources of Chemotherapeutic Agents

All of the agents mentioned here can be identified as originating from one of three backgrounds. Observations of certain differences between cancer cells or tumours, and normal cells or tissues, have led to the development of agents designed with the intention of exploiting those differences. Unfortunately, the original premise does not always correctly explain a particular agent's activity, as in the case of cyclophosphamide. The second origin is the screening of vast numbers of natural products. This route produced, among others, the antimitotic antibiotics and Taxol. Although the approach lacks a testable rationale, it is still a useful way of discovering agents with novel mechanisms of action. The third origin is the development of closely related structural analogues of agents from one of the first two groups in attempt to reduce the parent agent's toxic side effects, while retaining antitumour efficacy. This area of research represents a significant proportion of past and current anti-cancer drug design. In spite of some successes in developing analogues from parent agents, a fundamental understanding of how the chemical changes on a drug structure affects its antitumour efficacy and tumour specificity has not always been possible. Even though some of the agents employed clinically have been used for over 40 years and have been exhaustively studied, it is still not clear exactly how such chemically reactive drugs can produce specific biological effects (Hartley, 1990). A simple enantiomeric difference can equate to a completely different spectrum of activity, and with the

example of cytosine arabinoside, the difference between an essential DNA building block and a cellular poison. Structure-activity studies provide a useful insight into the relationship between changes in drug structure and biological activity.

The issue of molecular recognition is rapidly becoming one of great importance in all of medicine. It is now obvious that biological events are the result of chemical interactions that occur specifically at the molecular level. For example, an enzyme will perform a specific catalytic function or transformation efficiently only if the correct substrate is in place and only if allosteric sites are activated properly. DNA is the carrier of genetic information in cells and gene expression (or lack thereof) through the selective binding of promoters, suppressors and the transcription machinery is crucial to the cell and the organism.

The recent exponential growth of research in the fields of cellular and molecular biology has provided for a greater understanding of the processes involved in cell signalling, cell division, and DNA maintenance mechanisms. Many of the processes are either aberrant or lacking in malignant cells and this concomitantly suggests that these might be targeted by new, designed agents. This includes topoisomerase inhibitors, bioreductive agents that target the hypoxic conditions of solid tumours, and agents that target the MDR protein. Additionally, growth factors and their receptors and signal transduction pathways (Powis, 1993), positive and negative checkpoints on cell cycle progression (Hartwell & Kastan, 1994), and metastasis/angiogenesis processes (Weinstat & Steeg, 1994) have been suggested as potential alternative targets.

The fact that all of the alkylating agents and antimitotic antibiotics interact with DNA in some manner suggests that DNA is an important chemotherapeutic target. Because the different tumour types respond differently to chemotherapy, the implication is that some tumour types must be particularly susceptible to DNA damage. Additionally, most

differentiated cells are largely unaffected by the action of chemotherapeutic agents. The suggestion is that DNA damaging agents possessing a higher specificity than those currently used can be developed that may be able to exploit these differences. The design of novel DNA-targeted agents first requires an understanding of DNA structure and an understanding of the specific DNA interactions of the currently employed chemotherapeutics.

1.4 DNA Structure and Drug: DNA Interactions

1.4.1 DNA Structure and Modes of Binding

In one of the seminal discoveries of the 20th century, Watson and Crick proposed a structure for DNA based on knowledge of the chemical structures of each of the four bases and X-ray diffraction patterns (Watson & Crick, 1953). It is the hydrogen bonding interactions that occur between adenine and thymine, and between guanine and cytosine, that form the two base pairs and the core of the DNA structure. The bases are connected to the sugar phosphate backbone of the DNA through an *N*-glycosylic bond to the C1′ position of deoxyribose. The 3'-position of each sugar is linked to the 5'-position of the next through a negatively charged phosphate group. Composition of one strand is matched by the opposite strand of complementary bases, where the sugar linkages from 5' to 3' run in the opposite direction and together these form a double helix. The sugars assume non-planar conformations or 'puckers' in order to minimise steric clashes (Blackburn, 1990). Because the strands are anti-parallel the sugars do not diametrically oppose one another and this results in two 'grooves' of differing width, called the major and minor grooves. There are several different types of conformations DNA can adopt, each of which vary in groove width and depth, according to state of hydration and salt concentration. For the purposes of this discussion, a description will only entail B-DNA, as it is the most commonly found structure of genomic

DNA. The major groove of canonical B-DNA is wider (11.7 Å) and slightly deeper (8.8 Å) than the minor groove, with a width of 5.7 Å and depth of 7.5 Å. One complete turn of DNA consists of 10.5 base pairs with a rise of 3.3-3.4 Å per base pair (Blackburn, 1990). The width and shape of the grooves are altered, however, depending on the sequence composition. AT-rich sequences have a narrow minor groove (Fratini, *et al.*, 1982; Nelson, *et al.*, 1987), whereas GC-containing sequences are significantly wider (Fagan & Wemmer, 1992; Neidle, 1992).

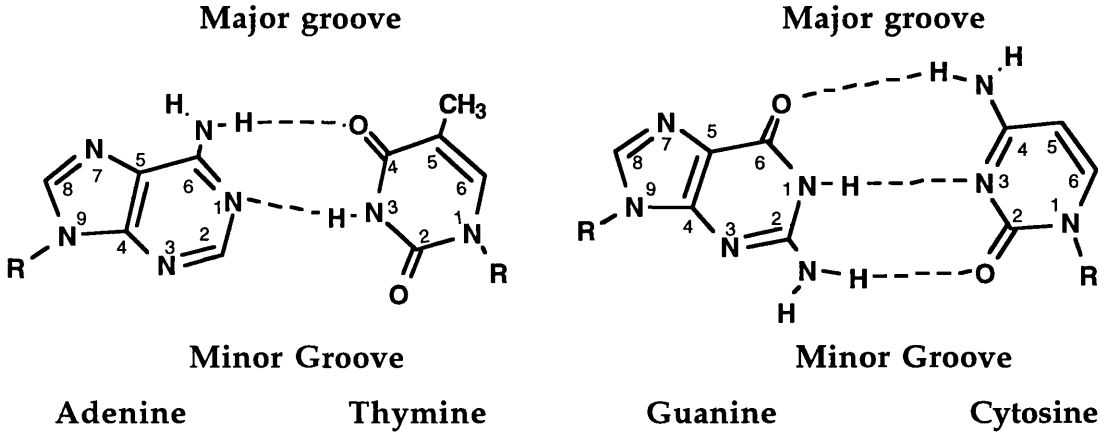

Figure 1.6. The DNA base pairs and hydrogen bonding.

The base pairing composition provides a source of electron rich sites and hydrogen bond donors and acceptors (Figure 1.6). The major groove contains more information as defined by the number and discriminatory capacity of hydrogen bond accepting and donating sites. The majority of proteins bind in the major groove, while certain polymerases operate via the minor groove and some proteins interact with both. Many xenobiotics including antibiotics bind to the minor groove. Because the majority of protein: DNA interactions occur in the major groove, the minor groove is relatively unoccupied in comparison and this is presumably the reason for the evolution of minor groove-binding antibiotics to attack the DNA of competing organisms (Lown, 1990).

In addition to major groove and minor groove binding, intercalation can also occur. Planar aromatic molecules can fit between the stacked base pairs, and the overlap of π clouds between the drug and the base pairs offer a stabilisation through binding. Stiffening and unwinding of the DNA helix occurs to accommodate intercalators. Due to the interactions, however, intercalators can only fit in between every other base pair, in what is known as nearest neighbour exclusion (Wilson, 1990). Because intercalators only interact with the immediate base pairs on either side, the sequence specificity of these agents is severely limited, although intercalators can be linked by a flexible linker in what are termed bis-intercalators (Wilson, 1990). The classic examples of intercalators are the DNA stain ethidium bromide and the antimitotic antibiotic actinomycin D.

A fourth mode of DNA binding that has been studied for possible exploitation is triple helix formation. It is known that polypyrimidine oligodeoxynucleotide strands composed of thymines and protonated cytosines can hydrogen bond with adenines and guanines, respectively, in polypurine-containing duplex DNA in what is termed Hoogsteen base pairing (Blackburn, 1990). The clear attraction to this approach is the exquisite sequence specificity that can be attained by base pairing complementation and there have been reported *in vitro* successes, but there are serious drawbacks in its biological application. Recognition of pyrimidines in mixed DNA by triple helix forming oligodeoxynucleotides has proven more difficult to achieve (Griffin, *et al.*, 1992), oligodeoxynucleotides are extremely vulnerable to degradation by the various exo- and endonucleases (Wickstrom, 1986) and cellular penetration is limited by the negatively charged backbone of the oligodeoxynucleotides and a majority are trapped by endocytic vesicles (Helene, 1991). Lastly, there are serious questions concerning the biological effects seen for DNA binding and RNA binding 'antisense' oligodeoxynucleotides and whether the

mechanism of action may be due to some other cellular response not associated with specific target binding (Gura, 1995).

1.4.2 Drug: DNA Interactions

The DNA interactions of the alkylating agents and the antimitotic antibiotics appear to be crucial for the expression of their biological and clinical activities. Elucidation of an agent's specific interactions with DNA becomes important in the full characterisation of that agent's profile. There are several levels of DNA interaction that can be explored. The first is understanding the non-covalent and covalent interactions. Non-covalent interactions are either one or a combination of electrostatic, hydrogen bonding, and van der Waals forces. Covalent interaction describes the formation of a chemical bond between an agent and DNA. Because of the confusion that may arise, the term 'bind' will refer to non-covalent interactions, and the term 'alkylate' will refer to covalent bond formation, even though this may not be strictly correct, as with cisplatin. Agents may either interact through non-covalent or covalent interactions, or they may possess non-covalent interactions that affect or direct ensuing covalent bond formation.

As mentioned above, each of the four DNA base pairs contain electron rich groups and these can act as nucleophiles. Agents that possess different electrophilic substituents can react with DNA nucleophiles with varying rates. Identifying the specific position where an agent alkylates (i.e., guanine-N7, adenine-N3) helps determine in which groove the agent preferentially alkylates. An agent may possess a sequence specificity or preferential reactivity for a base or base pair only within a specific sequence context. The agent may require a 'recognition sequence' for optimal interactions with DNA. Knowledge of the particular types of DNA lesions formed by an agent aids in determining which lesions are critical. It is well known that certain lesions are primarily mutagenic, while some are toxic,

and that different types of DNA damage are repaired by different repair enzymes (Sancar & Sancar, 1988). Knowledge of the spectrum of different lesions formed and repaired is essential for understanding repair mechanisms involved in resistance. Lastly, determination of the full profile of an agent helps aid in the design of novel analogues. Knowledge of the critical lesion formed by an agent or its active metabolite aids in the design of novel analogues which preferentially form that lesion, or which eliminate other types of lesions that could be detrimental.

1.5 Mechanism of DNA Interaction for the Alkylating Agents

1.5.1 Nitrogen Mustards and Chemical Reactivity

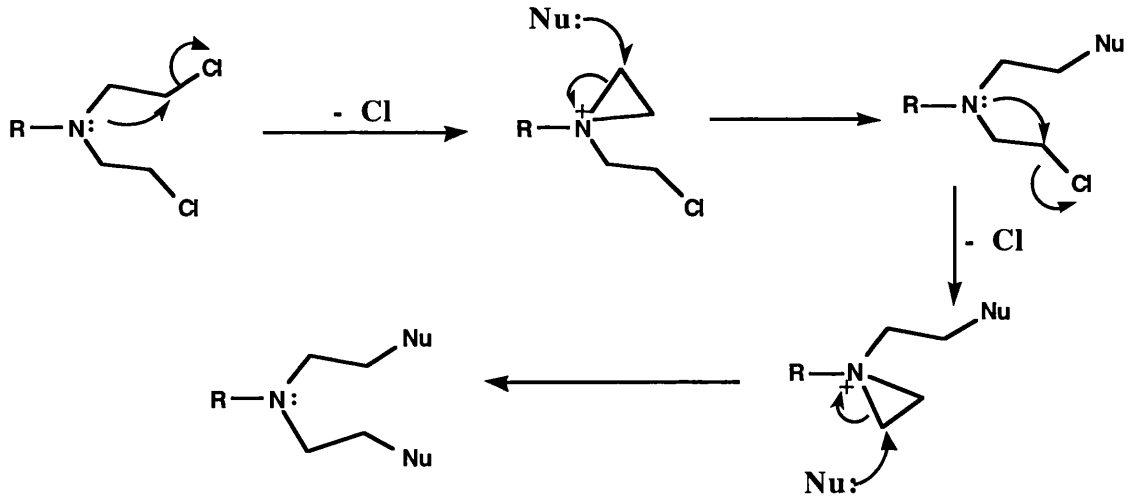

Figure 1.7. Aziridinium formation by a nitrogen mustard.

Nu: = Nucleophile.

The mechanism of action for the alkylating agents is now generally assumed to be DNA alkylation and, in the case of bifunctional agents, the formation of interstrand cross-links which prevent replication. The β-methylenes of the nitrogen mustards are electrophilic due to the presence of the electronegative chlorine, which is a good leaving group. The presence

of the nitrogen β to the electrophilic carbon means that the nitrogen mustards can undergo a cyclisation reaction whereby the nitrogen lone pair attacks a β-methylene carbon and, with loss of chloride, produces the positively charged aziridinium intermediate (Figure 1.7) (Williamson & Witten, 1967). The methylenes in the aziridinium cation are highly reactive and susceptible to attack by nucleophiles. The rate-limiting step is the aziridinium formation, which depends on the electronic influence of the R-group substituted on the nitrogen (Panthananickal, *et al.*, 1978). Mechlorethamine possesses an electron-donating methyl group on the nitrogen that accelerates aziridinium formation, while melphalan and chlorambucil possess an electron-withdrawing aromatic ring and these react more slowly (Wilman & Connors, 1983). DNA possesses several oxygens and nitrogens that can act as nucleophiles. If DNA provides the nucleophile in the reaction, nucleophilic attack and ring opening produces a monoalkylation on the DNA. The second chloroethyl arm can also undergo cyclisation to form an aziridinium ion. If simple hydrolysis occurs, then the lesion will most likely remain a monoalkylation. If the second nucleophile is on the opposite strand of DNA, then an interstrand cross-link has been completed (Figure 1.7).

1.5.2 DNA Alkylation and Cross-Linking by the Nitrogen Mustards

Because of the highly electrophilic nature of the aziridinium ion, a variety of cellular nucleophiles could potentially react with the nitrogen mustards. Early studies on alkylating agents, and the nitrogen mustard family in particular, found that bifunctional agents generally exerted a more powerful cytotoxic action than the corresponding monofunctional agents (Haddow, *et al.*, 1948; Loveless, 1951). It was hypothesised that this was probably the result of the ability to cross-link macromolecules, particularly those involved in duplication of the chromosomes (Goldacre, *et al.*, 1949). The first proposal that mechlorethamine formed DNA interstrand cross-

links stemmed from the observation that mechlorethamine-treated DNA did not denature normally (Geiduschek, 1961). Each of the DNA bases have oxygens and nitrogens that could potentially act as nucleophiles in reaction with an aziridinium, but the most nucleophilic position is the guanine-N7 position. A study using radio-labelled mustard gas demonstrated reaction with nucleic acids that identified the target as guanines, specifically the N7 position of guanine (Brookes & Lawley, 1960). Further studies demonstrated that monofunctional analogues of mustard gas and mechlorethamine produced guan-7-yl adducts, but mustard gas and mechlorethamine produced di(guan-7-yl) adducts, in addition to the monofunctional adducts (Brookes & Lawley, 1961). It was also shown that the bifunctional derivatives were much more cytotoxic than the monofunctional derivatives. The authors hypothesised that the increase in cytotoxicity was due to the ability of the bifunctional agents to form DNA interstrand cross-links and it was proposed that this occurred via opposite guanines in a 5'-CG sequence (Brookes & Lawley, 1961). The hypothesis that the nitrogen mustards form interstrand cross-links through the N7 position of guanines on opposite strands has now been broadly accepted, albeit now modified with the advent of sequencing methodologies (see below).

Direct demonstrations of DNA cross-linking began to support the hypothesis of cross-linking as the biological mechanism of action (Geiduschek, 1961; Kohn, *et al.*, 1966; Lawley & Brookes, 1967), but evidence of cross-linking in cells at pharmacologically reasonable doses did not to come until the advent of the technique of alkaline elution (Kohn, *et al.*, 1976). The distinct advantage of the technique was that it did not require prior isolation of the genomic DNA, which can subject the DNA to extensive and uncontrolled fragmentation. The technique proved sensitive enough to detect cross-links in cellular DNA after treatment with drug doses amounting to a log kill or less (Ewig & Kohn, 1977; Ross, *et al.*, 1978). Mechlorethamine, at sub-toxic doses, rapidly formed cross-links between

one and two hours after a 30 minute exposure to drug (Ewig & Kohn, 1977). The cross-links were then removed by a process that was virtually complete by 24 hours (Ewig & Kohn, 1977). Comparison of the time course of cross-link formation and removal by mechlorethamine and melphalan found very different rates (Ross, *et al.*, 1978). In contrast to mechlorethamine, cross-link formation by melphalan occurred rapidly between one and two hours after drug exposure, but then continued to gradually rise up to ten hours. Cross-link removal for melphalan was much more gradual and a significant amount of cross-links remained after 24 hours (Ross, *et al.*, 1978). The study did not distinguish between DNA interstrand and DNA: protein cross-linking.

A study on several cell lines that were made resistant to either Cisplatin or melphalan found a correlation between interstrand cross-linking and cytotoxicity. Comparisons between parent and resistant cell lines found a reduction in cross-linking of similar proportion to the increase in survival (Zwelling, *et al.*, 1981). Where cross-resistance occurred there was also a reduction in the amount of interstrand cross-linking. A strong correlation between the cytotoxicity and the total area under the curve for interstrand DNA cross-linking was found for mechlorethamine and melphalan, indicating that both the formation and rate of removal of the interstrand cross-links was important for the cytotoxic effects of the bifunctional alkylating agents (Hansson, *et al.*, 1987). Interstrand cross-link formation was found to correlate well with loss of colony survival, whereas DNA: protein cross-links did not correlate (O'Connor & Kohn, 1990). Examination of lymphocytes from untreated, treated sensitive, and treated resistant patients, found no difference in melphalan transport or intracellular concentration of melphalan but greater cross-linking in the untreated and treated sensitive samples indicating cross-link removal was a possible mechanism of resistance (Panasci, *et al.*, 1988). Comparison between the aromatic nitrogen mustards melphalan, chlorambucil and

benzoic acid mustard found that cytotoxicity correlated better with DNA cross-linking ability in isolated and cellular DNA than with hydrolysis rates (Sunters, *et al.*, 1992). For a series of monofunctional and bifunctional aminoacridine nitrogen mustards, the bifunctional analogues were more cytotoxic than the monofunctional analogues (Kohn, *et al.*, 1994).

1.5.3 DNA Sequence Preference of the Nitrogen Mustards

The introduction of DNA chemical sequencing methodologies was an important advance that allowed for the determination of the sequence specificity of drugs that interact with DNA, including the nitrogen mustards. Briefly, the Maxam and Gilbert method relies upon a series of chemical reactions that degrade the DNA (Maxam & Gilbert, 1980). The specific chemical reactions produce strand breaks at one or more of the four base pairs. Performing four different chemical reactions separately on singly end-labelled DNA fragment samples and subsequent electrophoresis on a denaturing polyacrylamide gel produces a 'ladder' of DNA strands differing in length by single nucleotides. The sequence of the DNA can be readily determined from the ladders.

In the sequencing reaction for guanines, dimethylsulfate (DMS) is used to methylate the N7 position. Subsequent treatment with hot piperidine leads to a strand break. DNA that has been alkylated at the N7 position of guanine by an alkylating agent such as a nitrogen mustard can also undergo the same treatment to produce a strand break (Figure 1.8) (Mattes, *et al.*, 1986b). Incubation of a singly end-labelled DNA fragment with an alkylating agent, followed by hot piperidine treatment allows for determination of the exact guanine alkylated. If the drug dose used equates to single hit kinetics, then a majority of the DNA fragment remains undamaged and there should only be one alkylation on the damaged strands. This allows for a determination of which guanines are preferentially alkylated in a given sequence (Mattes, *et al.*, 1986b).

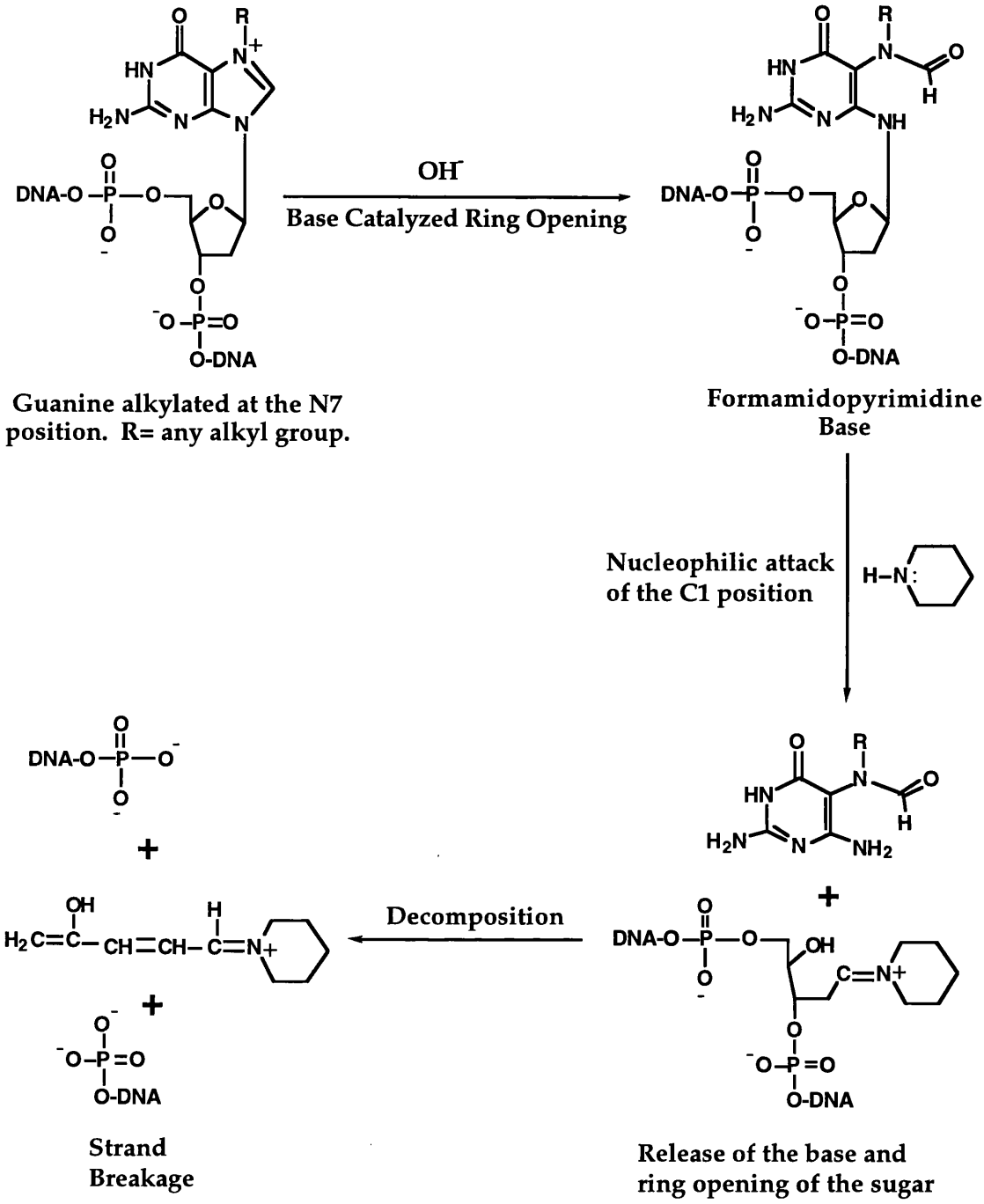

Figure 1.8. Piperidine-induced cleavage of guanine-N7 alkylated DNA.

It was shown that nitrogen mustards did not alkylate all guanines with equal intensity, but preferentially alkylated guanines within runs of guanines and less preference was seen for isolated guanines (Mattes, *et al.*, 1986a). The electrostatic potential of guanine located within various triplet base pairs, determined theoretically (Pullman & Pullman, 1981), was compared with the alkylation patterns for mechlorethamine and

melphalan. Although the correlation was not perfect, mechlorethamine and melphalan reacted preferentially with the most electronegative guanines, while the methylating agent DMS showed little sequence preference and a poor correlation with electrostatic potential (Kohn, *et al.*, 1987). Quinacrine mustard and uracil mustard possessed different sequence preferences, namely 5'-G(G/T)Pu and 5'-PyGC, respectively (Mattes, *et al.*, 1986a). It was hypothesised that quinacrine mustard favourably intercalated into its sequence before alkylation occurred, and a stabilising hydrogen bond could occur between the cytosine-4-NH_2 group of the 3'-C and the carbonyl group of uracil mustard (Kohn, *et al.*, 1987). The effect of ionic strength and the presence of different cationic DNA binding agents on the sequence specificity of alkylation for several nitrogen mustards has been studied (Hartley, *et al.*, 1990). The alkylation pattern for quinacrine mustard and uracil mustard were significantly affected by the minor groove binders netropsin and distamycin, but the alkylation pattern of melphalan was affected to a lesser extent. The discovery of the sequence specificity of alkylation for the nitrogen mustards led to a hypothesis that these agents may impart their biological effects because they target GC-rich regions (Hartley, *et al.*, 1988a; Mattes, *et al.*, 1988). Certain regions of the human genome including the regulatory regions of oncogenes (e.g. c-Ha-ras, c-sis) (Mattes, *et al.*, 1988) and the 3-Kb units of the Epstein Barr virus genome (Karlin, 1986) have an unusually high (>80%) GC content.

It has also been shown that the sequence specificity of alkylation for three different nitrogen mustards is retained in treated cells (Hartley, *et al.*, 1992). Sites of guanine-N7 alkylation were examined in human alpha DNA, a highly repetitive 340 base pair sequence comprising 1% of the human genome. The sequence preferences of mechlorethamine, uracil mustard, and quinacrine mustard, when the DNA from drug-treated cells and isolated DNA treated with the drugs were compared, were found to be essentially identical.

A more recent and important discovery was that the sequence specificity for cross-linking by mechlorethamine is between opposing guanine-N7 positions in the sequence 5'-GNC and not 5'-CG (Ojwang, *et al.*, 1989; Millard, *et al.*, 1990; Grueneberg, *et al.*, 1991; Rink, *et al.*, 1993). This would not be predicted by molecular modelling studies utilising a canonical B-DNA structure. A modelling study of phosphoramide mustard, the active metabolite of cyclophosphamide, predicted the sequence 5'-GC to be more favourable for cross-linking than the previously hypothesised 5'-CG (Hausheer, *et al.*, 1989). The distance between the opposing guanine-N7 positions separated by an intervening base pair in canonical B-DNA is 8.9 Å, but the constraints of the mechlorethamine structure dictate that the drug structure could not span a distance greater than 7.5 Å. It is now clear, however, that DNA cross-linked by mechlorethamine assumes a bent shape in order to accommodate the interstrand cross-link, and this has been shown theoretically and experimentally (Rink & Hopkins, 1995).

1.5.4 Adenine-N3 Alkylation by the Nitrogen Mustards

It should also be noted that adenine-N3 alkylation by some nitrogen mustards has been documented by several groups. A transcription termination assay using RNA polymerase found that the predominant transcription termination sites occurred at adenines for melphalan, and certain AG and GA repeats for CHL (Pieper, *et al.*, 1989). It was proposed that CHL and melphalan could form adenine-adenine intrastrand cross-links in the minor groove (Pieper & Erickson, 1990). The predominant mutations induced by melphalan in an SV-40 based shuttle vector replicated in human cells were surprisingly found to be A.T to T.A transversions, although the mutations induced by mechlorethamine and the active metabolite of cyclophosphamide were not (Wang, *et al.*, 1990). The sites of frequent transversion were also prominent sites for thermolabile adenine-N3 alkylation and the adenine adduct formation for CHL was nearly identical to

that seen for melphalan (Wang, *et al.*, 1991). The introduction of the minor groove and AT-binding distamycin suppressed the adenine adduct formation and mutation caused by CHL (Wang, *et al.*, 1994). A study with ^{14}C labelled CHL and HPLC isolation of the adducts found that the ratio of guanine to adenine adducts was 3:1 (Bank, 1992) and a recent HPLC isolation of mechlorethamine adducts found a guanine to adenine adduct ratio of 86:14 (Osborne, *et al.*, 1995).

1.5.5 Mechanism of Action of the Nitrosoureas

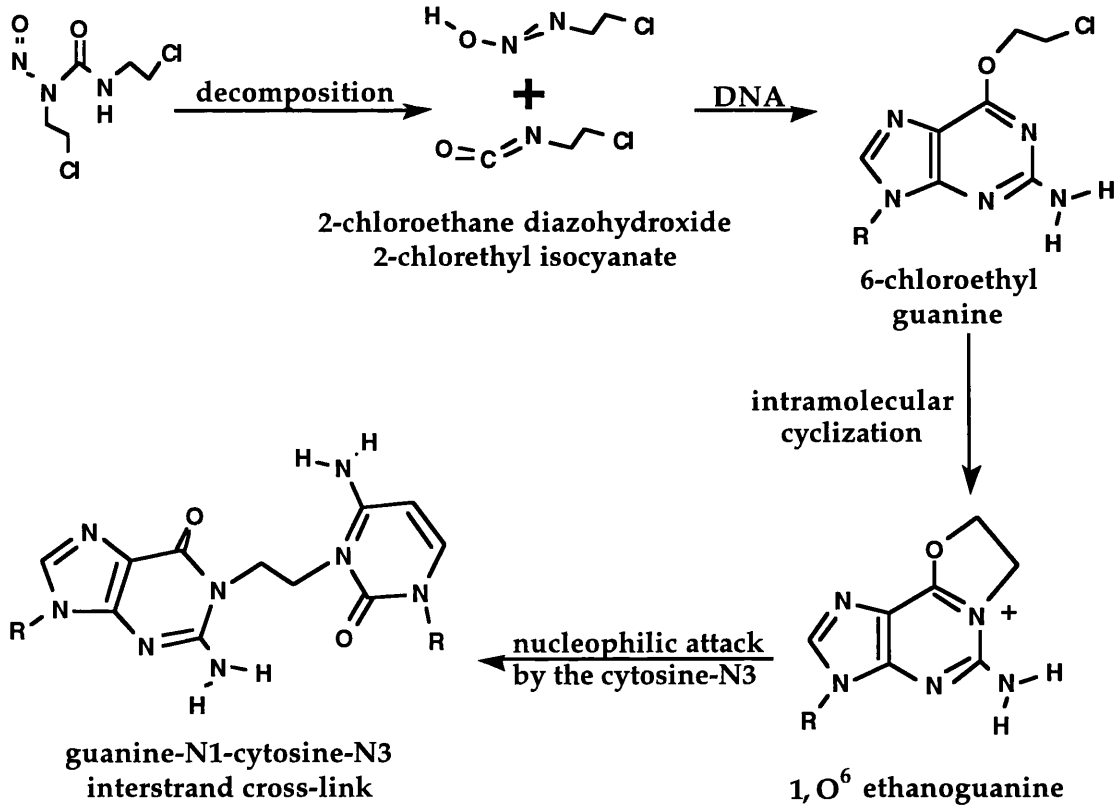

Figure 1.9. Cross-linking by the decomposition product of BCNU.

The nitrosoureas spontaneously decompose to a variety of compounds at physiological pH, but the chief products are 2-chloroethanediazohydroxide and 2-chloroethyl isocyanate, which decompose further to other products (Montgomery, 1986). The various decomposition products can react with DNA at several nucleophilic sites, but the majority of the alkylation occurs at the guanine-N7 position

(Gibson, *et al.*, 1985). The sequence specificity of guanine-N7 alkylation was shown to be guanines within runs of guanines and this correlates with the higher electronegativity of guanines flanked by guanines (Hartley, *et al.*, 1986). The primary mechanism of action, however, is thought to be interstrand cross-link formation, which is thought to be initiated by a different alkylation event. Chloroethylation of the guanine-O6 position by 2-chloroethanediazohydroxide, followed by an internal cyclisation with the N1 position and nucleophilic attack by an opposing cytosine-N3 forms a covalent cross-link between the guanine-N1 and cytosine-N3 positions of the complementary strands (Figure 1.9) (Tong, *et al.*, 1982). The hypothesis is supported by alkaline elution data that showed cross-linking increased up until approximately 6 hours after drug removal (Ewig & Kohn, 1977). Cells proficient in O6-AGT activity (termed Mer^+) accumulate fewer cross-links and are more resistant to BCNU than cells deficient in O6-AGT activity (Mer^-), indicating that cells which repair guanine-O6 alkylation are more resistant to the cytotoxic effects of the nitrosoureas (Erickson, *et al.*, 1980). This evidence supports the hypothesis that interstrand cross-link formation, initiated by guanine-O6 alkylation, is the mechanism of action for the nitrosoureas.

1.5.6 Cisplatin

Cisplatin produces a variety of DNA lesions, including monofunctional lesions, interstrand and intrastrand cross-links. These lesions have been determined utilising a variety of methods including alkaline elution, HPLC, atomic absorption spectroscopy (AAS), and enzyme-linked immunosorbant assay (ELISA) techniques (Reed & Kohn, 1990). It is now generally accepted that intrastrand cross-links at GG (65%) and AG (25%) sequences account for the majority of DNA platination (Eastman, 1986). The primary methods for determining the sequence specificity of cisplatin have been enzymatic, via exonuclease digestion or polymerase

inhibition, and this has been shown to be primarily guanines within runs of guanines and at AG sites (Comess & Lippard, 1993). The sequence specificity of cisplatin has also been studied in the single copy n-Ras gene in cells (Grimaldi, *et al.*, 1994). A lesion at the sequence 5'-TACT was seen in cells that did not occur on DNA treated with cisplatin.

The specific mechanism of action for cisplatin, with regards to the critical lesion, has been debated for some time. It is generally presumed that interstrand cross-links account for no more than 5% of total DNA platination (Comess & Lippard, 1993). DNA interstrand and DNA-protein cross-linking has been correlated with cytotoxicity by alkaline elution (Zwelling, *et al.*, 1981). Correlation of intrastrand cross-link formation with cytotoxicity has proven more difficult to establish. It has recently been shown that several high mobility group (HMG) proteins bind to the cisplatin: DNA intrastrand cross-links with an extremely high affinity, and it has been proposed that the intrastrand cross-links act as molecular decoys for transcription factors, called transcription factor hijacking (Treiber, *et al.*, 1994).

Studies utilising short oligodeoxynucleotide duplexes found that interstrand cross-linking occurred preferentially at the sequence 5'-GC (Hopkins, *et al.*, 1991) and modelling studies of the cisplatin: DNA interstrand cross-link indicate that the DNA bends significantly towards the major groove in order to accommodate the cross-link (Huang, *et al.*, 1995). Most recently, the structure of an oligodeoxynucleotide containing a cisplatin GG intrastrand cross-link was solved by X-ray crystallography, and the DNA was shown to be significantly bent towards the major groove (Takahara, *et al.*, 1995).

1.5.7 Triazenes and Imidazotetrazinones

DTIC belongs to the triazene family of agents. It has been shown that DTIC requires oxidative demethylation by liver microsomes, producing an

unstable form, which leads to the production of diazomethane (Montgomery, 1986). Diazomethane is highly reactive towards nucleophiles, including those on DNA and it is believed that DNA methylation is ultimately responsible for the activity of DTIC (Montgomery, 1986). The chloroethylating compound BIC is similar structurally to DTIC but was not pursued because of disappointing clinical trials.

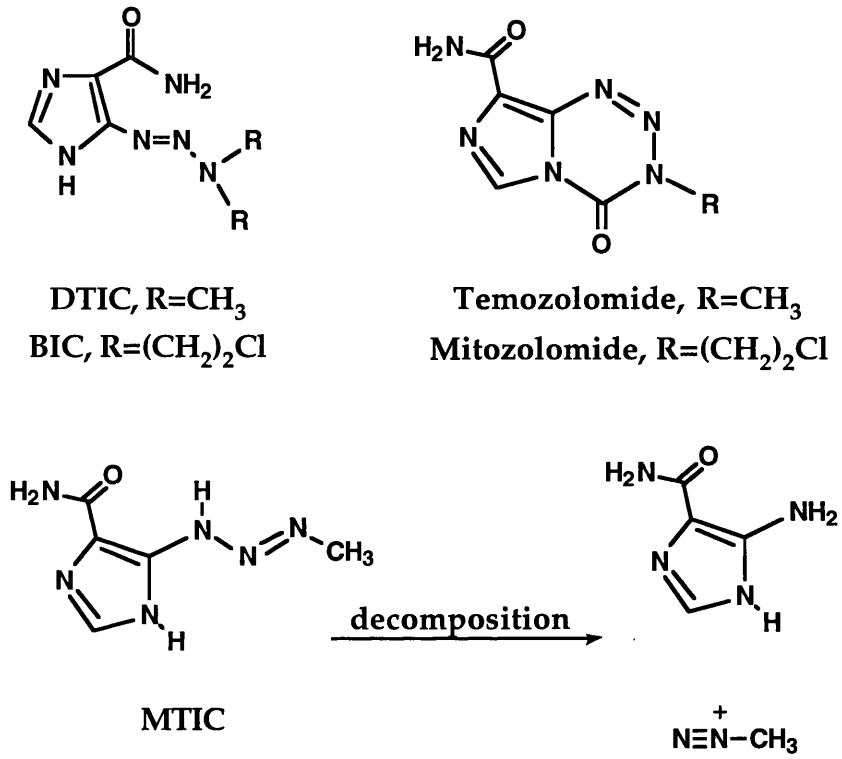

Figure 1.10. Triazenes, imidazotetrazinones, and the decomposition of MTIC to form the reactive diazomethane species.

Mitozolomide and temozolomide are imidazotetrazinones designed as prodrugs that do not require metabolic activation, but rely on acid or base catalysis to form the DNA-reactive species (Figure 1.10) (Stevens, *et al.*, 1984; Stevens, *et al.*, 1987). Pre-clinical studies on mitozolomide found that Mer^- cells were significantly more sensitive than Mer^+ cells, and interstrand cross-links were produced in Mer^- cells but not Mer^+ cells, indicating a chloroethylation reaction similar to the nitrosoureas (Gibson, *et al.*, 1985). Mitozolomide was the first of the imidazotetrazinones to enter clinical

trials, but the dose limiting toxicity, thrombocytopenia, was found to be unpredictable (Stevens & Newlands, 1993). Temozolomide lacks the chloroethyl arm of mitozolomide, thereby eliminating chloroethylation reactions and presumably the associated side effects and susceptibility to repair by O6-AGT (Stevens & Newlands, 1993). Temozolomide undergoes a base-catalysed decomposition to form MTIC (Figure 1.10), which alkylates the guanine-N7 position with a strong preference for guanines within runs of guanines (Hartley, *et al.*, 1988b). MTIC decomposes to form the reactive diazomethane species (Figure 1.10) (Denny, *et al.*, 1994a). Clinical evaluation of temozolomide against primary brain tumours has been encouraging (O'Reilly, *et al.*, 1993).

1.6 DNA Interactions for Clinical and Pre-Clinical Antibiotics

1.6.1 Anthracyclines

Several possible modes of action have been identified for the anthracyclines. The drugs' aglycone fused ring system can intercalate between the base pairs of DNA and inhibit DNA and RNA synthesis (Priestman, 1989). The drugs have been shown to bind to the membrane protein which is responsible for calcium transportation and there are two potential paths for producing free radicals which are known to cause DNA damage (Olson & Mushlin, 1990). The aglycone contains a semiquinone system that can be enzymatically reduced via one electron reduction to a semiquinone free radical. Alternatively, the agents can chelate several metals and oxygen free radicals may be generated non-enzymatically by the reaction of the ferric ion and molecular oxygen chelated to the anthracycline ring. As mentioned earlier, the anthracyclines have been shown to inhibit topoisomerase II by stabilising the 'cleavable complex' (Capranico & Zunino, 1990) and this causes DNA double-stranded breaks. Very recently it

has also been shown that adriamycin can cross-link DNA under extended incubation times (Cullinane, *et al.*, 1994).

1.6.2 Bleomycins

The mechanism of action is now generally assumed to be a catalytic, oxidative destruction of DNA that is oxygen and metal ion dependent (Natrajan & Hecht, 1994). The drug possesses a bithiazole moiety which acts as DNA binding domain, a metal chelating and oxygen binding domain, and a disaccharide group whose function remains unclear, although it has recently been shown that the first carbohydrate of the disaccharide may greatly influence the cleaving efficiency (Boger, *et al.*, 1995). The interaction of the bithiazole DNA binding portion appears to be primarily by intercalation (Manderville, *et al.*, 1995) and the strand breaks produced by bleomycin occur preferentially at 5'-GC and 5'-GT sequences (D'Andrea & Haseltine, 1978).

1.6.3 Mitomycin C

An early and influential study proposed a reduction of the quinone of mitomycin, activating two 'masked' functionalities, the aziridine and the carbamate. These were proposed to react with two nucleophiles on the opposite strands of DNA (Iyer & Szybalski, 1964). Isolation of the mitomycin C: DNA adducts were carried out by enzymatic digestion of calf thymus DNA and HPLC analysis, but the drug: DNA incubation conditions proved important in identifying the lesions. Enzymatic or chemical reduction in aerobic conditions led to the formation of a monofunctional mitomycin: guanine-2-NH_2 adduct (Tomasz, *et al.*, 1986), but anaerobic chemical reduction led to the isolation of the mitomycin: (guanine-2-NH_2)$_2$ cross-link (Figure 1.11) (Tomasz, *et al.*, 1987).

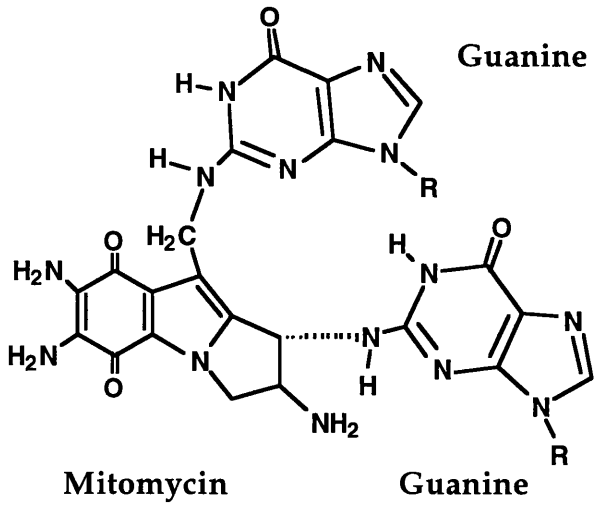

Figure 1.11. Mitomycin C: (guanine-2-NH_2)$_2$ cross-link.

The sequence specificity of cross-linking for mitomycin C was demonstrated by several groups to be exclusively at the 5'-CG sequence (Teng, *et al.*, 1989; Weidner, *et al.*, 1989; Borowy-Borowski, *et al.*, 1990). Examination of the specificity of the monoalkylation step by several groups found 5'-CG sequences to be the predominant site of alkylation, followed by less frequent alkylation at 5'-GG sequences (Li & Kohn, 1991; Kumar, *et al.*, 1992).

1.6.4 Bioreductive Agents

As mentioned earlier, it is well known that insufficient blood flow in solid tumours results in conditions of hypoxia. The field originally developed from the hope that agents could be developed that would target hypoxia and sensitise tumours to the effects of radiotherapy (Adams & Stratford, 1986). The initial clinical studies on the first 'radiosensitizer', misonidazole, proved disappointing, but hypoxia has remained an attractive target (Adams & Stratford, 1994; Hay, *et al.*, 1994). Development of DNA-damaging agents that first require reductive activation has been explored more recently. The different types of DNA-damaging bioreductive agents include the diaziridinyl benzoquinones (Hartley, *et al.*, 1991a) and quinone-containing compounds similar to mitomycin (Islam, *et al.*, 1991;

Workman, *et al.*, 1992; Huang, *et al.*, 1994), and nitroanilines (Palmer, *et al.*, 1992).

The diaziridinyl benzoquinones alkylate the guanine-N7 position with a preference for runs of guanines and cross-link in similar manner to the nitrogen mustards. The quinone moiety, however, can be chemically or enzymatically reduced to the hydroquinone, which facilitates aziridine ring opening. The cross-linking ability for the reduced form of 2,5-diaziridinyl-1,4-benzoquinone (DZQ) is increased by over 10-fold and the sequence specificity of alkylation is enhanced, such that a strong preference for the sequence 5'-TGC is exhibited (Hartley, *et al.*, 1991a). In addition, the sequence specificity of cross-linking for the oxidised form of DZQ was shown to be 5'-GNC, while the reduced form of DZQ preferentially cross-linked at 5'-GC (Berardini, *et al.*, 1993).

1.6.5 CC-1065 and Related Agents

The cyclopropylpyrroloindole (CPI)-containing antibiotic (+)-CC-1065 (Figure 1.12) was discovered by scientists at the Upjohn Company in fermentation broths of *Streptomyces zelensis* (Hanka, *et al.*, 1978). It was found to be extremely potent *in vitro*, and examined by the NCI drug screening program as an investigative drug. *In vivo* studies, however, revealed a delayed lethality in mice at sub-therapeutic doses that precluded it from further development (Hurley & Draves, 1993). Isolation and identification of the (+)-CC-1065: adenine-N3 adduct provided direct evidence for its covalent interaction with DNA (Hurley, *et al.*, 1984). Analysis of the sequence specificity was carried out by thermally inducing strand breaks at sites of adenine-N3 alkylation and revealed a preference for the 3'-adenine in the sequences 5'-AAAAA and 5'-PuNTTA. Space-filling modelling studies revealed a remarkably snug fit of the banana-shaped drug in the minor groove of DNA (Reynolds, *et al.*, 1985).

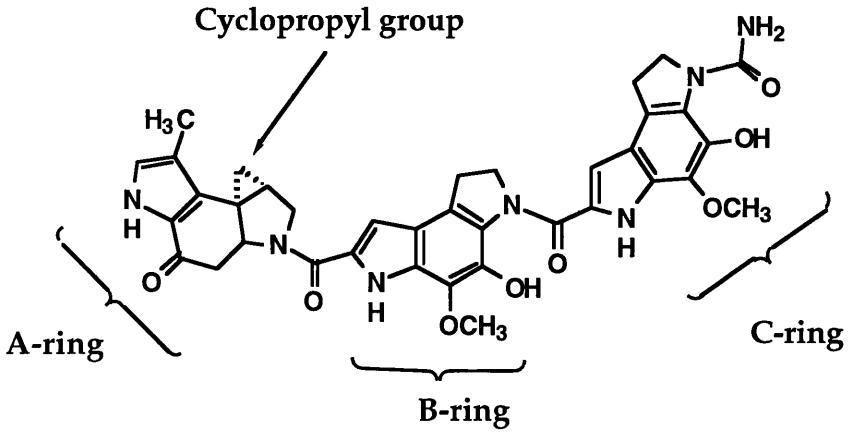

Figure 1.12. (+)-CC-1065.

A series of truncated analogues were synthesised in order to determine the molecular basis for the sequence specificity and it was found that the cyclopropyl-containing A-ring alkylated in a similar pattern to the ABC analogue, leading the authors to postulate that the A-ring was the determinant of the alkylation specificity, while the B- and C-rings facilitated non-covalent interactions (Hurley, *et al.*, 1988). These results proved controversial, however, and conflicting work has been published. Work from another group showed that the AB and ABC compounds recognised a subset of those alkylated by the A-ring analogue, and it was declared that, "the non-covalent binding selectivity of the agents may restrict the number of available DNA alkylation sites" (Boger, *et al.*, 1991). Work on the unnatural (-) enantiomers has also proved conflicting. Publication by Boger *et al.* of work on the unnatural enantiomer (-)-CC-1065 indicated that the compound only alkylated a subset of those alkylated by the truncated (-) A-ring analogue (Boger, *et al.*, 1990). Publication by Hurley *et al.* of (-) A-ring analogues found that this compound reacted detectably only at the same sites selected by (+)-CC-1065 (Hurley, *et al.*, 1990). Both groups agree that the (+) analogues are oriented in the 3'-5' direction, while the (-) analogues are oriented in the reverse 5'-3' direction. More recent work on various and numerous analogues has produced the hypothesis that the 'snugness' of the fit into the minor groove or the depth to which the drug can penetrate into

the groove is the determinant of the alkylation specificity (Boger, *et al.*, 1994). This work has been expanded to include the duocarmycin family, which have a similar cyclopropyl-pyrroloindole A-ring (Boger & Johnson, 1995a), and the hypothesis is further supported by the synthesis and determination of the alkylation specificity for an ABC analogue with the cyclopropyl group on the C-ring (Boger & Johnson, 1995b).

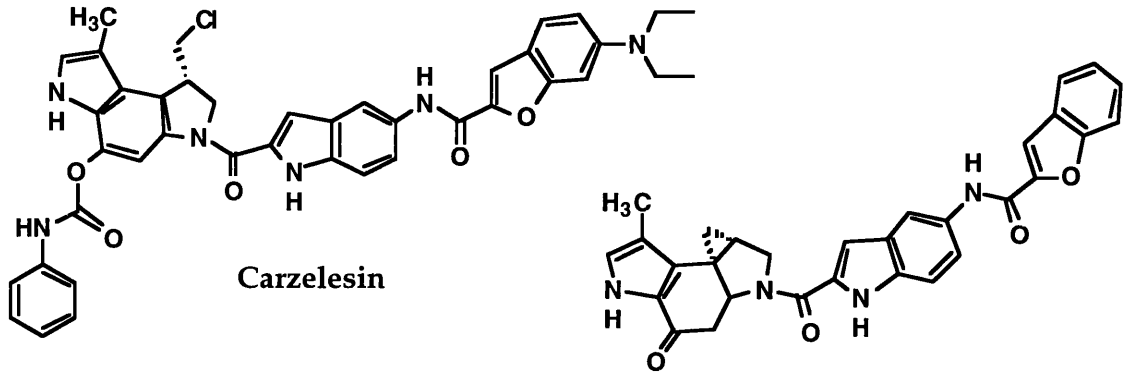

Carzelesin

Adozelesin

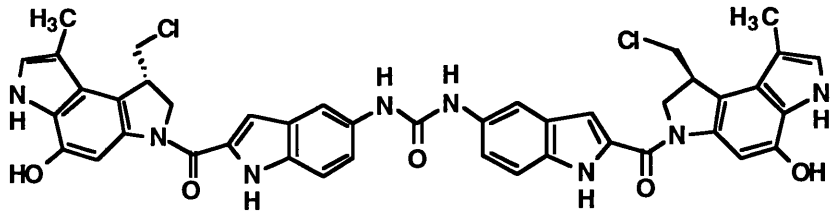

Bizelesin

Figure 1.13. Synthetic CPI analogues of CC-1065.

The Upjohn Company produced a series of CPI analogues based upon the repeating pyrroloindole units, some of which retained an antitumour efficacy without the delayed lethality seen with CC-1065. The three most promising agents, adozelesin, carzelesin and bizelesin, are now being evaluated in clinical trials (Figure 1.13) (Li, *et al.*, 1991; Workman, *et al.*, 1992). Carzelesin was designed as a prodrug that requires two steps for activation; hydrolysis of the phenylurethane substituent and ring closure to form the cyclopropyl group on the A-ring (Li, *et al.*, 1992). Bizelesin is a designed minor groove cross-linker which has been shown to efficiently

form cross-links *in vitro* (Lee & Gibson, 1991). Each of the analogues, however, appear to be susceptible to MDR (Zsido, *et al.*, 1992). The DNA alkylation specificity of adozelesin and bizelesin has been examined in cells using the technique of ligation-mediated PCR and it was found that the alkylation patterns were similar but not identical to that seen in isolated DNA (Lee, *et al.*, 1994). It has been suggested that the agents possessing the greatest stability of the cyclopropyl group may be expected to exhibit the most potent cytotoxic activity (Boger & Johnson, 1995a). A relationship between solvolysis stability and biological potency was observed with both simple and complex analogues of the CC-1065 and duocarmycin families (Boger & Johnson, 1995a).

1.6.6 The PBDs

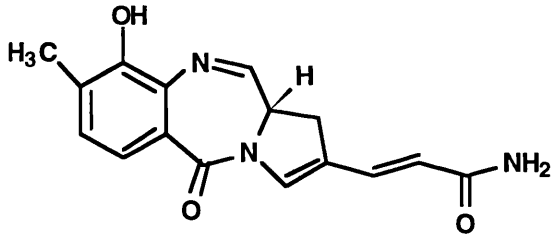

Anthramycin

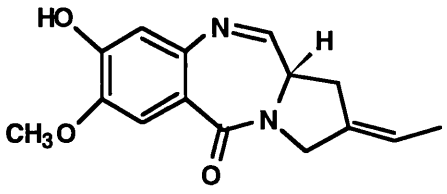

Tomaymycin

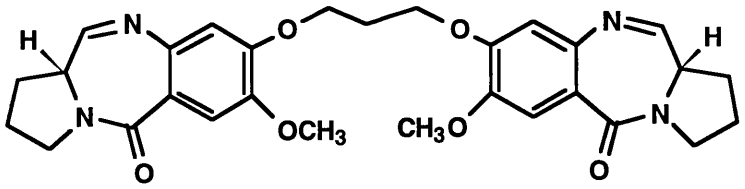

DSB-120

Figure 1.14. Pyrrolobenzodiazepines.

Agents with a common pyrrolobenzodiazepine structure, to which anthramycin and tomaymycin belong (Figure 1.14), have been explored as potential antitumour agents. These agents were also isolated from the fermentation broths of a *Streptomyces* species. Clinical application was

impeded by severe dose limiting toxicities, but other natural and designed agents of this class are being developed. The agents were found to bind in the minor groove, covalently bonding to the guanine-2-NH_2 position (Hurley & Petrusek, 1979; Hurley, *et al.*, 1980), and they preferentially alkylate at 5'-PuGPu sequences (Hertzberg, *et al.*, 1986). Designed minor groove cross-linking agents have been developed by linking two PBD units together (Bose, *et al.*, 1992). The linked PBDs are extremely toxic and produce cross-links in the minor groove that are not repaired (Smellie, *et al.*, 1994). Crosslinking by the agent DSB-120 occurred at the sequence 5'-GATC, which was predicted by molecular modelling (Jenkins, *et al.*, 1994a).

1.6.7 Enediynes

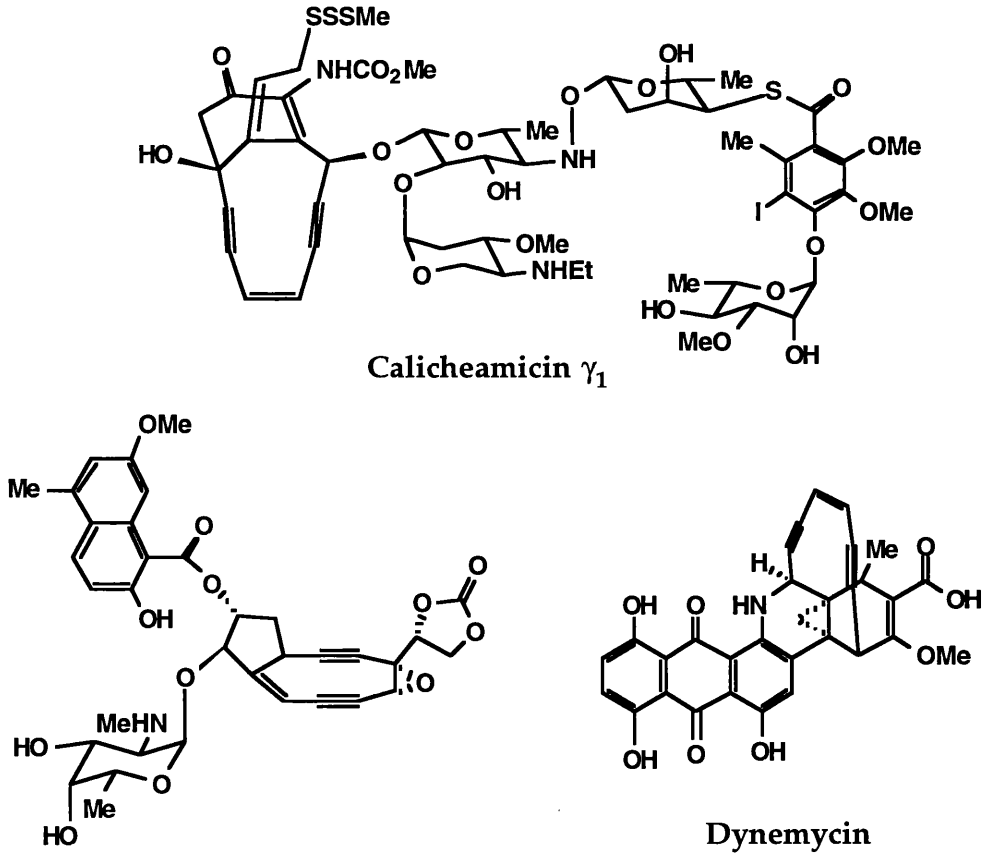

Figure 1.15. Enediyne-containing antibiotics.

The enediyne family is worth mentioning briefly because of their unique mechanism of action. The diverse natural products each have in common an enediyne functionality which can undergo a cycloaromatization via a highly reactive 1,4-benzenoid diradical intermediate (Nicolaou, *et al.*, 1993). Once the drugs have bound DNA, the diradical species efficiently catalyses double stranded breaks through hydrogen abstraction from the sugar backbone. These natural products are some of the most toxic compounds known to man and there is now great interest in attempting to exploit their unique biological properties.

1.7 Non-Covalent Minor Groove Binders

Netropsin and distamycin are the two exhaustively studied members of a general grouping of non-covalent minor groove binders that includes Hoechst 33258, DAPI, berenil, SN-6999, and pentamadine (Zimmer & Wahnert, 1986; Gilbert & Feigon, 1991; Neilson, 1991; Krugh, 1994; Geierstanger & Wemmer, 1995). Each have in common the general features of a cationic or dicationic nature that provides for an initial attraction to DNA and a shape that mirrors the convex shape of the minor groove.

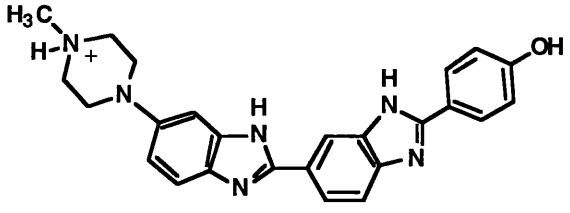

Hoechst 33258

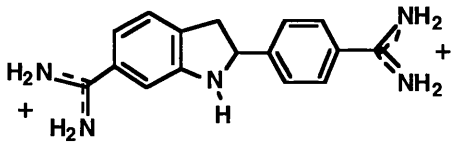

DAPI

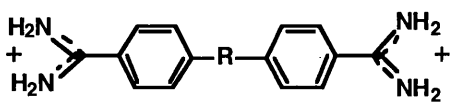

Pentamidine, R= $O(CH_2)_5O$

Berenil, R= N=N-NH

Figure 1.16a. Non-covalent minor groove binders.

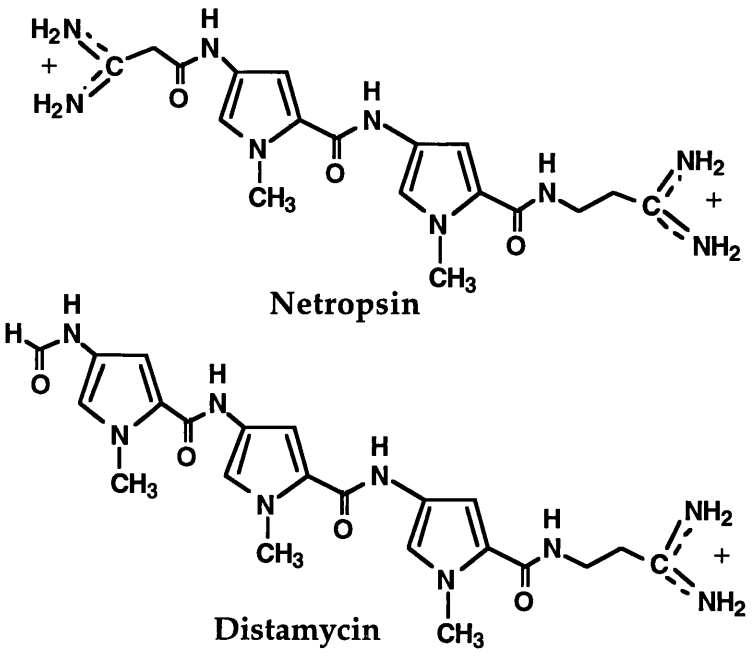

Figure 1.16b. Non-covalent minor groove binders.

1.7.1 Netropsin and Distamycin

Netropsin, the first of the pyrrole-amidine antibiotics to be discovered, was isolated from *Streptomyces netropsis* (Finlay, *et al.*, 1951). Distamycin, isolated from *Streptomyces distallicus*, was discovered by Arcamone and coworkers and was experimentally tested as an antiviral agent (Arcamone, 1993). It was the antiviral activity that suggested a strong interaction with DNA for both agents. ^{1}H NMR and X-ray crystal studies examining the structures of distamycin and netropsin showed that the molecules possess a concave shape which can mirror the shape of DNA (Berman, *et al.*, 1979). The concave shape also aligns the potential hydrogen bond donating amido groups on the face of the concave side.

Initial characterisation of the interactions of netropsin and distamycin with DNA employed biophysical techniques such as UV absorption, circular dichroism (CD), thermal melting and viscosity studies. CD, in particular, provided useful information. Briefly, circular dichroism relies on the differential absorption of circular polarised light by chiral molecules. Differential absorption of the light gives rise to an ellipticity that is represented in millidegrees in a positive or negative direction. These

interactions are termed Cotton effects and DNA exhibits a characteristic CD spectrum that differs for the A-, B-, and Z-forms. The interaction of drug molecules with DNA can cause changes in the CD spectrum, such as the appearance of drug-induced bands and/or alteration in the original spectrum. Achiral drugs do not exhibit CD spectra, so changes induced in the DNA's spectrum can be attributed to the interaction of the drug with the DNA(Zimmer & Wahnert, 1986).

The interaction of netropsin with various synthetic dA.dT and natural AT-rich DNA clearly indicated a high specificity for AT base pairs, whereas little or no interaction with GC-rich DNA was seen (Zasedatelev, *et al.*, 1974; Zimmer, *et al.*, 1979). In addition, strong interactions are seen with dI.dC containing duplexes. This strongly implicated that the 2-amino group of guanine must have an inhibitory effect on the binding to GC-rich sequences (Wartell, *et al.*, 1974). Distamycin showed a strong interaction with AT-rich DNA, but it also showed a weak induced CD spectrum with GC-rich DNA, which was attributed to weak binding to GC-rich sequences (Luck, *et al.*, 1977). A series of distamycin analogues with dansyl groups on the N-terminus and with one, two, or three pyrrole units were studied for their DNA binding affinity (Gursky, *et al.*, 1982). It was found that the monopyrrole analogue had a poor binding constant, and the di- and tripyrrole analogues had binding constants which were over an order and three orders of magnitude stronger, respectively (Gursky, *et al.*, 1982).

The technique of 'footprinting' is the most commonly used technique for determining the precise sequence specificity of a protein or drug. Briefly, a drug or protein is pre-incubated with a singly end-labelled DNA fragment, and then exposed to a chemical or enzymatic cleaving agent, which should cleave the DNA with minimum sequence preference. At sites where the drug or protein is bound, cleavage is suppressed because the cleaving agent cannot readily access the DNA. Where cleavage is suppressed due to drug/protein binding, bands do not appear on a DNA

sequencing gel. The gaps which appear on a sequencing gel are termed 'footprints' and the nucleotide sequence of the drug/protein binding site can be determined.

Development of the technique closely followed the introduction of the Maxam and Gilbert chemical sequencing methodologies. The original study utilised DNase I as the cleaving agent and studied the binding of the lac repressor to the lac operator (Galas & Schmitz, 1978). It quickly became an important method for determining the sequence specificity of DNA-binding drugs. The study utilised the DNA cleaving ability of DNase I to show that netropsin bound to AT sequences of four base pairs, in agreement with the biophysical data (Lane, *et al.*, 1983). An independent study reported by Van Dyke and Dervan utilised a designed chemical cleaving agent. The agent, called MPE, has an EDTA group linked to the intercalator methidium (Hertzberg & Dervan, 1982). The methidium group intercalates between base pairs via the minor groove, placing the EDTA group in proximity to the sugar phosphate backbone of DNA. The EDTA group can chelate an Fe(II) cation that coordinates oxygen molecules and produces diffusible hydroxyl radicals, in what is known as Fenton chemistry (Hertzberg & Dervan, 1984). The addition of a reducing agent such as dithiothreitol or ascorbate greatly enhances the reaction. Hydroxyl radicals are generally known to produce single stranded breaks on the backbone of DNA via hydrogen abstraction from the deoxyribose.

The footprinting studies on netropsin using MPE as the DNA cleaving agent revealed a strong affinity for AT sequences of four base pairs in length (Van Dyke, *et al.*, 1982). Distamycin demonstrated binding to AT sites five base pairs in length, with tolerance for a GC base pair in the binding site (Van Dyke, *et al.*, 1982; Harshman & Dervan, 1985). These results were corroborated by independent groups utilising different cleaving agents (Fox & Waring, 1984; Portugal & Waring, 1987). Footprinting has also been utilised to determine the DNA sequence specificity of a host of

other agents, including actinomycin, mithramycin, echinomycin, and all of the above listed non-covalent minor groove binders. The technique has proven valuable for determination of sequence specificity, but does not elucidate the specific interactions that occur between a drug and the base pairs of its recognition sequence.

Cocrystallization of netropsin and the dodecamer 5'-CGCGAATT^{Br}CGCG and solution by X-ray crystallography provided a detailed examination of the specific atomic interactions that occur between netropsin and DNA (Kopka, *et al.*, 1985). The drug was found to 'fit snugly into the minor groove of the DNA spanning the four AT base pairs.' The cationic ends of netropsin were found to be centered at the bottom of the groove, in proximity to the adenine-N3 positions at either end of the binding site, and not involved with the phosphates. The distances between the amido groups on the concave face of netropsin and the electron-rich sites on the floor of the minor groove, although long by classical hydrogen bond criteria, were proposed to contribute to stabilising the drug: DNA complex. Close contacts were also proposed to occur between the hydrogens of the pyrrole rings and the methylene groups of netropsin and the hydrogens in the minor groove of DNA. It was proposed that the AT specificity seen for netropsin arose from an 'avoidance' of GC base pairs, due to a steric clash which would occur between the protruding guanine-2-NH_2 group and the pyrrole C3 hydrogen. A concise description of netropsin binding to DNA is as follows. The electrostatic attraction of the dicationic drug for the negatively charged DNA provides for the initial interaction. A combination of hydrogen bonding and van der Waals forces provide the strength of binding by positioning the drug optimally in the groove. The binding that occurs in the minor groove for netropsin is enthalpy driven and this is due to the pyrrole-amide backbone, not the cationic ends (Breslauer, *et al.*, 1988).

1.7.2 Lexitropsins

The X-ray crystal study described above also predicted the possibility of designing compounds which could 'recognise' GC base pairs. Replacement of the pyrrole units with heterocycles such as imidazoles eliminates the steric clash caused by the protruding guanine-2-NH_2 group and these compounds were coined 'lexitropsins', or 'information reading oligopeptides' (Kopka, *et al.*, 1985). In addition to relieving the steric clash, the hydrogen-bond accepting nitrogen is placed in proximity to the guanine-2-NH_2 hydrogens in the minor groove.

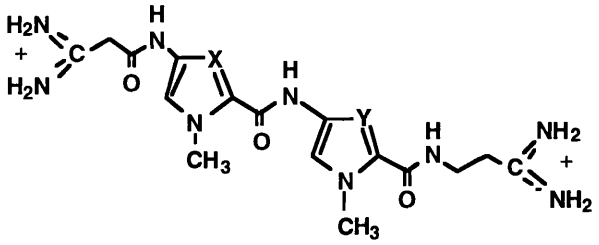

1, x=N, =N; 1a, x=N, y=CH; 1b, x=CH, y=N

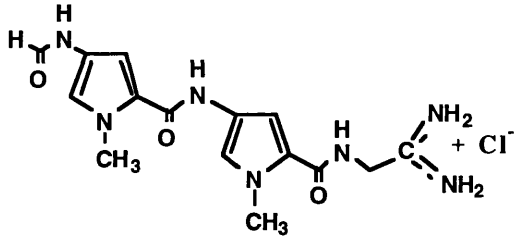

3

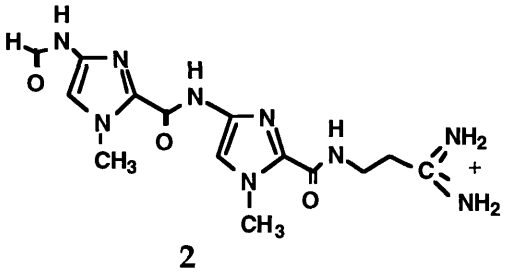

2

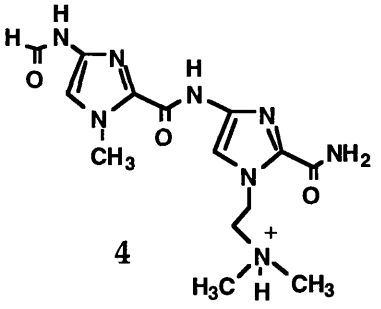

4

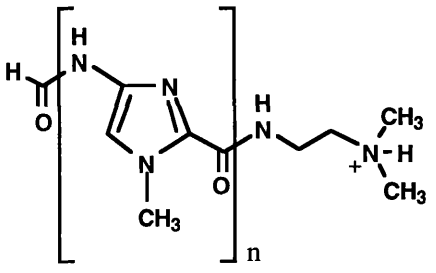

$Im_{n=1-4}$

Figure 1.17. Generations of lexitropsins.

A novel synthetic route to distamycin and netropsin (Lown & Krowicki, 1985) proved adaptable to the preparation of analogues which contained imidazoles (Lown, *et al.*, 1986; Krowicki & Lown, 1987), thiazoles (Rao, *et al.*, 1990; Rao, *et al.*, 1990), furans (Lee, *et al.*, 1989), and triazoles (Rao, *et al.*, 1991). The first generation lexitropsins contained imidazoles while retaining the positively charged N-terminal guanidinium and C-terminal amidinium groups (**1**, **1a**, **1b**, Figure 1.17) (Lown, *et al.*, 1986). The first generation lexitropsins, when studied by footprinting, were found to have an increased tolerance of GC-base pairs, but still bound to many of the AT-rich sites in similar manner to netropsin. It appeared that the lexitropsins retained a preference or 'memory' for AT-rich sequences. Theoretical studies on the electrostatic potentials of the minor groove of DNA had shown that AT-rich regions possess greater negative potential than GC-rich sequences (Lavery & Pullman, 1985). It was postulated that the dicationic nature was predisposing the lexitropsins for AT-rich sequences and it followed that a reduction in the cationic nature of the molecules could be beneficial. Replacement of the N-terminal guanidinium group with a formamido group, such as on the N-terminus of distamycin, produced the formamido-diimidazole lexitropsin (**2**, Figure 1.17) and it was found by footprinting studies to bind to the sequence 5'-CCGT (Kissinger, *et al.*, 1987). NMR studies of **2** bound to the oligodeoxynucleotide d[CATGGCCATG]$_2$ confirmed placement of the lexitropsin in the minor groove over 5'-CCAT with the N-terminal domain oriented in the 5'-direction and the C-terminal amidinium group oriented over the 3'-T (Lee, *et al.*, 1988a). This NMR study and an NMR study of **1** bound to the oligodeoxynucleotide d[CGCAATTGCG]$_2$ (Lee, *et al.*, 1988) offered insight into the recognition of the 3'-T in the binding sequence. It was argued that the hydrogens of the methylenes on the aminidium group provided a steric clash with the protruding G-2-NH_2 group of a GC base pair, resulting in a recognition of the 3'-AT base pair by default. A truncated lexitropsin **3** was

synthesised and its binding to the oligodeoxynucleotide d[CGCAATTGCG]$_2$ studied by NMR (Lee, *et al.*, 1988b). It was found that the lexitropsin **3** had shifted one base pair, from the sequence AATT to the sequence ATTG, indicating that removal of the methylene group allowed for recognition of a GC base pair at the C-terminus of this lexitropsin (Lee, *et al.*, 1988b).

There have been more recent studies evaluating modifications to lexitropsins. Formamido-imidazole lexitropsins that incorporate a dimethylaminoethyl group on the C-terminus were designed and synthesised (Figure 1.17) (Lee, *et al.*, 1993c). The series of lexitropsins Im$_{1-4}$, containing one to four imidazole units, were evaluated for their DNA binding properties. The Im$_1$ analogue demonstrated poor interactions with DNA. The Im$_2$ and Im$_3$ analogues, when studied by circular dichroism, demonstrated significant DNA-induced ellipticities that were more pronounced for poly(dG.dC) than for poly(dA.dT) DNA. Footprinting studies revealed the consensus recognition sequence for Im$_2$ to be the four base pair site 5'-(G.C)$_3$(A.T). Although differing from Im$_2$ by only one imidazole unit, Im$_3$ clearly recognised different sequences and its primary recognition sequence was 5'-TCGGGCT (Lee, *et al.*, 1993c).

Very recently a rationally designed lexitropsin overcame the 3'-terminal recognition of an AT base pair and bound to GC-exclusive sequences. The lexitropsin **4** (Figure 1.17) contains a completely truncated amido C-terminus and a dimethylaminoethyl group is attached to the first imidazole via the N1 position. The diimidazole analogue footprinted weakly at pure GC sites, predominantly at the sequence 5'-CGCC (Lee, *et al.*, 1994).

1.7.3 Linking Lexitropsins

A unique non-repeating sequence in the human genome would theoretically comprise 16-20 base pairs, although there are suspicions that lengths of 30-50 bases may be required for true uniqueness (Anderson, 1992).

More specifically, within the constraints of the AT and GC complementary nature of double helical DNA, for a binding size of *n* base pairs there are $(4^n)/2$ distinguishable sequences for odd *n* and for even *n*, there are $(4^n)/2 + (4^{n/2})/2$ (Dervan, 1986). The repeating pyrrole-amide units of netropsin and distamycin hinted at the possibility of recognising longer sequences by synthesising analogues with increasing numbers of the repeating units. Such a study was published on a series of distamycin analogues containing four to seven pyrrole units (Youngquist & Dervan, 1985). The increase in the number of pyrrole-amide units provided an increase in the binding site size that corresponded to "n+1" number of base pairs recognised for every "n" amido group on the concave face of the drug molecule (Dervan, 1986). More importantly, however, the binding became less favourable with the increase in the number of pyrrole units beyond four, indicating that the analogues of higher pyrrole-amide unit number did not interact with the DNA efficiently (Youngquist & Dervan, 1985).

A theoretical modelling study provided an interesting assessment of the structural aspects of ligands which bind to the minor groove of DNA (Goodsell & Dickerson, 1986). The minor groove distances between the base pairs of canonical B-DNA were compared with the repeat distances between the cyclic units of netropsin and other minor groove binding ligands. It was found that "the pyrrole-amide repeat of netropsin was inherently too long for perfect registration with B-DNA (Goodsell & Dickerson, 1986)." For each increase in the number of pyrrole-amide units in the DNA binding molecule, the important interactions between the drug and the base pairs of the minor groove become more 'out of phase' and less optimal.

Curvature is another important aspect of minor groove-binding ligands. In an early attempt at addressing curvature, two analogues were synthesised that had a β-alanine linker in place of either the central or C-terminal pyrrole. The analogues, which possessed the same number of amido groups but one less pyrrole than distamycin bound to DNA with a

weaker affinity than distamycin, as determined by UV and CD (Dasgupta, *et al.*, 1987). The binding affinities of benzyl-containing analogues decreased as the curvature decreased compared to distamycin (Rao, *et al.*, 1988).

The above mentioned work carried out on the formamido-imidazole lexitropsins containing one to four imidazole units addressed the aspect of curvature for these lexitropsins (Lee, *et al.*, 1993c). The Im_4 analogue, when studied by CD, demonstrated DNA-induced ellipticities that were not as great as those seen for Im_2 or Im_3, and additionally, Im_4 did not footprint. Modelling studies comparing the interactions of Im_3 and Im_4 with DNA indicated that the curvature of the molecules played a role in the recognition. When aligned in the minor groove, Im_3 closely fit the shape of the groove, but Im_4 was too curved to allow for a snug fit. When 'docked' into the minor groove, the two central imidazoles of Im_4 were too distant for interactions with the floor of the minor groove (Lee, *et al.*, 1993c). The curvature measured for netropsin and distamycin was found to match well with the curvature of an A_4 tract (Cory, *et al.*, 1992).

The concept of linking together binding units has been explored by several groups. The earliest example was a report of the synthesis and DNA binding properties of a group of head to tail, head to head, and tail to tail linked "bis-netropsin" compounds (Gursky, *et al.*, 1982). Each of the bis-netropsin analogues possessed significant binding constants, estimated to be greater than 10^8 M^{-1}, and the data from CD studies provided an estimation of binding sites of 10 to 11 base pairs. Three tetrapyrrole units were linked with β-alanine linkers to produce an agent which bound a 16 base pair AT-rich site (Youngquist & Dervan, 1987). There have been numerous other studies on linked lexitropsins, in which the pyrrole units have been connected by various linkers such as different numbers of methylene groups, and the units have been connected by the linkers in head to head and head to tail orientations (Lown, *et al.*, 1989; Kissinger, *et al.*, 1990; Rao, *et*

al., 1991). This has also been accomplished with imidazole-containing compounds (Lee, *et al.*, 1994b; Wyatt, *et al.*, 1994b).

1.7.4 Groove Width and Lexitropsin Binding

Although many of the X-ray and NMR studies of distamycin show a single drug molecule occupying the narrow minor groove of AT-rich binding sites, there has been high-field NMR evidence that two distamycin molecules can bind in an antiparallel, side by side dimeric motif at higher drug: DNA ratios (Pelton & Wemmer, 1989; Fagan & Wemmer, 1992). The work offered a rationale for the previously unexplained binding properties of several analogues synthesised and studied by Dervan and coworkers. Pyridine-2-carboxamide-netropsin (2-PyN, Figure 1.18), bound two very different sites, 5'-TTTTT and 5'-TGTCA (Wade & Dervan, 1987). It was found that 2-PyN bound the 5'-TTTTT site in a 1:1 complex, while the wider 5'-TGTCA site could favourably accommodate a 2:1 complex (Wade, *et al.*, 1992). The analogue 1-methylimidazole-2-carboxamide-netropsin (2-ImN, Figure 1.18) preferentially bound in a dimeric motif at the sequence 5'-TGTCA (Mrksich, *et al.*, 1992; Wade, *et al.*, 1992). Groove width proved to be the key factor in both this example and reports of dimeric binding by distamycin, where the minor groove of T tracts are much more narrow than those of mixed sequence.

These findings offered insight into the potential recognition of sequences of mixed AT/GC composition by designed oligopeptides that could bind in a dimeric motif. A series of 2-PyN linked dimer analogues (Figure 1.18) were synthesised that were covalently linked through the central pyrrole-N1 positions by methylene linkers (Dwyer, *et al.*, 1993; Mrksich & Dervan, 1993b). Covalently linking the peptides increased the binding affinity for the dimeric site 5'-TGTCA, relative to the monomeric site 5'-TTTTT, by over 25-fold.

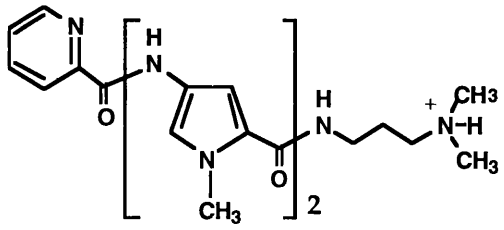

2-PyN

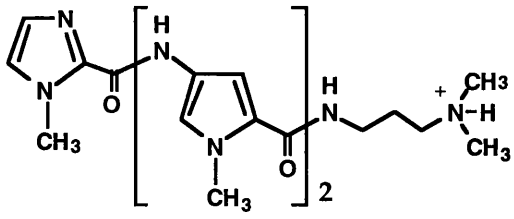

2-ImN

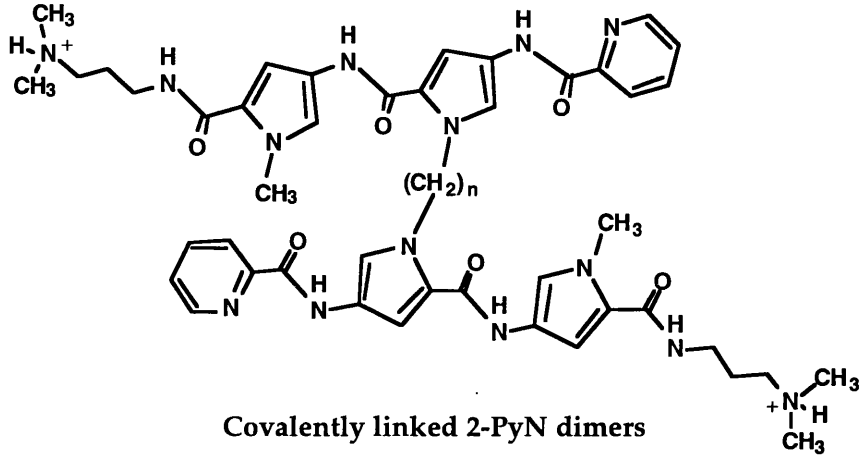

Covalently linked 2-PyN dimers

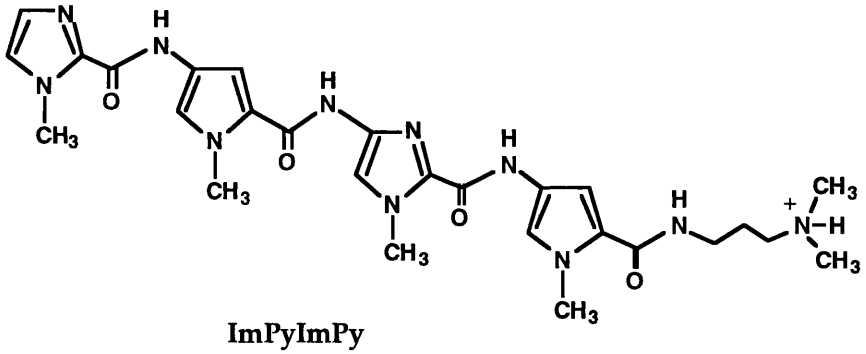

ImPyImPy

Figure 1.18 Designed dimeric-binding peptides.

It was also discovered that a tripyrrole distamycin analogue and the above mentioned 2-ImN bound the sequence 5'-TGTTA in an antiparallel heterodimeric fashion (Mrksich & Dervan, 1993a). Covalently linking the 2-ImN and distamycin analogue via a methylene linker produced a peptide heterodimer that bound the 5'-TGTTA site with a 3-fold higher affinity than the 5'-TGTCA site (Mrksich & Dervan, 1994). Covalent heterodimers have also been designed and synthesised that are linked in a head to tail fashion and bind as antiparallel dimers in a "hairpin" motif (Mrksich, *et al.*, 1994). The recognition of a GC-rich sequence has also been accomplished with a peptide designed to bind in a dimeric motif. The alternating ImPyImPy

analogue (Figure 1.18) was found to bind as an antiparallel dimer in the minor groove of the six base pair site 5'-(A.T)GCGC(A.T)-3' (Geierstanger, *et al.*, 1994b; Mrksich & B., 1995).

1.8 Lexitropsin Derivatives as DNA Vectors for Reactive Groups

There are numerous examples in the literature of agents which utilise the framework of distamycin as a DNA binding vector, to which a further group or groups can be attached. Examples of such groups include different types of DNA cleaving and alkylating groups (see below), intercalating groups such as ellipticine and acridines (Bailly & Henichart, 1994), the metal chelating domain of bleomycin (Owa, *et al.*, 1992; Huang, *et al.*, 1995), enediyne groups (Xie, *et al.*, 1993; Wittman, *et al.*, 1995), *o*-carborane groups designed for use in Boron neutron capture therapy (Yamamoto, *et al.*, 1995), photoactivatible groups such as psoralens (Lee, *et al.*, 1994a; Rao, *et al.*, 1994), coumarins (Hartley, *et al.*, 1994; Lee, *et al.*, 1994a), isoalloxazine (Herfeld, *et al.*, 1994), and pyrene (Hartley, *et al.*, 1995), and hypoxia-selective and radiosensitising groups such as nitroarenes and nitroimidazole (Parrick & Porssa, 1993; Jenkins, *et al.*, 1994b). These have been utilised variously as probes for DNA structure, DNA binding, and many have been screened as potential anti-cancer agents.

Attachment of an EDTA group onto distamycin analogues (Figure 1.19) creates an agent capable of producing strand breaks via the generation of hydroxyl radicals at sites of drug binding, in similar manner to that described for MPE. The first example of these 'affinity cleaving' agents were tripyrrole analogues possessing an EDTA group at either the N-terminus or C-terminus and the results from studying the affinity cleaving agents complemented the footprinting studies (Taylor, *et al.*, 1984).

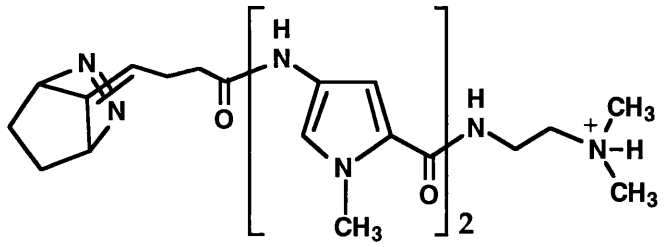

Diazene-Lexitropsin

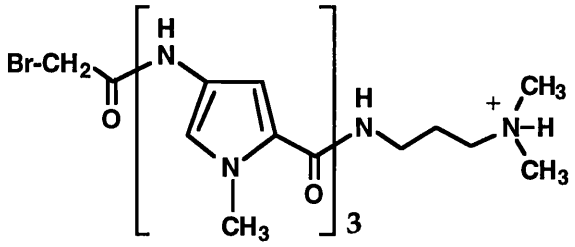

Bromoacetyl-Distamycin

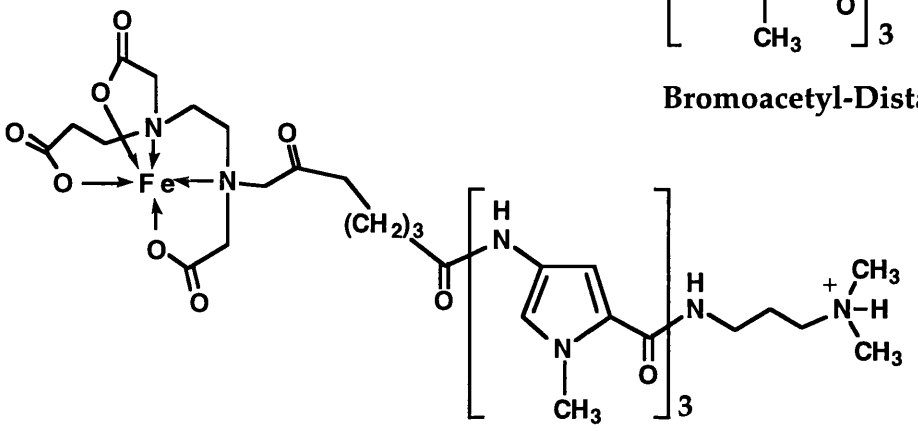

Fe(II)-EDTA-Distamycin

Figure 1.19. Diazene-lexitropsin, bromoacetyl-distamycin, and Fe(II)-EDTA-distamycin.

A simple electrophilic analogue, *N*-bromoacetyl distamycin (Figure 1.19), was shown to bind non-covalently to several AT sequences on a 157 base pair fragment identically to distamycin (Baker & Dervan, 1985; Baker & Dervan, 1989). Alkylation, however, occurred slowly in only one of the sites, at the adenine opposite the 3'-T in the sequence 5'-AGTTTA. More recently, a diazene-lexitropsin derivative has been shown to cleave DNA specifically at the preferred sites of netropsin binding, upon photoactivation (Bregant, *et al.*, 1994).

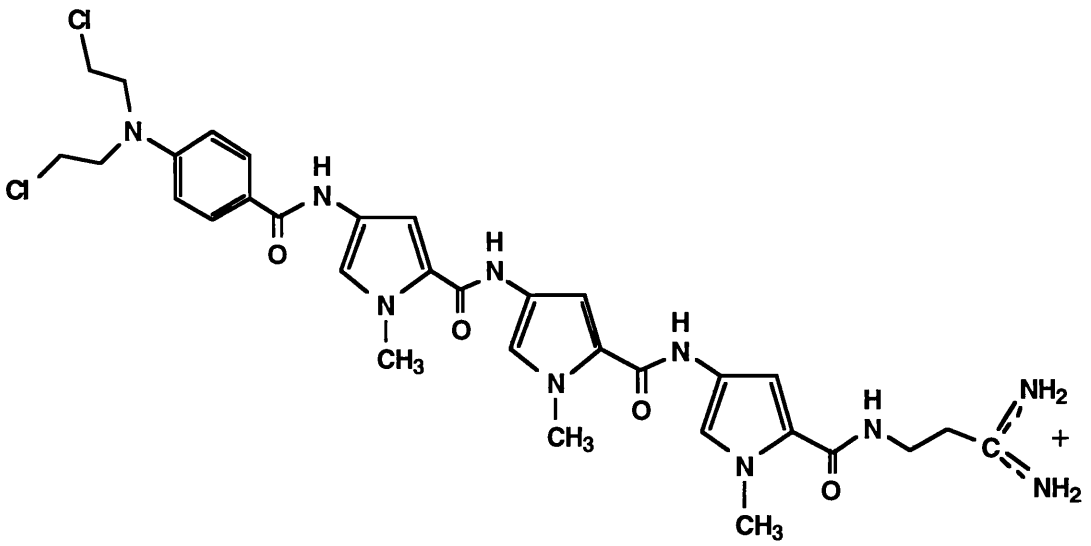

Figure 1.20. Tallimustine.

Many of the alkylating derivatives of distamycin analogues have been screened for antitumour activity. Tallimustine (FCE 24517, Figure 1.20) is a benzoic acid mustard derivative of distamycin, and was the most promising of several developed (Arcamone, *et al.*, 1989; D'Alessio, *et al.*, 1994). Studies on its mechanism of action revealed alkylation in the minor groove at selected adenines while showing no major groove guanine-N7 alkylation (Broggini, *et al.*, 1991). A footprinting study demonstrated identical binding sites to distamycin, which indicates that tallimustine has retained the preference for AT-rich sequences (Broggini, *et al.*, 1989). It is not cross-resistant with conventional nitrogen mustards, such as melphalan, but showed a cross-resistance with doxorubicin, indicating that it may possibly be susceptible to MDR (Pezzoni, *et al.*, 1991; Geroni, *et al.*, 1993). It has been shown to interfere with human ligase activity (Montecucco, *et al.*, 1991) and slowly forms covalent adducts at longer incubation times (Fontana, *et al.*, 1992). Recently, determination of the sequence specificity of alkylation using a thermal cleavage assay found that tallimustine only alkylated the 3'-adenine within the sequence 5'-TTTTPuA and a single base pair change in the consensus sequence prevented alkylation (Broggini, *et al.*, 1995). Tallimustine and distamycin have also

been shown to interfere with TATA box protein binding and *in vitro* transcription (Bellorini, *et al.*, 1995). Phase I clinical trials have now been reported (Sessa, *et al.*, 1994).

Cyclopropylcarbonyl, mono-, di-, and trichloroacetyl groups have been linked to netropsin units, but the resulting analogues demonstrated only weak cytotoxic activity and no analysis of the DNA sequence specificity of the analogues was performed (Krowicki, *et al.*, 1988). A bispyrazole analogue tethering a benzoyl nitrogen mustard (Figure 1.21) was synthesised and possessed activity *in vitro*, but was chemically unstable (Lee, *et al.*, 1991b). Dipyrrole lexitropsins were used to tether an *N*-(2-chloroethyl)-*N*-nitrosourea group (Figure 1.21), but the majority of the alkylation for the conjugates corresponded to that seen for the untethered CCNU (Church, *et al.*, 1990). The compounds also proved to be less toxic than the parent nitrosoureas (Chen, *et al.*, 1993). More recently uncharged dipyrrole lexitropsins tethering sulfonate ester groups were reported (Figure 1.21) which showed methylation at adenine sites in AT tracts (Zhang, *et al.*, 1993). The sites of methylation corresponded to the non-covalently bound sites of the drugs, as determined by footprinting. A bis-hydroxymethyl-pyrrole-oligopeptide conjugate (Figure 1.21) was shown to efficiently crosslink an oligodeoxynucleotide containing the core sequence CGAATTGC at the guanine-2-NH_2 positions (Sigurdsson, *et al.*, 1993) and was shown to have a comparable cytotoxicity to cisplatin in L1210 cells (Sigurdsson & Hopkins, 1994).

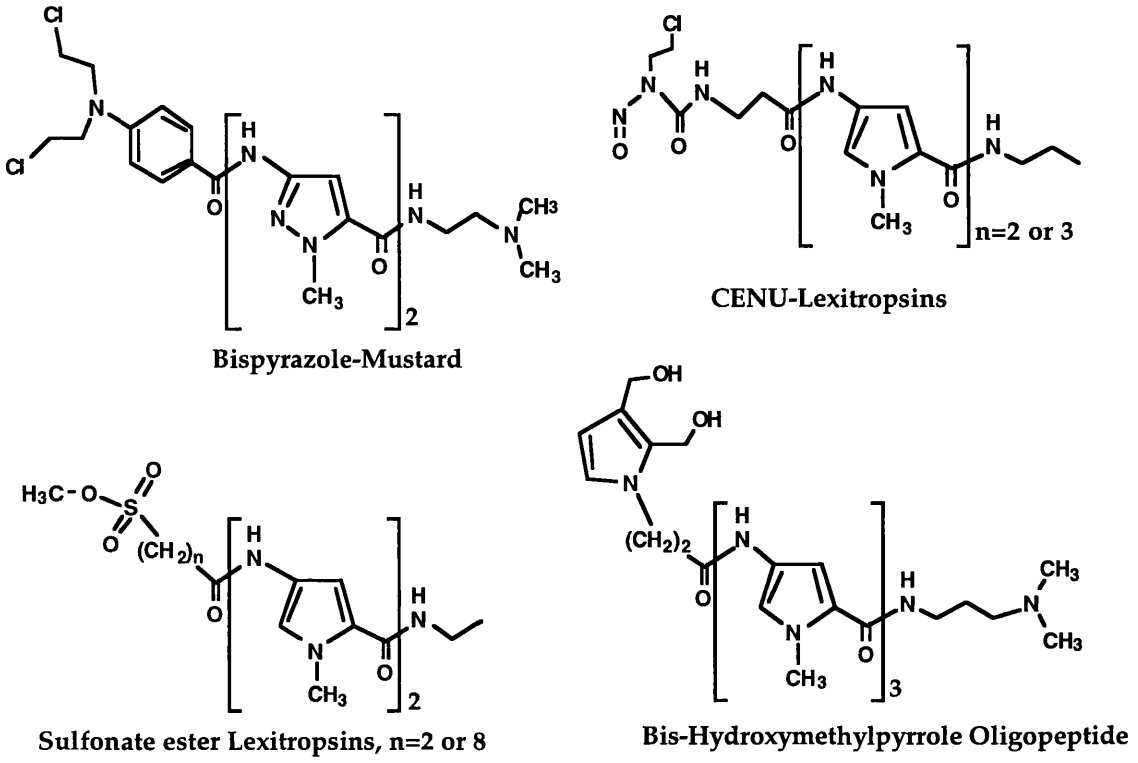

Figure 1.21. Alkylating lexitropsins.

Di- and triheterocyclic lexitropsins with mixed pyrrole/imidazole units and an N-terminal bis-(chloroethyl)amino group have recently been reported (Xie, *et al.*, 1995). However, all but one of the compounds were less active than distamycin. An analysis of the sequence specificity was reported, but the thermal cleavage assay and the piperidine cleavage assay were curiously combined into single experiments, consequently obscuring the results because there could be no discrimination between major groove and minor groove alkylation at adenines or guanines. Most recently, a novel linked bis-(dipyrrole benzoic acid mustard) lexitropsin has been reported, but the dimer was not as potent as the monomer (Chen, *et al.*, 1995).

Analogues of the Im_2 lexitropsin with various reactive groups were synthesised and evaluated for cytotoxicity (Lee, *et al.*, 1993a). The diimidazole analogues possessing either cyclopropyl, chloroacetyl, bromoacetyl groups were found to be relatively non-cytotoxic (Lee, *et al.*, 1993a). However, a benzoic acid mustard derivative was found to be cytotoxic, and additionally, a triimidazole and benzoic-acid mustard

derivative was synthesised and found to be more cytotoxic than the diimidazole derivative (Lee, *et al.*, 1993a) (Chapter Two).

1.9 Aims of the Experimental Work

Previous work with the nitrogen mustards has implicated the DNA interstrand cross-link as the critical lesion in their mechanism of cytotoxicity. Cross-link formation and subsequent removal has been shown to correlate with cell survival. The nitrogen mustards have a poor affinity for DNA and a sequence preference which is limited. Because of the weak affinity for DNA and the lack of sequence specificity, it was reasoned that tethering a nitrogen mustard functionality to a minor groove binding vector could prove beneficial. The vector could efficiently deliver the nitrogen mustard to the minor groove of DNA. The approach of utilising lexitropsins as DNA binding vectors has been attempted with several types of alkylating groups. Tallimustine's advance to clinical evaluation has demonstrated that the approach can be exploited. In all of the above mentioned studies, however, the effect of the lexitropsin on the alkylating functionality and the effect of the alkylating functionality on the lexitropsin were not examined in thorough detail.

The aims of the experimental work were to elucidate a structure-activity relationship for a series of minor groove binding lexitropsins which conjugate an aromatic nitrogen-mustard. Comparison between two aromatic nitrogen mustard groups that possess different reactivities should permit analysis of the effect of a lexitropsin portion on the reactivity and specificity of the nitrogen mustard. The heterocyclic units chosen for the lexitropsin portion in each family were either AT-recognising pyrroles or GC-recognising imidazoles. The effect of targeting different regions of DNA can thus be examined. Each family of conjugates contains a mono-, di-, and triheterocyclic conjugate. By examining conjugates which possess DNA binding vectors of increasing DNA affinity and binding site size, the effect of

targeting the nitrogen mustard in a more sequence-specific manner can be examined. In addition, the increase in the reading frame portion of the lexitropsin should allow for examination of the effect of the nitrogen mustard group on the binding specificity of the lexitropsin portion. Lastly, a half-mustard triimidazole conjugate was prepared for evaluation, in order to determine the importance of the second chloroethyl arm of nitrogen mustards when tethered to lexitropsins.

CHAPTER TWO: CYTOTOXICITY AND DNA CROSS-LINKING IN PLASMID AND CELLULAR DNA FOR THE NITROGEN MUSTARD CONJUGATES

2.1 Introduction

The lexitropsins tethering aromatic nitrogen-mustards are presented in Figure 2.1. The nitrogen-mustard chosen was either benzoic acid mustard (BAM) or chlorambucil (CHL), and was located on the N-terminus of the lexitropsin. CHL is the more reactive of the two mustards, forming cross-links more efficiently and being more cytotoxic than BAM (Sunters, *et al.*, 1992). CHL possesses an electron donating alkyl substituent *para* on the aniline to the nitrogen. BAM, however, has an electron withdrawing carboxamido group in the *para* position. In addition, the carboxamido linkage of BAM holds the benzoyl group approximately planar to the lexitropsin portion, while the chlorambucil moiety has a flexible $(CH_2)_3$ linker.

The heterocyclic units chosen for the lexitropsin portion in each family were either AT-recognising pyrroles or GC-recognising imidazoles. As mentioned earlier, the pyrrole-amide framework of distamycin provides for an AT-sequence specificity due to an avoidance of GC base pairs. The imidazole framework, however, allows for recognition of GC-rich sequences. Targeting AT- or GC-rich regions may have separate advantages or disadvantages, such as modulating transcription factor: DNA interactions (Broggini & D'Incalci, 1994), including interfering with the proteins that bind to promoter regions such as the TATA box (Chiang, *et al.*, 1994), or GC-rich regions, such as those in oncogenes (Hartley, *et al.*, 1988a; Mattes, *et al.*, 1988). The pyrrole and imidazole lexitropsins have a dimethylamino group on the C-terminus, in place of the amidinium group of netropsin and distamycin. This change was incorporated in order to facilitate synthetic preparation of the lexitropsin conjugates, because the precursors are soluble in organic solvents. The amino functionality has a pKa value of 9.3, so the

drugs remain cationic at a pH of 7. A tripyrrole distamycin analogue that possesses the C-terminal dimethylamino group substituted for the amidinium group footprinted at the same AT-rich sequences as distamycin (Wade, *et al.*, 1993).

Each family contains a mono-, di-, and triheterocyclic conjugate. Previously studied monoheterocyclic analogues possessed poor DNA affinities compared to di- and triheterocyclic lexitropsins, which occupied binding sites of four and five base pairs, respectively (Gursky, *et al.*, 1982; Lee, *et al.*, 1993c). By examining conjugates that possess DNA binding vectors of increasing DNA affinity and binding site size, the effect of targeting the nitrogen mustard can be closely examined.

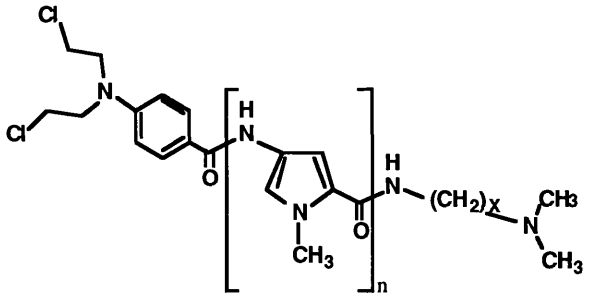

Pyrrole-BAM conjugates
BAM-(Py)$_1$, n=1, x=2, BAM-(Py)$_2$, n=2, x=3, BAM-(Py)$_3$, n=3, x=3

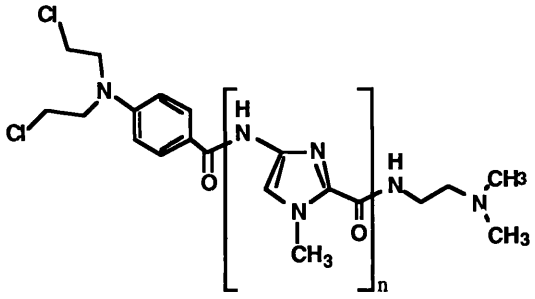

Imidazole-BAM conjugates
BAM-(Im)$_1$, n=1, BAM-(Im)$_2$, n=2, BAM-(Im)$_3$, n=3

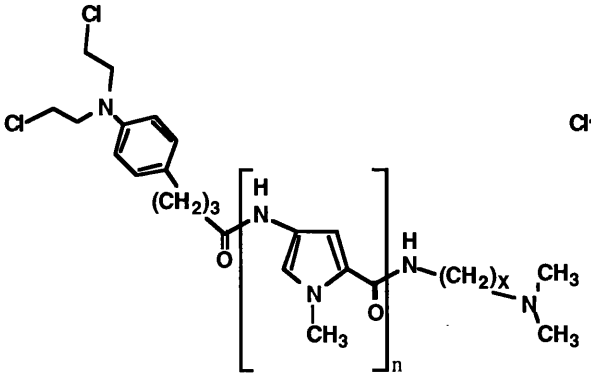

Pyrrole-CHL conjugates
CHL-(Py)$_1$, n=1, x=2, CHL-(Py)$_2$, n=2, x=2, CHL-(Py)$_3$, n=3, x=3

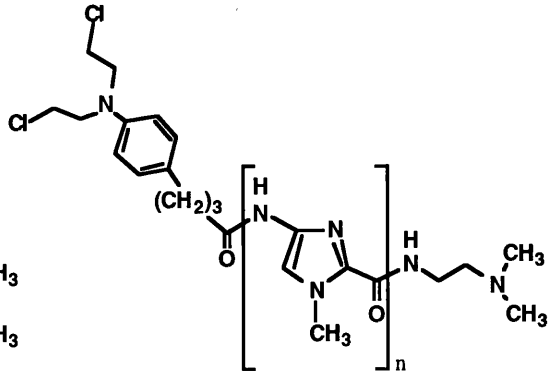

Imidazole-CHL conjugates
CHL-(Im)$_1$, n=1, CHL-(Im)$_2$, n=2, CHL-(Im)$_3$, n=3

Figure 2.1. The nitrogen-mustard lexitropsin conjugates.

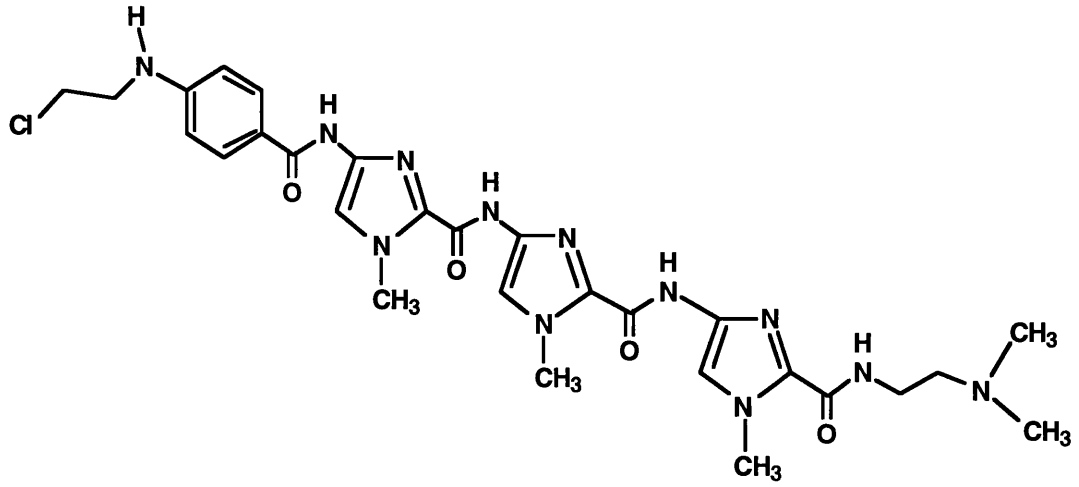

Figure 2.2. The half-mustard triimidazole conjugate.

One additional structural feature is to be examined. A half-mustard triimidazole conjugate was prepared for evaluation (Figure 2.2). The half-mustard triimidazole conjugate consists of a chloroethylamino benzamido group on the N-terminus of the triimidazole vector. Evaluation of the half-mustard conjugate should allow for an examination of the importance of bifunctionality for the nitrogen mustard group when conjugated to minor groove binding vectors.

The initial characterisation of the profiles for the series of conjugates, presented in this Chapter, was the determination of cytotoxicity and interstrand cross-linking, in plasmid and cellular DNA. The cytotoxicity was evaluated using the MTT assay (Carmichael, *et al.*, 1987; Twentyman & Luscombe, 1987). The cross-linking ability of the conjugates in plasmid DNA was determined by a neutral agarose gel assay (Hartley, *et al.*, 1991b). DNA cross-linking in cells was determined by the technique of alkaline elution (Kohn, *et al.*, 1981).

2.2 Materials and Methods

2.2.1 Materials

Drugs.

Drugs were kindly provided by Dr. Moses Lee, Department of Chemistry, Furman University, Greenville SC, USA. The synthesis and characterisation of the drugs have been reported (Lee, *et al.*, 1993a; Lee, *et al.*, 1993b; Hartley, *et al.*, 1994; Wyatt, *et al.*, 1994a). Drugs, of a minimum of 1 mg, were dissolved in DMSO and 1 molar equivalent HCl at a 10 mM stock concentration and stored at -20° C until immediately prior to use. Drug dilutions in the appropriate buffer for each experiment were prepared fresh for each experiment.

Plasmid DNA.

Plasmid pBR322 (260 μg/ml) DNA was obtained from Northumbria Biologicals (NBL) and was stored in 10 mM Tris-HCl (pH 7.8), 1 mM EDTA at -20° C.

Radioisotopes.

The following radioisotopes were purchased from Amersham International: [γ-^{32}P] ATP (5000 Ci/mmol, 10 mCi/ml) and [2-^{14}C]Thymidine: (53 mCi/mmol, 50 μCi/ml).

Chemicals.

Tris-hydroxymethyl-methylamine (Tris) and tris-hydroxymethyl-methylamine hydrochloride salt (Tris-HCl) were purchased from Sigma. Triethanolamine, MTT, and sodium hydroxide (NaOH) pellets were purchased from Aldrich. Ethylenediaminetetraacetic acid (EDTA), ethylenediaminetetraacetic acid disodium salt (Na_2EDTA), concentrated hydrochloric acid (HCl, 12 M), glacial acetic acid and dimethyl sulfoxide (DMSO) were purchased from BDH. Phosphate buffered saline tablets were purchased from Oxoid. Ultrapure agarose was purchased from Bethesda Research Laboratories (BRL).

Enzymes.

Bam H1: 8-12 units/μl in 50 mM Tris-HCl (pH 7.5), 200 mM KCl, 0.5 mM EGTA, 1 mM DTT, 0.5 mg/ml BSA, 50% (v/v) glycerol, 0.1% w/v) Triton X-100. Purchased from BRL.

T4 polynucleotide kinase (PNK): 5 units/μl in 50 mM Tris-HCl (pH 7.5), 25 mM KCl, 5 mM DTT, 0.1 μM ATP, 50% v/v glycerol, 0.2 mg/ml BSA. Purchased from BRL.

Bacterial alkaline phosphatase (BAP): 100 units/μl in 10 mM Tris-HCl (pH 8.0), 0.12 M NaCl , 50% v/v glycerol. Purchased from BRL.

Buffers.

Bam H1 (10x) buffer: 50 mM Tris-HCl (pH 8.0), 10 mM $MgCl_2$, 100 mM NaCl.

BAP (5x) buffer: 50 mM Tris-HCl (pH 8.0), 600 mM NaCl.

Forward reaction (5x) buffer: 200 mM Tris-HCl (pH 8.0), 75 mM 2-mercaptoethanol, 50 mM $MgCl_2$, 1.65 μM ATP.

Stop Solution: 0.6 M sodium acetate, 20 mM Na_2EDTA, 100 μg/ml tRNA.

TEOA buffer: 25 mM triethanolamine, 1 mM Na_2EDTA, pH 7.2.

TAE agarose gel running buffer: 40 mM Tris, 20 mM acetic acid, 2 mM Na_2EDTA, pH 8.1.

Strand separation buffer: 30% DMSO, 1 mM Na_2EDTA, 0.04% bromophenol blue and 0.04% xylene cyanol in distilled and deionized water.

Sucrose loading buffer: 0.6% sucrose, 0.04% bromophenol blue, and 0.04% xylene cyanol in distilled and deionized water.

Materials for Alkaline Elution:

Polycarbonate filters, 2 μM pore size, 25 mm diameter were obtained from Costar Nucleopore.

Sarcosyl-(N-laurylsarcosine), proteinase K and sodium chloride (NaCl) were purchased from Sigma. Tetraethylammonium hydroxide (40%, wt.) was purchased from Aldrich.

Scintillation fluid: Ecoscint A was purchased from National Diagnostics and, before use, glacial acetic acid was added for a final concentration of 0.7%, to prevent chemiluminescence in the alkaline solutions.

Sarcosyl lysis buffer: 0.2% sarcosyl(N-lauryl sarcosine), 2 M NaCl , 0.04 M Na_2EDTA, (pH 10.0). The solution was filtered before use.

Alkaline elution buffer: 5.84 g EDTA was dissolved in 35-40 ml 40% tetraethylammonium hydroxide and diluted with water to a final volume of one litre. The pH was adjusted to 12.1 by addition of small volumes of tetraethylammonium hydroxide. The solution was filtered before use.

2.2.2 Cell Culture

The K562 human myeloid leukaemia cell line (Andersson, *et al.*, 1979) was used for all experiments carried out *in vitro*. The cells were grown in suspension culture in RPMI 1640 medium supplemented with 5% foetal calf serum and 2 mM glutamine. The cells were kept at 37° C in a 5% CO_2 atmosphere in the dark and maintained at a concentration of between 5 X 10^4 and 1 X 10^6, within log phase growth. The cells were harvested by centrifugation for five minutes at 300g, 37° C, the supernatant poured off and discarded and the cells resuspended in the appropriate amount of medium for the experiment. Mycoplasm screening was performed every two months.

Labelling of the Cells with ^{14}C Thymidine for Alkaline Elution.

Cells were counted prior to labelling to ensure logarithmic growth. Cells were labelled with ^{14}C thymidine (5 µl/ml of a 3.3 µCi/ml working stock) eighteen hours before drug treatment. One hour before drug treatment, cells were spun and resuspended in fresh medium to remove unincorporated label.

Drug Treatment for Alkaline Elution.

Cells, at a concentration of 3.3-4 X 10^5/ml, were treated with drug in a volume of 8 ml for one hour at 37° C in the dark. Cells were then spun and resuspended in drug free medium and incubated for four hours at 37° C.

Irradiation for Alkaline Elution.

The cells were then placed on ice and single strand breaks introduced to the appropriate samples by X-ray irradiation (4 Gy) at 0° C. Following irradiation, the cells were diluted in 10 ml sterile, ice cold PBS.

2.2.3 MTT Cytotoxicity Assay

Cells were counted 24 hours and just prior to use to ensure cells were in logarithmic growth. The proper volume of cells for a final cell density of 1×10^4 cells per well were spun and the supernatant poured off. The cells were resuspended in fresh medium (21 ml per plate), and distributed in 2 ml aliquots per tube. Drug was then added, the tubes inverted to mix the drug and cells and left to incubate for one hour in the dark at 37° C. Following the incubation, the cells were spun at 300g for five minutes, and the medium removed. The cells were resuspended in 2 ml fresh medium, then plated out in a 96-well round bottom plate, 8 wells per sample, 200 µl per well. The plates were left to incubate for three days in the dark at 37° C in a humidified atmosphere. After three days, 20 µl of a 5 mg/ml solution of MTT in sterile PBS was added to each well and the plates were left to incubate at 37° C for a further five hours. The plates were spun at 300g for five minutes to pellet the dye at the bottom of the well. The medium was removed with care being taken not to disturb the pellet and leaving 10 to 20 µl in the well. DMSO (200 µl) was added to each well and the pellet was carefully and completely dissolved in the solvent, so that there were no air bubbles in the wells. The absorption spectra of the wells were collected on a Dynatech MR 700 Microplate Reader. The absorbance readings, an average of the eight wells per sample, were then plotted as percentage of control untreated cells to determine the IC_{50} for each drug.

2.2.4 Plasmid DNA Preparation

Linearization of plasmid pBR322 DNA.

The closed circular plasmid pBR322 DNA (20 µg) was linearised with Bam H1 in its buffer for one hour at 37° C. Following the incubation the DNA was precipitated by addition of one tenths volume 3 M sodium acetate and 3 volumes of 95% ethanol. The samples were chilled in a dry ice/ethanol

bath for ten minutes and then spun in a microfuge for ten minutes at 13000 rpm. After centrifugation, the supernatant was removed and the DNA pellet lyophilised to remove all ethanol. The DNA pellet was resuspended in distilled and deionized water (40 µl).

Dephosphorylation of the linear DNA.

The DNA (20 µg) was dephosphorylated with bacterial alkaline phosphatase for one hour at 65° C in its buffer, and in a final volume of 100 µl. Following the incubation, one volume of phenol was added, vortexed thoroughly and spun for five minutes at 13000 rpm in a microfuge. The organic layer was removed, and the aqueous layer washed twice with 100 µl aliquots of 24:1 chloroform/isoamyl alcohol. The organic layers were back extracted with a 50 µl aliquot of distilled water, the aqueous layers were combined and the DNA precipitated as described above.

5'-end labelling of the dephosphorylated DNA with [γ-^{32}P]ATP.

The DNA was 5'-end labelled with T4 polynucleotide kinase, [γ-^{32}P]ATP (10 µCi), and forward reaction buffer (20 µl final volume) at 37° C for 30 minutes. Following incubation, the DNA was precipitated with one volume of 7.5 M ammonium acetate and three volumes 95% ethanol. The DNA was chilled and spun as described above. The supernatant was removed and the DNA pellet resuspended in 50 µl of distilled and deionized water. The DNA was precipitated with 5 µl of 3 M sodium acetate and 165 µl 95% ethanol, then chilled and spun. After removing the supernatant, the pellet was dried by lyophilisation.

2.2.5 Agarose Gel Cross-Link Assay

Drug: DNA reactions.

Approximately 100 ng of 5'-end labelled DNA was used for each experimental point. Drug dilutions from the stock were in TEOA buffer. Reactions with drug were performed in TEOA buffer at 37° C for the times given and terminated by addition of an equal volume of stop solution,

followed by three volumes of 95% ethanol. The samples were chilled and spun, the supernatant was removed, and 75 µl of 70% ethanol added. The samples were spun for another ten minutes, the supernatant removed and the DNA pellets dried by lyophilisation. Samples were resuspended in 10 µl of strand separation buffer, then heated to 90° C for two minutes and immediately placed on ice. The non-denatured control was taken up in 10 µl of sucrose loading buffer and not heated.

Electrophoresis and Quantitation.

The samples were loaded onto a 0.8% agarose gel (25 x 20 x 1 cm) and electrophoresed for 15 hours at 40 volts. After electrophoresis the gel was placed onto a sheet of Whatman filter paper and a sheet of 3 mm filter paper. The gels were dried on a BioRad 5850 gel dryer and X-ray film (hyperfilm, Amersham) exposed to the gel. Densitometry was carried out on a BioRad GS-670 densitometer interfaced with a 7100/60 PowerPC.

2.2.6 Alkaline Elution

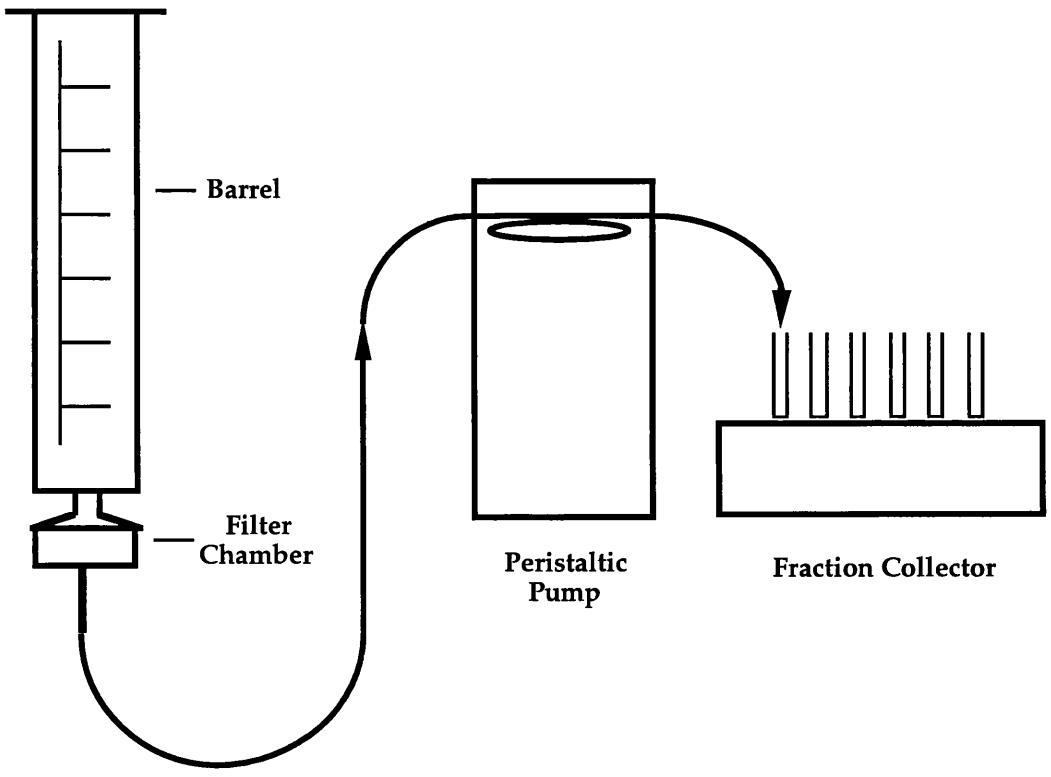

Figure 2.3. Schematic representation of the alkaline elution apparatus.

Elution preparation.

The filters were mounted in the filter chambers and, with the funnel in place on a vacuum flask, 10 ml of ice cold PBS was added to the barrel (Figure 2.3). The air from the filter chamber was evacuated by filling it with solution using a 1 ml pipette. When half of the PBS had flowed through, the vacuum was stopped and the cells were added. The number of cells loaded onto each filter was approximately 0.6-0.8 X 10^6. The funnels were protected from light and the solution was allowed to drip under gravity until the flow had stopped. The cells were lysed with 5 ml of lysis buffer by very carefully adding the first 2 ml directly to the filter chamber with a 1 ml pipette. The filters were protected from light and the lysis solution was allowed to drip by gravity into 20 ml polypropylene scintillation vials (L.I.P.). The tubes from the pump were then connected to the needle. A ProK solution of 2 ml (0.5 mg/ml in elution buffer) was very carefully added to the filter chamber, followed by addition of 40 ml of the alkaline elution buffer to the barrel.

Elution and workup.

Elution occurred over fifteen hours, with the pumps calibrated to elute through 2 ml an hour, and fractions of 6 ml were collected every three hours. When the elution was complete fractions were transferred to scintillation vials. After fifteen hours, the elution buffer remaining in each funnel was discarded and the pump run to collect the solution remaining in the line and filter chamber in a new fraction. The filters were then removed and placed in scintillation vials to which 0.4 ml 1 N HCl was added. The vials were sealed and heated in an oven at 60° C for 1 hour to depurinate the DNA. At the end of the hour, 2.5 ml 0.4 M NaOH was added and the vials left to cool for 1 hour. The line tubing and funnels were washed through with 10 ml 0.4 M NaOH, which was collected as a separate fraction.

A 2 ml aliquot of the lysis solution, 2.5 ml of the wash and all of the other fractions collected were transferred to 20 ml polypropylene scintillation vials. Water was added to the lysis solution, the wash and the filters to give a final volume of 6 ml. The fractions were then mixed with 10 ml Ecoscint A scintillation fluid and the radioactivity counted on a Beckman LS1800 scintillation counter. The values were plotted as fraction of DNA remaining on a log scale versus time to produce the elution profiles. The cross-link index for the drugs at the doses studied were calculated using the formula

$$XLI = \sqrt{[(1-R_0)/(1-R)]} - 1$$

where R_0 and R are the relative retention values at 12 hours for the control and drug samples, respectively.

2.3 Results

2.3.1 Cytotoxicity

The cytotoxicity of each conjugate was determined on the K562 human myeloid leukaemia cell line for a one hour exposure to drug. Following drug exposure, the cells were resuspended in drug-free medium and allowed to grow for three days, at the end of which the MTT was added. Following a five hour incubation period to allow the MTT to be metabolised, the dye was pelleted and the supernatant removed. The pellets were dissolved in DMSO and the absorbance measured. The absorbance, an average of eight wells per lane, was plotted as a percentage of the absorbance of the control untreated lane. A representative plot of percent absorbance versus concentration is shown for BAM and CHL in Figure 2.4. The IC_{50} values are extrapolated from the plots where the absorbance percentage has been reduced by half. The IC_{50} values for the BAM and CHL conjugates are shown in Table 2.1 and 2.2, and are an average of three independent experiments for each drug. Distamycin and the Im_3 lexitropsin showed little cytotoxicity at concentrations up to 600 μM and 500 μM, respectively,

under these conditions. In agreement with previous studies on distamycin, an alkylating functionality is required for appreciable cytotoxicity with this class of minor groove-binding agent.

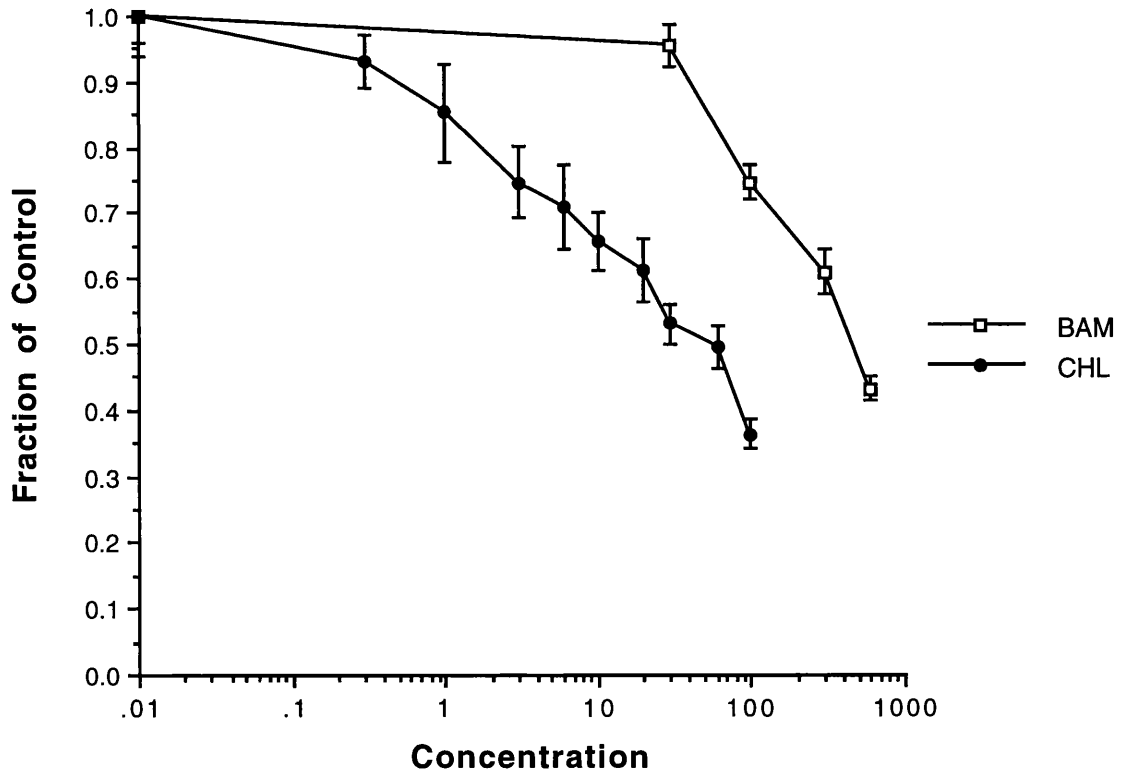

Figure 2.4. Plot of the absorbance as a fraction of the control versus the drug concentration on a log scale for BAM and CHL.

The BAM Conjugates.

Under these conditions, BAM had an IC_{50} value of 500 μM (Table 2.1). The BAM conjugates were more cytotoxic than BAM and showed a clear increase in cytotoxicity for each increase in the number of pyrrole or imidazole units. The monoimidazole conjugate showed a modest improvement over BAM of approximately 3.5-fold, while the monopyrrole conjugate's IC_{50} value was 10-fold lower than BAM. The di- and triheterocyclic conjugates were significantly more cytotoxic than BAM or the monoheterocyclic conjugates. The dipyrrole conjugate was 25-fold more cytotoxic than BAM and the diimidazole conjugate was over 40-fold more cytotoxic. The triheterocyclic analogues were the most cytotoxic in each family. The tripyrrole conjugate was over 50-fold more cytotoxic than BAM and the triimidazole conjugate was approximately 500-fold more cytotoxic than BAM. Comparison between the imidazole and pyrrole families reveal that, while the monopyrrole conjugate was more cytotoxic than the monoimidazole conjugate, the di- and triimidazole conjugates were more cytotoxic than their corresponding pyrrole conjugates. The triimidazole conjugate was the most cytotoxic of all the BAM conjugates. The cytotoxicity of tallimustine (FCE 24517) was determined under identical conditions, and its IC_{50} value was 5 μM (Table 2.1). This value was slightly lower than the tripyrrole-BAM conjugate, from which it only differs in the substitution of the dimethylaminopropyl group instead of the amidinium group on the C-terminus. The half-mustard imidazole conjugate was inactive in the dose range studied, up to 100 μM (Table 2.1).

Compound	IC_{50} (μM)	Compound	IC_{50} (μM)
BAM	500		
BAM-$(Py)_1$	50(±5)	BAM-$(Im)_1$	140(±20)
BAM-$(Py)_2$	20(±2)	BAM-$(Im)_2$	12(±1)
BAM-$(Py)_3$	9(±0.5)	BAM-$(Im)_3$	1(±2)
FCE 24517	5(±1)	Half-$(Im)_3$	>100

Table 2.1. The IC_{50} values for BAM and the BAM conjugates determined on the K562 cell line following a one hour exposure to drug. Errors represent the average of three independent experiments.

Compound	IC_{50} (μM)	Compound	IC_{50} (μM)
CHL	70(±10)		
CHL-$(Py)_1$	13(±2)	CHL-$(Im)_1$	>150
CHL-$(Py)_2$	6(±2)	CHL-$(Im)_2$	21(±2)
CHL-$(Py)_3$	5(±1)	CHL-$(Im)_3$	9(±1)

Table 2.2. IC_{50} values for CHL and the CHL conjugates determined on the K562 cell line following a one hour exposure to drug. Errors represent the average of three independent experiments.

The CHL Conjugates.

The cytotoxicity values for the CHL conjugates were determined utilising the procedure described above and are presented in Table 2.2. Under these conditions, the parent mustard CHL had an IC_{50} value of 70 μM. The CHL conjugates were more cytotoxic than the parent mustard, with the exception of the monoimidazole conjugate. For each increase in the number of heterocyclic units there was an increase in the cytotoxicity. These differences, however, were not as marked as those seen for the BAM conjugates. The monoimidazole conjugate showed no activity at the highest dose studied of 150 μM, but the di- and triimidazole conjugates were more cytotoxic than the parent mustard, by approximately 3-fold and 7-fold, respectively. Each of the pyrrole conjugates were more cytotoxic than CHL itself and the differences were not as great with each increase from one to three pyrrole units, between 5-fold and 14-fold. Comparison between the imidazole and pyrrole families shows that the pyrrole conjugates were more cytotoxic than the corresponding imidazole conjugates. The tripyrrole conjugate was the most cytotoxic of the CHL conjugates.

2.3.2 Interstrand Cross-Linking in Plasmid DNA

The DNA cross-linking ability of each analogue was evaluated using an agarose gel cross-link assay. The presence of a cross-link between the two DNA strands prevents complete separation of the strands upon denaturation such that the cross-linked DNA reanneals in a neutral agarose gel to run as double-stranded (Hartley, *et al.*, 1991b). Quantitation of the amount of the double-stranded versus single-stranded DNA gives a measure of the extent of cross-linking in a given DNA sample. The drug: DNA incubations were for two hours at 37° C and a representative gel is shown in Figure 2.5. In the gel shown, a dose dependent increase in the cross-linking by CHL is evident (lanes c-e), such that at 100 μM (lane e), a significant portion of the DNA is cross-linked and runs as double-stranded.

The cross-linking results for all of the conjugates are summarised in Tables 2.3 and 2.4. The tables show the cross-linking for each of the analogues at a dose range of 1, 10, and 100 μM.

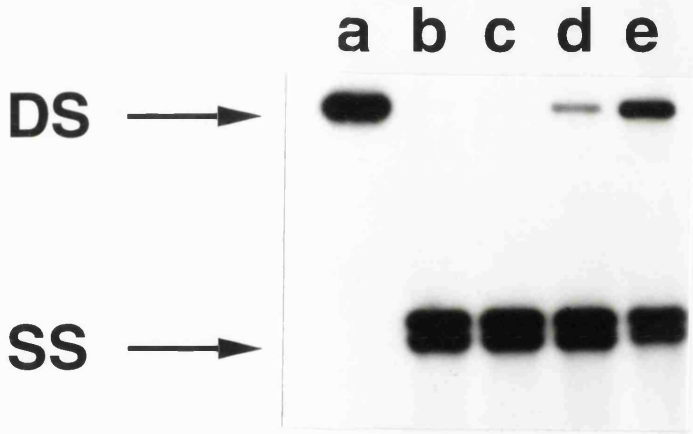

Figure 2.5. Agarose gel showing the dose-dependent cross-link formation by CHL following a two hour exposure to drug at 37° C. Lane a, double stranded control; lane b, denatured control; lane c, CHL, 1 μM; lane d, CHL, 10 μM; lane e, CHL, 100 μM.

The BAM Conjugates.

The BAM conjugates cross-linked DNA poorly, even at doses as high as 100 μM (Table 2.3). This is in agreement with BAM, which also cross-links DNA poorly. Furthermore, the cross-linking ability of the BAM conjugates did not improve with the increase in number of heterocyclic units. The monopyrrole-BAM conjugate showed an elevated cross-linking ability compared to BAM and the dipyrrole- and tripyrrole-BAM conjugates at the highest dose. The di- and tripyrrole conjugates, however, showed only a slight improvement compared to BAM and very low level of cross-link formation overall. The pattern of results was seen with the imidazole conjugates. The monoimidazole-BAM conjugate showed significant cross-linking at the highest dose used, but the di- and triimidazole conjugates showed a very low level of cross-linking at the doses studied. The gel in Figure 2.6 shows the cross-linking efficiency for the tripyrrole-BAM and tripyrrole-CHL conjugates at doses of 0.1, 1, and 10 μM for two hours. The tripyrrole-CHL conjugate clearly shows cross-link formation while the tripyrrole-BAM conjugate shows little evidence of cross-link formation.

The effect of increasing the incubation time on the cross-linking ability of the mono-, di-, and tripyrrole-BAM conjugates was studied and at a dose of 5 μM, the cross-linking ability was not affected by incubation times of up to five hours. It should be noted that the concentration of 5 μM and incubation conditions of five hours at 37° C were those used to determine the sequence specificity of alkylation, presented in Chapter Three. It appears that the increase in the DNA binding portion does not offer an increase in cross-linking ability for the BAM conjugates.

Compound	Cross-linking (%)		
	1 μM	10 μM	100 μM
BAM	0	0	0[a]
BAM-$(Py)_1$	0	0	24
BAM-$(Py)_2$	0	9	5
BAM-$(Py)_3$	0	7	2
BAM-$(Im)_1$	0	12	53
BAM-$(Im)_2$	0	0	5
BAM-$(Im)_3$	0	0	5

Table 2.3 Percent cross-linking for the BAM conjugates at the doses listed following a two hour exposure to drug at 37° C. [a]Little cross-linking was seen for BAM at doses as high as 1 mM.

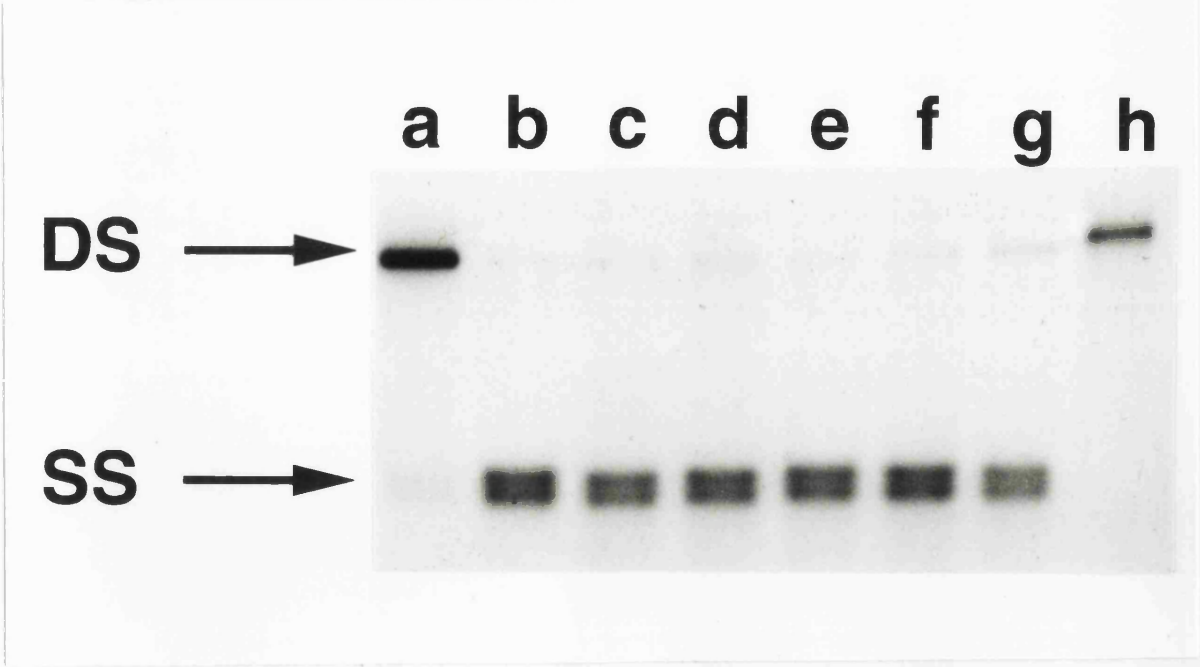

Figure 2.6 Agarose gel showing the cross-link formation for the tripyrrole-BAM and tripyrrole-CHL conjugates. Lane a, double-stranded control; lane b, single-stranded control; lanes c-e, BAM-$(Py)_3$, 0.1 μM, 1 μM, 10 μM; lanes f-h, CHL-$(Py)_3$, 0.1 μM, 1 μM, 10 μM.

The CHL Conjugates.

CHL demonstrates an improved cross-linking ability compared to BAM. This is presumably a result of its higher reactivity. It is clear from the data in Table 2.4 that each of the mono-, di-, and triheterocyclic-CHL conjugates showed an increased cross-linking ability in comparison to the parent mustard CHL. This difference was more pronounced with the pyrrole conjugates, where the dose required to induce cross-linking was greater than 10-fold lower than that required by CHL. The imidazole conjugates show a slight increase in the efficiency of cross-linking with each increase in the number of imidazole units, but the pyrrole conjugates show little difference in cross-linking ability. An agarose cross-link gel showing the time course of cross-link formation for the tripyrrole and triimidazole-CHL conjugates is shown in Figure 2.7. It appears that the cross-linking for the tripyrrole-CHL conjugate occurs rapidly, while the cross-linking for the triimidazole-CHL conjugate rises at a more steady rate (Figure 2.8).

Compound	Cross-linking (%)		
	1 μM	10 μM	100 μM
CHL	0	15	45
CHL-$(Py)_1$	24	100	100
CHL-$(Py)_2$	28	100	100
CHL-$(Py)_3$	23	100	100
CHL-$(Im)_1$	nd	36	100
CHL-$(Im)_2$	4	43	100
CHL-$(Im)_3$	17	64	100

Table 2.4. Percent cross-linking for the CHL conjugates at the doses listed following a two hour exposure to drug at 37° C. nd= not determined.

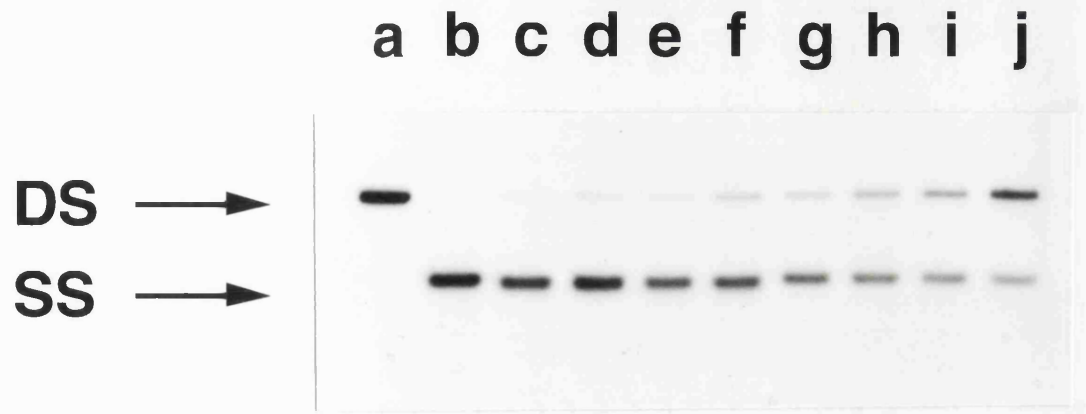

Figure 2.7. Agarose cross-link gel showing the time course of cross-link formation for the triimidazole- and tripyrrole-CHL conjugates. Reactions were carried out at 37° C for the times listed. Lane a, double-stranded control; lane b, single-stranded control; lanes c-f, CHL-$(Py)_3$, 2.5 μM, and lanes g-j, CHL-$(Im)_3$, 5 μM; 20, 40, 60, and 120 minutes, respectively.

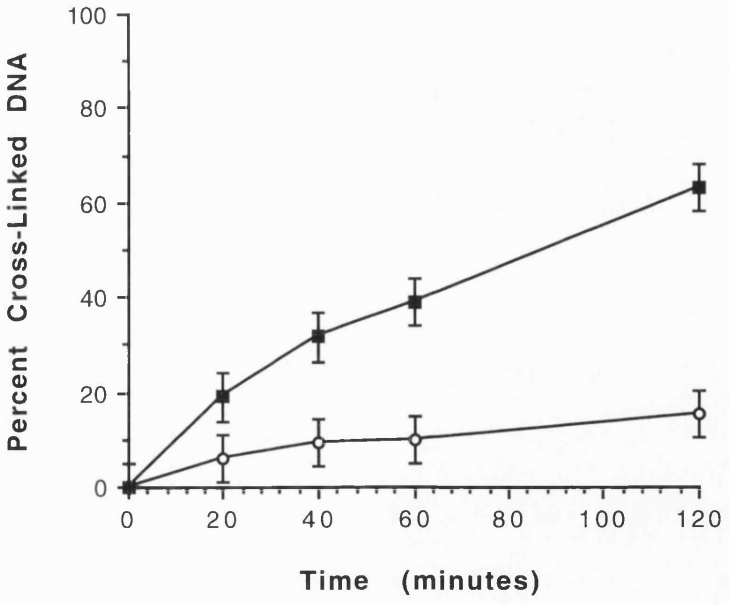

Figure 2.8. Plot of the percent cross-linked DNA versus time for the triimidazole- and tripyrrole-CHL conjugates, taken from the gel in Figure 2.7. Square represents the CHL-$(Im)_3$ conjugate and circle represents the CHL-$(Py)_3$ conjugate.

2.3.3 DNA Interstrand Cross-linking in Cells

The conjugates were examined for their DNA cross-linking ability in cells by the method of alkaline elution. The cells were labelled with ^{14}C thymidine prior to drug treatment, and the drug incubation was for one hour followed by a four hour post-incubation period. The cells were then placed on ice and strand breaks were introduced to half of the samples through X-ray irradiation. The samples were lysed on two micron filters, and the DNA eluted with an alkaline buffer which denatures the DNA. Unirradiated DNA is mostly retained on the filter, while DNA containing random strand breaks elutes through the filters more rapidly and at a constant rate. The presence of DNA interstrand cross-links in irradiated samples, however, retards the DNA in comparison to the irradiated controls. All eluted fractions are collected, recorded by scintillation counting, and the numbers, two averaged per data point, plotted on a log scale of percentage of DNA retained on filter versus elution time. The graph for the unirradiated control should show little decrease versus time, while the graph for the irradiated controls should show a steady decrease. If there are cross-links present in the irradiated, drug-treated samples, then there should be an increase in the graph relative to the irradiated controls. If the drug induces strand breaks, then the graph of the unirradiated, drug-treated samples should show a decrease relative to the unirradiated controls. The time point at 12 hours was used to determine the cross-link index for each drug.

The BAM Conjugates.

The alkaline elution profile for the monopyrrole-BAM conjugate, shown in Figure 2.9, shows that at a dose of 50 μM, its IC_{50} value, no evidence of cross-link formation was seen. The graph for the tripyrrole-BAM conjugate (Figure 2.10a) does not show any cross-link formation at either a 5 μM dose or a 50 μM dose, greater than five times its IC_{50} value.

The triimidazole-BAM conjugate (Figure 2.10b), at a dose of 3 μM (three times its IC_{50} value), does not show cross-link formation. The pattern was the same with the diheterocyclic conjugates, with neither the pyrrole or imidazole conjugate showing any evidence of cross-linking at doses equal to or greater than their IC_{50} values. The results are in agreement with the studies in plasmid DNA, in that the BAM conjugates do not demonstrate a significant cross-linking ability. It should also be noted that the BAM conjugates did not appear to produce strand breaks, as evidenced by the similar elution profiles for the unirradiated control and drug treated samples.

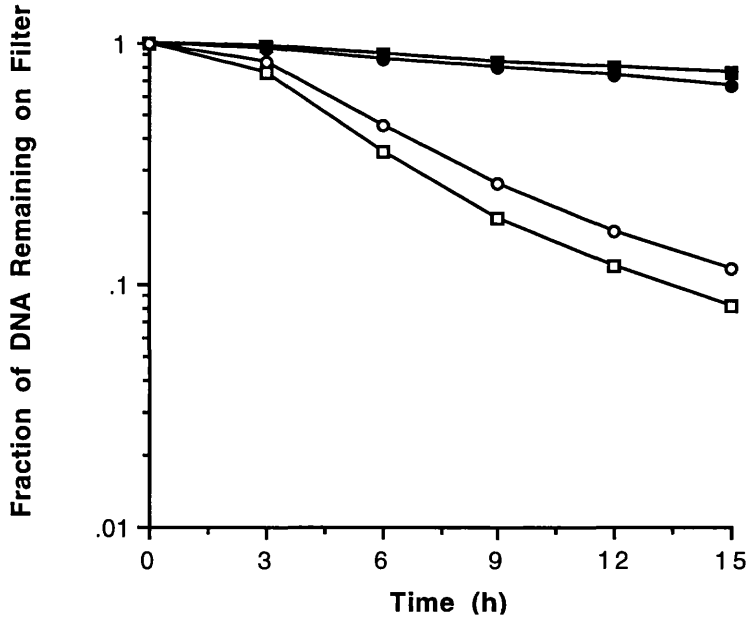

Figure 2.9. Alkaline elution profile for the monopyrrole-BAM conjugate. Drug treatment was for one hour, followed by a four hour post-incubation period in drug-free medium. Unirradiated control (■), irradiated control (□), BAM-$(Py)_1$, 50 μM dose, unirradiated (●) and irradiated (○).

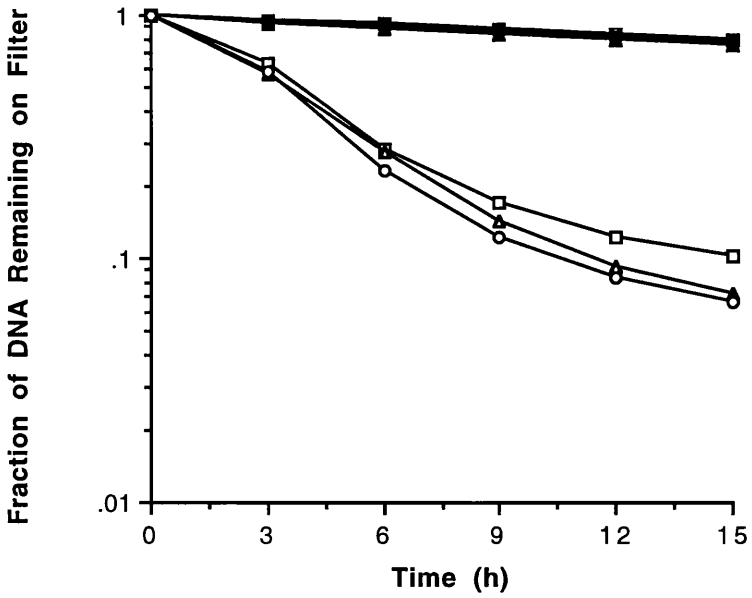

Figure 2.10a. Elution profile for the tripyrrole-BAM conjugate. Drug treatment was for one hour, followed by a four hour incubation period in drug-free medium. Unirradiated control (■), irradiated control (□), BAM-$(Py)_3$, 5 μM dose, unirradiated (●) and irradiated (○), BAM-$(Py)_3$, 50 μM dose, unirradiated (▲) and irradiated (△).

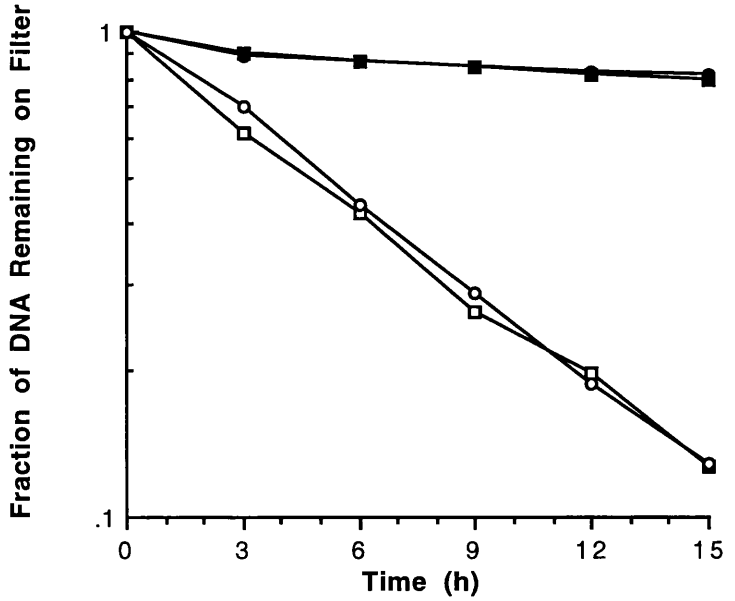

Figure 2.10b. Alkaline elution profile of the triimidazole-BAM conjugate. Drug treatment was for one hour, followed by a four hour incubation period in drug-free medium. Unirradiated control (■), irradiated control (□), BAM-$(Im)_3$, 3 μM dose, unirradiated (●) and irradiated (○).

The CHL Conjugates.

The plot for the diimidazole- and dipyrrole-CHL conjugates is shown in Figure 2.11. At a dose of 10 μM, both conjugates clearly induce significant cross-linking. The pattern was similar for the triheterocyclic conjugates, shown in Figure 2.12a and 2.12b. The plot for the tripyrrole-CHL conjugate (Figure 2.12a) shows clear evidence of cross-link formation at a dose of 5 μM, its IC_{50} value. A dose of 3 μM for the triimidazole-CHL conjugate, one third its IC_{50} value, produced significant cross-linking (Figure 2.12b). The crosslinking indices for the di- and triheterocyclic conjugates are shown in Table 2.5.

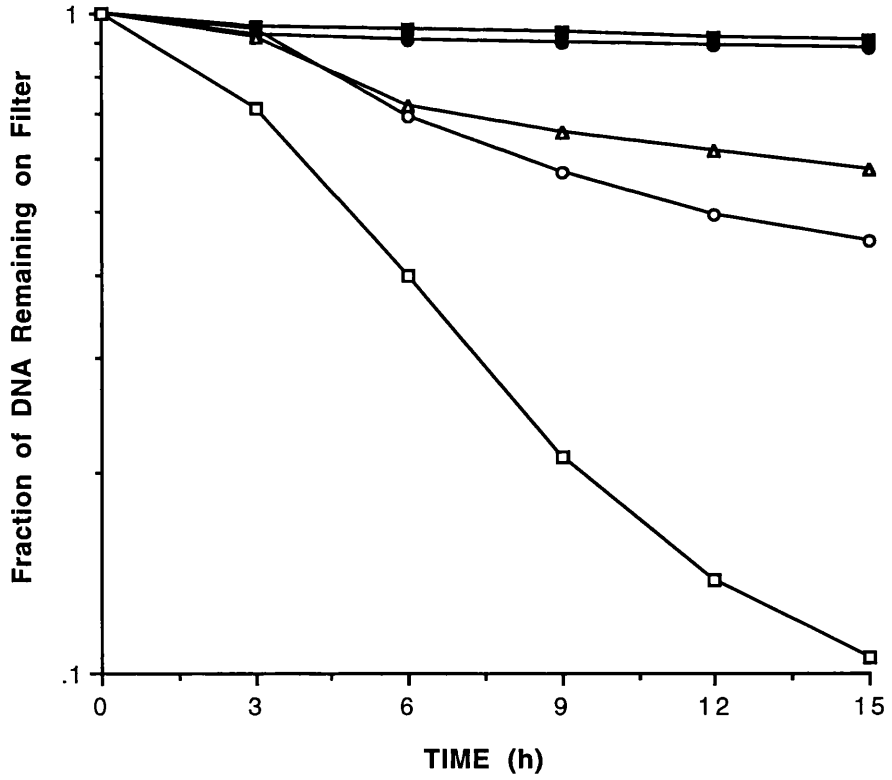

Figure 2.11. Alkaline elution profile of the diimidazole- and dipyrrole-CHL conjugate. Drug treatments were for one hour, followed by a four hour incubation period in drug-free medium. Unirradiated control (■), irradiated control (□), CHL-$(Im)_2$, 10 μM dose, unirradiated (●) and irradiated (○), CHL-$(Py)_2$, 10 μM dose, irradiated (Δ).

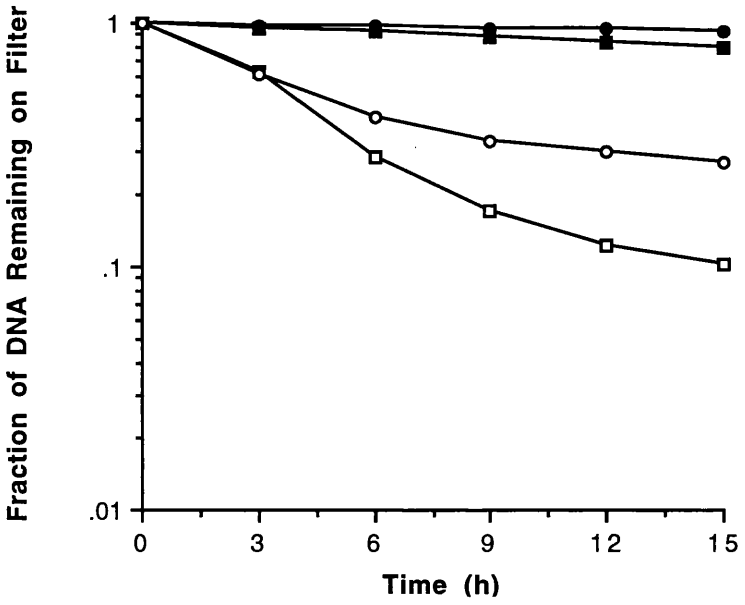

Figure 2.12a. Alkaline elution profile of the tripyrrole-CHL conjugate. Drug treatment was for one hour, followed by a four hour incubation period in drug-free medium. Unirradiated control (■), irradiated control (□), CHL-$(Py)_3$, 5 μM dose, unirradiated (●) and irradiated (○).

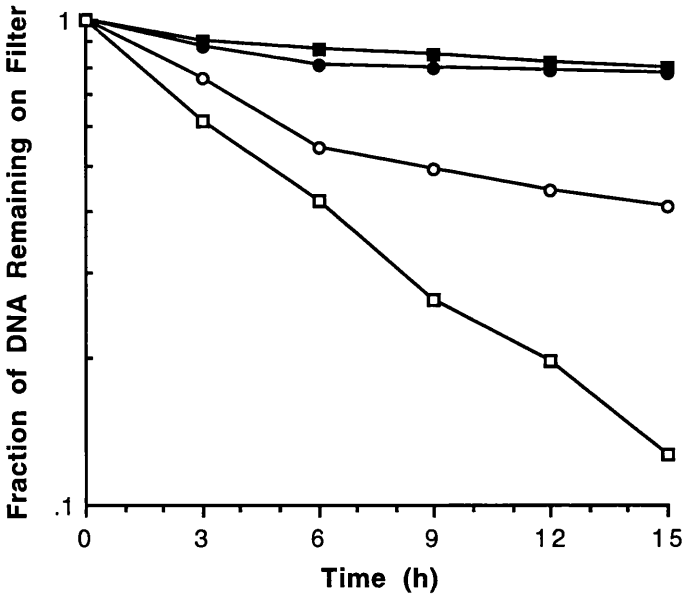

Figure 2.12b. Alkaline elution profile of the triimidazole-CHL conjugate. Drug treatment was for one hour, followed by a four hour post-incubation period in drug-free medium. Unirradiated control (■), irradiated control (□), CHL-$(Im)_3$, 3 μM dose, unirradiated (●) and irradiated (○).

Drug	IC_{50} Value (μM)	Drug Dose (μM)	Cross-link Index
BAM-$(Py)_2$	20	40	0.0
BAM-$(Im)_2$	12	10	0.0
BAM-$(Py)_3$	5	5	0.0
BAM-$(Im)_3$	1	3	0.0
CHL-$(Py)_2$	6	10	0.49
CHL-$(Im)_2$	21	10	0.31
CHL-$(Py)_3$	6	5	0.12
CHL-$(Im)_3$	9	3	0.20

Table 2.5. The cross-link indices, calculated using the formula listed in Materials and Methods, for the di- and triheterocyclic conjugates at the doses listed for the alkaline elution experiments.

2.4 Discussion

It is clear that tethering nitrogen mustards to minor groove binding vectors produces conjugates which are more cytotoxic than the parent mustards. The vectors themselves are essentially inactive, indicating that the DNA alkylating functionality is necessary for cytotoxic activity. This is in agreement with previous studies on distamycin and on netropsin derivatives that did not contain DNA-reactive groups (Debart, *et al.*, 1989). With the exception of the monoimidazole-CHL conjugate, each conjugate offered an improvement in cytotoxicity compared to the respective parent mustard. As discussed in the introduction, CHL cross-links DNA at lower doses and is more cytotoxic than BAM. Examination of the structure of CHL reveals that an electron donating alkyl substituent is *para* to the bis-(chloroethyl) nitrogen on the aniline. BAM, however, has an electron withdrawing carboxylic acid group *para* to the bis-(chloroethyl) nitrogen on the aniline group. The presence of a net-electron withdrawing group *para* to the nitrogen would destabilise the formation of the aziridinium intermediate, and presumably decelerate DNA alkylation and cross-link formation. The presence of a net-electron donating group *para* to the nitrogen would stabilise the aziridinium formation, and thus accelerate DNA alkylation and cross-link formation (Wilman & Connors, 1983).

The CHL and BAM conjugates have propyl and carboxamido groups, respectively, in the *para* position. It is presumed that similar electronic influences exist for the bis-(chloroethyl) nitrogen in each conjugate as those that act on the nitrogen of the parent nitrogen mustards. The cross-linking abilities of the conjugates resemble the parent mustards' cross-linking abilities, in that the CHL conjugates cross-link DNA at much lower doses than the BAM conjugates. The improvements in cytotoxicity in reference to the parent mustards, however, are greater for the BAM conjugates than for the CHL conjugates. Assuming the chemical reactivity of the nitrogen mustard group in the conjugates has not been altered in an unexpected

manner, the lexitropsin portions must be exerting their influence via the delivery of the nitrogen mustard groups to the DNA.

The improvement in cytotoxicity the triheterocyclic conjugates offered over the corresponding parent mustards was significant. With the exception of the pyrrole-CHL family, the triheterocyclic conjugates were the most cytotoxic for each family. The trend in the cytotoxicity seen within each family corresponded to the increase from one to three heterocyclic units. This was clearly evident for the BAM conjugates. The increase in the number of imidazole units from one to three in the previously mentioned formamido-imidazole lexitropsins provided an increase in the non-covalent DNA binding affinity (Lee, *et al.*, 1993c). Knowledge concerning the non-covalent DNA binding affinities for each of the conjugates, therefore, is helpful in determining the importance of the lexitropsin portion and its affinity for DNA.

The non-covalent DNA binding affinities for each of the conjugates were determined by Moses Lee and coworkers at Furman University, utilising an ethidium displacement assay and have been published (Lee, *et al.*, 1993a; Lee, *et al.*, 1993b; Wyatt, *et al.*, 1994a). The principle feature of the assay is the measurement of the fluorescence of ethidium bromide, which is enhanced approximately 25-fold when intercalated into DNA (Morgan, *et al.*, 1979). Displacement of the ethidium by another drug's binding will lower the fluorescence. The binding constants of the titrated drugs can be estimated and compared by measuring the loss of ethidium fluorescence as a function of the added drug. The drug concentration which produces a 50% reduction of fluorescence is approximately inversely proportional to the apparent binding constant (Debart, *et al.*, 1989). The apparent binding constant provides an indication of the non-covalent binding affinity.

Compound	DNA			
	Calf Thymus	T4	poly(dA.dT)	poly(dG.dC)
Distamycin	7.7	6.5	350	2.0
BAM-$(Py)_1$	2.4	4.7	3.1	1.5
BAM-$(Py)_2$	15	33	71	11
BAM-$(Py)_3$	37	87	71	26
CHL-$(Py)_1$	3.5	5.7	2.8	1.9
CHL-$(Py)_2$	47	nd	40	26
CHL-$(Py)_3$	21	58	25	21

Table 2.6. Estimated DNA binding constants for distamycin and the pyrrole conjugates (K_{App}, $\pm 0.5X10^5M^{-1}$). nd= not determined.

Compound	DNA			
	Calf Thymus	T4	poly(dA.dT)	poly(dG.dC)
Im_3	7.7	3.3	4.8	5.3
BAM-$(Im)_1$	4.6	2.4	4.8	4.6
BAM-$(Im)_2$	4.6	2.4	4.8	4.6
BAM-$(Im)_3$	5.9	1.7	9.5	5.0
Half-$(Im)_3$	23	39	5.5	9.0
CHL-$(Im)_1$	0.11	0.05	0.06	0.06
CHL-$(Im)_2$	0.11	0.13	0.11	0.13
CHL-$(Im)_3$	0.22	0.19	0.13	0.16

Table 2.7. Estimated DNA binding constants for the Im_3 lexitropsin and the imidazole conjugates (K_{App}, $\pm 0.5X10^5M^{-1}$).

The binding constants for the conjugates are presented in Table 2.6 and 2.7. The binding affinities for each drug were determined on four representative DNAs: calf thymus DNA, T4 DNA, and the synthetic poly(dA.dT) and poly(dG.dC) DNA. T4 DNA has an obstructed major groove due to the α-glycosylation of the cytosines and interaction with this DNA infers minor groove binding. Each of the conjugates showed a level of interaction with T4 DNA. It is clear from the table that the monoheterocyclic conjugates have poorer non-covalent affinities than their corresponding di- an triheterocyclic analogues.

Generally, there is an increase in binding affinities with each increase in number of heterocyclic units. The pyrrole conjugates demonstrated stronger affinities for poly(dA.dT) than poly(dG.dC), indicating that the pyrrole conjugates have retained the preference for AT-rich sequences, although the magnitude was significantly less than that seen for distamycin. The pyrrole conjugates possessed higher non-covalent affinities than the imidazole conjugates. The imidazole conjugates possessed similar or greater affinities to poly(dG.dC) than to poly(dA.dT), which indicates an increased tolerance of GC base pairs. There appears to be little difference in the non-covalent affinities for the pyrrole-BAM and pyrrole-CHL conjugates, but the imidazole-CHL conjugates had significantly weaker binding affinities than the imidazole-BAM conjugates. Lastly, the half-mustard imidazole conjugate demonstrated a significant non-covalent interaction, indicating that it non-covalently bound DNA at least as strongly as the triimidazole-BAM conjugate.

Circular dichroism studies carried out at Furman University on the di- and triheterocyclic conjugates supported the results found with the ethidium displacement assay. The induced ellipticities seen for the pyrrole conjugates indicated strong interaction with calf thymus DNA and poly(dA.dT) but little or no interaction with poly(dG.dC) (Wyatt, *et al.*, 1994a). The imidazole conjugates demonstrated greater induced ellipticities

for poly(dG.dC) than for poly(dA.dT) (Lee, *et al.*, 1993a; Lee, *et al.*, 1993b). Comparison between the BAM and CHL conjugates revealed that the BAM conjugates had greater induced ellipticities than the CHL conjugates.

As mentioned previously, monopyrrole lexitropsins did not interact appreciably with DNA when measured by circular dichroism (Gursky, *et al.*, 1982), and the formamido-monoimidazole analogue Im_1 did not demonstrate measurable interactions with DNA when studied by circular dichroism and footprinting (Lee, *et al.*, 1993c). The reason that the monoheterocyclic conjugates possess poor but measurable non-covalent interactions may be due to the addition of the nitrogen mustard functionality. In agreement with previous work on lexitropsins, the di- and triheterocyclic conjugates possess higher non-covalent affinities than the monoheterocyclic conjugates. The ethidium displacement and circular dichroism studies provide an estimation of the relative strength of non-covalent DNA binding for the conjugates.

The CHL conjugates showed an improved DNA cross-linking ability in comparison to CHL itself, while the BAM conjugates did not cross-link DNA efficiently. The appraisal of the cross-linking ability for each conjugate in plasmid DNA proved to be an accurate prediction of cross-linking ability in cells, as was shown for melphalan, CHL and BAM (Sunters, *et al.*, 1992). The di- and triheterocyclic-CHL conjugates demonstrated significant cross-link formation in cells at doses equal to or below their IC_{50} values. The BAM conjugates consistently did not show evidence for interstrand cross-link formation in cells at doses in excess of their IC_{50} values. It is interesting to note that the cross-linking ability in plasmid DNA was not significantly affected by the number of heterocyclic units. The monoheterocyclic conjugates in each family cross-linked DNA just as effectively, or better than, the corresponding di- and triheterocyclic analogues. Non-covalent DNA binding affinity does not affect the cross-linking ability for these nitrogen mustard containing conjugates. As previously described, an

increase in cross-linking ability for conventional nitrogen mustards corresponds to an increase in cytotoxicity (Sunters, *et al.*, 1992). This does not hold true, however, for nitrogen mustards tethered to minor groove-binding vectors, and cross-linking is not a good indication of cytotoxicity in this case.

The CHL conjugates are more cytotoxic than the parent mustard and this is probably due to the ability of the lexitropsin portion to efficiently deliver the nitrogen mustard functionality to the DNA. The CHL conjugates produce cross-links in plasmid DNA at doses lower than that required by CHL. The lexitropsin portion contains a dimethylamino group which, as discussed in the introduction, would be protonated at a pH of 7. Cationic DNA binding agents have a natural affinity for the negatively charged DNA structure. The significant cross-linking seen in cells for the CHL conjugates indicates that DNA interstrand cross-linking is the mechanism of action for these analogues.

It seems possible that the pyrrole-CHL conjugates are more cytotoxic than their corresponding imidazole conjugates due to their increased DNA binding affinities, which are on average over an order of magnitude higher than the imidazole conjugates. Cross-link formation in plasmid DNA occurs at lower doses for the pyrrole conjugates than for the imidazole conjugates. This explanation does not, however, exclude other possibilities, including drug uptake and the repair of these lesions.

The considerations are somewhat different for the BAM conjugates. It is obvious that tethering BAM to the minor groove binding vectors produces conjugates which are much more cytotoxic than the parent mustard. This increase in cytotoxicity cannot be explained by an increase in cross-linking ability. The lack of cross-linking in cells indicates that cross-linking is not the mechanism of action for the BAM conjugates. In light of the knowledge concerning lexitropsin derivatives lacking alkylating groups, it seems certain that a DNA alkylation event is occurring. The lexitropsin

portion, therefore, is both efficiently delivering the BAM portion to the DNA, but may be directing the BAM portion away from its natural target in the major groove. It would appear that the BAM conjugates are producing specific and highly cytotoxic monoalkylations in the minor groove, where the lexitropsin portion preferentially binds (see Chapter Three).

The half-mustard imidazole conjugate was not cytotoxic at the dose range studied, which implies that the second chloroethyl arm of the benzoic acid-mustard portion is important for the BAM conjugates. There are several possibilities to consider. The aziridinium formation could be affected by the replacement of the second chloroethyl arm with a hydrogen. There may be other lesions formed by the triimidazole-BAM conjugate, such as DNA-protein or DNA intrastrand cross-links. Alternatively, the DNA sequence specificity of alkylation for the half-mustard imidazole conjugate may be different from that of the triimidazole conjugate. These considerations will be addressed in Chapter Three.

It is attractive to speculate that the differences seen in cytotoxicity between the imidazole- and pyrrole-BAM conjugates could be due to the targeting of different regions of DNA. The triimidazole conjugate proved to be the most cytotoxic of the all the conjugates, in spite of its poorer non-covalent DNA binding affinity in comparison to the tripyrrole-BAM conjugate and the half-mustard imidazole conjugate.

In order to determine the types of DNA lesions and the sequence specificity of alkylation for the conjugates, a *Taq* stop assay and several modified sequencing techniques were utilised. These studies allowed for the determination of the effect of the lexitropsin portion on the reactivity and sequence specificity of the nitrogen mustard functionality. These studies also allowed for an examination of the effect of the nitrogen mustard functionality on the sequence specificity of the lexitropsin portion. The next chapter presents the results of this work.

CHAPTER 3: SEQUENCE SPECIFICITY OF ALKYLATION

3.1 Introduction

A study of the sequence specificity of alkylation for the parent mustards and each family of the conjugates was undertaken to evaluate the influence of the lexitropsin portion on the reactivity and specificity of the nitrogen mustard functionality, and the influence of the mustard group on the DNA binding properties of the lexitropsin group. The technique initially used to identify the sequence specificity of alkylation was the *Taq* stop assay (Ponti, *et al.*, 1991). This technique has the flexibility to examine several regions of DNA and detect different types of alkylation damage. Two modified sequencing techniques were utilised to confirm the specific lesions detected by the *Taq* polymerase stop assay. The piperidine cleavage assay was used to examine the sequence specificity of alkylation for guanine-N7 lesions (Mattes, *et al.*, 1986b). The thermal cleavage assay was used to determine the sequence specificity of alkylation for adenine-N3 or guanine-N3 lesions (Reynolds, *et al.*, 1985; Mitchell, *et al.*, 1993). The technique of MPE footprinting was used to determine non-covalent DNA binding specificity (Van Dyke, *et al.*, 1982).

3.2 Materials and Methods

3.2.1 Materials

The regions of pBR322 DNA (Chapter Two materials) are referred to by sequence number as listed (Figure 3.1) (Maniatis, *et al.*, 1982). The GC-rich Bam H1/Sal 1 region (375-651) is 276 base pairs long with a GC content of 65% and 18 tracts of four or more GC base pairs. The 213 base pair region defined between base pair number 3090 and 3303 has a GC content of 36% and 11 tracts of four or more AT base pairs.

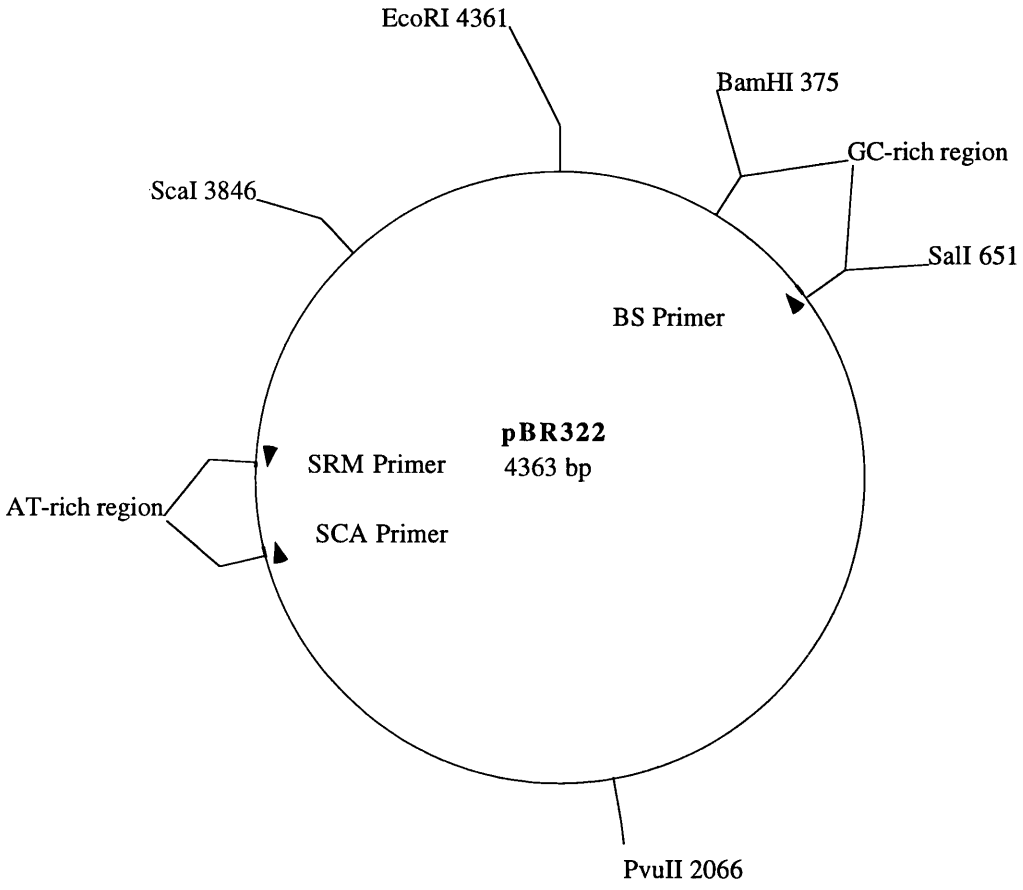

Figure 3.1. Plasmid map of pBR322 DNA, including labelling of the AT- and GC-regions, cutting sites of the restriction enzymes utilised, and the binding locations of the primers used for the *Taq* polymerase stop assay.

Chemicals.

Boric acid was purchased from BDH. Ammonium persulfate (APS), piperidine, dithiothreitol, ammonium iron(II) sulfate hexahydrate, and tetramethylethylenediamene (TEMED) were purchased from Aldrich. The Sequagel kit including 10X buffer, concentrate (acrylamide), and diluent (8 M urea) were purchased from National Diagnostics. X-ray film was purchased from Amersham (hyperfilm) or Kodak (bluefilm). Low melting point (LMP) agarose was purchased from BRL. Sodium citrate was purchased from BDH. Methidiumpropyl-EDTA was a gift from Professor Peter Dervan, California Institute of Technology.

3.2.2 *Taq* Polymerase Stop Assay

Enzymes.

Bam H1: as described in Chapter 2.

Pvu II: 8-12 U/μl in 20 mM Tris-HCl, pH 7.4, 50 mM KCl, 0.1 mM EDTA, 1.0 mM DTT, 200 μg/ml BSA, 50% (v/v) glycerol. Purchased from Northunbria Biologicals Ltd (NBL).

Sca I: 8-12 U/μl in 20 mM Tris-HCl, pH 7.4, 50 mM KCl, 0.1 mM EDTA, 1.0 mM DTT, 200 μg/ml BSA, 50% (v/v) glycerol, purchased from NBL.

Taq polymerase: 5 U/μl , purchased from Advanced Biotechnologies.

Red hot *Taq* polymerase: 5 U/μl , purchased from Advanced Biotechnologies.

Buffers.

Pvu II (10x) buffer: 10 mM Tris-HCl, pH 7.8, 50 mM NaCl, 10 mM $MgCl_2$, 1 mM DTT, purchased from NBL.

Sca I (10x) buffer: 50 mM Tris-HCl, pH 7.8, 100 mM NaCl, 10 mM $MgCl_2$, 1 mM DTT, purchased from NBL.

TEOA buffer as described in Chapter 2.

Stop Solution as described in Chapter 2.

Taq polymerase (10X) reaction buffer IV: 20 mM $(NH_4)_2SO_4$, 75 mM Tris-HCl pH 9.0, 0.01% Tween, and separate stock solution of 25 mM $MgCl_2$ were purchased from Advanced Biotechnologies.

Deoxynucleoside triphosphates (dNTPs): Ultrapure 100 mM solutions of the dNTPs were purchased from Pharmacia Biotech.

Synthetic oligodeoxynucleotide primers.

The synthetic primer 5′-TATGCGACTCCTGCATTAGG-3′, identified as BS, binds to the sequence 640-621 and was used to examine damage to the top strand of the GC-rich Bam H1/Sal 1 region. The synthetic primer 5′-GCAGCAGATTACGCGCAGAA-3′, identified as SCA, binds to the complementary strand at position 3090-3109 and was used to examine alkylation on the bottom strand of the AT-rich region. The primer 5′-

GCATTGGTAACTGTCAGACC-3′, identified as SRM, binds to the sequence 3303-3284 and was used to examine the top strand of the AT-rich region.

Drug: DNA reactions.

Before the drug: DNA incubations, the plasmid was linearised with an appropriate restriction enzyme, in order to provide a downstream block for the *Taq* polymerase. For examination of the top strand of the GC-rich region, the plasmid was restricted with Bam H1, as described in Chapter 2. Extension by the *Taq* polymerase results in a 265 base pair full length fragment. For examination of the top strand of the AT-rich region, the DNA was linearised with PVU II (2 units per μg of DNA) in its buffer for one hour at 37° C, precipitated and then resuspended in 40 μl water. For examination of the bottom strand of the AT-rich region, the plasmid was linearised with Sca I (2 units per μg of DNA) in its buffer for one hour at 37° C, precipitated and then resuspended in 40 μl water. Approximately 500 ng DNA was used for each experimental point and drug reactions were in a total volume of 50 μl TEOA buffer. Incubations were for either two or five hours at 37° C, followed by precipitation with stop solution and 95% ethanol as described in Chapter 2. Samples were washed with 70% ethanol, then dried by lyophilisation.

5′-End labelling of the primers.

The oligodeoxynucleotide primers were 5′-end labelled using T4 polynucleotide kinase and [γ-^{32}P]ATP, as described in Chapter 2, in a final volume of 25 μl. At the end of the 30 minute incubation, 30 μl of distilled water was added and the 55 μl was gently loaded onto the top of the BioSpin column. The Bio-Rad BioSpin columns were prepared just prior to use by spinning to pack the column and remove the storage buffer and then eluting through 250 μl of distilled water. The samples were loaded onto the dry columns and the column was spun for four minutes at 1200g to collect the primer in the eluent. The primer was then aliquoted directly into the primer extension mixture.

Primer Extension.

The dried, control or drug-treated, DNA samples were resuspended in 50 µl of water. The primer extension of each DNA sample was carried out in a total volume of 100 µL containing 0.5 µg template DNA, 5 pmoles labelled primer, 125 µM of each dNTP, 1 U *Taq* polymerase, reaction buffer IV, 2.5 mM $MgCl_2$, 0.05% gelatine. The dNTP, $MgCl_2$, gelatine, and reaction buffer IV solutions were all stored as 10X stocks at 4° C until use. The *Taq* polymerase, stored at -20° C, was diluted immediately prior to use. The cycling conditions, carried out using a PTC-100 Programmable Thermal Cycler (MJ Research, inc.), consisted of an initial four minute denaturation step at 94° C, followed by a cycle of one minute at 94° C, one minute at 60° C and one minute at 72° C, for a total of 30 cycles. After primer extension the samples were precipitated with three volumes 95% ethanol and washed with 70% ethanol. Samples were dried by lyophilisation and then taken up in 3 µl of formamide loading dye prior to polyacrylamide electrophoresis.

3.2.3 Preparation of 5'-Singly End-Labelled Fragments

Buffers.

TAE: as described in Chapter 2.

Sucrose loading buffer: as described in Chapter 2.

50X GELase™ buffer: (Epicentre Technologies).

Enzymes:

GELase™: (Epicentre Technologies).

For the GC-rich region.

DNA was linearised with Bam H1, dephosphorylated and 5'-end labelled as described in Chapter 2. The DNA was subjected to a second restriction digest with Sal 1, which cuts at a single site 276 base pairs downstream from the Bam H1 restriction site. After incubation the DNA was precipitated with sodium acetate and ethanol, dried by lyophilisation, and then taken up in sucrose loading buffer (Chapter 2). Samples were loaded onto a 1.0% LMP

agarose gel containing ethidium bromide (5 µl/100 ml of gel of a 10 mg/ml solution) and electrophoresed for 90 minutes at 75 V in TAE buffer. After electrophoresis, the bands were visualised by UV fluorescence. The slice of gel containing the 276 base pair fragment was excised and collected in a 1.5 ml eppendorf, along with the appropriate amount of GELase^{TM} 50X buffer. The gel slice was then melted in a 65° C water bath for 10 to 15 minutes and then placed in a 45° C bath for 10 minutes. The GELase^{TM} was added and allowed to digest the agarose for 3 hours. At the end of the digestion, one volume of 5 M ammonium acetate and 3 volumes of 95% ethanol were added and the samples spun in a microfuge for 30 minutes at 13000 rpm. The supernatant was removed and the DNA pellet dried by lyophilisation. The pellet was resuspended in 100 µl water, washed with chloroform/isoamyl alcohol (24:1), and then precipitated and dried. The DNA pellet was then taken up in the buffer required by the experiment and stored at -20° C until use.

For the AT-rich region.

Preparation of 5'-singly end-labelled fragments for the AT-rich region was carried out by exponential amplification of the strands with one of the two primers labelled. The plasmid pBR322 DNA was restricted with the enzyme Ban I, in its buffer for one hour at 50° C. Restriction with Ban I produces 10 fragments, the longest of which is 2024 base pairs long and contains the AT-region of interest. The cut plasmid was run down a 1.0% LMP gel and the fragment of interest isolated and purified via GELase^{TM} digestion as described above. This fragment provided a template for exponential amplification with the SCA and SRM primers described above. Exponential amplification of each DNA sample was carried out in a total volume of 100 µL containing 0.2 µg template DNA, 50 pmoles each of SCA and SRM primer, 125 µM of each dNTP, 1 U *Taq* polymerase, reaction buffer IV, 2.5 mM $MgCl_2$, 0.05% gelatine. The cycling conditions consisted of an initial four minute denaturation step at 94° C, followed by a cycle of one minute at

94° C, one minute at 60° C and one minute at 72° C, for a total of 30 cycles. After amplification the samples were precipitated with three volumes 95% ethanol and washed with 70% ethanol. Samples were dried by lyophilisation. An aliquot of resulting DNA from this amplification was subsequently used as a template for a second round of exponential PCR, with one of the primers 5'-end labelled. The PCR conditions were identical to those described for the first round of exponential amplification. In order to examine the top strand, the SCA primer was 5'-end labelled prior to PCR, as described for the *Taq* stop assay. For the bottom strand, the SRM primer was 5'-end labelled prior to PCR, as described for the *Taq* stop assay. The resulting product from the PCR was precipitated and run down a 1.0% LMP gel, the band excised and purified as described above. The lyophilised fragment was taken up in the buffer required by the experiment and stored at -20° C until use.

3.2.4 Piperidine Cleavage Assay

The 5'-singly end-labelled DNA, prepared as described above, and drugs were incubated in a TEOA buffer solution (final volume of 50 µl) at 37° C for either two or five hours, as described in Chapter 2. Following incubation, the DNA was precipitated with sodium acetate and ethanol and dried by lyophilisation. The DNA pellet was resuspended in 100 µl of a freshly diluted and chilled 10% piperidine solution and incubated at 90° C for 15 minutes to quantitatively convert sites of guanine-N7 alkylation into strand breaks (Mattes, *et al.*, 1986b). Samples were then immediately snap frozen with a dry ice/ethanol bath and lyophilised to dryness. Samples were lyophilised with two additional 20 µl aliquots of water to remove all piperidine, washed with 70% ethanol and dried by lyophilisation. Samples were taken up in 3 µl of formamide loading dye, heated to 90° C for two minutes, then placed on ice before loading onto the polyacrylamide gel.

3.2.5 Thermal Cleavage Assay

Buffers.

Sodium citrate buffer: 1.5 mM sodium citrate, 15 mM NaCl, pH 7.2.

The 5'-singly end-labelled DNA, prepared as described above, and drugs were incubated in a TEOA buffer solution (final volume of 50 µl) at 37° C for either two or five hours, as described in Chapter 2, followed by precipitation with sodium acetate and ethanol. Samples were taken up in 100 µl of a sodium citrate buffer (pH 7.2) and heated to 90° C for 30 minutes, as described previously (Reynolds, *et al.*, 1985). Following heat treatment, the samples were chilled in an ice bath, precipitated with sodium acetate and ethanol, and then dried. Samples were taken up in 3 µl of formamide loading dye, heated to 90° C for two minutes, then placed on ice before loading onto the gel.

3.2.6 Methidiumpropyl-EDTA Footprinting

Buffers.

Footprinting buffer: 10 mM Tris, 50 mM NaCl, pH 7.6.

The 5'-singly end-labelled fragment, prepared as described above, and drugs were incubated at room temperature for two hours in footprinting buffer with 3 µg of calf thymus DNA, in a total volume of 30 µl. Immediately prior to the end of the incubation, the following solutions were made up fresh and kept on ice: 100 µM solution of ferrous ammonium sulfate, 100 µM solution of the MPE. A 35.8 mM stock solution of DTT was thawed and kept on ice. At the end of the incubation, 6 µl of a 1:1 mix of the Fe(II) solution and MPE solution was added to the drug: DNA solution. After a gentle mixing, 2 µl of the DTT solution was added, the samples gently mixed again and allowed to react at room temperature for fifteen minutes. Samples were then snap frozen, lyophilised and then washed with 70% ethanol.

3.2.7 Polyacrylamide Gel Electrophoresis

Buffers.

Tris-boric acid buffer: 90 mM Tris-HCl, 90 mM boric acid, 2 mM EDTA, pH 8.3.

Formamide loading dye: 0.04% bromophenol blue, 0.04% xylene cyanol, 98% deionised formamide.

Electrophoresis was carried out on a BioRad Sequi-Gen sequencing gel apparatus and the gel size was 80 cm x 40 cm x 0.4 mm. The 6% polyacrylamide denaturing sequencing gels were prepared using a National Diagnostics Sequagel kit consisting of concentrate (19:1 acrylamide: bisacrylamide), diluent (8 M urea), and buffer (10X TBE buffer). For each gel, the concentrate (24 ml), diluent (66 ml) and buffer (10 ml) were mixed fresh. The base of the gels were sealed with 15 ml of the mix to which 75 µl of TEMED and 105 µl of the APS solution (0.25 mg/ml) was added. After the base was sealed, 39 µl of TEMED and 337 µl of APS solution were added to the remainder of the mix and the gels were poured. Each gel was prerun with TBE buffer for approximately 30 minutes in order to bring the temperature of the gel up to approximately 50° C. Once samples were loaded, electrophoresis conditions varied between 2500 and 3000 V, in order to maintain a gel temperature of between 50 and 60° C. Each electrophoresis run was terminated when the bromophenol blue marker had migrated approximately 70 cm. The gels were removed from the plate using a sheet of Whatman paper, and a sheet of 3mm paper was placed between the Whatman sheet and the porous gel drying support. Gels were dried for 2 hours at 80° C, and X-ray film was exposed to each gel. Exposure times for the gels varied, depending on the amount of radioactivity captured on the filter paper, but were on average overnight for the gels from the polymerase stop assay, and one week for the gels from the other assays, without screens.

Overnight exposures for the gels from the other assays were obtained using an intensifying screen and by storing the cassette containing the gel, film and screen at -70° C. Densitometry of the autoradiograms was carried out on a BioRad GS-670 densitometer interfaced with a Power PC.

3.3 Results

3.3.1 BAM and the Pyrrole-BAM Conjugates

GC-Rich Region.

Initially the drugs were examined on a 265 base pair GC-rich region of pBR322 DNA (375-640) using the *Taq* polymerase stop assay. BAM, at a concentration of 500 μM (its IC_{50} value), produced a pattern of alkylation consistent with that seen for other conventional nitrogen mustards (Ponti, *et al.*, 1991). The predominant sites of alkylation were guanines within runs of guanines and in the sequence 5'-TGG (Figure 3.2, lane d). Although the pattern was quantitatively similar to that seen for other conventional nitrogen mustards, the dose of BAM required to produce detectable amounts of damage was higher and indicates that the drug is significantly less reactive. The inclusion of equimolar amounts of distamycin did not significantly alter the alkylation pattern of BAM (Figure 3.2, lane f). Distamycin (lane b) did not produce any blockages to the *Taq* polymerase and this is presumably because it does not form covalent adducts with DNA and is displaced during the precipitation and wash steps prior to primer extension.

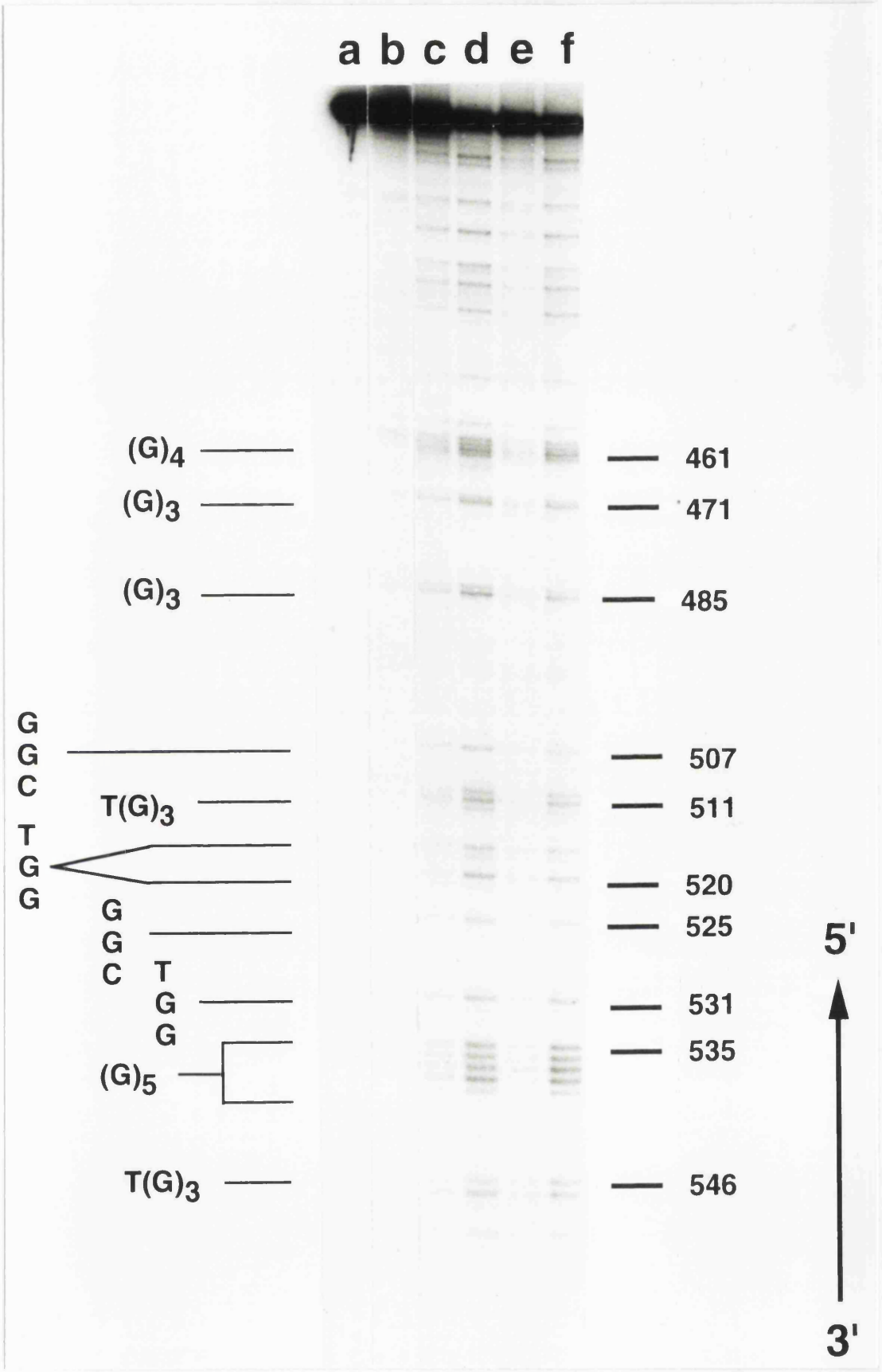

Figure 3.2. *Taq* polymerase gel examining damage to the top strand of the GC-rich region (defined in materials and methods) caused by BAM alone or in the presence of distamycin. Lane a, control; lane b, distamycin 500 μM; lane c, BAM, 100 μM; lane d, BAM, 500 μM; lane e, BAM + distamycin, 100 μM, lane f, BAM + distamycin, 500 μM. Drug: DNA incubations were for 5 hours at 37° C.

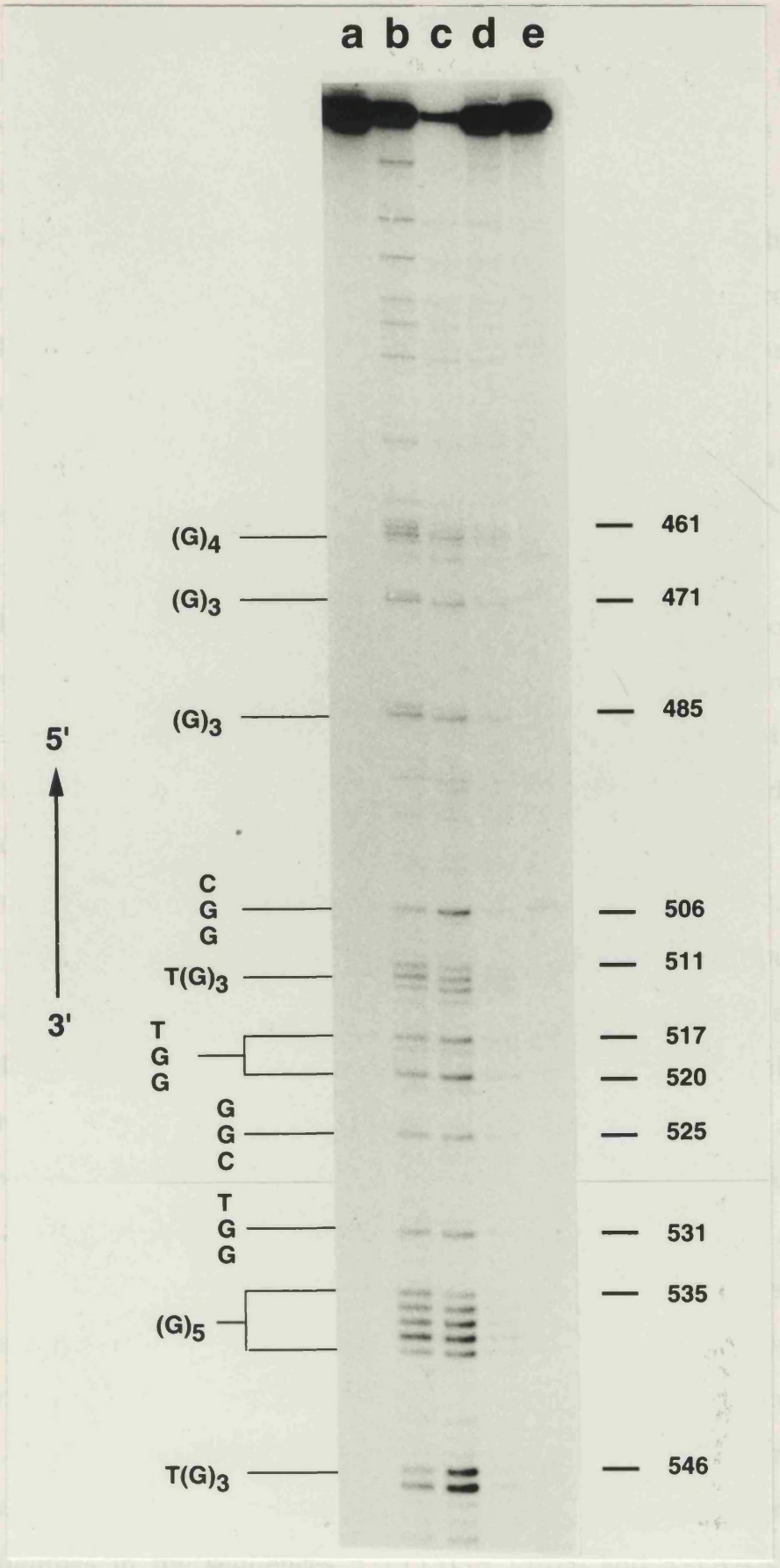

Figure 3.3. *Taq* **polymerase gel examining damage to the top strand of the GC-rich region caused by the BAM-Py conjugates. Lane a, control; lane b, BAM, 500 μM; lane c, BAM-$(Py)_1$, 10 μM; lane d, BAM-$(Py)_2$, 10 μM; lane e, BAM-$(Py)_3$, 10 μM. Drug: DNA incubations were for 5 hours at 37° C.**

The monopyrrole-BAM conjugate, at a concentration of 10 μM, (5-fold lower than its IC_{50} value), also produced a similar pattern in this region, but the intensities of several of the bands differed (Figure 3.3, lane c). The dose which produced a similar amount of damage to that produced by BAM on the fragment was at least 50-fold lower. The dipyrrole and tripyrrole conjugates did not produce any significant covalent lesions in this region under identical conditions (Figure 3.3, lanes d and e), in spite of their higher non-covalent affinity for DNA, as measured by ethidium displacement.

AT-Rich Region.

The 213 base pair AT-rich region of pBR322 DNA defined from 3090 to 3303 was examined to further elucidate the specificity of alkylation of the pyrrole-BAM conjugates. This region was chosen because of its high incidence of AT runs which are known sites of non-covalent binding for pyrrole-containing lexitropsins. Examination of the bottom and top strands was carried out utilising the *Taq* polymerase stop assay, initially. BAM reacted weakly with guanines and including equimolar amounts of distamycin in the incubation did not alter the alkylation specificity seen for BAM (data not shown). The results for BAM and the pyrrole-BAM conjugates are shown in Figures 3.4 and 3.5 for the bottom and top strands, respectively. The pyrrole-BAM conjugates (lanes c-e) showed a markedly altered alkylation specificity from that of BAM (lane b) in this AT-rich region. The lesions seen were concentration dependent within a dose range that ensured single hit kinetics. On both strands of this region, the monopyrrole conjugate demonstrated preferential alkylation at adenines within AT-rich sequences, and in an overall pattern that bore little resemblance to that seen for BAM. The preferential sites of alkylation were those adenines in the sequences 5'-TTTTG<u>A</u> (3205) and 5'-TAA<u>A</u> (3250). Sites alkylated to a lesser extent included 5'-TT<u>A</u>A (3232) and 5'-ATTG<u>A</u> (3256).

Figure 3.4. *Taq* **polymerase gel examining damage to the bottom strand of the AT-rich region caused by BAM and the BAM-Py conjugates. Lane a, control; lane b, BAM, 500 μM; lane c, BAM-$(Py)_1$, 5 μM; lane d, BAM-$(Py)_2$, 5 μM; lane e, BAM-$(Py)_3$, 5 μM. Drug: DNA incubations were for 5 hours at 37° C.**

The dipyrrole conjugate alkylated fewer sites overall on the strand, while retaining strong alkylation at the adenine in the sequences 5'-TTTTGA (3205) and 5'-TTTAAA (3250), with weaker alkylation observed at 5'-ATTGA (3256) and two occurrences of 5'-TTTAA (3232 and 3237). The tripyrrole conjugate, at the same dose as the mono- or dipyrrole conjugate, only strongly alkylated at one sequence on the bottom strand, 5'-TTTTGA (3205). It is clear, therefore, that for each increase in the number of pyrroles there is alkylation at fewer sites. For example, while the adenine in the sequence 5'-TTTTGA (3205) is strongly alkylated by each of the conjugates, the adenine in the sequence 5'-TTTAAA (3250) shows a relative decrease in alkylation with the increase in pyrrole units.

Examination of the top strand, shown in Figure 3.5, revealed results consistent with those seen for the bottom strand. The monopyrrole conjugate showed alkylation at several sites, including strong alkylation at the sequences 5'-TTTTAA (3254 and 3235), 5'-TTAA (3240), and 5'-TTTTGG (3193), while some of the bases alkylated to a weaker extent corresponded to the guanines alkylated by BAM. The dipyrrole conjugate showed alkylation at fewer sites and strong alkylation at the sequences 5'-TTTTGG (3193), 5'-TTTTAA (3254) and 5'-ATATGA (not shown). Weaker alkylation was observed at the sites 5'-ATTAA (3240), 5'-TTTTAA (3235) and 5'-AATGA (3246). The tripyrrole conjugate only strongly alkylated at the sequence 5'-TTTTGG (3193). In agreement with the results from the bottom strand, for each increase in the number of pyrroles there is strong alkylation at fewer sites. Two occurrences of the sequence 5'-TTTTAA (3254 and 3235) in particular, are strongly alkylated by the monopyrrole conjugate, alkylated to a lesser extent by the dipyrrole conjugate but only alkylated weakly, if at all, by the tripyrrole conjugate. Interestingly, an occurrence of the 5'-TTTTAA sequence on the other strand (3237, Figure 3.4) is only weakly alkylated by the dipyrrole conjugate.

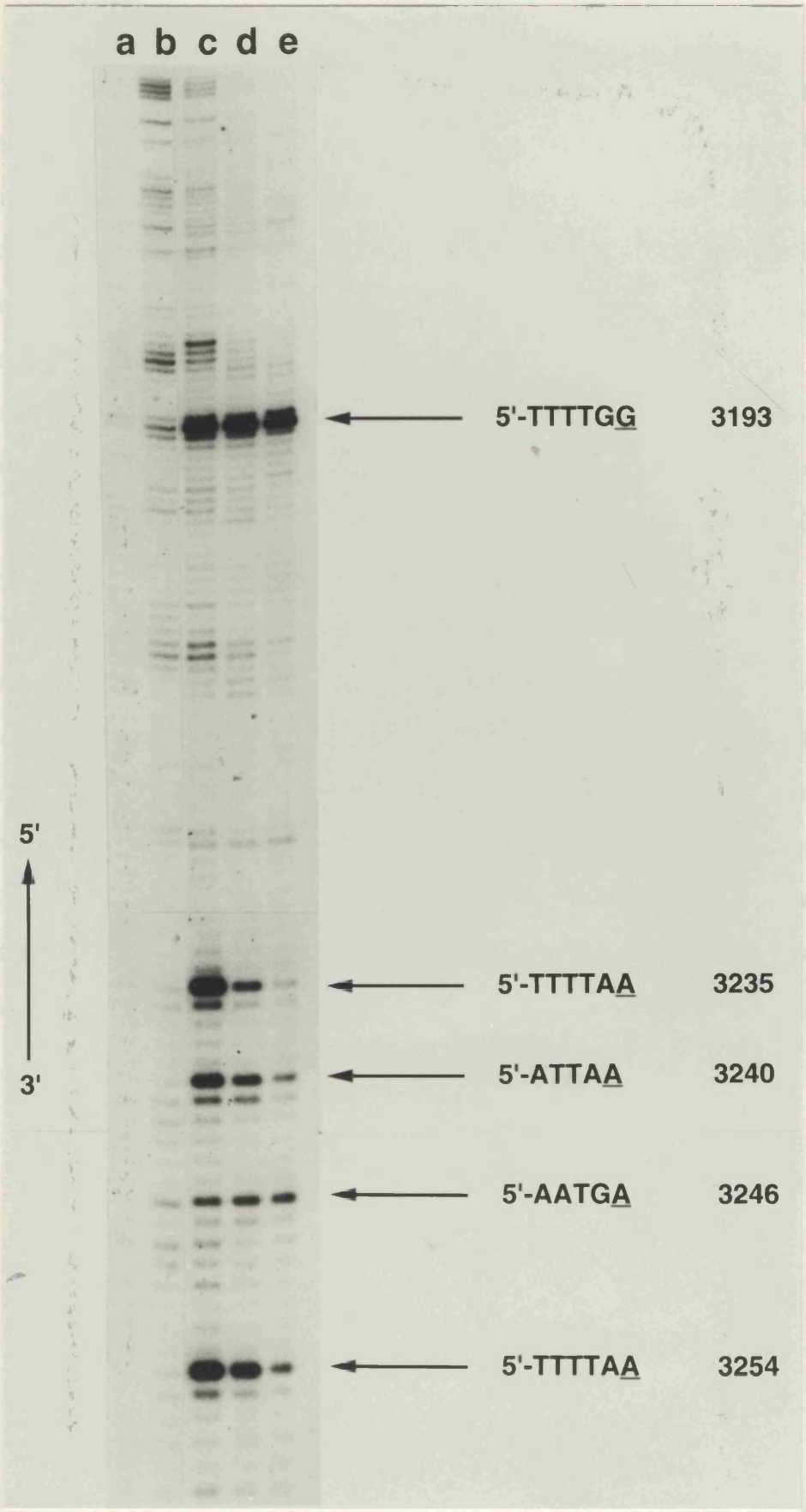

Figure 3.5. Resolvable region of *Taq* polymerase gel examining damage to the top strand of the AT-rich region caused by the BAM-Py conjugates. Lane a, control; lane b, BAM, 500 μM; lane c, BAM-$(Py)_1$, 5 μM; lane d, BAM-$(Py)_2$, 5 μM; lane e, BAM-$(Py)_3$, 5 μM.

The adenine lesions seen on the bottom strand were qualitatively confirmed as minor groove adenine-N3 lesions for the conjugates (Figure 3.6a, lanes d-f), using the thermal cleavage assay. These included the alkylation seen in Figure 3.4 by all three conjugates at 5'-TTTTGA (3205) and the site in the sequence 5'-TTTAAA (3250) by the monopyrrole conjugate. For the top strand, the adenine lesions and the guanine lesion (3193) were confirmed as adenine-N3 and guanine-N3 lesions, respectively, using the thermal cleavage assay (Figure 3.6b, lanes c-e). These included the strongest site of alkylation seen in Figure 3.5 for the conjugates, 5'-TTTTGG (3193), and 5'-TTTTAA (3235 and 3254) for the monopyrrole conjugate.

The lesions detected by the *Taq* polymerase assay for BAM were confirmed as guanine-N7 lesions by piperidine treatment of a 5'-singly end-labelled fragment of the same region (Figure 3.7, top strand, lane c). As shown on the gel, BAM alkylated both guanines equally strongly at the sequence 5'-TTGG (3192 and 3193, Figure 3.7, lane c). The monopyrrole conjugate showed alkylation of both guanine-N7 positions and a three-fold preference for the 3'-guanine (lane d). In Figure 3.6b, however, the thermal depurination assay clearly shows that the alkylation in the minor groove occurs only at the 3'-guanine.

Figure 3.6a. Thermal cleavage gel showing purine-N3 lesions to the bottom strand of the AT-rich region caused by the BAM-Py conjugates. Lane a, control heat treated; lane b, control no heat; lane c, G+A marker lane (formic acid); lane d, BAM-$(Py)_1$, 10 μM; lane e, BAM-$(Py)_2$, 10 μM; lane f, BAM-$(Py)_3$, 10 μM. Drug: DNA incubations were for 5 hours at 37° C.

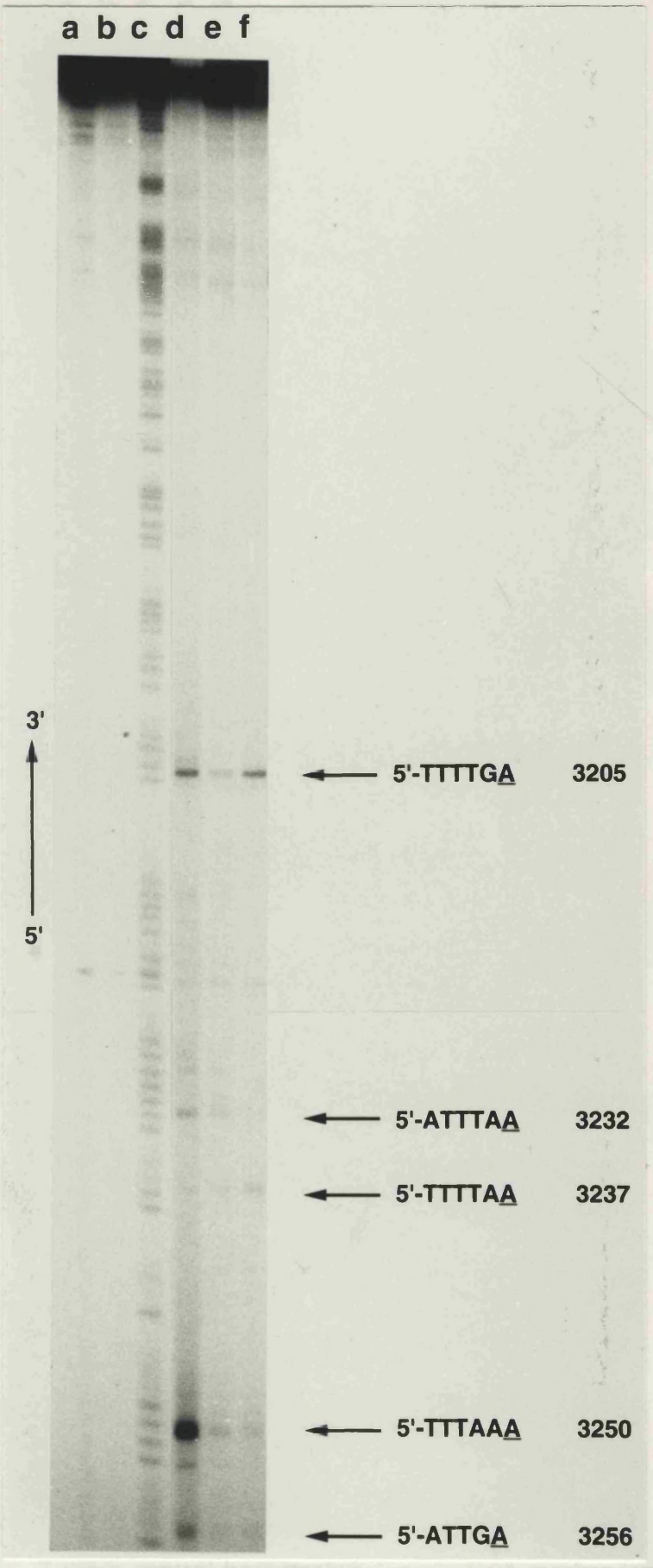
a b c d e f
3'
5'
5'-TTTTGA 3205
5'-ATTTAA 3232
5'-TTTTAA 3237
5'-TTTAAA 3250
5'-ATTGA 3256

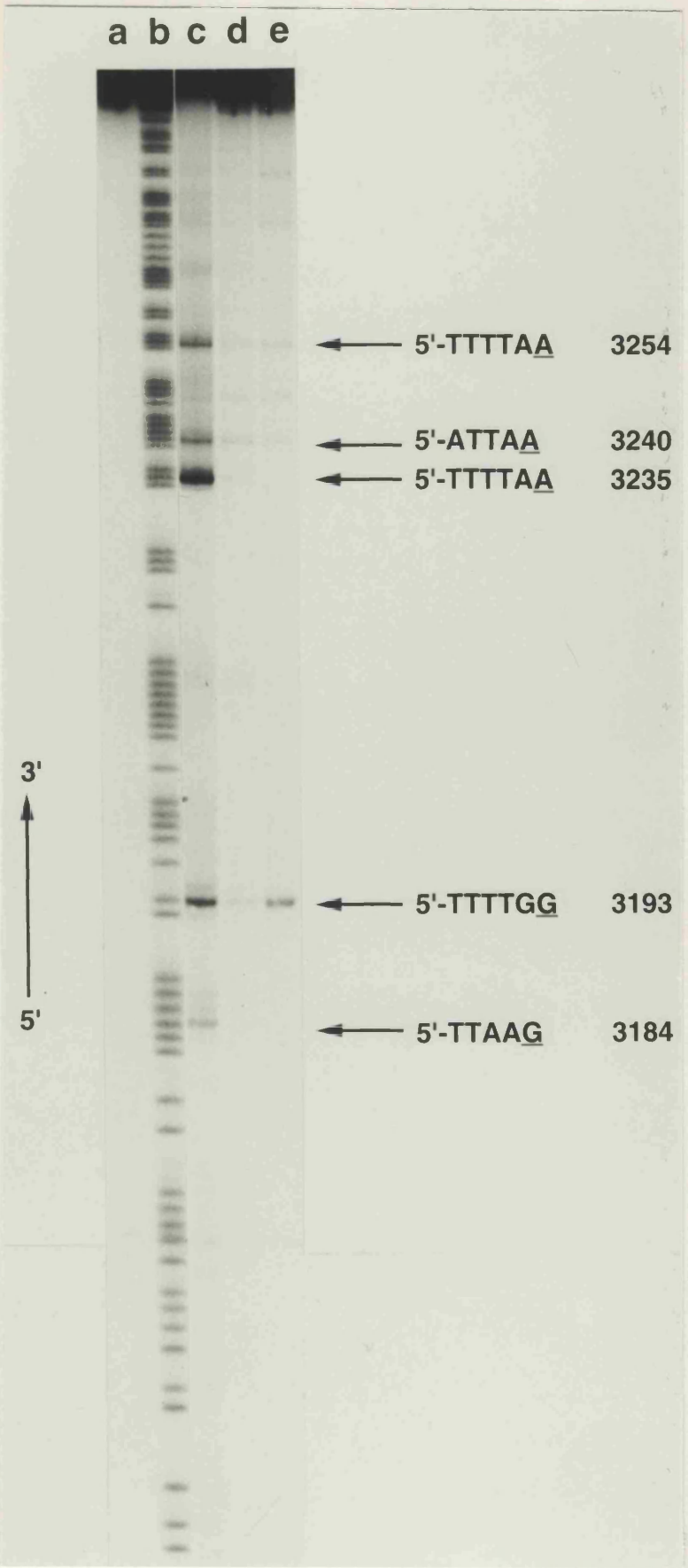

Figure 3.6b. Thermal cleavage gel showing purine-N3 lesions to the top strand of the AT-rich region. Lane a, control heat treated; lane b, G+A marker lane; lane c, BAM-$(Py)_1$, 10 μM; lane d, BAM-$(Py)_2$, 10 μM; lane e, BAM-$(Py)_3$, 10 μM.

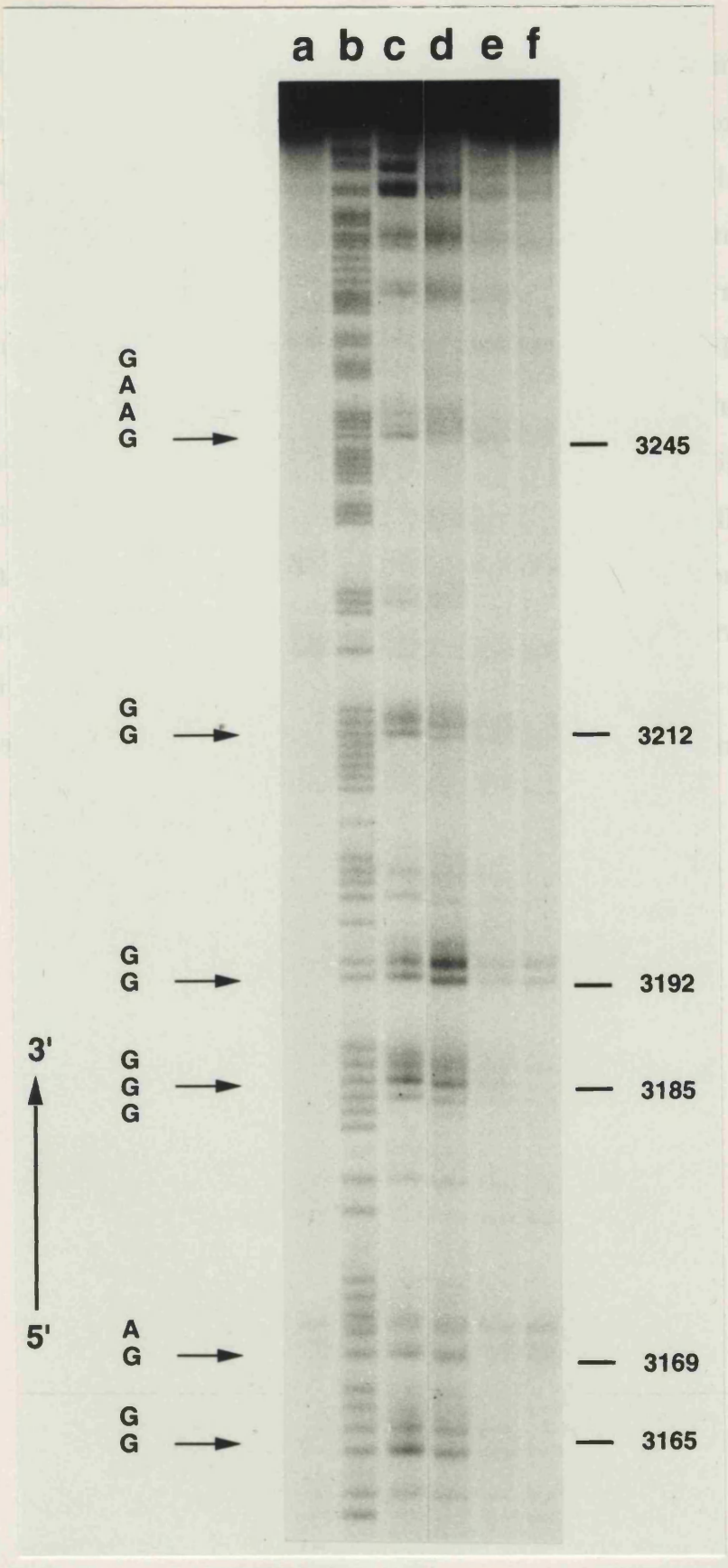

Figure 3.7. Piperidine cleavage gel showing guanine-N7 lesions to the top strand of the AT-rich region. Lane a, control piperidine treated; lane b, G+A marker lane (formic acid); lane c, BAM, 500 μM; lane d, BAM-$(Py)_1$, 10 μM; lane e, BAM-$(Py)_2$, 10 μM; lane f, BAM-$(Py)_3$, 10 μM. Drug:DNA incubations were for 5 hours at 37°C.

Quantitation of the gels in Figure 3.4 and 3.5 by densitometry shows the alkylation pattern for each of the conjugates (Figure 3.8). Comparison of the alkylation on both strands, shown in Figure 3.8a, revealed that the preferred sites of alkylation for the monopyrrole conjugate were the sequences 5'-TTGPu, 5'-TTAA, and 5'-TAAA. The preferred sites of alkylation for the dipyrrole conjugate were the sequences 5'-TTTGPu, 5'-TTTAA, 5'-TATGA, and 5'-TTAAA (Figure 3.8b), while for the tripyrrole conjugate the consensus sequence was 5'-TTTTGPu (Figure 3.8c). Examination of the strand opposite the two preferred sites of alkylation, 5'-TTTTGPu, did not reveal a corresponding lesion, providing strong evidence that the non-covalent binding and alkylation which occurs in the minor groove does not lead to interstrand crosslink formation with these conjugates, even though they possess a nitrogen mustard functionality.

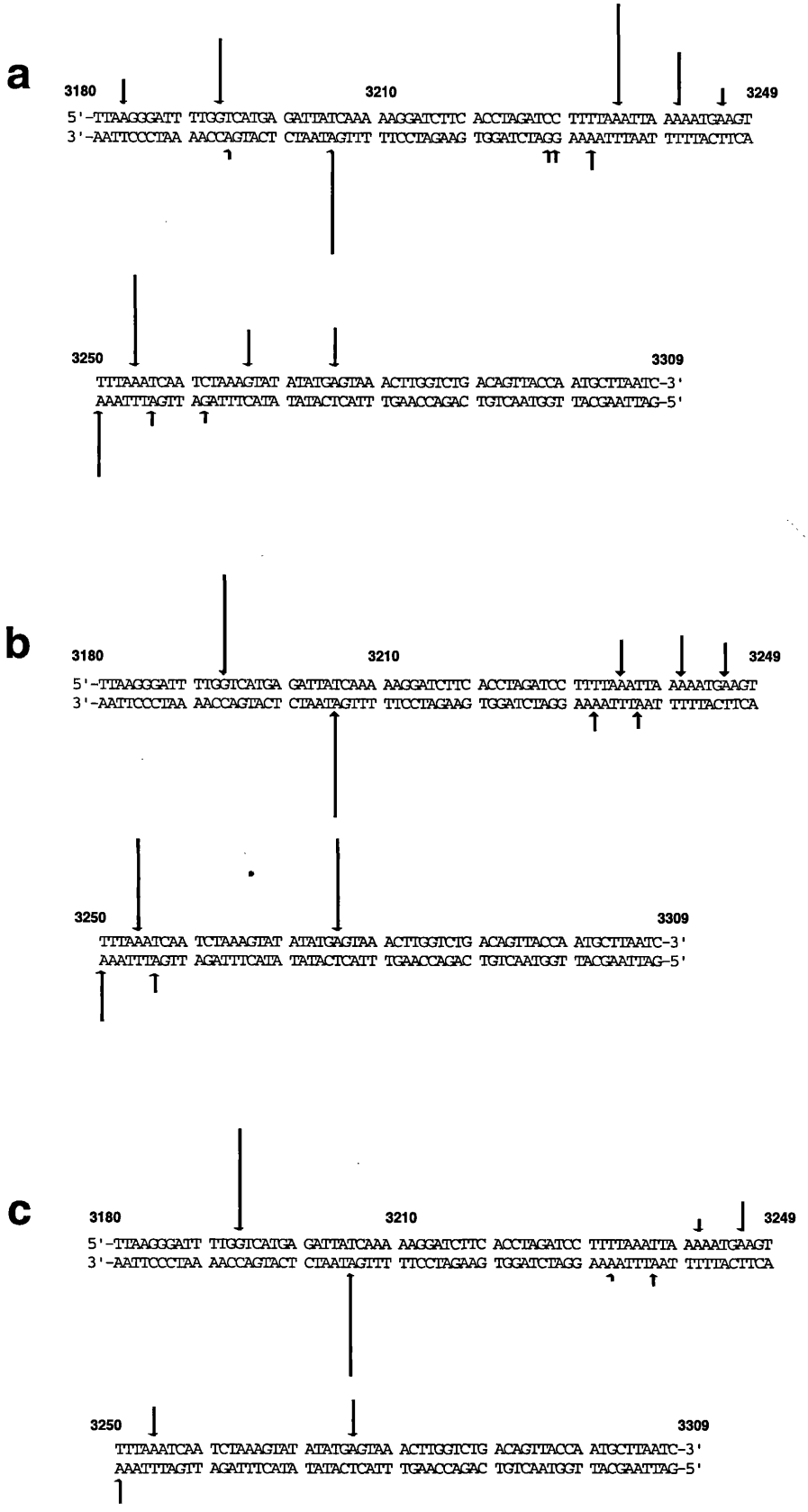

Figure 3.8. Quantitation of the alkylation patterns of the pyrrole-BAM conjugates on the top and bottom strands of the AT-rich region taken from the gels in figures 3.4 and 3.5. Alkylation on each strand is normalised to the site of strongest alkylation; (a), BAM-$(Py)_1$; (b), BAM-$(Py)_2$; (c), BAM-$(Py)_3$.

3.3.2 Tallimustine

As mentioned earlier, prior studies using the thermal cleavage assay found alkylation only in the sequence 5'-TTTTGA, and a single base pair change in the sequence abolished alkylation (Broggini, *et al.*, 1995). In order to confirm this result, the sequence specificity of alkylation for tallimustine was compared under identical conditions in the AT-rich region using the *Taq* polymerase stop assay. The results for the bottom strand, shown in Figure 3.9, clearly show alkylation at the single occurrence of 5'-TTTTGA in pBR322 DNA (lane d). In addition, alkylation was also seen at the sequence 5'-TTTTAA, a site that was only weakly alkylated by the tripyrrole-BAM conjugate (Figure 3.4, lane e). The DNA template incubated with distamycin shows no blockages. On the bottom strand, strong alkylation is seen for tallimustine at the 5'-TTTTGG site seen for the tripyrrole-BAM conjugate and of the two occurrences of 5'-TTTTAA on the strand, one site (3254) is only weakly alkylated by tallimustine, while the other (3235) is not detectably alkylated (data not shown).

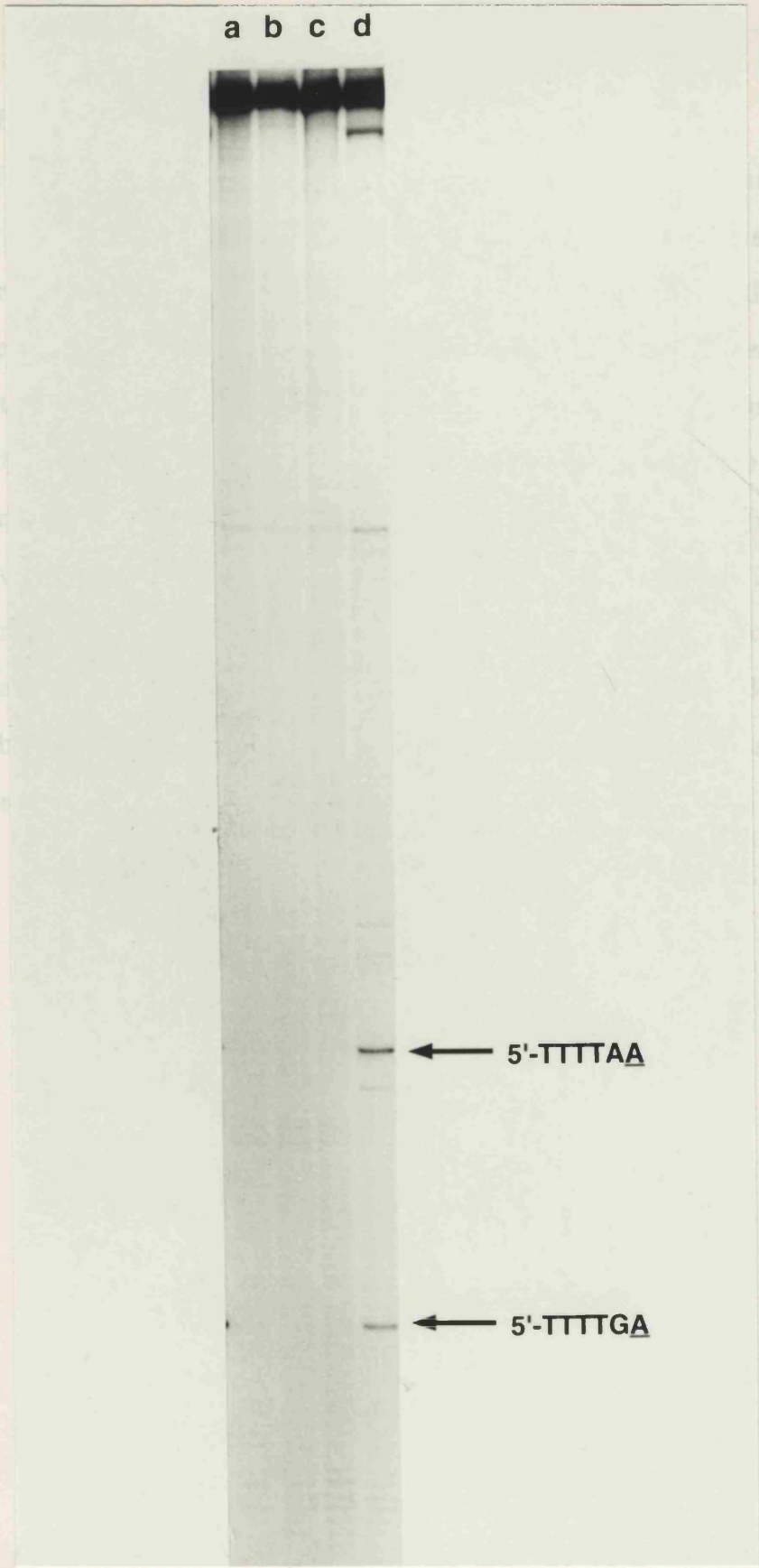

Figure 3.9. ***Taq*** **polymerase gel examining damage to the bottom strand of the AT-rich region caused by tallimustine. Lane a, control; lane b, distamycin 1 μM; lane c, distamycin 10 μM; lane d, tallimustine 1 μM. Drug: DNA incubations were for 5 hours at 37° C.**

3.3.3 MPE Footprinting

MPE footprinting studies were performed on the top strand of the AT-rich region in order to determine the non-covalent sequence specificity for the tripyrrole-BAM conjugate relative to distamycin and tallimustine. The gel, pictured in Figure 3.10, shows the results which are represented by the densitometric scans in Figures 3.11a-d. It is clear from the densitometric scan of the control MPE-cleaved lane that MPE does not cleave with the same efficiency throughout the strand. The stretch of DNA that showed the greatest variability in cleavage was the 43 base pair run from 3230-3273 which contains only 5 GC base pairs. The cleavage at A or T tracts of 4 or more base pairs, including 3139-3142, 3170-3174, 3207-3211 and 3188-3191 was affected, but to a lesser degree. The implications of this will be considered in the discussion.

Figure 3.10. MPE Footprinting gel examining the top strand of the AT-rich region. Lane a, control uncleaved; lane b, G+A marker lane (formic acid); lane c, MPE cleaved (no drug); lane d, distamycin, 100 μM; lane e, BAM-$(Py)_3$, 50 μM; lane f, BAM-$(Py)_3$, 100 μM; lane g, tallimustine, 50 μM; lane h, tallimustine, 100 μM; lane i, BAM-$(Im)_3$, 50 μM; lane j, BAM-$(Im)_3$, 100 μM; lane k, Im_3 lexitropsin, 100 μM. Drug: DNA incubations were for 2 hours at room temperature.

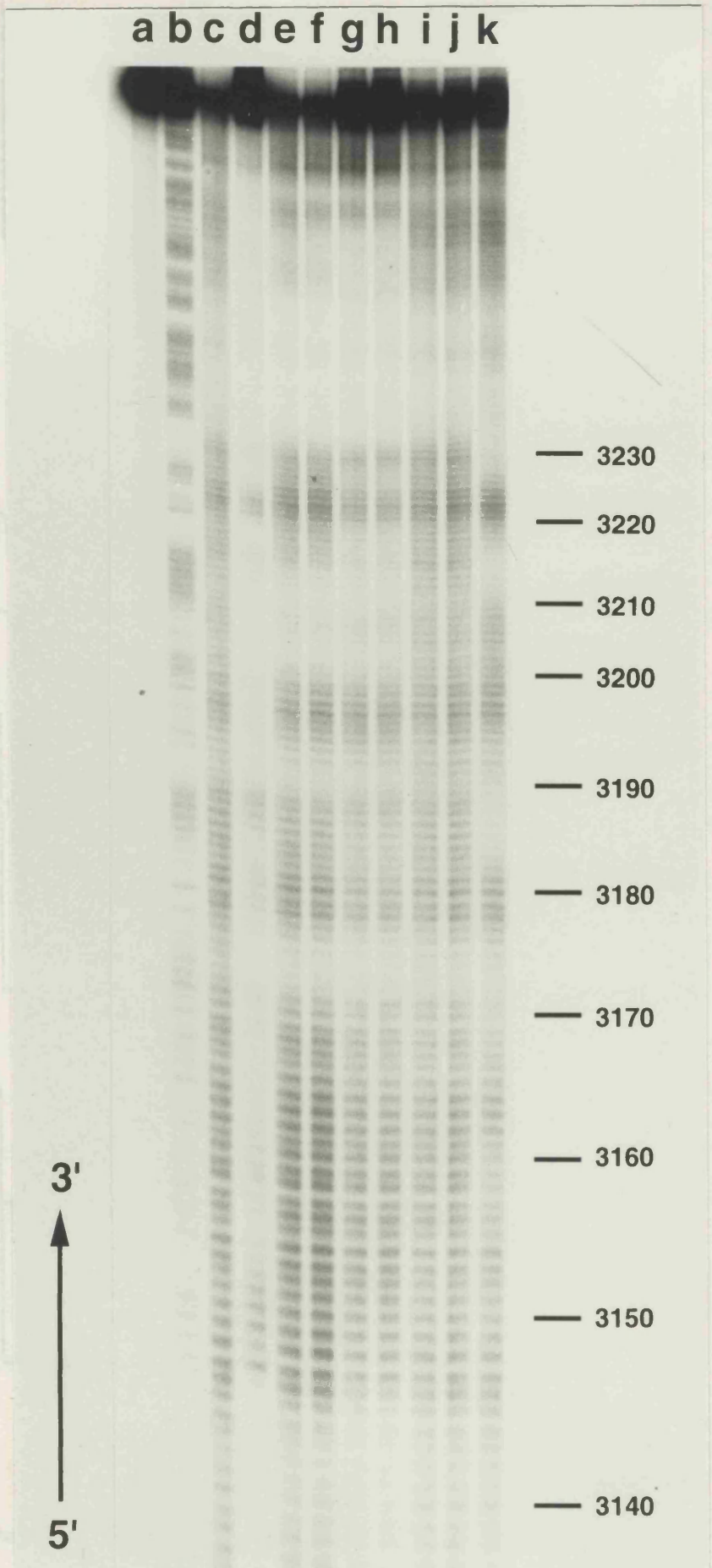
a b c d e f g h i j k
3230
3220
3210
3200
3190
3180
3170
3160
3150
3140
3'
5'

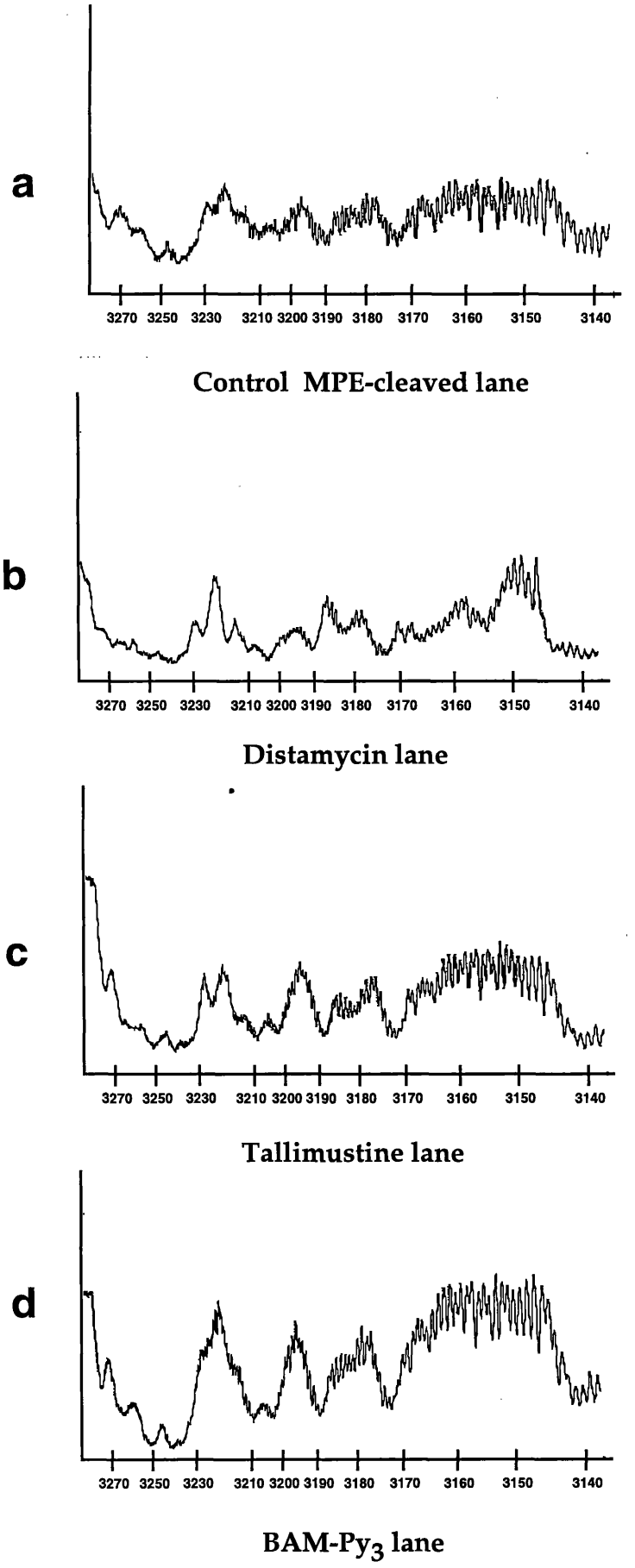

Figure 3.11. Densitometric scans of the lanes from the gel in Figure 3.10. (a), scan for control lane c; (b), scan for distamycin 100 μM lane d; (c), scan for tallimustine 100 μM lane f; (d), scan for the BAM-$(Py)_3$ 100 μM lane h.

Box diagrammatic representations of the non-covalent binding sites are presented in Figure 3.12. Where cleavage compared to the control untreated lane was detectable but less than 50%, hatched boxes are used. Where cleavage compared to the control lane was inhibited by greater than 50%, filled boxes are used. Distamycin clearly footprinted several AT-rich sites with GC base pairs on either side of the sites (Figure 3.12a). These included 5′-TTTTC (3139), 5′-AAAAC (3170), 5′-TTTTG (3188), 5′-TTATC (3202), 5′-AAAAA (3207), 5′-ATCTT (3214), and 5′-ATATG (3270). Weaker sites included 5′-TCTGA (3151), 5′-TGGAA (3163), 5′-TTAAG (3180), and 5′-TAGAT (3223). Binding was evident in the AT run from 3230-3273, but the determination of the exact binding sites in this stretch was impossible due to the inefficient cleavage by MPE and overlapping binding sites for distamycin and has been labelled with a hatched box.

Tallimustine footprinted with a weaker affinity compared to distamycin, while binding several of the sites strongly bound by distamycin. The strong sites included 5′-TTTTC (3139), 5′-AAAAC (3170), 5′-TTTTG (3188), 5′-TTATC (3202) and 5′-AAAAA (3207). Weaker sites included 5′-TTAAG (3180), 5′-ATCTT (3214), and 5′-TAGAT (3223) (Figure 3.12b). Tallimustine non-covalently recognises the same sites that distamycin binds, with the exception of two weak distamycin sites that were missed. The tripyrrole-BAM conjugate footprinted in similar fashion to that seen for tallimustine, except for the following sites which were missed or weakly bound: 5'-TTAAG (3180), 5′-ATCTT (3214), 5′-TAGAT (3223) (Figure 3.12c). Most of the sites footprinted by tallimustine and the tripyrrole-BAM conjugate were not sites of strong alkylation, indicating that the agents do not alkylate at all sites where non-covalent binding has occurred.

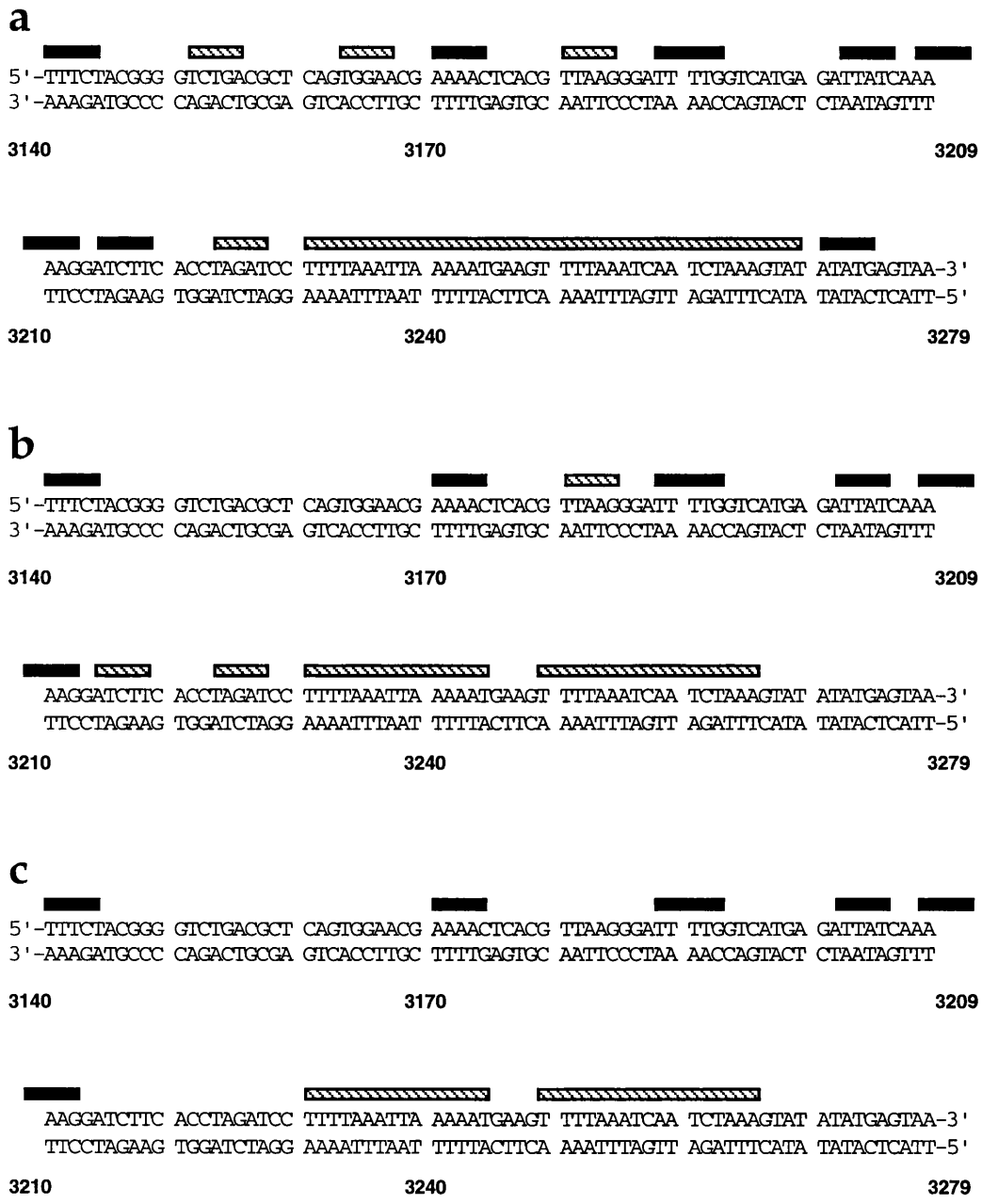

Figure 3.12. Box diagrammatic representations of the recognition sites for distamycin, tallimustine and BAM-$(Py)_3$ on the top strand of the AT-rich region. Where cleavage compared to the control untreated lane was between 10% to 50%, hatched boxes are used. Where cleavage compared to the control lane was inhibited by greater than 50%, filled boxes are used. (a), distamycin; (b), tallimustine; (c), BAM-$(Py)_3$.

3.3.4 The Imidazole-BAM Conjugates

GC-Rich Region.

Initially the drugs were examined on the GC-rich region of pBR322 DNA (375-640) using the *Taq* polymerase stop assay. The monoimidazole conjugate (Figure 3.13, lane c) produced an alkylation pattern that was qualitatively similar to that seen for BAM (lane b). One exception was an additional band within the sequence 5'-AGC (495) for the monoimidazole conjugate. The di- and triimidazole conjugates did not alkylate in this region to any appreciable extent (Figure, 3.13, lanes d and e). Additionally, the diimidazole- and triimidazole-BAM conjugates did not produce footprints in this region (data not shown). This contrasted with the Im_2 and Im_3 lexitropsins, which footprinted strongly at the sequences 5'-$(G.C)_3$(A.T), and 5'-TCGGGCT, respectively (Lee, *et al.*, 1993c).

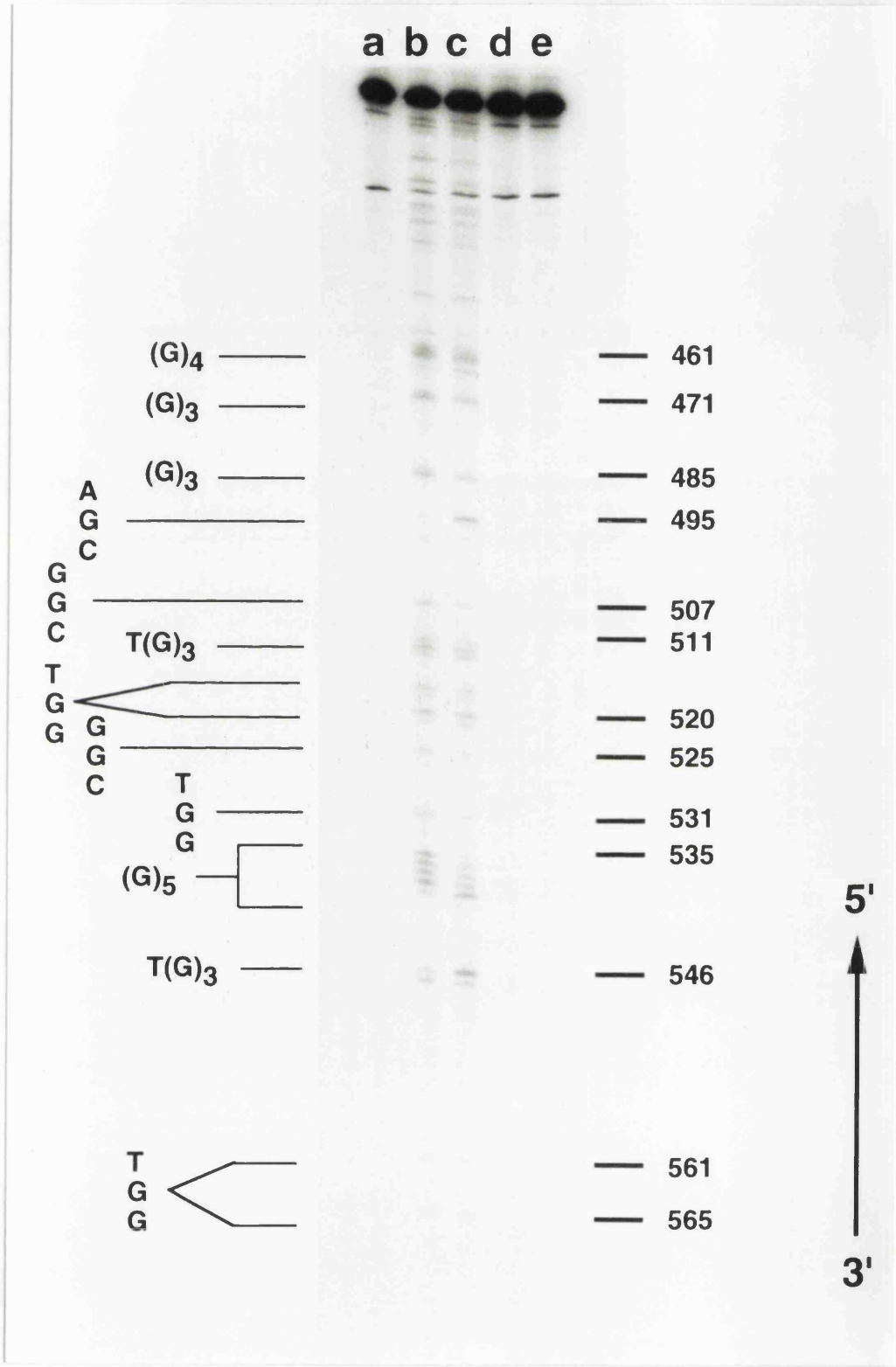

Figure 3.13. *Taq* polymerase gel examining damage to the top strand of the GC-rich region caused by BAM and the BAM-Im conjugates. Lane a, control; lane b, BAM, 500 μM; lane c, BAM-$(Im)_1$, 5 μM; lane d, BAM-$(Im)_2$, 5 μM; lane e, BAM-$(Im)_3$, 5 μM. Drug: DNA incubations were for 5 hours at 37° C.

AT-Rich Region.

Examination of the AT-rich region revealed that the monoimidazole conjugate alkylated in a similar pattern to that seen for BAM, but the intensity of some of the bands differed (Figure 3.14, lane b). The sites of alkylation that were common for BAM and the monoimidazole-BAM conjugate are listed on the left side of Figure 3.14, and include GG sites (3212-13, 3192-93), a GGG site (3184-86), and a G_4 site (3147-50). Lesions at the adenines alkylated strongly by the monopyrrole-BAM conjugate were also detectable, but only faintly. The strongest of the same minor groove sites was the sequence 5′-TTTTAA (3235, lane d). The diimidazole-BAM conjugate clearly recognises fewer sites than BAM or the monoimidazole conjugate. As with the dipyrrole-BAM conjugate, the diimidazole-BAM conjugate does not strongly alkylate at guanines alkylated by BAM. The sites of strongest alkylation were 5′-TTTTGG (3193), 5′-AATGA (3246), and two occurrences of 5′-TTTTAA (3235, 3254, lane g). This preference closely resembled the alkylation specificity of the dipyrrole-BAM conjugate. Additionally, alkylation was evident at 5′-ATTAAAA (3240, 3242) and AAAAGG (3212, lane g).

The strongest site of alkylation for the triimidazole conjugate was the 5′-TTTTGG site (3193), while weaker alkylation was detected at 5′-TTTTAA (3254) and 5′-AATGA (3246, lane j). In agreement with the dipyrrole- and tripyrrole-BAM conjugates, the triimidazole conjugate strongly alkylates fewer sites than the diimidazole conjugate. The alkylation specificity of the triimidazole conjugate closely resembled that seen for the tripyrrole conjugate, particularly in that both the triimidazole and tripyrrole conjugates show comparable alkylation at the two occurrences of 5′-TTTTAA (i.e., stronger alkylation at 3254 than at 3235, lane j).

Figure 3.14. ***Taq*** **polymerase gel examining damage to the top strand of the AT-rich region. Lane a, control; lane b, BAM, 500 μM; lane c, BAM-$(Im)_1$, 1 μM; lane d, BAM-$(Im)_1$, 10 μM; lane e, BAM-$(Im)_2$, 1 μM; lane f, BAM-$(Im)_2$, 5 μM; lane g, BAM-$(Im)_2$, 10 μM; lane h, BAM-$(Im)_3$, 1 μM; lane i, BAM-$(Im)_3$, 5 μM; lane j, BAM-$(Im)_3$, 10 μM. Drug: DNA incubations were for 5 hours at 37° C.**

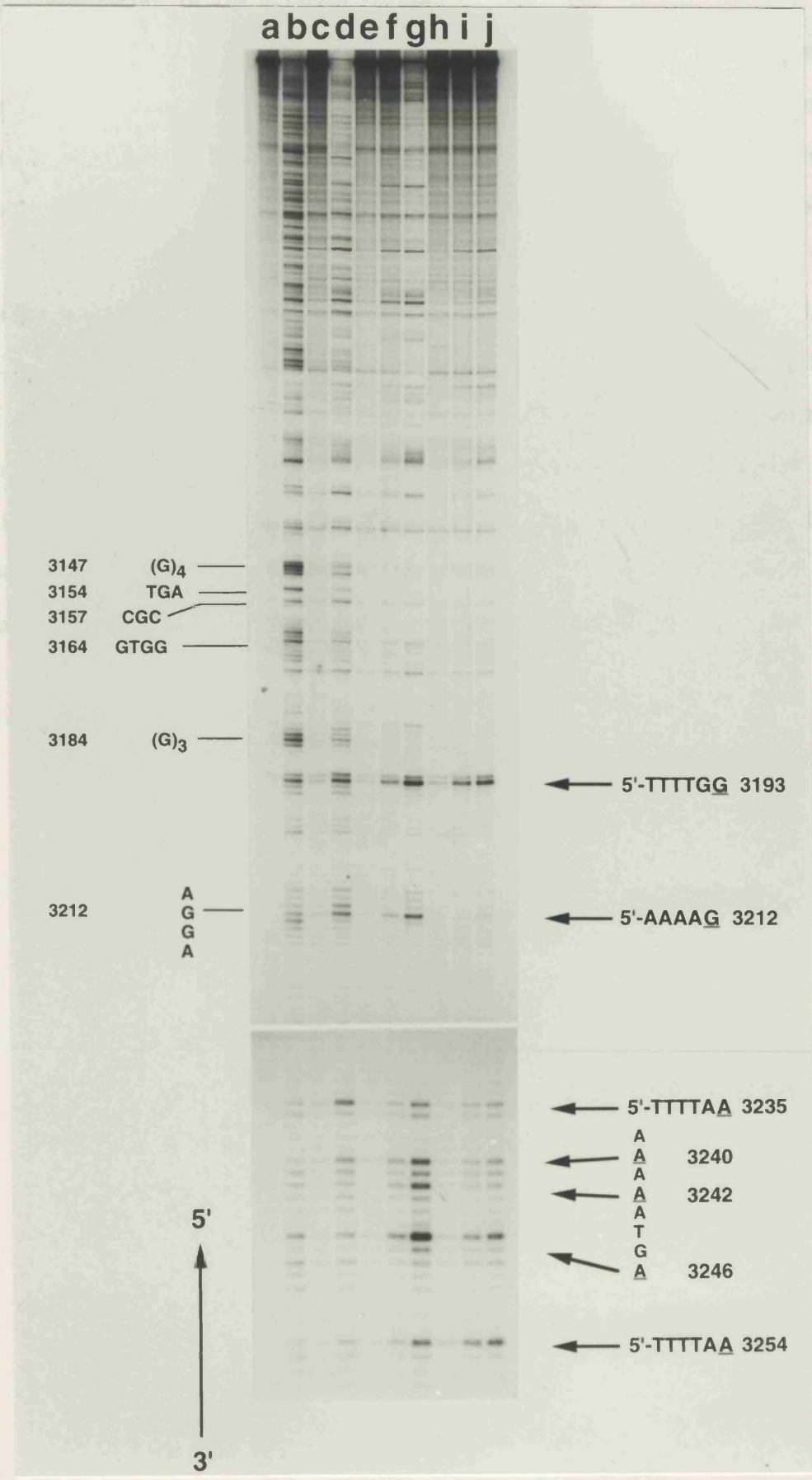
a b c d e f g h i j
3147 (G)4
3154 TGA
3157 CGC
3164 GTGG
3184 (G)3
3212 A G G A
5'-TTTTGG 3193
5'-AAAAG 3212
5'-TTTTAA 3235
A A A A T G A
3240
3242
3246
5'-TTTTAA 3254
5'
3'

MPE Footprinting in the AT-rich region.

Footprinting studies for the triimidazole-BAM conjugate and the Im_3 lexitropsin were carried out on the AT-rich region and were included on the gel in Figure 3.10 (lanes j and k, respectively). The densitometric scans for the control lane c, triimidazole-BAM conjugate lane j, and Im_3 lexitropsin, lane k, are presented in Figure 3.15. The Im_3 lexitropsin produced three strong footprints at the sequences 5'-AGGGA (3184), 5'-AAGGA (3210), and 5'-ATCCT (3227), while the remainder of the cleavage pattern was similar to that seen in the control lane (Figure 3.15b). The profile of the densitometric scan for the triimidazole-BAM conjugate was nearly identical to that seen for the control lane, making interpretation of the AT runs difficult, but it appears that the triimidazole-BAM conjugate produces no clear non-covalent binding sites when studied by MPE footprinting (Figure 3.15c).

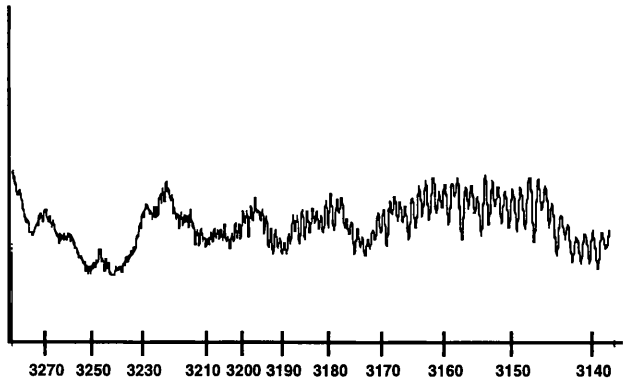

Control Lane

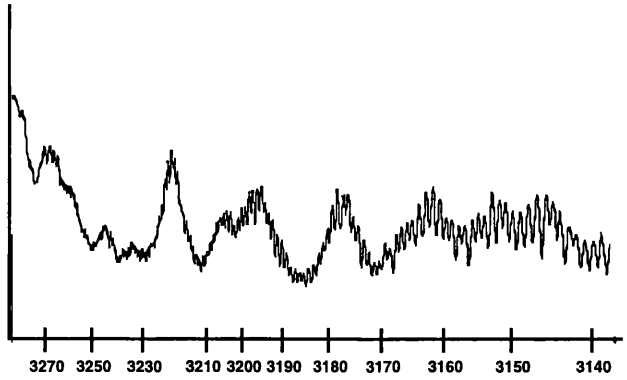

Im_3 Lexitropsin Lane

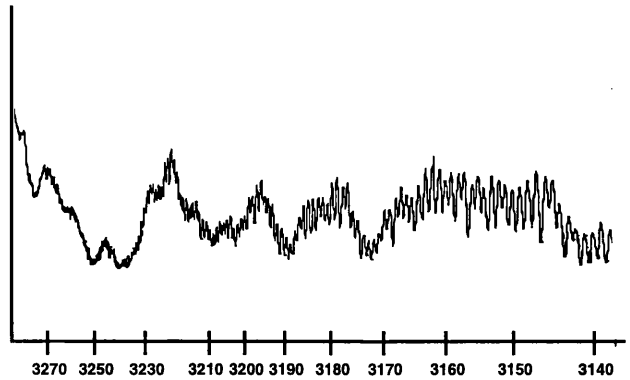

BAM-Im_3 Lane

Figure 3.15. Densitometric scans from the gel in Figure 3.10. (a), control lane c; (b), Im_3 lane k; (c), BAM-$(Im)_3$ lane j.

3.3.5 The Effect of pH on the Alkylation Specificity of the Pyrrole- and Imidazole-BAM Conjugates

The effect of pH on the alkylation specificity of the diimidazole- and triimidazole-BAM conjugates and the tripyrrole-BAM conjugate was examined by carrying out the drug: DNA incubations in buffers of pH 5.0, 7.2, or 9.3. The primer extension was then performed in identical manner and damage to the top strand of the AT-rich region was compared. The tripyrrole-BAM conjugate alkylated the preferred site, 5′-TTTTGG (3193), with equal intensity at pH 5.0, 7.2, or 9.3 (Figure 3.16, lanes h, i, and j, respectively). Additionally, the alkylation specificity and intensity seen for the tripyrrole-BAM conjugate in the 43 base pair stretch from 3230-3274 was unaffected (data not shown). Incubation at acidic pH introduced additional sites of alkylation for the tripyrrole-BAM conjugate, which included 5′-AACGAA (3171) and, to a lesser extent, AAGGGA (3187) immediately upstream of the 5′-TTTTGG site (Figure 3.16, lane h). One additional site at pH 5 was seen in the unresolvable region on the gel, but the alkylation pattern was otherwise unaffected in comparison to neutral or basic pH. There were no detectable changes in the alkylation specificity or intensity between pH 7.2 and pH 9.3. The alkylation pattern for BAM in the pH range studied showed essentially no difference in the alkylation pattern and intensity (data not shown).

Figure 3.16. ***Taq*** **polymerase gel comparing the effect of pH on damage to the top strand of the AT-rich region caused by BAM-$(Im)_2$, BAM-$(Im)_3$ and BAM-$(Py)_3$. Lane a, control; lane b, BAM-$(Im)_2$, 5 μM, pH 5.0; lane c, BAM-$(Im)_2$, 5 μM, pH 7.2; lane d, BAM-$(Im)_2$, 5 μM, pH9.3; lane e, BAM-$(Im)_3$, 5 μM, pH 5.0; lane f, BAM-$(Im)_3$, 5 μM, pH 7.2; lane g, BAM-$(Im)_3$, 5 μM, pH9.3; lane h, BAM-$(Py)_3$, 5 μM, pH 5.0; lane i, BAM-$(Py)_3$, 5 μM, pH 7.2; lane j, BAM-$(Py)_3$, 5 μM, pH9.3. Drug: DNA incubations were for 5 hours at 37° C.**

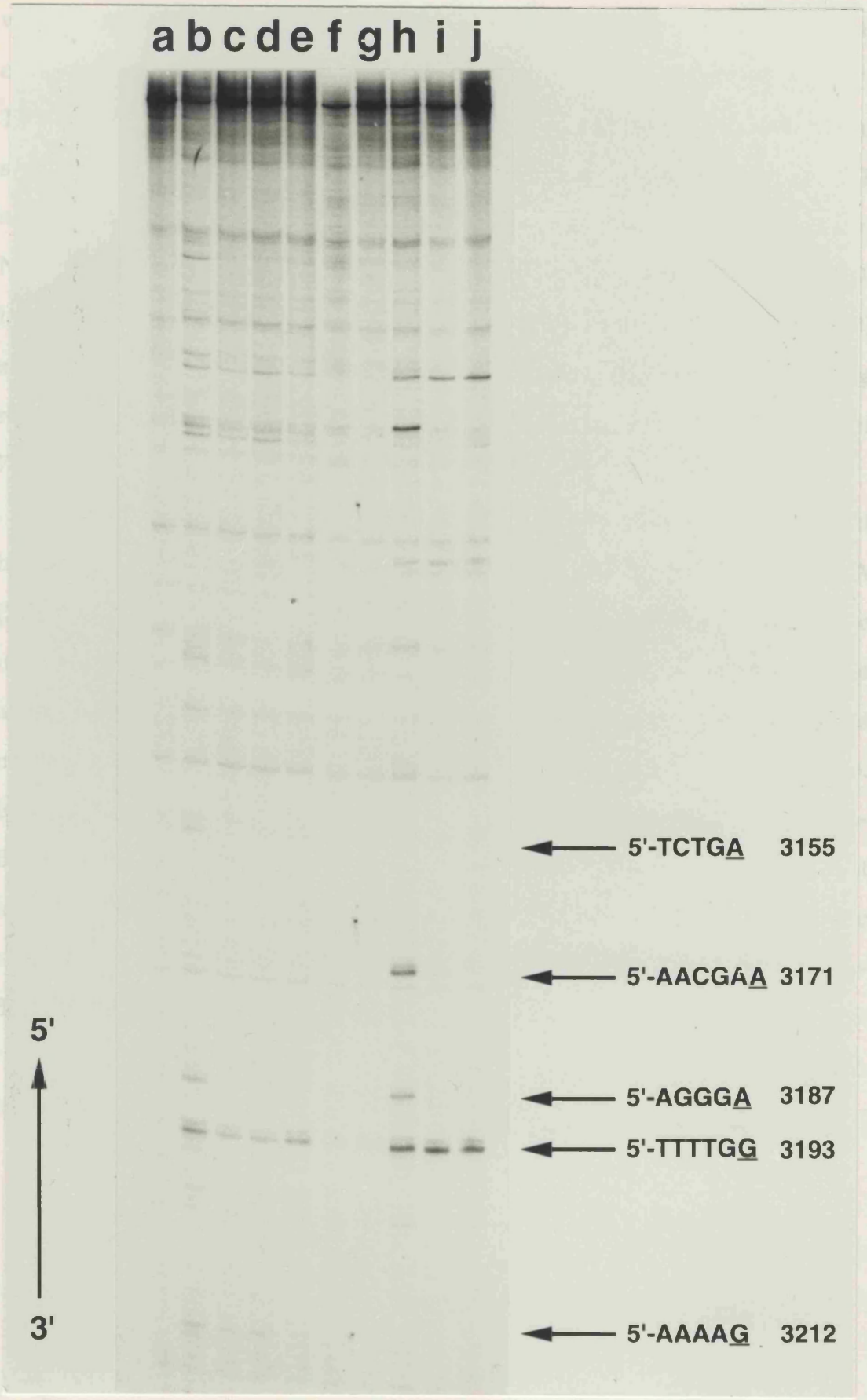
a b c d e f g h i j
5'-TCTGA 3155
5'-AACGAA 3171
5'-AGGGA 3187
5'-TTTTGG 3193
5'-AAAAG 3212
5'
3'

The alkylation specificity seen for the diimidazole-BAM conjugate was affected by pH in the following ways. The change from acidic to neutral or basic pH decreased the alkylation intensity at the preferred site 5'-TTTTGG (3193) by at least 2-fold (lanes b, c, d, pH 5.0, 7.2, 9.3). The alkylation seen at 5'-AAAAG site at (3212), as well as the alkylation seen in the AT stretch from 3230-3273 (data not shown), was affected in identical manner. New sites were alkylated by the diimidazole-BAM conjugate at pH 5.0, including AGGGA (3187) immediately upstream of the 5'-TTTTGG (3193) site, and, to a lesser extent, 5'-TCTGA (3155) (Figure 3.16, lane b). There were no noticeable changes in the alkylation specificity or intensity between pH 7.2 and pH 9.3.

The alkylation seen for the triimidazole-BAM conjugate was reduced by at least 2-fold at the preferred 5'-TTTTGG site (3193) and at 5'-TTTTAA (3254, data not shown) by the change from pH 5.0 to pH 7.2. At the dose used for the triimidazole-BAM conjugate, it did not appear that new sites of alkylation were introduced at pH 5.0. There were no detectable differences in the alkylation specificity or intensity between pH 7.2 and pH 9.3. Examination of the alkylation specificity for the tripyrrole- and triimidazole-BAM conjugates in the GC-rich region over the same pH range did not uncover any lesions for either conjugate (data not shown). Therefore, acidic or basic pH did not introduce new sites of alkylation for the triheterocyclic-BAM conjugates in the GC-rich region.

3.3.6 Comparison of the Alkylation Specificity of the Half-Mustard and Triimidazole-BAM Conjugates

The covalent sequence specificity of the half-mustard triimidazole conjugate was directly compared to the triimidazole-BAM conjugate using the *Taq* polymerase stop assay. When examined in the GC-rich region, the half-mustard conjugate alkylated selected guanines in the region (Figure 3.17, lane c), in contrast to the triimidazole-BAM conjugate, which showed no detectable alkylation in the region at the doses used (lane e). The strongest sites of alkylation were 5'-GGG (546) and AGC (495) and the half-mustard conjugate appeared to be more specific than CHL or BAM.

Examination of the AT-rich region clearly shows that the half-mustard conjugate and triimidazole-BAM conjugate have different patterns of alkylation (Figure 3.18). A higher drug dose was required in order to produce similar amounts of damage (as judged by the amount of full-length undamaged template) for the half-mustard conjugate compared to the triimidazole-BAM conjugate. It is interesting to note that the half-mustard conjugate does not alkylate at the 5'-TTTTGG site favoured by the BAM conjugates (Figure 3.18, lanes d and e). Nor does it alkylate at the sites within the AT stretch from 3230-3273 that were alkylated with varying intensity by the BAM conjugates (data not shown), but there was one strong shared site of alkylation in the unresolvable region of the gel. At the highest drug dose, the strongest alkylation was in a run of four guanines (3147-50), while other guanines were alkylated to a lesser extent (Figure 3.18, lane e).

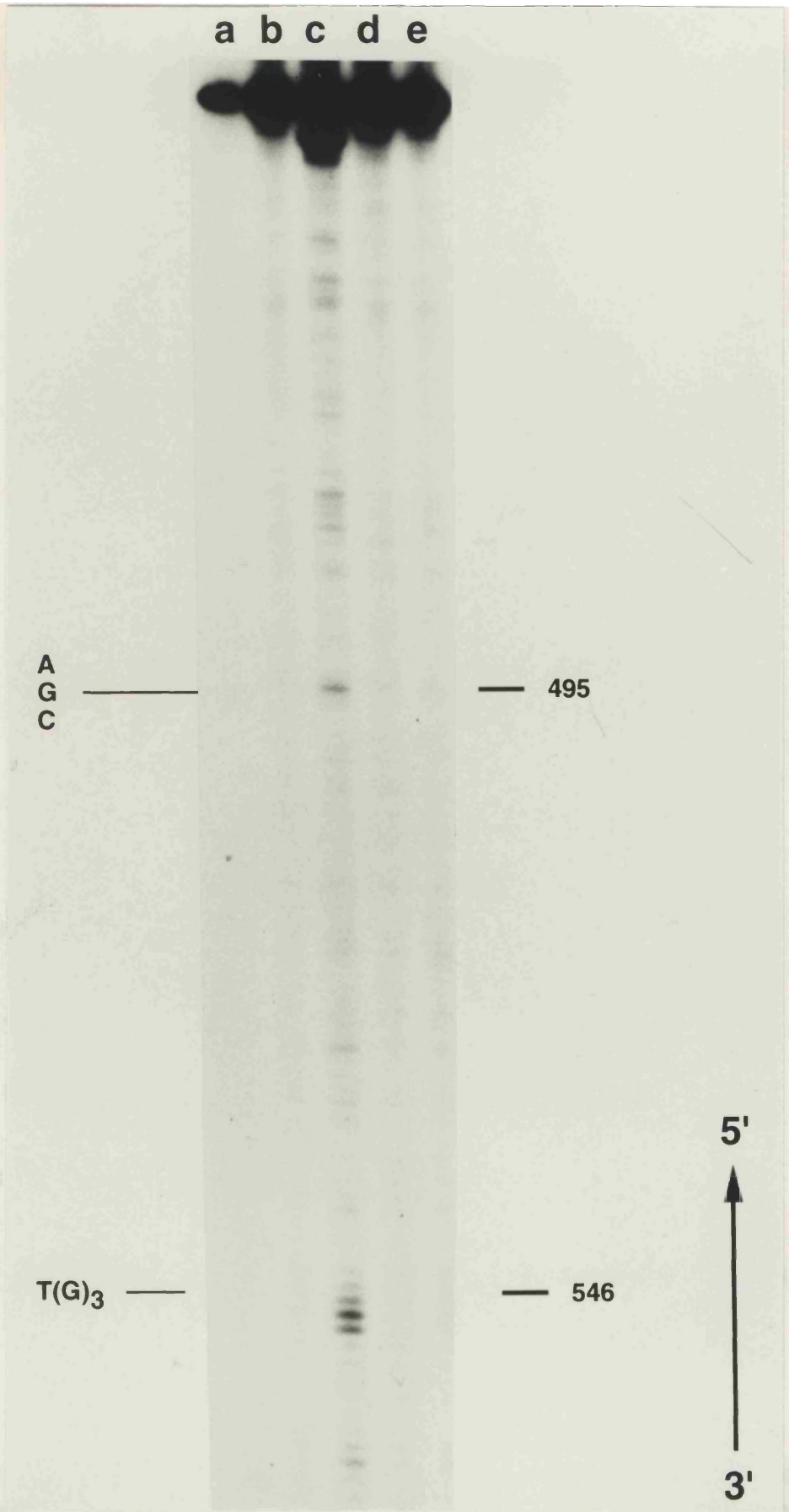

Figure 3.17. *Taq* polymerase gel comparing damage to the top strand of the GC-rich region caused by the half-mustard conjugate and BAM-$(Im)_3$. Lane a, control; lane b, half-mustard, 1 μM; lane c, half-mustard, 10 μM; lane d, BAM-$(Im)_3$, 1 μM; lane e, BAM-$(Im)_3$, 10 μM. Drug: DNA incubations were for 5 hours at 37° C.

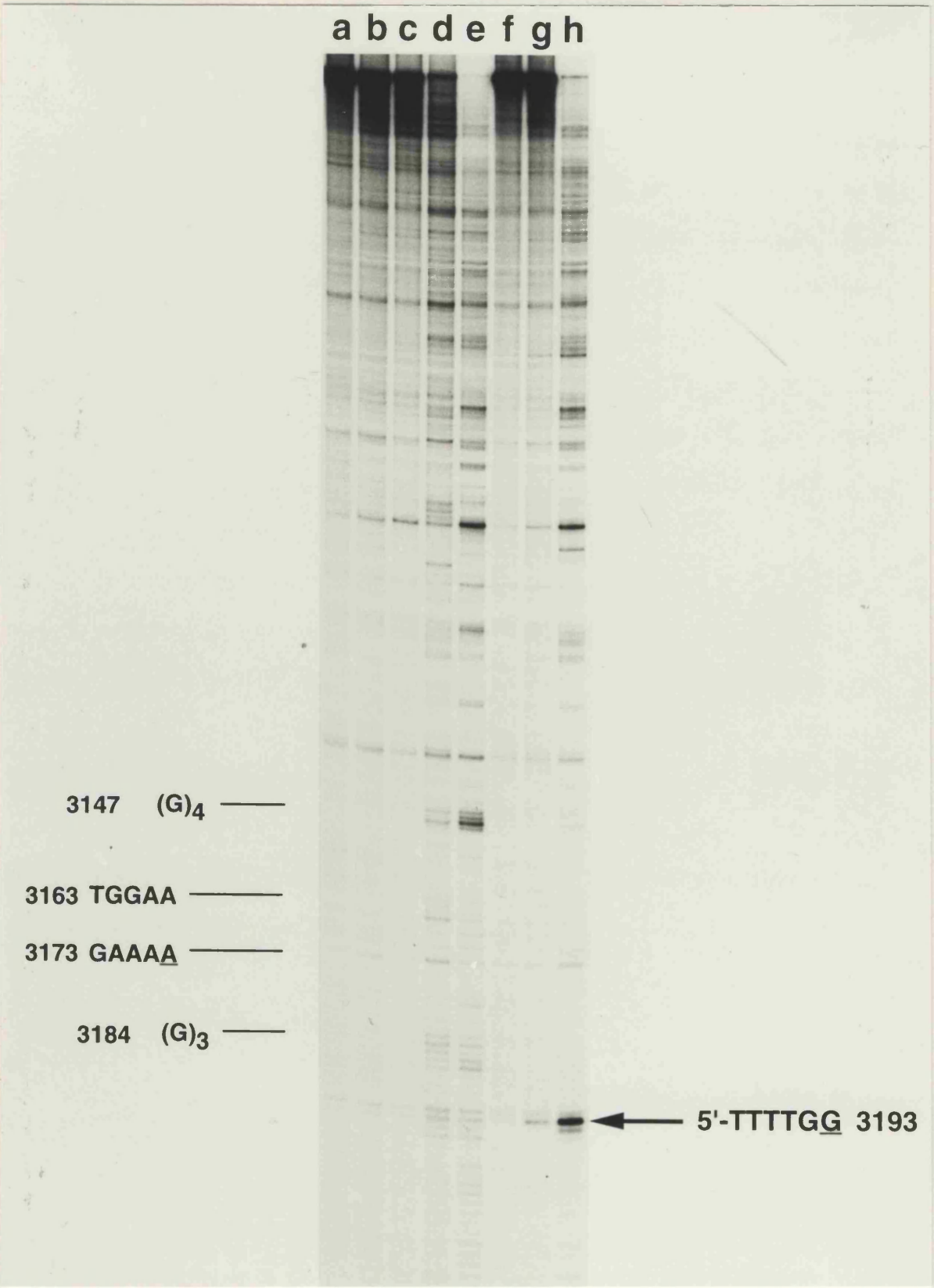

Figure 3.18. *Taq* polymerase gel comparing damage to the top strand of the AT-rich region caused by the half-mustard triimidazole conjugate and BAM-$(Im)_3$. Lane a, control; lane b, half-mustard, 0.1 μM; lane c, half-mustard, 1 μM; lane d, half-mustard, 10 μM; lane e, half-mustard, 50 μM; lane f, BAM-$(Im)_3$, 0.1 μM; lane g, BAM-$(Im)_3$, 1 μM; lane h, BAM-$(Im)_3$, 10 μM. Drug: DNA incubations were for 5 hours at 37° C.

3.3.7 CHL and the CHL Conjugates

The sequence specificity of CHL and the CHL conjugates was examined on the GC-rich region of pBR322 DNA (375-640) using the *Taq* polymerase stop assay. At a concentration of 100 μM, CHL produced a pattern of alkylation consistent with that seen for BAM. The dose used, however, was 5-fold lower than that used for BAM, indicative of the greater reactivity of CHL. The predominant sites of alkylation were guanines within runs of guanines and in the sequence 5'-TGG (Figure 3.19, lane c) and the pattern was nearly identical to that seen for BAM. The inclusion of equimolar amounts of distamycin did not alter the alkylation pattern of CHL (Figure 3.19, lanes d and e).

The diimidazole- and triimidazole-CHL conjugates were found to produce equivalent amounts of damage at a 10-fold lower dose than CHL (Figure 3.20, lanes c-f). However, the alkylation pattern was similar to that seen for CHL, and the lesions were confirmed as guanine-N7 lesions using the piperidine cleavage assay (data not shown). The dipyrrole- and tripyrrole-CHL conjugates also produced an alkylation pattern at a 10-fold lower dose that was similar to CHL, but with one obvious exception. A strong band was clearly evident within the sequence 5'-AGA (466-8) (Figure 3.20, lanes h and j).

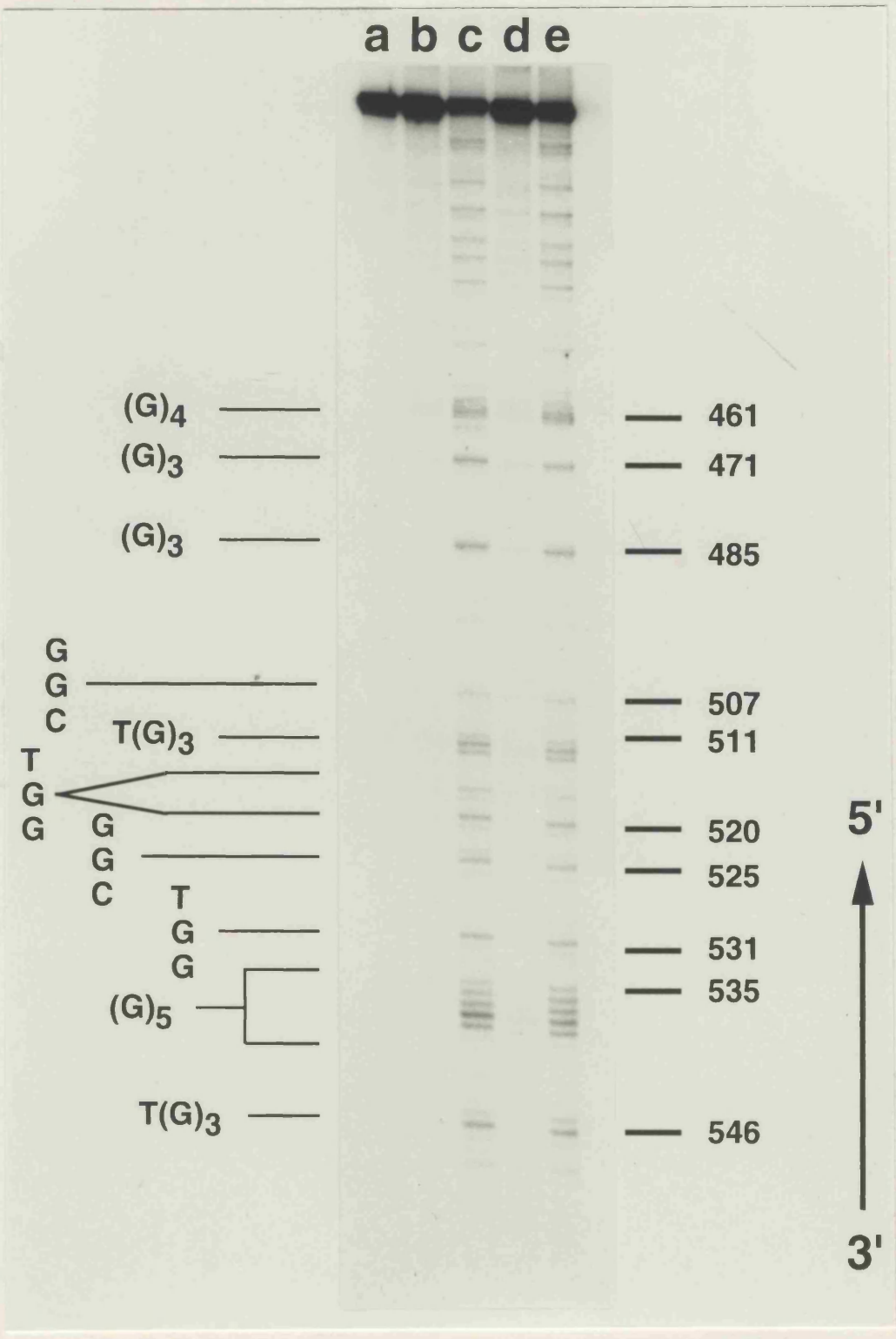

Figure 3.19. *Taq* **polymerase gel examining damage to the top strand of the GC-rich region caused by CHL alone or in the presence of distamycin. Lane a, control; lane b, distamycin 100 μM; lane c, CHL, 100 μM; lane d, CHL + distamycin, 10 μM; lane e, CHL + distamycin, 100 μM. Drug: DNA incubations were for 2 hours at 37° C.**

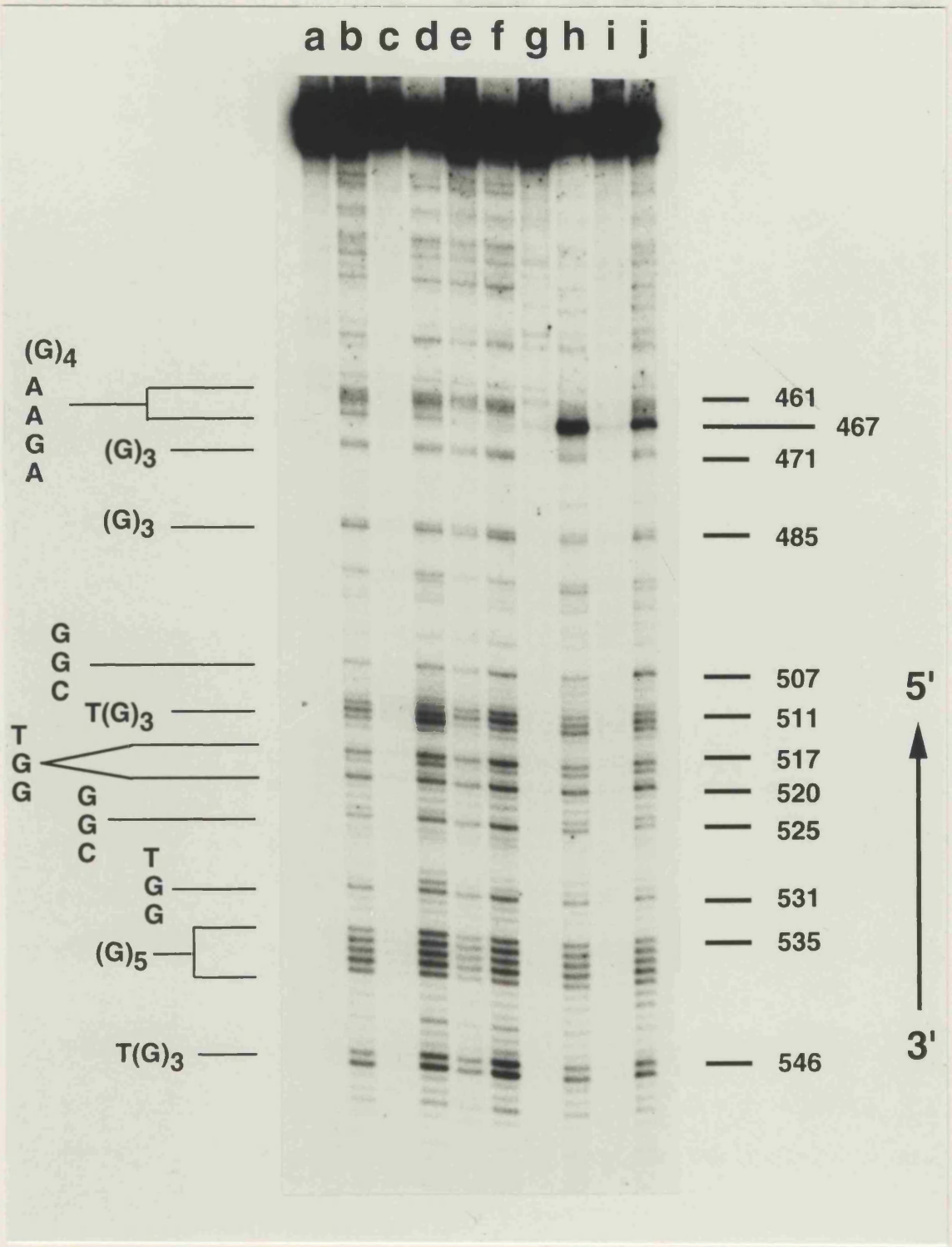

Figure 3.20. *Taq* polymerase gel examining damage to the top strand of the GC-rich region caused by the CHL conjugates. Lane a, control; lane b, CHL, 100 μM; lane c, CHL-$(Im)_2$, 1μM; lane d, CHL-$(Im)_2$, 10 μM; lane e, CHL-$(Im)_3$, 1 μM; lane f, CHL-$(Im)_3$, 10 μM; lane g, CHL-$(Py)_2$, 1 μM; lane h, CHL-$(Py)_2$, 10 μM; lane i, CHL-$(Py)_3$, 1 μM; lane j, CHL-$(Py)_3$, 10 μM. Drug: DNA incubations were for 2 hours at 37° C.

The guanine-N7 alkylation pattern of CHL (Figure 3.21a, lane g), and the dipyrrole- and tripyrrole-CHL conjugates (lanes d and f, respectively) was confirmed using the piperidine cleavage assay. Interestingly, however, neither CHL or the pyrrole-CHL conjugates alkylated the N7 position of the guanine (467) shown to be strongly alkylated by the *Taq* polymerase stop assay. In order to determine whether the lesions produced by the pyrrole-CHL conjugates at the site (466-8) in Figure 3.20 were minor groove lesions, the thermal cleavage assay was used, and the results are shown in Figure 3.21b. The dipyrrole-CHL conjugate clearly produced a doublet at the site, alkylating both the adenine- and guanine-N3 positions (466-7) (Figure 3.21b, lane e). The tripyrrole-CHL conjugate only strongly alkylated the guanine-N3 position (Figure 3.21b, lane f). The strong bands that appeared on the *Taq* stop assay gel within the sequence 5′-AAGAT were thus assigned as minor groove adenine-N3 and guanine-N3 lesions. Aside from the strong bands which appear at the AG (466-7) site for the di- and tripyrrole conjugates, there are several other weaker bands on the thermal cleavage gel at the higher drug concentration used. These bands nearly all correspond to guanines identified as guanine-N7 lesions from the piperidine gel (Figure 3.21a). It is possible that there may be weak alkylation in the minor groove at these sites, but the heat treatment may induce a background depurination and strand breakage at guanine-N7 alkylated sites. With the exception of the unique minor groove site of alkylation for the pyrrole-CHL conjugates, the CHL conjugates largely retain the alkylation specificity of the CHL group.

Figure 3.21a. Piperidine cleavage gel showing guanine-N7 lesions to the top strand of the GC-rich region caused by the CHL-Py conjugates. Lane a, control piperidine treated; lane b, G+A marker lane (formic acid); lane c, CHL-$(Py)_2$ 0.5 μM; lane d, CHL-$(Py)_2$ 5 μM; lane e, CHL-$(Py)_3$, 0.5 μM; lane f, CHL-$(Py)_3$, 5 μM; lane g, CHL 100 μM. Drug: DNA incubations were for 2 hours at 37° C.

Figure 3.21b. Thermal cleavage gel showing purine-N3 lesions to the top strand of the GC-rich region caused by the CHL conjugates. Lane a, control heat treated; lane b, G+A marker lane (formic acid); lane c, CHL-$(Py)_2$, 1 μM; lane d, CHL-$(Py)_3$, 1 μM; lane e, CHL-$(Py)_2$, 10 μM; lane f, CHL-$(Py)_3$, 10 μM.

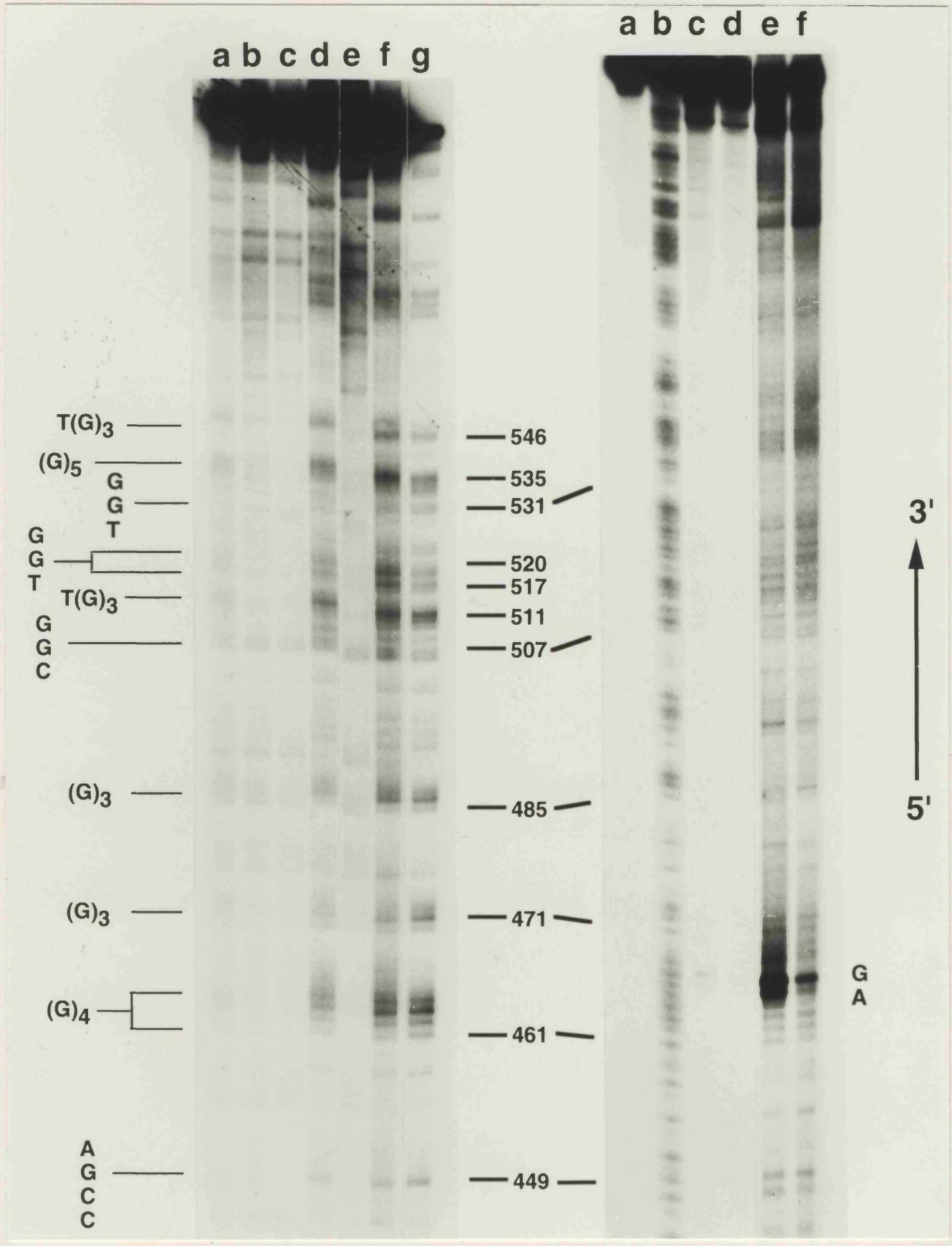

Figure 3.21a.

Figure 3.21b.

3.4 Discussion

Conventional nitrogen mustards have been shown to alkylate guanines preferentially in runs of guanines (Mattes, *et al.*, 1986a), and this has been confirmed using the *Taq* polymerase stop assay (Ponti, *et al.*, 1991). The electrostatic potential of guanine surrounded by different combinations of base pairs were the most electronegative when guanine was surrounded by two guanines, and this roughly correlates with the sequence specificity of guanine-N7 alkylation seen for the nitrogen mustards (Kohn, *et al.*, 1987). There have been reports of adenine-N3 alkylation by the aromatic nitrogen mustards melphalan and chlorambucil (Pieper & Erickson, 1990; Wang, *et al.*, 1991), and the adenine-N3 alkylation seen for CHL was inhibited by the inclusion of distamycin (Wang, *et al.*, 1994). The results from the *Taq* stop assay with or without the inclusion of distamycin and the results from piperidine cleavage assay do not disprove that BAM and CHL can alkylate adenine-N3 positions, but suggest that guanine-N7 lesions are the predominant lesions formed at the doses used for CHL and BAM in both regions. This consisted of guanines within runs of guanines and in the sequence 5′-TGG. BAM and CHL showed essentially no difference in their sequence specificity. The agents do differ in the dose required to produce similar amounts of damage, which is 5-fold less for CHL. A longer incubation time was used for BAM in order to provide a direct comparison with the BAM conjugates, but there was no indication that the longer incubation time affected either alkylation specificity or intensity. The higher reactivity of CHL does not produce an altered sequence preference compared to BAM.

The 10-fold lower doses for the diimidazole- and triimidazole-CHL conjugates which produced similar amounts of damage compared to CHL indicates a more efficient delivery of the nitrogen mustard group to the DNA. The sequence preference of the CHL group, however, has not been

altered by the lexitropsin portion. The alkylation pattern for the diimidazole- and triimidazole-CHL conjugates is nearly identical to that seen for CHL. The guanine-N7 alkylation pattern for the pyrrole-CHL conjugates, which comprised the majority of the total alkylation, is similar to that seen for CHL. The exception was a unique site (466-7) strongly alkylated by the pyrrole conjugates, but not by the imidazole conjugates or CHL. The alkylation at this site was assigned as minor groove adenine- and guanine-N3 lesions, based upon the results of the thermal cleavage assay. The same technique confirmed the presence of a guanine-N3 lesion, originally detected by a DNA polymerase stop assay, formed by the minor-groove specific and CPI-containing natural product duocarmycin A (Mitchell, *et al.*, 1993) and the guanine-N3 lesions of duocarmycin have been isolated by HPLC (Asai, *et al.*, 1994). All other alkylation seen on the *Taq* stop gel was assigned as guanine-N7 alkylation. It would therefore appear that while the overall alkylation pattern is essentially guanine-N7 alkylation reminiscent of CHL, the lexitropsin portion has contributed to the introduction of a novel site of alkylation. Because the site is not preferentially alkylated by the imidazole-CHL conjugates, it is assumed that the effect is specific for the AT-binding pyrrole lexitropsins. It would be difficult to offer a rationale for the strong alkylation preference seen for the AG bases within the extended 5′-AAGATC sequence. The AT-rich stretch of five base pairs with a single GC base pair would be a potential non-covalent binding site for the di- and tripyrrole lexitropsin moiety. The alkylation, however, occurs in the middle of the binding site and the sequence to the 5′-end is a $(G)_4$ tract and $(G)_3$ on the 3′-end. It may be possible that the site offers a unique conformation that allows for tight minor groove binding by the pyrrole conjugates, while simultaneously accommodating the flexibility of the $(CH_2)_3$ linker of CHL such that the central G and A sites are alkylated.

Comparison of the sequence specificity of the pyrrole-BAM conjugates versus the pyrrole-CHL conjugates clearly reveals that the less reactive mustard has been targeted more effectively. The CHL portion of the conjugates is being delivered to the DNA more efficiently than when not conjugated to a DNA-binding agent (as judged by the 10-fold lower doses required to produce similar amounts of damage), but the delivery is not in a sequence specific manner. The fact that the CHL alkylation pattern is maintained in spite of the lexitropsin portion suggests that CHL is too reactive a nitrogen mustard to be exclusively targeted to the minor groove by the lexitropsin framework. In addition, the flexibility the CHL moiety possesses due to the $(CH_2)_3$ linker may be detrimental. The BAM portion is fixed relatively planar in comparison to the lexitropsin portion, and this presumably places an additional requirement on the alkylation event. It has been shown by modelling that, although the triimidazole lexitropsin portion can sit in the minor groove, it is still possible for the CHL portion to intercalate between the base pairs, placing the bis-(chloroethyl)amino group in proximity to the guanine-N7 position (Lee, *et al.*, 1993b). In light of the similarities between the alkylation pattern for CHL and the pyrrole-CHL conjugates, it seems more likely that the reactivity of the CHL portion is the ultimate determinant of the sequence specificity of alkylation for the CHL conjugates.

In a GC-rich stretch of DNA, the monopyrrole-BAM conjugate clearly shows a pattern of alkylation qualitatively similar to BAM itself, albeit at 50-fold lower doses. This difference may simply be due to the cationic C-terminus of the lexitropsin portion and its affinity for DNA. BAM alkylated guanines in the AT-rich region in a consistent manner with conventional nitrogen mustards. In the same AT-rich fragment, however, the monopyrrole conjugate preferentially alkylated sites in the minor groove, as detected by the *Taq* polymerase stop assay. The minor groove lesions were

confirmed as adenine-N3 and guanine-N3 lesions using the thermal cleavage assay. Interestingly, the sequence 5'-TTTTAA is not alkylated to the same extent in all three occurrences in this region, implying that the sequence conformation of the neighbouring regions might also play a role in the alkylation event.

The dipyrrole- and tripyrrole-BAM conjugates possess a higher non-covalent affinity for DNA, as measured by an ethidium displacement assay (Wyatt, *et al.*, 1994a), and show little if any retention of the alkylation preference of BAM. Alkylation is limited to labile sites in the minor groove of AT-rich sequences where the lexitropsin preferentially binds. The increase in the reading frame portion of the molecule by the addition of a third pyrrole-amide group offers a corresponding increase in the sequence specificity of alkylation. The alkylation pattern is similar to the dipyrrole conjugate, but strong alkylation only occurs at two very similar sites, inferring that the third pyrrole group places an additional requirement on the alkylation event. This is most closely met by the consensus sequence 5'-TTTTGPu.

The alkylation specificity of tallimustine, determined using the thermal cleavage assay, was confirmed using the taq polymerase stop assay. In addition to the alkylation seen at an occurrence of 5'-TTTTGA in the AT-rich region, alkylation was also clearly evident at 5'-TTTTGG and one of three occurrences of 5'-TTTTAA. The alkylation pattern is very similar to the tripyrrole-BAM conjugate, but the relative intensities of alkylation seen are different. It is interesting to note that tallimustine strongly alkylated at the 5'-TTTTAA site on the bottom strand that was only weakly alkylated by the tripyrrole-BAM conjugate. However, two occurrences of 5'-TTTTAA on the top strand were weakly alkylated, if at all, and this agreed with the results for the tripyrrole-BAM conjugate. The non-covalent sequence specificity for tallimustine and the tripyrrole-BAM conjugate was very

similar, although tallimustine appears to bind with a higher affinity and some sites that were weak sites for tallimustine were missed by the tripyrrole-BAM conjugate. Both tallimustine and the tripyrrole-BAM conjugate non-covalently bound the same sites that were strongly bound by distamycin, which were AT-rich regions flanked by a GC base pair. Distamycin additionally footprinted at several sites that were missed by tallimustine and the tripyrrole-BAM conjugate.

The incorporation of the C-terminal dimethylaminopropyl group instead of the amidinium group has introduced two subtle changes in the binding and alkylating characteristics of the tripyrrole-BAM conjugate compared to tallimustine. It has apparently lowered the affinity, while not appreciably affecting the non-covalent sequence specificity of the tripyrrole-BAM. The strong alkylation by tallimustine at one of three occurrences of the sequence 5'-TTTTAA is the other change. It may be that the difference in intensity of alkylation seen for tallimustine is affected by its higher non-covalent binding affinity. A higher non-covalent binding affinity may not explain the fact that two occurrences of 5'-TTTTAA are only weakly alkylated or missed, however. Furthermore, the footprinting studies provide evidence that the alkylation event does not always occur following non-covalent binding. This result is in agreement with the work on *N*-bromoacetyl distamycin, which showed non-covalent binding at several AT sites identically to distamycin, but alkylation at only one of the sites, at the adenine opposite the 3'-T in the sequence 5'-AGTTTA (Baker & Dervan, 1989). The local sequence conformation of the DNA must be crucial in determining whether alkylation is favourable.

In a GC-rich region, the monoimidazole-BAM conjugate alkylated guanines in a similar pattern to BAM, albeit at a 10-fold lower dose, and in agreement with the results seen for the monopyrrole-BAM conjugate. Although the delivery of the nitrogen mustard has been enhanced, the

monoheterocyclic lexitropsin portion does not possess enough of a reading frame to alter the alkylation pattern in the GC-rich region. The diimidazole- and triimidazole-BAM conjugates show little alkylation preference for guanines in the region, indicating that these conjugates no longer possess the alkylation preference of the BAM portion. If one were to strictly predict sites of alkylation based upon the sequence preference of the lexitropsin portion, the footprinting sites on the strand for Im_2 and Im_3 at 5'-$(G.C)_3$(A.T) and 5′-TCGGGCT sequences, respectively, would have been prime candidates. The footprinting studies and the *Taq* stop assay results clearly demonstrate that the di- and triimidazole conjugates do not detectably interact with the GC-rich region. It would initially appear, therefore, that the BAM group has altered the sequence specificity of the imidazole vector.

The results from the AT-rich region proved insightful, if not surprising. The monoimidazole conjugate alkylated guanines in a consistent pattern to that seen for BAM. It also alkylated selected minor groove adenine-N3 sites, but not with the strong preference seen for the monopyrrole-BAM conjugate. The diimidazole- and triimidazole-BAM conjugates alkylated in similar manner to the dipyrrole- and tripyrrole-BAM conjugates. Adenines within AT-rich sequences were the sites of alkylation and the consensus sequence 5′-TTTTG<u>Pu</u> proved to be the site of strongest alkylation for the di- and triimidazole conjugates. It appears that the BAM group has caused a reversion of the imidazole recognition features, predisposing alkylation for AT-rich sites. When examined by MPE footprinting, the triimidazole-BAM conjugate did not show detectable non-covalent interactions.

The effect of pH on the intensity of alkylation seen for the BAM conjugates introduced another consideration for the lexitropsin conjugates. Additional sites were clearly alkylated at a pH of 5 for both pyrrole- and imidazole-BAM conjugates. The intensity of alkylation for the tripyrrole-

BAM conjugate at the preferred site on the strand, 5'-TTTTGG (3193) was not affected by the change in pH. The alkylation seen for the diimidazole- and triimidazole-BAM conjugates, however, was reduced by at least 2-fold at neutral or basic pH compared to a pH of 5. Demonstration of a pH effect logically suggests that protonation is involved, and that this effect markedly alters the alkylation event for the imidazole-BAM conjugates at the preferred sites of alkylation.

Replacement of the bis-(chloroethyl)amino group with a chloroethylamino group produced an analogue with a substantially altered sequence specificity of alkylation. Most interestingly, the half-mustard analogue did not alkylate at the sequence 5'-TTTTGG which was preferentially alkylated by both imidazole and pyrrole-BAM conjugates. This suggests that the substitution of the second chloroethyl arm with a hydrogen has either altered the specific interactions that occur in the minor groove prior to alkylation or it has altered either the formation or reactivity of the aziridinium group, which affects the alkylation event. If proton loss occurs following aziridinium formation for the half-mustard conjugate, then the cationic charge is lost. This could possibly explain the difference in the sequence specificity of alkylation seen for the half-mustard conjugate compared to the triimidazole-BAM conjugate.

Two strong explanations for the alkylation specificity of the diimidazole- and triimidazole-BAM conjugates would be either an increase in the cationic nature of the imidazole conjugates, or a structural feature of the DNA that ideally suits both pyrrole- and imidazole-containing lexitropsins. There are two possibilities of increasing the cationic nature of the imidazole conjugates. The first is that the formation of an aziridinium on the mustard portion adds additional positive charge to the lexitropsin. As mentioned in Chapter 1, the minor groove of AT-rich regions are more electronegative than the minor groove of GC-rich regions. The first generation of imidazole containing lexitropsins were dicationic and they

retained a preference or 'memory' for AT-rich sites. The removal of the C-terminal cationic group created a lexitropsin which preferentially bound to GC-rich sites, and the monocationic Im_2 and Im_3 lexitropsins preferentially bind to GC-rich sequences. It could be argued that because aziridinium ion formation adds to the cationic nature of the molecules, the bias for AT-rich sequences is being re-introduced to the imidazole conjugates, causing a reversal of the non-covalent sequence specificity and predisposing the alkylation event towards AT-rich sites. Alternatively, the cationic nature of the imidazole conjugates could be increased by protonation of the imidazole-N3 nitrogens. Not only would this add to the cationic nature of the conjugates, but the presence of a hydrogen on the imidazole would reintroduce the steric clash that occurs with the guanine-2-NH_2 hydrogens. The fact that the alkylation intensity for the diimidazole- and triimidazole-BAM conjugates at the preferred site was affected by pH, but the alkylation intensity of the tripyrrole-BAM conjugate was not affected might suggest this possibility.

If a complete reversal of the sequence specificity of the imidazole BAM conjugates due to an increase in the cationic nature has occurred, however, then there are several inconsistencies that are evident. An effect of protonation on the imidazole groups should also be seen for the non-alkylating imidazole lexitropsins, but Im_2 and Im_3 clearly and preferentially bind to GC-rich sequences. Even when examined in the AT-rich region, the Im_3 lexitropsin footprinted to different sequences compared to distamycin, and the strongest site contained a G_3 tract and 3'-terminal AT base pair. If the added cationic nature of the aziridinium were the sole explanation, one might expect the monoimidazole-BAM conjugate to behave similarly to the monopyrrole conjugate. The sites strongly alkylated by the monopyrrole-BAM conjugate within the 43 base pair AT stretch are only weakly alkylated, if at all, by the monoimidazole-BAM conjugate. Additionally, the aziridinium is only a transiently formed reactive intermediate and

presumably would not remain long enough to effect the binding characteristics. Lastly, one might expect the triimidazole-BAM conjugate to non-covalently recognise AT-rich sites similarly to the tripyrrole-BAM conjugate, but it does not footprint at either AT- or GC-rich sequences.

The second explanation is that structural aspects of the DNA in addition to the base pair composition (i.e., either AT or GC) dictate the alkylation specificity seen by both the pyrrole- and imidazole-BAM conjugates. Specifically, the local sequence conformation may either offer a unique groove shape that allows for particularly tight non-covalent binding by all lexitropsins, or the local conformation may determine whether alkylation is favourable by serving as a catalyst for the alkylation event. Pyrrole-containing compounds do not bind to GC-rich sequences due to steric clashes that occur between hydrogens on the drug and guanine-2-NH_2 group. Imidazoles do not have hydrogens that protrude from the concave face of the molecules, and hence can favourably interact with GC-rich sequences. The imidazoles can still bind to AT base pairs, however. Aside from potential hydrogen bonding that can occur between the guanine-2-NH_2 groups and the imidazole nitrogens on the concave face of the lexitropsin, imidazole lexitropsins lack the ability to discriminate between AT and GC sites. The major structural determinant for the alkylation event, then, may be groove width and shape. These values, as mentioned in the introduction, are different for AT- and GC-rich sequences.

Within the past 15 years the paradigm of B-DNA as structurally homogeneous has been substantially altered and a renewed interest in DNA structure determination has occurred. The ability to synthesise oligodeoxynucleotides of known sequence in milligram quantities allowed for detailed examination of DNA structure by single crystal X-ray studies and high-field NMR. Additionally, a naturally occurring kinetoplast DNA with anomalous electrophoretic and biophysical properties was found to be

intrinsically bent (Marini, *et al.*, 1982). The bending was proposed to be due to the phased distribution of A-tracts at 10 base pair intervals (Crothers, *et al.*, 1990). It is now well known from X-ray crystallography and high-field NMR studies that DNA stretches of differing A.T/G.C content have different conformational flexibilities and that A-tracts are distinct in this respect.

In addition to the techniques of NMR and X-ray crystallography, the utilisation of chemical probes to study the local sequence conformation of A-tracts within longer fragments of DNA has provided useful information. It has been shown that DNA containing phased A tracts is not cleaved randomly by hydroxyl radical (Burkhoff & Tullius, 1987). The reactivity of the hydroxyl radical species gradually decreased from the 5'- to 3'- direction along each A tract and the authors proposed that this was due to a progressive narrowing of the width of the minor groove. The pattern was very reproducible and occurs in A tracts surrounded by DNA of mixed content. A study of the visible-light induced cleavage of DNA by the intercalator ethidium bromide (EtBr) showed that EtBr bound A tracts poorly, while also binding the ends of the A tracts tightly (Krishnamurthy, *et al.*, 1990). Chemical cleavage studies utilising $KMnO_4$, which attacks the 5-6 double bond of thymine from above or below the base, and DEPC, which attacks the purine-N7 position with a strong preference for adenines, found similar results (McCarthy, *et al.*, 1990). While most thymines were randomly cleaved following treatment with $KMnO_4$, thymines within T tracts, i.e. those in a stacked arrangement, were protected from cleavage. The exception was the 3'-T, implying that the stacked arrangement abruptly changes at this base pair. DEPC was found to induce cleavage at all adenines in A tracts, except for the 3'-adenine (McCarthy, *et al.*, 1990). A minimum of 3 base pairs in the A tract was necessary. Studies on the naturally bent kinetoplast DNA using the same chemical probes found that "a 5'-TG step favours a highly stacked conformation." Furthermore, the authors

proposed that "the A tract function 5'-TG-3' acts to accentuate the overall bend of an A tract" (McCarthy, *et al.*, 1993).

An additional benefit to the MPE footprinting studies performed on the AT-rich region is that the cleavage pattern of the MPE alone offers insight into the local DNA conformation in similar manner to the above mentioned chemical probes. The densitometry of the MPE cleavage of the AT-rich region, shown in Figure 3.11, offers clear indication of local sequence-dependent variation in DNA conformation. Cleavage induced by MPE is suppressed at A or T tracts of 4 or more base pairs. The 43 base pair stretch of DNA from 3230 to 3273 is unique. In addition to the fact that there are only five GC base pairs within this stretch, there are two T_4 tracts, three A_3 tracts and an A_5 tract. The MPE induced cleavage of this area is greatly suppressed, strongly suggesting that the region possesses an unusual conformation. The cleavage throughout the fragment occurred most efficiently in stretches of mixed AT/GC content. It is clear that the intercalator MPE behaves similarly to EtBr, in that binding to A tracts is reduced compared to DNA of mixed composition.

Distamycin footprints AT-rich sites, some of which possess a 3'-terminal GC base pair. Close examination of the previously reported footprinting studies of distamycin would not suggest that the specific site 5'-TTTTG is bound with an enhanced or preferential non-covalent binding compared to other binding sites of similar composition. The strong site for alkylation on this strand, 5'-TTTTGG, lies outside the AT stretch mentioned above and the cleavage of the immediately surrounding base pairs is relatively uniform. Cleavage is clearly suppressed within the site, indicating it possesses a narrow minor groove that is disrupted by the TG step. Although it is more difficult to interpret the strength of binding due to the suppressed cleavage, it does not appear that the binding that occurs at the 5'-TTTTG site is more favoured or enhanced compared to the other binding sites for distamycin.

Tallimustine and the tripyrrole-BAM conjugate footprinted in similar manner to that seen for distamycin, with the exception that some of the weaker distamycin sites were only weakly footprinted or missed. Non-covalent interactions clearly occurred at the 5'-TTTTGG sequence, but not to any greater extent than those seen at several other AT sites. Nor is there evidence that distamycin preferentially footprinted at the site. The Im_3 lexitropsin does not footprint at the site, but strongly footprints at a nearby GC-rich site. It appears that the strong alkylation seen at the 5'-TTTTGPu sites is not due to an enhanced non-covalent binding of both imidazole and pyrrole-containing analogues, but to a local sequence conformation which enhances the alkylation step once non-covalent binding has occurred.

The strongest sites of alkylation were those containing a 5'-TTTTG step, where the junction bend seen at the junctions of A tracts with mixed DNA is accentuated further by the presence of guanine. The structure and conformation of a number of synthetic oligonucleotides containing 5'-T_4G, 5'-T_4GG and 5'-T_4GA sequences have been investigated by high field NMR and X-ray crystallography studies. NMR [5'-dCCGTTTTGCC-3' (Nadeau & Crothers, 1989), 5'-dGGAAATTTTTGG-3' (Chen, *et al.*, 1992), 5'-dCTTTTGCAAAAG-3' (Searle & Embrey, 1990), 5'-dGCGTTTTG-3' (Walker, *et al.*, 1994), and 5'-dGCATTTTGAAACC-3' (Katahira, *et al.*, 1990)] and X-ray studies [5'-dCGCTTTTTTGCG-3' (Nelson, *et al.*, 1987)] on oligonucleotides containing the 5'-TTTTG-3' sequence indicate significant narrowing (3.8-3.9 Å) and propeller twisting (17-25°) in the minor groove of the T-tract from the 5' to 3' terminus. In addition, at the T-G junction the minor groove width expands to >4.5 Å indicating an abrupt disruption of the compression caused by the stacked A.T base pairs. These results are consistent with junction-induced bending observed for the decamer 5'-CGTTTTGGCC-3' as indicated by its anomalous gel electrophoretic mobilities (Koo, *et al.*, 1986).

The monopyrrole- and dipyrrole-BAM conjugates alkylated at several different sites of varying AT composition. It should be noted that each of

these sites possess a pyrimidine-purine step two nucleotides from the base alkylated. Tallimustine displays the requirement of the T_4 tract, followed by a purine step. The fact that alkylation is seen at only one of three occurrences of 5'-TTTTAA indicates that the sequence itself may not be as important in the alkylation process as the local conformation of the DNA. The alkylation pattern is nearly identical to that seen for the tripyrrole-BAM conjugate and indicates that the change incorporated on the C-terminus of the tripyrrole-BAM conjugate has not affected the sequence specificity of alkylation, but the intensity of alkylation seen at those sites.

It is proposed that the primary determinant of the sequence specificity of alkylation seen for the imidazole and pyrrole-BAM conjugates and tallimustine is the local DNA structural conformation, which is a junction bend caused by the 5'-T_n-Purine step in the sequence. This structural feature, and not the direct drug: DNA base pair contacts, has the greater effect in determining the sequence specificity of alkylation for the BAM conjugates. The 5'-T_n-purine step disrupts the base stacking and may possibly offer an ideal conformational shape that catalyses the alkylation step. Once bound, favourable hydrogen-bonding interactions may occur between electron-rich sites and the amido hydrogen of the carboxamido group which is *para* to the bis-chloroethyl nitrogen. Hydrogen bond formation between an electron-rich site and the amido hydrogen would alter the electron density on the carboxamido group. Through the conjugation of the aniline group, this could possibly catalyse aziridinium formation via an increase in electron density on the nitrogen. This would result in a site-specifically activated alkylation. If this particular hydrogen, bonding interaction was to occur only at the unique sequence conformation then it may offer an explanation as to why strong alkylation occurs for the BAM conjugates or tallimustine at a site where the non-covalent interactions do not appear to be enhanced.

A concise description of the speculative model is as follows: non-covalent interactions occur which allow the drugs to bind to several AT-rich sequences. In the case of the imidazole conjugates, these interactions are very weak. The mono- and diheterocyclic BAM conjugates are not as restricted due to their smaller size and can alkylate at sites that possess a narrow minor groove, followed by a 5'-pyrimidine-purine step. At the specific sequences where a 5'-TG step disrupts the stacking of the thymines and "accentuates the overall bend of the A tract", a unique sequence conformation occurs that allows a favourable hydrogen bond interaction between the amido hydrogen of the carboxamido group *para* to the bis-(chloroethyl) nitrogen and a minor groove electron-rich site, and this catalyses the alkylation event.

CHAPTER FOUR: DISCUSSION

The exponential growth of the field of cellular and molecular biology has provided opportunities to explore many questions of medicine on the molecular level. Molecular medicine can be defined as the discovery of fundamental molecular components that determine normal cellular behaviour, the dissection of aberrant genetic expression or interaction, and the modulation or correction of those aberrations for the purpose of disease prevention and cure (Karp & Broder, 1994). Important processes in the cell cycle, cell signalling, and in the maintenance of the genome's integrity are constantly being discovered. Each of these new processes potentially represent a novel target in diseases where that particular process or function is either impaired, altered or amplified. Modern organic chemistry has proved adaptable enough to be able to synthesise the most complex molecules found in nature. Upon discovery of biologically active molecules, the flexibility to synthesise closely related analogues greatly aids the determination of how changes in a molecule's structure affects its biological activity. If the biological target is an enzyme of defined function, possibly one for which a crystal structure has been solved, or a well-characterised receptor protein, then the task may be challenging but straightforward. Problems concerning interpretation of biological results can quickly arise, however, if the precise nature of the target is not properly understood for both normal and incorrect functions, or worse, if there are other biological targets affected that are not accounted for.

The alkylating agents are potent cytotoxic compounds that can cause serious side effects when used clinically. It is generally presumed that the serious side effects are a result of the chemical reactivity the molecules possess that enable them to modify a host of biological macromolecules. This can presumably affect many different cellular processes and the agents indiscriminately harm both normal proliferating and cancerous cells.

Additionally, the agents are potent carcinogens and mutagens that can have harmful effects on normal chromosomal integrity. In spite of all of the serious drawbacks, however, the alkylating agents are still frequently used in the treatment of cancer, and in combination therapy, can induce long-term remissions and cures in some types of cancer.

Determination of the primary biological target should be the first step in the evaluation of any biologically active agent. The predominance of the evidence suggests that the target for the alkylating agents is DNA. The variety of mechanisms that act to combat endogenous and exogenous DNA damage have only recently been fully appreciated. For instance, the 'cell cycle checkpoint' p53 protein monitors DNA damage and can block progression through the cell cycle to either allow repair to occur or initiate a programmed cell death in order to prevent a cell with a damaged genome to replicate. The fact that a mutant form of this protein is found in many different types of cancer indicates its importance in DNA damage recognition (Lane, 1992). The variety of DNA repair pathways that act to repair DNA damage combine to maintain the integrity of the chromosomes. All of the above underscores the prime importance of DNA and its protection from damaging events.

There are a host of possibilities now being explored in attempt to better target the agents of chemotherapy and modulate their side effects. The premise of antibody directed enzyme prodrug therapy (ADEPT) is the conjugation of an enzyme to an antibody specific for cancer cells. The prodrug is then given and the targeted enzyme produces the active drug specifically at the tumour site (Kerr, *et al.*, 1995; Springer & Niculescu-Duvaz, 1995). Alternatively, prodrugs that are activated by local conditions, such as hypoxia or pH changes, have been developed (Stevens & Newlands, 1993; Denny, *et al.*, 1994b). If some of these approaches rely on a DNA

damaging event for cell kill, however, understanding drug: DNA interactions in isolated and cellular DNA remains extremely important. The mechanism of action for the nitrogen mustards is presumed to be the formation of interstrand cross-links. Additionally, it is well known that the nitrogen mustards possess a) a high chemical reactivity; b) a poor DNA binding affinity; c) a modest sequence preference for guanines within runs of guanines, although they can modify most of the nucleophilic groups on DNA with varying rates; and d) they are susceptible to detoxification by cellular mechanisms that act to protect the cell and the integrity of the genome.

Assuming that the most probable target is DNA and that the currently used alkylating agents possess a poor affinity and specificity, attempting to improve the specificity by more effectively targeting DNA is a molecular approach in the design of novel chemotherapeutic agents. Tethering nitrogen mustard groups to DNA minor groove binding vectors is an attempt to direct the DNA alkylation event in a sequence specific manner. The minor groove of DNA has remained a popular target for rational anticancer drug design largely due to the precedents provided by various non-covalent and covalent DNA-binding natural products. Knowledge of the specific DNA interactions of natural and synthetic agents suggested that a more efficient and specific targeting was possible. This approach has been attempted with different minor groove binding vectors including the pyrrole framework of distamycin and netropsin. The continued clinical evaluation of tallimustine and the CPI analogues of CC-1065 will bear out whether the approach has resulted in useful clinical agents. The previous studies of lexitropsin vectors tethering reactive groups did not explore structure-activity relationships. Specifically, detailed examinations of the influence of the reactive groups on the specificity of the lexitropsin, and the influence of lexitropsin on the specificity of the

nitrogen mustard were not carried out. The work presented above represents one attempt at such a structure-activity study.

There are several conclusions that can be drawn from the work presented above, with regards to the design of future lexitropsins that tether reactive groups. Attaching aromatic nitrogen mustards to minor groove binding lexitropsins creates conjugates that are more cytotoxic than the parent mustards. It should be noted that conjugates are not always more cytotoxic than the parent compound, as was seen with the *N*-(2-chloroethyl)-*N*-nitrosourea lexitropsins (Chen, *et al.*, 1993), the lexitropsin conjugating the metal binding domain of bleomycin (Owa, *et al.*, 1992), and the di- and triheterocyclic lexitropsins with mixed pyrrole/imidazole units and an N-terminal bis-(chloroethyl)amino group (Xie, *et al.*, 1995). Altering the manner in which either domain of a conjugate reacts with its target can produce an inactive conjugate.

The trends in cytotoxicity for each family clearly demonstrate a beneficial effect of tethering an aromatic nitrogen mustard to a DNA-binding vector and this may be true for many different types of DNA-binding agents. DNA-intercalating aminoacridine groups that tether nitrogen mustards were substantially more cytotoxic than the parent nitrogen mustards (Gourdie, *et al.*, 1990). The differences in cytotoxicity compared to the parent nitrogen mustard for each increase in the number of heterocyclic units vary between families, but were substantially greater for the BAM conjugates than for the CHL conjugates. The difference was greatest for the imidazole-BAM conjugates and least for the pyrrole-CHL conjugates. An increase in the DNA delivery for nitrogen mustard groups produces an increase in cytotoxicity, but the magnitude depends primarily on the nitrogen mustard reactivity and to a lesser extent on the lexitropsin portion chosen. The study reporting the aminoacridine-nitrogen mustard conjugates stated that, "the *in vitro* cytotoxicities of the more reactive

mustards were improved the least by DNA targeting, while those of the less reactive were improved the most" (Gourdie, *et al.*, 1990).

The mechanism of action for the CHL conjugates appears to be similar to conventional nitrogen mustards, i.e., guanine-N7 alkylation and DNA interstrand cross-linking in the major groove. The CHL conjugates all cross-linked DNA more efficiently than CHL and, with the exception of the monoimidazole-CHL conjugate, were more cytotoxic than CHL. The lexitropsin portion did not, however, markedly alter the sequence specificity of alkylation for the CHL portion. The one significant difference between the conventional nitrogen mustards and the CHL conjugates was that there was no clear correlation between cross-linking and cytotoxicity. The monoimidazole-CHL conjugate cross-linked DNA more efficiently than CHL, but was less cytotoxic. The monopyrrole-CHL conjugate cross-linked DNA as efficiently as the di- or tripyrrole-CHL conjugates, but was less cytotoxic.

The increase in cytotoxicity for the CHL conjugates compared to CHL may be due to an increased delivery to the DNA. The fact that the pyrrole-CHL conjugates were more cytotoxic than the imidazole-CHL conjugates might be explained as due to their greater than 10-fold higher non-covalent binding affinities. Unfortunately, the correlation is not perfect, and this interpretation ignores several other possibilities, in particular the fact that the dipyrrole- and tripyrrole-CHL conjugates alkylated a unique minor groove site strongly. Speculation that the higher cytotoxicity seen for the pyrrole-CHL conjugates is due to the unique minor groove site would be extremely difficult to validate.

The results and observations on the BAM conjugates was quite different from the CHL conjugates and conventional nitrogen mustards. The cytotoxicity increased for each increase in the number of heterocyclic units, and the differences were significant. The diheterocyclic- and

triheterocyclic-BAM conjugates did not efficiently cross-link plasmid or cellular DNA, and the conjugates efficiently alkylated in the minor groove at AT-rich sites. Furthermore, for each increase in the number of heterocyclic units, there was a corresponding increase in the sequence specificity of alkylation, such that the triheterocyclic conjugates strongly alkylated fewer sites than BAM or the mono- and diheterocyclic conjugates.

The di- and triheterocyclic-BAM conjugates did not alkylate major groove guanine-N7 positions as BAM did, but the di- and triheterocyclic-CHL conjugates largely retained the alkylation preference of CHL. The less reactive nitrogen mustard was delivered more efficiently to the minor groove where the lexitropsin portion preferentially binds. If the reactivity of the alkylating group is too great, the lexitropsin portion cannot exclusively deliver it to the minor groove. The earlier mentioned example of the *N*-(2-chloroethyl)-*N*-nitrosourea lexitropsins offers corroborating evidence. It was shown that, while minor groove alkylation does occur, the predominance of the alkylation remained that seen for the parent compound CCNU (Church, *et al.*, 1990). The same group later published work on sulfonate esters tethered to lexitropsins. The sulfonate esters are simple methylating agents which are less reactive and produce far less complex DNA adducts than the nitrosoureas. The sulfonate ester lexitropsins predominantly methylated in the minor groove of AT tracts where the lexitropsins non-covalently bound (Zhang, *et al.*, 1993). In addition to the higher reactivity, the flexibility of the $(CH_2)_3$ linker of the CHL conjugates may be detrimental. For the BAM conjugates, there are structural requirements for the alkylation event that are distinct from the non-covalent binding of the conjugates. The combination of flexibility and higher reactivity might increase the possibility of the nitrogen mustard portion reacting before it is properly targeted by the lexitropsin.

The BAM group offers several advantages to CHL when conjugated to the lexitropsins. The lower reactivity probably limits the opportunities

for reaction with nucleophiles other than those in the minor groove. The mustard portion of the BAM conjugates is fixed approximately planar to the lexitropsin portion and this most likely places an added requirement on the alkylation event. Monoheterocyclic lexitropsins bind to DNA poorly when compared to di- or triheterocyclic lexitropsins. Although the BAM portion, when tethered to the monoheterocyclic lexitropsin, is more efficiently delivered to the DNA than when not conjugated, the DNA-binding portion is not substantial enough to exclusively target the minor groove. It was interesting to note that, whereas the monopyrrole-BAM conjugate strongly alkylated minor groove sites in AT-rich stretches, the monoimidazole conjugate did not, and the monopyrrole conjugate was 3-fold more cytotoxic than the monoimidazole conjugate. Speculation that the minor groove alkylation seen for the monopyrrole-BAM conjugate is responsible for the increased cytotoxicity compared to the monoimidazole-BAM conjugate would be difficult to validate, however. The dihetereocyclic- and triheterocyclic-BAM conjugates effectively directed alkylation into the minor groove, where the lexitropsin portion binds. The fact that the greater difference in cytotoxicity compared to the parent nitrogen mustard was seen for the BAM conjugates, and that the alkylation was limited to the minor groove may suggest that selective minor groove alkylation is more toxic than indiscriminate major groove alkylation.

The finding that the imidazole-BAM conjugates alkylated in similar pattern to their pyrrole counterparts would not have been predicted based on studies of the non-alkylating lexitropsins and suggests that caution be taken before making such predictions. The pyrrole-containing lexitropsins bind to AT-rich sequences because of a clash that occurs between the guanine-2-NH_2 groups and the pyrrole hydrogens. The Im_2 and Im_3 lexitropsins bind to GC-rich sequences, but not because of an avoidance of AT base pairs. Binding to AT-rich sites is still theoretically possible, although, in the case of Im_2 and Im_3, this does not occur. For the pyrrole-

BAM conjugates, the specificity increases with the number of pyrrole units, from one to three, such that the tripyrrole conjugate strongly alkylated very few sites. Evidence that tallimustine and the tripyrrole-BAM conjugate non-covalently bound several AT-rich sites, including those where little or no alkylation was seen, implies that the alkylation event is not solely dictated by the non-covalent binding.

Two possible explanations for the AT-selectivity of the diimidazole- and triimidazole-BAM conjugates were presented. The first was that an increase in the cationic nature of the conjugates had biased binding and alkylation at the more electronegative AT-rich sequences. Following aziridinium formation, the ensuing dicationic conjugate could bind to AT-rich sequences in similar manner to the first generation lexitropsins. The pH effect on the alkylation intensity seen for the di- and triimidazole-BAM conjugates, but not for the tripyrrole-BAM conjugate, implies that additional protonation on the imidazole-BAM conjugates increases the cationic character and predisposes the molecules for the more electronegative AT-rich sites.

There are a couple of inconsistencies concerning the role of protonation. First, the monoimidazole-BAM conjugate did not strongly alkylate the minor groove sites in the AT-rich region. If it were simply the added cationic character caused by aziridinium formation, then it would not be unreasonable to assume that the monoimidazole and monopyrrole conjugates would alkylate similarly. This also presumes that the aziridinium ion would exist long enough to have an effect on the non-covalent interactions of the lexitropsin. Secondly, The Im_2 and Im_3 lexitropsins preferentially bound to GC-rich sites, specifically 5'-$(G.C)_3$(A.T) and 5'-TCGGGCT respectively. An effect of protonation on the imidazole portion of the conjugates should also have been seen with the Im_2 and Im_3 lexitropsins. Even when examined on the AT-rich region, the Im_3 lexitropsin retained its non-covalent preference for GC-rich sites.

Lastly, the triimidazole-BAM conjugate did not footprint to either GC- or AT-rich sequences. This presents the most interesting piece of evidence, because it indicates that favourable non-covalent interactions with the minor groove do not detectably occur for this conjugate. Yet the alkylation event clearly occurs and in very similar manner to that seen for the tripyrrole conjugate. This evidence, coupled with the fact that alkylation does not occur at all sites of non-covalent binding for the tripyrrole-BAM conjugate and tallimustine, implies that the non-covalent interactions are not the primary recognition feature that dictates the alkylation event.

It seems most likely that the local sequence conformation plays a primary role in the alkylation specificity for the di- and triheterocyclic-BAM conjugates. The imidazole-BAM conjugates, because they can potentially bind to both AT and GC sites, now recognise a second structural feature of the DNA, which is the shape of the DNA the local sequence adopts, and this takes precedent over the AT/GC sequence recognition. The unique shape that the T_4GPu sequence adopts may also act as a catalyst for the alkylation event. An NMR study demonstrated that the state of hydration for 5'-TTAA steps is different from that seen for 5'-AATT steps, and indicates that a disruption of the spine of hydration has occurred at the 5'-TTAA site (Liepinsh, *et al.*, 1994). The results were correlated with the larger width of the minor groove in d-$(TTAA)_2$ segments compared to d-$(AATT)_2$ segments. It has been proposed, based on the examination of the X-ray solution of several different oligodeoxynucleotides of differing AT-GC content, that the preferred positions of the water oxygens in the minor groove depend predominantly on groove width rather than on base sequence (Chuprina, *et al.*, 1991).

There are in the literature several examples of drugs that alkylate DNA upon site-specific activation . It has been proposed that a catalytic activation of the alkylation step for CC-1065 occurs and involves both

ordered water molecules and a phosphate from the DNA backbone (Lin, *et al.*, 1991a). This catalytic activation, in addition to the conformational flexibility of the DNA (Sun, *et al.*, 1993a), was proposed to be at least partially responsible for the sequence specificity of CC-1065. In a model of the interaction of temozolomide with DNA, based on NMR and molecular modelling investigations, it was proposed that the ring opening to form MTIC and methylation of DNA by the diazomethane species is facilitated by the basic microenvironment of guanine-rich sequences and that an 'activated' water molecule is ideally positioned to initiate the ring opening of temozolomide (Denny, *et al.*, 1994a).

An NMR study of dimeric complexes of the 2-ImN analogue and distamycin with an oligodeoxynucleotide demonstrated that the heterodimeric complexes were formed in preference to the homodimeric complexes of either drug. It was also mentioned in the publication that the 1: 1: 1 complex of 2-ImN: distamycin : DNA exhibited a significantly higher stability than a 1: 1: 1 complex of 2-ImN: DNA and the tripyrrole distamycin analogue with the dimethylaminopropyl group on the C-terminus substituted for the amidinium group. It was suggested that, "differences in shape, charge distribution, or hydrogen bonding could be responsible for the difference in binding affinity" and "the nature of the cationic ligand tail group may be important for specificity and overall stability of these complexes" (Geierstanger, *et al.*, 1994a). Although the alkylation specificity is very similar for the tripyrrole-BAM conjugate and tallimustine, there are some subtle but significant differences. The incorporation of the change on the C-terminus has affected the intensity of alkylation for the tripyrrole-BAM conjugate versus tallimustine, which might be due to the stability of the respective complexes prior to alkylation. The implication is that structural modifications to drugs, however small or apparently insignificant they appear to be, may introduce a subtle change in the DNA interactions.

In addition to the specifically mentioned examples of DNA sequence-dependent structural features, there are many other studies examining the role of sequence-dependent recognition of DNA by drugs and the structural changes that occur to the DNA upon drug binding or bonding. It has been suggested that the sequence specificity of alkylation seen for tomaymycin and anthramycin is partially determined by the flexibility of the local sequence conformation and that both agents bend the DNA upon alkylation (Kizu, *et al.*, 1993). Solution of the X-ray crystal structure of the oligodeoxynucleotide CCAACGTTGG with two anthramycin molecules covalently bound in the minor groove has been reported (Kopka, *et al.*, 1994). It was proposed in the study that the origin of the alkylation specificity for anthramycin for the 5'-PuGPu sequence was not due to specific hydrogen-bond interactions but due to the low twist angles adopted by the purine-purine step in B-DNA (Kopka, *et al.*, 1994).

Effects on local DNA structure caused by CC-1065 and its CPI analogues have also been studied. It has been shown that CC-1065, and the AB and ABC ring analogues bend the DNA upon alkylation towards the minor groove. The induced bend is of similar magnitude and direction (towards the minor groove) to that seen for naturally bent A-tracts (Lee, *et al.*, 1991a; Lin, *et al.*, 1991b; Sun, *et al.*, 1993a). This property of entrapping/inducing a bend in DNA has led to the use of CC-1065 as a chemical probe to explore the DNA bending induced by a DNA-bending protein (Ding, *et al.*, 1993). Bizelesin, the designed cross-linking CPI analogue of CC-1065, has been shown to alkylate normally unreactive bases in what was termed a "proximity-driven manner." It was shown that if a highly favoured monoalkylation by the first arm were to occur, then the second alkylation that forms the cross-link was possible with normally unreactive bases such as guanine or cytosine due to the covalent immobilisation of the drug molecule by the monoalkylation (Sun, *et al.*, 1993b). It has also been shown that bizelesin eliminates the intrinsic bend

seen for A-tracts upon minor groove cross-link formation in an effect that differs from CC-1065 in that bizelesin can entrap/induce a straight form of DNA (Thompson & Hurley, 1995; Thompson, *et al.*, 1995).

As a footnote to the controversy surrounding the structural basis for the sequence specificity of alkylation seen for CC-1065, there should be mention of the non-covalent interactions. Hurley states that "while non-covalent binding in the minor groove must take place as a prelude [to alkylation], this binding might, as in the case of (+)-A, be very weak and need not be sequence selective" (Hurley & Draves, 1993). Boger *et al.* state that their interpretation that the snugness of the fit determines the alkylation specificity "should not be misconstrued to imply that AT-rich binding leads necessarily to productive DNA alkylation" (Boger, *et al.*, 1994). The observations are not mutually exclusive, and there are certain aspects of both arguments that need to be highlighted with specific reference to the results presented in this thesis. Although non-covalent interactions for the triimidazole-BAM conjugate are detectable using circular dichroism and an ethidium displacement assay (Lee, *et al.*, 1993a), it clearly does not produce footprints, and this is a nearly identical result to that seen for CC-1065 (Hurley, *et al.*, 1988). However, the triimidazole-BAM conjugate clearly alkylates fewer sites than the monoimidazole- or diimidazole-BAM conjugate, and the increase in the 'reading frame' of the lexitropsin must be limiting the number of sites alkylated. Additionally, the results of the footprinting studies for the tripyrrole-BAM conjugate and tallimustine show that the alkylation event does not occur at all sites of non-covalent binding.

NMR characterisations of the enediyne antibiotic calicheamicin complexed with different oligodeoxynucleotides has provided an interesting assessment of its non-covalent interactions with DNA. It has been shown that the position of the groove binding oligosaccharide is essentially identical in the seemingly unrelated sequences 5'-ACCT, 5'-

TCCT and 5'-TTTT. The cleavage selectivity of calicheamicin was proposed to represent a new kind of selectivity that is neither AT- or GC-selective but seems to bind to runs of pyrimidines, which is possibly driven by the flexibility that pyrimidine runs possess and may be able to distort readily to accommodate the drug (Kahne, 1995).

As mentioned in the introduction, Hoechst 33258 is a non-covalent minor groove binder that displays an AT-sequence specificity. Several complexes of Hoechst with oligodeoxynucleotides have been examined and although there is general agreement on the AT-sequence specificity and groove positioning for hydrogen bonding and van der Waals interactions reminiscent of that seen for netropsin, there has been some debate as to the positioning of the non-planar piperazine ring in the groove. Specifically, some of the studies have shown the entire drug molecule to fit entirely within four base pair AT binding sites, while some studies have shown that the drug molecule has shifted one base pair, such that the piperazine ring overlaps into a neighbouring GC-base pair. The more recent of these studies compared the X-ray crystal structures of Hoechst 33258 bound to an oligodeoxynucleotide containing a core AAATTT sequence with a previously solved drug: core AATT complex, where the drug bound to the central four AT base pairs (Spink, *et al.*, 1994). It was found that the drug was positioned over the ATTTG sequence in the longer AT oligodeoxynucleotide and this was proposed to be due to the narrower groove width and greater propeller twist of the AAATTT sequence compared to the AATT sequence.

A recent X-ray crystallography study of an analogue of Hoechst 33258 containing an imidazole group substituted for the piperazine complexed with the oligodeoxynucleotide $d(CGCGAATTCGCG)_2$ highlighted groove width as an important feature in the non-covalent binding of these structures (Wood, *et al.*, 1995). The groove width at the 3'-end of the 5'-AATT binding site for the oligodeoxynucleotide complexed with the

imidazole analogue was narrower than that seen for the oligodeoxynucleotide complexed with Hoechst 33258. This was consistent with the narrower cross-section of the imidazole group compared with the piperazine ring, and the tighter fit into the narrower groove was offered as an explanation of the higher non-covalent binding affinity seen for the imidazole analogue compared to Hoechst (Wood, *et al.*, 1995).

The precise nature of the drug: DNA adducts at the preferred sequences 5'-TTTTGPu cannot be commented on without precise structural data from either X-ray crystallography or high-field NMR. It would also be difficult to speculate on what specific aspect of the sequence allows for favourable alkylation, although the predominance of the structural evidence would suggest that it might be due to the combination of the narrow minor groove width of the T_4 tract and a junction bend at the 5'-TG step. Indeed, there is still some debate as to the precise structural causes of bending in DNA (Crothers, *et al.*, 1990; Dickerson, *et al.*, 1994; Sprous, *et al.*, 1995). An NMR study of tallimustine non-covalently bound to the sequence 5'-d$(CGTATACG)_2$ has been reported, and although the study demonstrated an exchange between two non-covalently bound modes, there was no insightful information about the alkylation event (Mazzini, *et al.*, 1994). Initial attempts to characterise a covalent adduct of tallimustine bound to an oligodeoxynucleotide containing the 5'-TTTTGA sequence has been unsuccessful (M. D'Incalci, personal communication). An abbreviated oligodeoxynucleotide may not provide the proper DNA structure required to catalyse the alkylation event.

Studies on N to C linked imidazole conjugates offer an interesting comparison to the oligoimidazole lexitropsins. Formamido-imidazole lexitropsins containing two or three imidazole units, and with a β-methylene group linking the C-terminal imidazole to the rest of the molecule, were examined for their non-covalent interactions. The β-

methylene linked triimidazole lexitropsin strongly footprinted at GC-rich sites of six base pairs, in contrast to the tetraimidazole analogue that did not footprint (Wyatt, *et al.*, 1994b). This indicated that the inclusion of a flexible linker in the molecule allowed for binding to six base pairs in a manner that overcame the problem of curvature in the Im_4 lexitropsin. Interestingly, however, BAM analogues of the N to C linked lexitropsins were essentially inactive, with IC_{50} values of greater than 100 μM (Lee, *et al.*, 1994). It is interesting to note that although the flexibility of the β-methylene linker created a compound with a better non-covalent binding affinity, it did not provide for a more cytotoxic mustard analogue. The linked BAM conjugates, because of the flexibility of the linker, may not fulfil structural requirements of the lexitropsin in order to strongly alkylate at the preferred site of the BAM conjugates. Studies to directly compare the alkylation specificity for the linked BAM conjugates are underway.

There would be several ways of testing whether the primary influence is either due to the question of protonation or the local DNA structure. BAM conjugates with uncharged alkyl groups on the C-terminus instead of the physiologically protonated dimethylamino group could be synthesised. The sulfonate ester lexitropsins discussed in the introduction contained the uncharged ethyl group and the methylation seen occurred in the minor groove of AT-rich sequences. The alkyl-containing BAM conjugates would remain uncharged until aziridinium formation occurred, upon which the drug molecule would then be monocationic. A truer half-mustard conjugate comparison would be an *N*-chloroethyl-*N*-ethylamino group because it would provide a much closer estimation of the aziridinium formation and steric requirements in order to provide a direct comparison with bis-(chloroethyl)amino derivative. It would be difficult to precisely determine the importance of the second chloroethyl arm as being due to a steric requirement that plays a role in the alkylation event, or if the bifunctionality plays a biological role.

As the understanding of the molecular basis of sequence specificity for the variety of minor groove binding agents increases, more subtle features of DNA structure are being discovered. Indeed, the paradigm of considering the B-DNA structure as structurally homogeneous has changed, such that the DNA structure is now known to be considerably flexible and the flexibility is defined by local sequence conformation. This has had the logical effect on the understanding of drug: DNA interactions. As the complexity of the drugs and our understanding of the drug: DNA interactions increase, there will be more considerations to take into account in the design of future sequence specific agents. It may now be possible to design agents that recognise different structural aspects of DNA, in addition to the AT or GC base composition of a particular sequence.

There are several drawbacks to the approach of utilising minor groove binders as vectors to which DNA reactive groups can be tethered. First and foremost, there must remain a strong rationale for the approach of targeting reactive groups that interact with DNA, if a DNA binding vector is being employed. Unfortunately, literature examples that do not provide such a rationale exist, for instance a protein kinase C binding domain attached to a lexitropsin, when PKC is involved in a signal transduction pathway and is located on the cell surface. One could argue against the benefits of such a conjugation.

Extremely toxic agents that damage DNA do not represent all past and potentially useful chemotherapeutic agents. The design of prodrugs that are activated in some manner requires two general principles that do not necessarily demand producing an extremely toxic species. These are a very large difference in toxicity between the prodrug and the active species, and the requirement that the active metabolite should be site-specifically produced, be it at the site of the tumour or in the nucleus instead of in the blood or cytoplasm of the cell. The NCI drug screening program is now

structured so that an investigational drug is tested against a panel of some 70+ cell lines derived from different types of tumours. The grading system then allows for identification of new drugs that are not necessarily toxic to all cells grown in culture but may display high activity against a particular tumour cell-line type. Comparison of a new drug's spectrum of activity against the panel to agents with a well-known spectrum of activity allows for a tentative classification of the new drug's mechanism of action, and this can now be accomplished with complex computer algorithms that aid in the process (van Osdol, *et al.*, 1994).

Definitive assignment of a structure-activity relationship when activity is defined as 'biological activity' should be restrained where there is no data concerning cellular uptake, nuclear concentration, and interaction with non-DNA targets. More importantly, the repair of individual lesions, particularly complex lesions, in different regions of the genome in living cells remains largely unexplored. Damage and repair studies for a variety of agents have been performed at the level of the genome, and at the level of the gene. Techniques to study damage and repair at the level of a gene fragment or at nucleotide resolution have only recently been developed. Confirmation of the covalent sequence specificity of drugs in cells is an important step in the rational design of novel DNA binding agents designed as anticancer agents. Those agents designed using models that are predicted from studies with isolated DNA must be shown to bind to cellular DNA with the same sequence specificity, or else the model will have no biological significance.

In preliminary work on different examples of alkylating agents, the results are somewhat encouraging, but also provide the necessary warning of extrapolating from isolated DNA fragments to the cellular DNA damage event. Studies examining the sequence specificity in cells for mechlorethamine and cisplatin in human alpha-DNA, a highly reiterative sequence 340 base pair sequence in the human genome, found an essentially

similar pattern of alkylation (Hartley, *et al.*, 1992; Murray, *et al.*, 1992). The sequence specificity of adozelesin and bizelesin was examined in cells using a ligation-mediated PCR technique. The alkylation patterns in cellular DNA for each agent were similar but not identical to those seen in DNA fragments (Lee, *et al.*, 1994). Examination of the nucleotide preference of cisplatin in the N-ras gene in human cells revealed a binding site not seen in isolated DNA (Grimaldi, *et al.*, 1994). The PBD dimer analogue AT-486 has been shown by the technique of single-strand ligation mediated-PCR to alkylate at the same sequence in cellular DNA as it does in isolated DNA fragments (Smellie *et al.*, in preparation). The sequence specificity of alkylation for tallimustine in cells is currently being examined and will be of great interest, particularly with regards to the formation and repair of such complex lesions (personal communication, Dr. Patrizia Beccaglia).

It will be extremely important to determine the biological consequences downstream of the DNA damage event. The recognition of the damage and repair of these lesions by the cellular machinery will be crucial in determining the important and unimportant lesions formed by a sequence-specific drug. A highly specific lesion that is easily recognised and removed by the DNA repair systems may not have the same impact as those lesions that are not easily recognised or repaired. The minor groove cross-links formed by the PBD dimer DSB-120 were not repaired, whereas mechlorethamine cross-links were. Different types of DNA lesions have different biological consequences and an agent designed to preferentially form cytotoxic lesions compared to mutagenic lesions would presumably be beneficial.

The day when a DNA-targeted drug can be rationally designed 'from scratch' for a specific medicinal purpose, be it cancer or any other disease, still seems a long way off. This appears due to the fact that a full understanding of the biological consequences of drug: DNA interactions remains elusive. This lack of understanding prevents a complete

determination of structure-activity relationships, particularly if activity is defined as 'biological consequence' or 'cytotoxicity.' Further studies on the responses to DNA damaging events are necessary, including those designed to see whether drugs are capable of producing a cell cycle block, what cellular responses are induced, such as repair or apoptosis, whether the lesions are repaired and, if so, by what repair pathway.

What the approach offers is some insight into the process of DNA recognition by small molecules that can covalently modify DNA, and this may have long-term implications for the design of DNA-targeted agents. For molecules that target DNA, a sequence specificity can be extrapolated from studies with relatively short DNA fragments that offer insight into the recognition features of the molecules (and DNA). A better knowledge of the particular variances in DNA structure would greatly aid in the rational design of the next generation of sequence specific drugs. As the drugs grow in complexity and the DNA targets grow in size, additional considerations such as DNA groove width and local conformational features must be taken into account. A more thorough understanding of all the local and global variations of DNA structure is one requirement for the next generation of lexitropsins, if the sequence specificity is to be further improved.

REFERENCES

Adams, G. E., & Stratford, I. J. (1986). Hypoxia-mediated nitro-heterocyclic drugs in the radio- and chemotherapy of cancer. *Biochem. Pharmacol.*, **35**, 71-76.

Adams, G. E., & Stratford, I. J. (1994). Bioreductive drugs for cancer therapy: the search for tumor specificity. *Int. J. Rad. Oncol. Biol. Phys.*, **29**, 231-238.

Allegra, C. J. (1990). Antifolates. In Cancer Chemotherapy: Principles and Practice. B. A. Chabner and J. M. Collins, eds. Philadelphia, J. B. Lippencott Company. 110-153.

Anderson, C. (1992). NIH and DNA patent rejected; backers want to amend law. *Nature*, **359**, 263.

Andersson, L. C., Nilsson, K., & Gahmberg, C. G. (1979). K562-A human erythroleukemic cell line. *Int. J. Cancer*, **23**, 143-147.

Arcamone, F. (1993). Synthesis and DNA binding selectivity of pyrrole-amidine oligopeptides. *Farmaco*, **48**, 143-150.

Arcamone, F. M., Animati, F., Barbieri, B., Configliacchi, E., D'Alessio, R., Geroni, C., Giuliani, F. C., Lazzari, E., Menozzi, M., & Mongelli, N. (1989). Synthesis, DNA-binding properties, and antitumor activity of novel distamycin derivatives. *J. Med. Chem.*, **32**, 774-778.

Asai, A., Naguamura, S., & Saito, H. (1994). A novel property of duocarmycin and its analogues for covalent reaction with DNA. *J. Am. Chem. Soc.*, **116**, 4171-4177.

Bailly, C., & Henichart, J.-P. (1994). Molecular pharmacology of intercalator-groove binder hybrid molecules. In Molecular Aspects of Anticancer Drug-DNA Interactions. S. Neidle and M. J. Waring, eds. Basingstoke, MacMillan Press. 162-196.

Baker, B. F., & Dervan, P. B. (1985). Sequence-specific cleavage of double-helical DNA. *N*-bromoacetyldistamycin. *J. Am. Chem. Soc.*, **107**, 8266-8268.

Baker, B. F., & Dervan, P. B. (1989). Sequence-specific cleavage of DNA by *N*-bromoacetyldistamycin. Product and kinetic analysis. *J. Am. Chem. Soc.*, **111**, 2700-2712.

Bank, B. B. (1992). Studies of chlorambucil-DNA adducts. *Biochem. Pharmacol.*, **44**, 571-575.

Bellorini, M., Moncollin, V., D'Incalci, M., Mongelli, N., & Mantovani, R. (1995). Distamycin A and tallimustine inhibit TBP binding and basal *in vitro* transcription. *Nucleic Acids Res.*, **23**, 1657-1663.

Benkovic, S. J. (1980). On the mechanism of action of folate- and biopterin-requiring enzymes. *Ann. Rev. Biochem.*, **49**, 227-251.

Berardini, M. D., Souhami, R. L., Lee, C. S., Gibson, N. W., Butler, J., & Hartley, J. A. (1993). Two structurally related diaziridinylbenzoquinones preferentially cross-link DNA at different sites upon reduction with DT-diaphorase. *Biochemistry*, **32**, 3306-3312.

Bergel, F., & Stock, J. A. (1954). Cyto-active amino-acid and peptide derivatives part I. Substituted phenylalanines. *J. Chem. Soc.*, 2409.

Berman, H. M., Neidle, S., Zimmer, C., & Thrum, H. (1979). Netropsin, a DNA-binding oligopeptide. Structural and binding studies. *Biochim. Biophys. Acta*, **561**, 124-131.

Blackburn, G. M. (1990). DNA and RNA structure. In Nucleic Acids in Chemistry and Biology. G. M. Blackburn and M. J. Gait, eds. Oxford, Oxford University Press. 17-70.

Boger, D. L., Coleman, R. S., Invergo, B. J., Sakya, S. M., Ishizaki, T., Munk, S. A., Zarrinmayeh, H., Kitos, P., & Thompson, S. C. (1990). Synthesis and evaluation of aborted and extended CC-1065 functional analogues: (+)- and (-)-CPI-PDE-I_1, (+)- and (-)-CPI-$CDPI_1$, and (±)-, (+)-, an d(-)-CPI-$CDPI_3$. Preparation of key partial structures and definition of an additional functional role of the CC-1065 central and right-hand subunits. *J. Am. Chem. Soc.*, **112**, 4623-4632.

Boger, D. L., & Johnson, D. S. (1995a). CC-1065 and the duocarmycins: unravelling the keys to a new class of naturally derived DNA alkylating agents. *Proc. Natl. Acad. Sci. U.S.A.*, **92**, 3642-3649.

Boger, D. L., & Johnson, D. S. (1995b). Second definitive test of proposed models for the origin of the CC-1065 and duocarmycin DNA alkylation specificity. *J. Am. Chem. Soc.*, **117**, 1443-1444.

Boger, D. L., Johnson, D. S., Yun, W., & Tarby, C. M. (1994). Molecular basis for sequence selective DNA alkylation by (+)- and ent-(-)-CC-1065 and related agents: alkylation site models that accommodate the offset AT-rich adenine N3 alkylation selectivity. *Bioorg. Med. Chem.*, **2**, 115-135.

Boger, D. L., Teramoto, S., & Zhou, J. (1995). Key synthetic analogs of bleomycin A2 that directly address the effect and role of the disaccharide: demannosyl-bleomycin A2 and α-D-mannopyranosyl-deglycobleomycin A2. *J. Am. Chem. Soc.*, **117**, 7344-7356.

Boger, D. L., Zarrinmayeh, H., Munk, S. A., Kitos, P. A., & Suntornwat, O. (1991). Demonstration of a pronounced effect of noncovalent binding selectivity on the (+)-CC-1065 DNA alkylation and identification of the pharmacophore of the alkylation subunit. *Proc. Natl. Acad. Sci. U.S.A.*, **88**, 1431-1435.

Borman, S. (1991). Taxol, a novel natural product from the Pacific Yew tree. *Chem. Eng. News*, **Sept. 2**, 11-14.

Borowy-Borowski, H., Lipman, R., & Tomasz, M. (1990). Recognition between mitomycin C and specific DNA sequences for cross-link formation. *Biochemistry*, **29**, 2999-3006.

Bose, D. S., Thompson, A. S., Ching, J., Hartley, J. A., Berardini, M. D., Jenkins, T. C., Neidle, S., Hurley, L. H., & Thurston, D. E. (1992). Rational design of a highly efficient irreversible DNA interstrand cross-linking agent based on the pyrrolobenzodiazepine ring system. *J. Am. Chem. Soc.*, **114**, 4939-4941.

Bregant, T. M., Groppe, J., & Little, R. D. (1994). New class of DNA-cleaving agents based on trimethylenemethane. *J. Am. Chem. Soc.*, **116**, 3635-3636.

Breslauer, K. J., Ferrante, R., Marky, L. A., Dervan, P. B., & Youngquist, R. S. (1988). The Origins of the DNA binding affinity and specificity of minor groove directed ligands: correlations of thermodynamic and structural data. In Structure and Expression. R. H. Sarma and M. H. Sarma, eds. NY, Adenine Press. 273-290.

Broggini, M., Coley, H., Mongelli, N., Grandi, M., Wyatt, M. D., Hartley, J. A., & D'Incalci, M. (1995). DNA sequence specific adenine alkylation by the novel antitumor drug tallimustine (FCE 24517), a benzoyl nitrogen mustard derivative of distamycin. *Nucleic Acids Res.*, **23**, 81-87.

Broggini, M., & D'Incalci, M. (1994). Modulation of transcription factor--DNA interactions by anticancer drugs. *Anticancer Drug Des.*, **9**, 373-387.

Broggini, M., Erba, E., Ponti, M., Ballinari, D., Geroni, C., Spreafico, F., & D'Incalci, M. (1991). Selective DNA interaction of the novel distamycin derivative FCE 24517. *Cancer Res.*, **51**, 199-204.

Broggini, M., Ponti, M., Ottolenghi, S., D'Incalci, M., Mongelli, N., & Mantovani, R. (1989). Distamycins inhibit the binding of OTF-1 and NFE-1 transfactors to their conserved DNA elements. *Nucleic Acids Res.*, **17**, 1051-1059.

Brookes, P., & Lawley, P. D. (1960). The reaction of mustard gas with nucleic acids in-vitro and in-vivo. *Biochem. J.*, **77**, 478-484.

Brookes, P., & Lawley, P. D. (1961). The reaction of mono- and di-functional alkylating agents with nucleic acids. *Biochem. J.*, **80**, 498-503.

Brown, J. M., & Giaccia, A. J. (1994). Tumour hypoxia: the picture has changed in the 1990s. *Int. J. Radiat. Biol.*, **65**, 95-102.

Burkhoff, A. M., & Tullius, T. D. (1987). The unusual conformation adopted by the adenine tracts in kinetoplast DNA. *Cell*, **48**, 935-943.

Capranico, G., & Zunino, F. (1990). Structural requirements for DNA topoisomerase II inhibition by anthracyclines. In Molecular Basis of Specificity in Nucleic Acid-Drug Interactions. B. Pullman and J. Jortner, eds. Dordrecht, Kluwer Academic Publishers. 167-176.

Carmichael, J., DeGraff, W. G., Gazdar, A. F., Minna, J. D., & Mitchell, J. B. (1987). Evaluation of a tetrazolium-based semiautomated colorimetric assay: assessment of chemosensitivity testing. *Cancer Res.*, **47**, 936-942.

Chabner, B. A. (1990). Bleomycin. In Cancer Chemotherapy: Principles and Practice. B. A. Chabner and J. M. Collins, eds. Philadelphia, J. B. Lippincott Company. 341-355.

Chen, F. X., Zhang, Y., Church, K. M., Bodell, W. J., & Gold, B. (1993). DNA crosslinking, sister chromatid exchange and cytotoxicity of *N*-2-chloroethylnitrosoureas tethered to minor groove binding peptides. *Carcinogenesis*, **14**, 935-940.

Chen, S.-M., Leupin, W., & Chazin, J. (1992). Conformational studies of the duplex d-(CCAAAAATTTCC).d-(GGAAATTTTTGG) containing a $(dA)_5$ tract using two-dimensional ^1H NMR spectroscopy. *Int. J. Biol. Macromol.*, **14**, 57-63.

Chen, Y.-H., Liu, J.-X., & Lown, J. W. (1995). Design, synthesis and evaluation of novel bismustard cross-linked lexitropsins. *Bioorg. Med. Chem. Lett.*, **5**, 2223-2228.

Chiang, S. Y., Welch, J., Rauscher, F. J., & Beerman, T. A. (1994). Effects of minor groove binding drugs on the interaction of TATA box binding protein and TFIIA with DNA. *Biochemistry*, **33**, 7033-7040.

Chuprina, V. P., Heinemann, U., Nurislamov, A. A., Zielenkiewicz, P., Dickerson, R. E., & Saenger, W. (1991). Molecular dynamics simulation of the hydration shell of a B-DNA decamer reveals two main types of minor-groove hydration depending on groove width. *Proc. Natl. Acad. Sci. U.S.A.*, **88**, 593-7.

Church, K. M., Wurdeman, R. L., Zhang, Y., Chen, F. X., & Gold, B. (1990). *N*-(2-chloroethyl)-*N*-nitrosoureas covalently bound to nonionic and monocationic lexitropsin dipeptides. Synthesis, DNA affinity binding characteristics, and reactions with ^{32}P-end-labeled DNA. *Biochemistry*, **29**, 6827-6838.

Clapper, M. L., & Tew, K. D. (1989). Alkylating agent resistance. In Drug Resistance in Cancer Therapy. R. F. Ozols, ed. Kluwer Academic Publishers. 125-150.

Colvin, M., & Chabner, B. A. (1990). Alkylating agents. In Cancer Chemotherapy: Principles and Practice. B. A. Chabner and J. M. Collins, eds. Philadelphia, J. B. Lippincott Company. 276-313.

Comess, K. M., & Lippard, S. J. (1993). Molecular aspects of platinum-DNA interactions. In Molecular Aspects of Anticancer Drug-DNA Interactions. S. Neidle and M. J. Waring, eds. Basingstoke, Macmillan Press. 134-168.

Cory, M., Tidwell, R. R., & Fairley, T. A. (1992). Structure and DNA binding activity of analogues of 1,5-bis(4-amidinophenoxy)pentane (pentamidine). *J. Med. Chem.*, **35**, 431-438.

Crothers, D. M., Haran, T. E., & Nadeau, J. G. (1990). Intrinsically bent DNA. *J. Biol. Chem.*, **265**, 7093-7096.

Cullinane, C., Van Rosmalen, A., & Phillips, D. R. (1994). Does adriamycin induce interstrand cross-links in DNA? *Biochemistry*, **33**, 4632-4638.

D'Alessio, R., Geroni, C., Biasoli, G., Pesenti, E., Grandi, M., & Mongelli, N. (1994). Structure-activity relationship of novel distamycin A derivatives: synthesis and antitumor activity. *Bioorg. Med. Chem. Lett.*, **4**, 1467-1472.

D'Andrea, A. D., & Haseltine, W. A. (1978). Sequence specific cleavage of DNA by the antitumor antibiotics neocarzinostatin and bleomycin. *Proc. Natl. Acad. Sci. U.S.A.*, **75**, 3608-3612.

Dasgupta, D., Parrack, P., & Sasisekharan, V. (1987). Interaction of synthetic analogues of distamycin with poly(dA.dT): role of the conjugated *N*-methylpyrrole system. *Biochemistry*, **26**, 6381-6386.

Debart, F., Periguad, C., Gosselin, D., Mrani, D., Rayner, B., Le Ber, P., Auclair, C., Balzarini, J., De Clercq, E., Paoletti, C., & Imbach, J.-L. (1989). Synthesis, DNA binding, and biological evaluation of synthetic precursors and novel analogues of netropsin. *J. Med. Chem.*, **32**, 1074-1083.

Denny, B. J., Wheelhouse, R. T., Stevens, M. F., Tsang, L. L., & Slack, J. A. (1994a). NMR and molecular modeling investigation of the mechanism of activation of the antitumor drug temozolomide and its interaction with DNA. *Biochemistry*, **33**, 9045-9051.

Denny, W. A., Wilson, W. R., Tercel, M., Van, Z. P., & Pullen, S. M. (1994b). Nitrobenzyl mustard quaternary salts: a new class of hypoxia-selective cytotoxins capable of releasing diffusible cytotoxins on bioreduction. *Int. J. Radiat. Oncol. Biol. Phys.*, **29**, 317-21.

Dervan, P. B. (1986). Design of sequence-specific DNA-binding molecules. *Science*, **232**, 464-471.

Dickerson, R. E., Goodsell, D. S., & Neidle, S. (1994). "...the tyranny of the lattice...". *Proc. Natl. Acad. Sci. U.S.A.*, **91**, 3579-3583.

Ding, Z. M., Harshey, R. M., & Hurley, L. H. (1993). (+)-CC-1065 as a structural probe of Mu transposase-induced bending of DNA: overcoming limitations of hydroxyl-radical footprinting. *Nucleic Acids Res.*, **21**, 4281-7.

Dwyer, T. J., Geierstanger, B. H., Mrksich, M., Dervan, P. B., & Wemmer, D. E. (1993). Structural analysis of covalent peptide dimers, bis(pyridine-2-carboxamidenetropsin)$(CH_2)_{3-6}$, in complex with 5'-TGACT-3' sites by two-dimensional NMR. *J. Am. Chem. Soc.*, **115**, 9900-9906.

Eastman, A. (1986). Reevaluation of interaction of cis-dichloro(ethylenediamine)platinum(II) with DNA. *Biochemistry*, **25**, 3912-3915.

Erickson, L. C., Laurent, G., Sharkey, N. A., & Kohn, K. W. (1980). DNA cross-linking and monoadduct repair in nitrosourea-treated human tumour cells. *Nature*, **288**, 727-729.

Evertt, J. L., Roberts, J. J., & Ross, W. C. J. (1953). Aryl-2-halogenoalkylamines: Part XII. Some carboxylic derivatives of *N*, *N*-di-2-chlorethylanaline. *J. Chem. Soc.*, 2386-2392.

Ewig, R. A., & Kohn, K. W. (1977). DNA damage and repair in mouse leukemia L1210 cells treated with nitrogen mustard, 1,3-bis(2-chloroethyl)-1-nitrosourea, and other nitrosoureas. *Cancer Res.*, **37**, 2114-2122.

Fagan, P., & Wemmer, D. E. (1992). Cooperative binding of distamycin-A to DNA in the 2:1 mode. *J. Am. Chem. Soc.*, **114**, 1080-1081.

Finlay, A. C., Hochstein, F. A., Sobin, B. A., & Murphy, F. X. (1951). Netropsin, a new antibiotic produced by a Streptomyces. *J. Am. Chem. Soc.*, **73**, 341-343.

Fontana, M., Lestingi, M., Mondello, C., Braghetti, A., Montecucco, A., & Ciarrocchi, G. (1992). DNA binding properties of FCE 24517, an electrophilic distamycin analogue. *Anticancer Drug Des.*, **7**, 131-141.

Fox, K. R., & Waring, M. J. (1984). DNA structural variations produced by actinomycin and distamycin as revealed by DNase I footprinting. *Nucleic Acids Res.*, **12**, 9271-9285.

Fratini, A. V., Kopka, M. L., Drew, H. R., & Dickerson, R. E. (1982). Reversible bending and helix geometry in a B-DNA dodecamer: CGCGAATT^{Br}CGCG. *J. Biol. Chem.*, **257**, 14686-14707.

Galas, D. J., & Schmitz, A. (1978). DNase footprinting: a simple method for the detection of protein-DNA binding specificity. *Nucleic Acids Res.*, **5**, 3157-3170.

Geiduschek, E. P. (1961). "Reversible" DNA. *Proc. Acad. Natl. Sci. U.S.A.*, **47**, 950-955.

Geierstanger, B. H., Jacobsen, J. P., Mrksich, M., Dervan, P. B., & Wemmer, D. E. (1994a). Structural and dynamic characterization of the heterodimeric and homodimeric complexes of distamycin and 1-methylimidazole-2-carboxamide-netropsin bound to the minor groove of DNA. *Biochemistry*, **33**, 3055-3062.

Geierstanger, B. H., Mrksich, M., Dervan, P. B., & Wemmer, D. E. (1994b). Design of a G.C-specific DNA minor groove-binding peptide. *Science*, **266**, 646-650.

Geierstanger, B. H., & Wemmer, D. E. (1995). Complexes of the minor groove of DNA. *Ann. Rev. Biophys. Biomol. Struct.*, **24**, 463-493.

Geroni, C., Pesenti, E., Tagliabue, G., Ballinari, D., Mongelli, N., Broggini, M., Erba, E., D'Incalci, M., Spreafico, F., & Grandi, M. (1993). Establishment of L1210 leukemia cells resistant to the distamycin-A derivative (FCE 24517): characterization and cross-resistance studies. *Int. J. Cancer*, **53**, 308-314.

Gibson, N. W., Mattes, W. B., & Hartley, J. A. (1985). Identification of specific DNA lesions induced by three classes of chloroethylating agents: chloroethylnitrosoureas, chloroethylmethanesulfonates and chloroethylimidazotetrazines. *Pharmac. Ther.*, **31**, 153-163.

Gilbert, D. E., & Feigon, J. (1991). Structural analysis of drug-DNA interactions. *Cur.. Opin. Struct. Biol.*, **1**, 439-445.

Gilman, A., & Phillips, F. S. (1946). The biological actions and therapeutic applications of β-chloroethyl amines and sulfides. *Science*, **103**, 409-415.

Goldacre, R. J., Loveless, A., & Ross, W. C. J. (1949). Mode of production of chromosome abnormalities by the nitrogen mustards. *Nature*, **163**, 667-669.

Goldenberg, G. J., & Begleiter, A. (1980). Membrane transport of alkylating agents. *Pharmacol. Ther.*, **8**, 237-274.

Goodsell, D., & Dickerson, R. E. (1986). Isohelical analysis of DNA groove binding drugs. *J. Med. Chem.*, **29**, 727-733.

Gourdie, T. A., Valu, K. K., Gravatt, G. L., Boritzki, T. J., Baguley, B. C., Wakelin, L. P., Wilson, W. R., Woodgate, P. D., & Denny, W. A. (1990). DNA-directed alkylating agents. 1. Structure-activity relationships for acridine-linked aniline mustards: consequences of varying the reactivity of the mustard. *J. Med. Chem.*, **33**, 1177-1186.

Griffin, L. C., Kiessling, L. L., Beal, P. A., Gillespie, P., & Dervan, P. B. (1992). Recognition of all four base pairs of double-helical DNA by triple-helix formation: Design of nonnatural deoxyribonucleosides for pyrimidine.purine base pair binding. *J. Am. Chem. Soc.*, **114**, 7976-7982.

Grimaldi, K. A., McAdam, S. R., Souhami, R. L., & Hartley, J. A. (1994). DNA damage by anticancer agents resolved at the nucleotide level of a single copy gene: evidence for a novel binding site for cisplatin in cells. *Nucleic Acids Res.*, **22**, 2311-2317.

Grueneberg, D. A., Ojwang, J. O., Benasutti, M., Hartman, S., & Loechler, E. L. (1991). Construction of a human shuttle vector containing a single nitrogen mustard interstrand, DNA-DNA cross-link at a unique plasmid location. *Cancer Res.*, **51**, 2268-2272.

Gura, T. (1995). Antisense has growing pains. *Science*, **270**, 575-577.

Gursky, G. V., Zasedatelev, A. S., Zhuze, A. L., Khorlin, A. A., Grokhovsky, S. L., Streltsov, S. A., Surovaya, A. N., Nikitin, S. M., Krylov, A. S., Retchinsky, V. O., Mikhailov, M. V., Beaubealashivili, R. S., & Gottikh, B. P. (1982). Synthetic sequence-specific ligands. *Cold Spring Harbor Symp. Quant. Biol.*, **47**, 367-378.

Haddow, A., Kon, G. A. R., & Ross, W. C. J. (1948). Effects upon tumours of various haloalkylarylamines. *Nature*, **162**, 824-825.

Hanka, L. J., Dietz, S. A., Gerpheide, S. A., Kuentzel, S. L., & G., M. D. (1978). CC-1065 (NSC-298223), a new antitumor antibiotic. Production, *in vitro* biological activity, microbiological assays and taxonomy of the producing microorganism. *J. Antibiot.*, **31**, 1211-1217.

Hansson, J., Lewensohn, R., Ringborg, U., & Nilsson, B. (1987). Formation and removal of DNA cross-links induced by melphalan and nitrogen mustard in relation to drug-induced cytotoxicity in human melanoma cells. *Cancer Res.*, **47**, 2631-2637.

Harshman, K. D., & Dervan, P. B. (1985). Molecular recognition of B-DNA by Hoechst 33258. *Nucleic Acids Res.*, **13**, 4825-4835.

Hartley, J. A. (1990). Mechanisms of DNA sequence selective modifications by alkylating agents. In Molecular Basis of Specificity in Nucleic Acid-Drug Interactions. B. Pullman and J. Jortner, eds. Dordrecht, Kluwer Academic Publishers. 513-530.

Hartley, J. A., Berardini, M., Ponti, M., Gibson, N. W., Thompson, A. S., Thurston, D. E., Hoey, B. M., & Butler, J. (1991a). DNA cross-linking and sequence selectivity of aziridinylbenzoquinones: a unique reaction at 5'-GC-3' sequences with 2,5-diaziridinyl-1,4-benzoquinone upon reduction. *Biochemistry*, **30**, 11719-11724.

Hartley, J. A., Berardini, M. D., & Souhami, R. L. (1991b). An agarose gel method for the determination of DNA interstrand crosslinking applicable to the measurement of the rate of total and "second-arm" crosslink reactions. *Anal. Biochem.*, **193**, 131-134.

Hartley, J. A., Bingham, J. P., & Souhami, R. L. (1992). DNA sequence selectivity of guanine-N7 alkylation by nitrogen mustards is preserved in intact cells. *Nucleic Acids Res.*, **20**, 3175-3178.

Hartley, J. A., Forrow, S. M., & Souhami, R. L. (1990). Effect of ionic strength and cationic DNA affinity binders on the DNA sequence selective alkylation of guanine N7-positions by nitrogen mustards. *Biochemistry*, **29**, 2985-2991.

Hartley, J. A., Gibson, N. W., Kohn, K. W., & Mattes, W. B. (1986). DNA sequence selectivity of guanine-N7 alkylation by three antitumour chloroethylating agents. *Cancer Res.*, **46**, 1943-1947.

Hartley, J. A., Lown, J. W., Mattes, W. B., & Kohn, K. W. (1988a). DNA sequence specificity of antitumor agents. Oncogenes as possible targets for cancer therapy. *Acta Oncol.*, **27**, 503-510.

Hartley, J. A., Mattes, W. B., Vaughan, K., & Gibson, N. W. (1988b). DNA sequence specificity of guanine N7-alkylations for a series of structurally related triazenes. *Carcinogenesis*, **9**, 669-674.

Hartley, J. A., McAdam, S. R., Das, S., Roldan, M. C., Haskell, M. K., & Lee, M. (1994). Molecular and cellular pharmacology of novel photoactive psoralen and coumarin conjugates of pyrrole- and imidazole-containing analogues of netropsin. *Anticancer Drug Des.*, **9**, 181-197.

Hartley, J. A., Webber, J., Wyatt, M. D., Bordenick, N., & Lee, M. (1995). Novel cytotoxic DNA sequence and minor groove targeted photosensitizers: conjugates of pyrene and netropsin analogues. *Bioorg. Med. Chem.*, **3**, 623-629.

Hartley, J. A., Wyatt, M. D., Garbiras, B. G., Richter, C., & Lee, M. (1994). Probing the importance of the second chloroethyl arm of a benzoic acid mustard derivative of an imidazole-containing analogue of distamycin. *Bioorg. Med. Chem. Lett.*, **4**, 2421-2424.

Hartwell, L. H., & Kastan, M. B. (1994). Cell cycle control and cancer. *Science,* **266**, 1821-1828.

Hausheer, F. H., Singh, U. C., Saxe, J. D., & Colvin, O. M. (1989). Identification of local determinants of DNA interstrand crosslink formation by cyclophosphamide metabolites. *Anticancer Drug Des.*, **4**, 281-294.

Hay, M. P., Wilson, W. R., Moselen, J. W., Palmer, B. D., & Denny, W. A. (1994). Hypoxia-selective antitumor agents. 8. Bis(nitroimidazolyl)-alkanecarboxamides: a new class of hypoxia-selective cytotoxins and hypoxic cell radiosensitisers. *J. Med. Chem.*, **37**, 381-91.

Heidelberger, C., Chaudhuari, N. K., Danenberg, P., Mooren, D., Greisbach, L., Duschinsky, R., Schnitzer, R. J., Pleven, E., & Scheiner, J. (1957). Fluorinated pyrimidines, a new class of tumor-inhibitory compounds. *Nature,* **179**, 663-666.

Helene, C. (1991). The anti-gene strategy: control of gene expression by triplex-forming-oligonucleotides. *Anticancer Drug Des.*, **6**, 569-584.

Herfeld, P., Helissey, P., Giorgi-Renault, S., Goulaouic, H., Pager, J., & Auclair, C. (1994). Poly(pyrrolecarboxamides) linked to photoactivable chromophore isoalloxazine. Synthesis, selective binding, and DNA cleaving properties. *Bioconj. Chem.*, **5**, 67-76.

Hertzberg, R. P., & Dervan, P. B. (1982). Cleavage of double helical DNA by methidiumpropyl EDTA iron(II). *J. Am. Chem. Soc.*, 313-315.

Hertzberg, R. P., & Dervan, P. B. (1984). Cleavage of DNA with methidiumpropyl-EDTA-Iron(II): reaction conditions and product analyses. *Biochemistry,* **23**, 3934-3945.

Hertzberg, R. P., Hecht, S. M., Reynolds, V. L., Molineux, I. J., & Hurley, L. H. (1986). DNA sequence specificity of the pyrrolo[1,4]benzodiazepine antitumor antibiotics. Methidiumpropyl-EDTA-iron(II) footprinting analysis of DNA binding sites for anthramycin and related drugs. *Biochemistry,* **25**, 1249-1258.

Hopkins, P. B., Millard, J. T., Woo, J., & Weidner, M. F. (1991). Sequence preferences of DNA interstrand cross-linking agents: importance of minimal DNA structural reorganization in the cross-linking reactions of mechlorethamine, cisplatin, and mitomycin C. *Tetrahedron*, **47**, 2475-2489.

Huang, H., Woo, J., Alley, S. C., & Hopkins, P. B. (1995). DNA-DNA interstrand cross-linking by cis-diamminedichloroplatinum (II):N7(dG)-to-N7(dG) cross-linking at 5'-d(GC) in synthetic oligonucleotides. *Bioorg. Med. Chem.*, **3**, 659-670.

Huang, J., Pratum, T. K., & Hopkins, P. B. (1994). Covalent structure of the DNA-DNA interstrand cross-link formed by reductively activated FR66979 in synthetic DNA duplexes. *J. Am. Chem. Soc.*, **116**, 2703-2709.

Huang, L., Quada, J. C., & Lown, J. W. (1995). Design, synthesis and sequence selective DNA cleavage of functional models of bleomycin. 1. Hybrids incorporating a simple metal-complexing moiety of bleomycin and lexitropsin carriers. *Bioconj. Chem.*, **6**, 21-33.

Hurley, L. H., & Draves, P. H. (1993). Molecular aspects of the interaction of (+)-CC-1065 with DNA. In Molecular Aspects of Anticancer Drug-DNA Interactions. M. Waring and S. Neidle, eds. Basingstoke, MacMillan Press. 89-133.

Hurley, L. H., Lee, C. S., McGovren, J. P., Warpehoski, M. A., Mitchell, M. A., Kelly, R. C., & Aristoff, P. A. (1988). Molecular basis for sequence-specific DNA alkylation by CC-1065. *Biochemistry*, **27**, 3886-3892.

Hurley, L. H., & Petrusek, R. (1979). Proposed structure of the anthramycin-DNA adduct. *Nature*, **282**, 529-31.

Hurley, L. H., Reynolds, V. L., Swenson, D. H., Petzold, G. L., & Scahill, T. A. (1984). Reaction of the antitumor antibiotic CC-1065 with DNA. Structure of an adduct with DNA sequence specificity. *Science*, **226**, 843-844.

Hurley, L. H., Rokem, J. S., & Petrusek, R. L. (1980). Proposed structures of the pyrrolo(1,4)benzodiazepine antibiotic-deoxyribonucleic acid adducts. *Biochem. Pharmacol.*, **29**, 1307-1310.

Hurley, L. H., Warpehoski, M. A., Lee, C. S., McGovren, J. P., Scahill, T. A., Kelly, R. C., Mitchell, M. A., Wicnienski, N. A., Gebhard, I., Johnson, P. D., & Bradford, V. S. (1990). Sequence specificity of DNA alkylation by the unnatural enantiomer of CC-1065 and its synthetic analogues. *J. Am. Chem. Soc.*, **112**, 4633-4649.

Islam, I., Skibo, E. B., Dorr, R. T., & Alberts, D. S. (1991). Structure-activity studies of antitumor agents based on pyrrolo[1,2-a]benzimidazoles: new reductive alkylating DNA cleaving agents. *J. Med. Chem.*, **34**, 2954-2961.

Iyer, V. N., & Szybalski, W. (1964). Mitomycin and porfiromycin: chemical mechanism of activation and cross-linking of DNA. *Science*, **145**, 55-58.

Jenkins, T. C., Hurley, L. H., Neidle, S., & Thurston, D. E. (1994a). Structure of a covalent DNA minor groove adduct with a pyrrolobenzodiazepine dimer: evidence for sequence-specific interstrand cross-linking. *J. Med. Chem.*, **37**, 4529-4537.

Jenkins, T. C., Parrick, J., & Porssa, M. (1994b). DNA-binding properties of nitroarene oligopeptides designed as hypoxia-selective agents. *Anticancer Drug Des.*, **9**, 477-493.

Kahne, D. (1995). Strategies for the design of minor groove binders: a re-evaluation based on the emergence of site-selective carbohydrate binders. *Chemistry and Biology*, **2**, 7-12.

Karlin, S. (1986). Significant potential secondary structures in the Epstein-Barr virus genome. *Proc. Natl. Acad. Sci. U.S.A.*, **83**, 6915-6919.

Karp, J. E., & Broder, S. (1994). New directions in molecular medicine. *Cancer Res.*, **54**, 653-665.

Kartner, N., & Ling, V. (1989). Multidrug resistance in cancer. *Sci. Am.*, **260**, 44-51.

Katahira, M., Sugeta, H., & Kyogoku, Y. (1990). A new model for the bending of DNAs containing the oligo(dA) tracts based on NMR observations. *Nucleic Acids Res.*, **18**, 613-618.

Kerr, D. E., Schreiber, G. J., Vrudhula, V. M., Svensson, H. P., Hellstrom, I., Hellstrom, K. E., & Senter, P. D. (1995). Regressions and cures of melanoma xenografts following treatment with monoclonal antibody β-lactamase conjugates in combination with anticancer prodrugs. *Cancer Res.*, **55**, 3558-3563.

Kissinger, K., Dabrowiak, J. C., & Lown, J. W. (1990). Molecular recognition between oligopeptides and nucleic acids: DNA binding specificity of a series of bis netropsin analogues deduced from footprinting analysis. *Chem. Res. Toxicol.*, **3**, 162-168.

Kissinger, K., Krowicki, K., Dabrowiak, J. C., & Lown, J. W. (1987). Molecular recognition between oligopeptides and nucleic acids. Monocationic imidazole lexitropsins that display enhanced GC sequence dependent DNA binding. *Biochemistry*, **26**, 5590-5595.

Kizu, R., Draves, P. H., & Hurley, L. H. (1993). Correlation of DNA sequence specificity of anthramycin and tomaymycin with reaction kinetics and bending of DNA. *Biochemistry*, **32**, 8712-8722.

Kohn, K. W., Erickson, L. C., Ewig, R. A., & Friedman, C. A. (1976). Fractionation of DNA from mammalian cells by alkaline elution. *Biochemistry*, **15**, 4629-4637.

Kohn, K. W., Ewig, R. A., Erickson, L. C., & Zwelling, L. A. (1981). Measurement of strand breaks and crosslinks by alkaline elution. In DNA Repair. A Laboratory Manual of Research Procedures. E. C. Freidberg and P. C. Hanawalt, eds. New York, Marcel Dekker Inc. 379-401.

Kohn, K. W., Hartley, J. A., & Mattes, W. B. (1987). Mechanisms of DNA sequence selective alkylation of guanine-N7 positions by nitrogen mustards. *Nucleic Acids Res.*, **15**, 10531-10549.

Kohn, K. W., Orr, A., O'Connor, P. M., Guziec, L. J., & Guziec, F. J. (1994). Synthesis and DNA-sequence selectivity of a series of mono- and difunctional 9-aminoacridine nitrogen mustards. *J. Med. Chem.*, **37**, 67-72.

Kohn, K. W., Spears, C. L., & Doty, P. D. (1966). Inter-strand crosslinking of DNA by nitrogen mustard. *J. Mol. Biol.*, **19**, 266-288.

Koo, H. S., Wu, H. M., & Crothers, D. M. (1986). DNA bending at adenine.thymine tracts. *Nature,* **320**, 501-506.

Kopka, M. L., Goodsell, D. S., Baikalov, I., Grzeskowiak, K., Cascio, D., & Dickerson, R. E. (1994). Crystal structure of a covalent DNA-drug adduct: anthramycin bound to C-C-A-A-C-G-T-T-G-G and a molecular explanation of specificity. *Biochemistry,* **33**, 13593-13610.

Kopka, M. L., Yoon, C., Goodsell, D., Pjura, P., & Dickerson, R. E. (1985). The molecular origin of DNA-drug specificity in netropsin. *Proc. Natl. Acad. Sci. U.S.A.,* **82**, 1376-1380.

Krishnamurthy, G., Polte, T., Rooney, T., & Hogan, M. E. (1990). A photochemical method to map ethidium bromide binding sites on DNA: application to a bent DNA fragment. *Biochemistry,* **29**, 981-988.

Krowicki, K., Balzarini, J., De, C. E., Newman, R. A., & Lown, J. W. (1988). Novel DNA groove binding alkylators: design, synthesis, and biological evaluation. *J. Med. Chem.,* **31**, 341-345.

Krowicki, K., & Lown, J. W. (1987). Synthesis of novel imidazole-containing DNA minor groove binding oligopeptides related to the antiviral antibiotic netropsin. *J. Org. Chem.,* **52**, 3493-3501.

Krugh, T. R. (1994). Drug-DNA interactions. *Cur.. Opin. Struct. Biol.,* **4**, 351-364.

Kufe, D. W., Major, P. P., Egan, E. M., & Beardsly, G. P. (1980). Correlation of cytotoxicity with incorporation of ara-C into DNA. *J. Biol. Chem.,* **255**, 8997-9000.

Kumar, S., Lipman, R., & Tomasz, M. (1992). Recognition of specific DNA sequences by mitomycin C for alkylation. *Biochemistry,* **31**, 1399-1407.

Lane, D. P. (1992). Worrying about p53. *Current Biology,* **2**, 581-583.

Lane, M. J., Dabrowiak, J. C., & Vournakis, J. N. (1983). Sequence specificity of actinomycin and netropsin binding to pBR322 DNA analyzed by protection from DNase I. *Proc. Natl. Acad. Sci. U.S.A.,* **80**, 3260-3264.

Lavery, R., & Pullman, B. (1985). The dependence of the surface electrostatic potential of B-DNA on environmental factors. *J. Biomol. Struct. Dyn.*, **2**, 1021-1032.

Lawley, P. D., & Brookes, P. (1967). Interstrand cross-linking of DNA by difunctional alkylating agents. *J. Mol. Biol.*, **25**, 143-160.

Lee, C. S., & Gibson, N. W. (1991). DNA damage and differential cytotoxicity produced in human carcinoma cells by CC-1065 analogues, U-73,975 and U-77,779. *Cancer Res.*, **51**, 6586-6591.

Lee, C. S., Pfeifer, G. P., & Gibson, N. W. (1994). Mapping of DNA alkylation sites induced by adozelesin and bizelesin in human cells by ligation-mediated polymerase chain reaction. *Biochemistry*, **33**, 6024-6030.

Lee, C. S., Sun, D., Kizu, R., & Hurley, L. H. (1991a). Determination of the structural features of (+)-CC-1065 that are responsible for bending and winding of DNA. *Chem. Res. Toxicol.*, **4**, 203-213.

Lee, H. H., Boyd, M., Gravatt, G. L., & Denny, W. A. (1991b). Pyrazole analogues of the bispyrrolecarboxamide anti-tumour antibiotics: synthesis, DNA binding and anti-tumour properties. *Anticancer Drug Des.*, **6**, 501-517.

Lee, M., Chang, D. K., Hartley, J. A., Pon, R. T., Krowicki, K., & Lown, J. W. (1988). Structural and dynamic aspects of binding of a prototype lexitropsin to the decadeoxyribonucleotide d(CGCAATTGCG)$_2$ deduced from high-resolution ^{1}H NMR Studies. *Biochemistry*, **27**, 445-455.

Lee, M., Garbiras, B. J., Young, C., Blair, B., Wyatt, M. D., & Hartley, J. A. (1994). Synthesis, DNA binding, cytotoxic properties, and structure activity relationship of a series of head to tail, and tail to tail linked imidazole-, and pyrrole-containing analogs of distamycin with N-terminal benzoic acid mustard groups. *Med. Chem. Res.*, **4**, 123-130.

Lee, M., Hartley, J. A., Pon, R. T., Krowicki, K., & Lown, J. W. (1988a). Sequence specific molecular recognition by a monocationic lexitropsin of the decadeoxyribonucleotide d-[CATGGCCATG]$_2$: structural and dynamic aspects deduced from high field ^{1}H-NMR studies. *Nucleic Acids Res.*, **16**, 665-684.

Lee, M., Krowicki, K., Hartley, J. A., Pon, R. T., & Lown, J. W. (1988b). Molecular recognition between oligopeptides and nucleic acids: influence of van der Waals contacts in determining the 3'-terminus of DNA sequences read by monocationic lexitropsins. *J. Am. Chem. Soc.*, **110**, 3641-3649.

Lee, M., Krowicki, K., Shea, R. G., Lown, J. W., & Pon, R. T. (1989). Molecular recognition between oligopeptides and nucleic acids. Specificity of binding of a monocationic bis-furan lexitropsin to DNA deduced from footprinting and 1H NMR studies. *J. Mol. Recognit.*, **2**, 84-93.

Lee, M., Preti, C. S., Vinson, E., Wyatt, M. D., & Hartley, J. A. (1994). GC Sequence specific recognition by an *N*-formamido, C-terminus-modified and imidazole-containing analogue of netropsin. *J. Med. Chem.*, **37**, 4073-4075.

Lee, M., Rhodes, A. L., Wyatt, M. D., D'Incalci, M., Forrow, S., & Hartley, J. A. (1993a). *In vitro* cytotoxicity of GC sequence directed alkylating agents related to distamycin. *J. Med. Chem.*, **36**, 863-870.

Lee, M., Rhodes, A. L., Wyatt, M. D., Forrow, S., & Hartley, J. A. (1993b). Design, synthesis, and biological evaluation of DNA sequence and minor groove selective alkylating agents. *Anticancer Drug Des.*, **8**, 173-192.

Lee, M., Rhodes, A. L., Wyatt, M. D., Forrow, S., & Hartley, J. A. (1993c). GC base sequence recognition by oligo(imidazolecarboxamide) and C-terminus-modified analogues of distamycin deduced from circular dichroism, proton nuclear magnetic resonance, and methidiumpropyl-ethylenediaminetetraacetate-iron(II) footprinting studies. *Biochemistry*, **32**, 4237-4245.

Lee, M., Roldan, M. C., Haskell, M. K., McAdam, S. R., & Hartley, J. A. (1994a). *In vitro* photoinduced cytotoxicity and DNA binding properties of psoralen and coumarin conjugates of netropsin analogues: DNA sequence-directed alkylation and cross-link formation. *J. Med. Chem.*, **37**, 1208-1213.

Lee, M., Walker, C., Cooper, M., Forrow, S. M., & Hartley, J. A. (1994b). Sequence selective molecular recognition of long DNA sequences by oligomethylene-linked oligoimidazole analogs of distamycin. *J. Bio. Comp. Polymers*, **9**, 3-28.

Lewin, M. (1986). Principles of Cancer Chemotherapy. In American Cancer Society, The Cancer Book. A. I. Holleb, ed. Garden City, N. Y., Doubleday and Company.

Li, L. H., DeKoning, T. F., Kelly, R. C., Krueger, W. C., McGovren, J. P., Padbury, G. E., Petzold, G. L., Wallace, T. L., Ouding, R. J., Prairie, M. D., & Gebhard, I. (1992). Cytotoxicity and antitumor activity of carzelesin, a prodrug cyclopropylpyrroloindole analogue. *Cancer Res.*, **52**, 4904-4913.

Li, L. H., Kelly, R. C., Warpehoski, M. A., McGovren, J. P., Gebhard, I., & DeKoning, T. F. (1991). Adozelesin, a selected lead among cyclopropylpyrroloindole analogs of the DNA-binding antibiotic, CC-1065. *Invest. New Drugs*, **9**, 137-148.

Li, V., & Kohn, H. (1991). Studies on the bonding specificity for mitomycin C-DNA monoalkylation processes. *J. Am. Chem. Soc.*, **113**, 275-283.

Liepinsh, E., Leupin, W., & Otting, G. (1994). Hydration of DNA in aqueous solution: NMR evidence for a kinetic destabilization of the minor groove hydration of d-$(TTAA)_2$ versus d-$(AATT)_2$ segments. *Nucleic Acids Res.*, **22**, 2249-2254.

Lin, C. H., Beale, J. M., & Hurley, L. H. (1991a). Structure of the (+)-CC-1065-DNA adduct: critical role of ordered water molecules and implications for involvement of phosphate catalysis in the covalent reaction. *Biochemistry*, **30**, 3597-3602.

Lin, C. H., Sun, D. Y., & Hurley, L. H. (1991b). (+)-CC-1065 produces bending of DNA that appears to resemble adenine/thymine tracts. *Chem. Res. Toxicol.*, **4**, 21-26.

Liotta, L. A. (1992). Cancer cell invasion and metastasis. *Sci. Am.*, **266**, 54-59.

Long, H. J. (1994). Paclitaxel (Taxol): a novel anticancer chemotherapeutic drug. *Mayo Clin. Proc.*, **69**, 341-345.

Loveless, A. (1951). Qualitative aspects of the chemistry and biology of radiomimetic (mutagenic) substances. *Nature*, **167**, 338-342.

Lown, J. W. (1990). Molecular mechanisms of DNA sequence recognition by groove binding ligands: biochemical and biological consequences. In Molecular Basis of Specificity in Nucleic Acid-Drug Interactions. B. Pullman and J. Jortner, eds. Dordrecht, Kluwer Academic Publishers. 106-122.

Lown, J. W., & Krowicki, K. (1985). Efficient total synthesis of the oligopeptide antibiotics netropsin and distamycin. *J. Org. Chem.*, **50**, 3774-3779.

Lown, J. W., Krowicki, K., Balzarini, J., Newman, R. A., & De Clercq, E. (1989). Novel linked antiviral and antitumor agents related to netropsin and distamycin: synthesis and biological evaluation. *J. Med. Chem.*, **32**, 2368-2375.

Lown, J. W., Krowicki, K., Bhat, U. G., Skorobogaty, A., Ward, B., & Dabrowiak, J. C. (1986). Molecular recognition between oligopeptides and nucleic acids: novel imidazole-containing oligopeptides related to netropsin that exhibit altered DNA sequence specificity. *Biochemistry*, **25**, 7408-7416.

Luck, G., Zimmer, C., Reinert, K. E., & Arcamone, F. (1977). Specific interactions of distamycin A and its analogs with (A-T) rich and (G-C) rich duplex regions of DNA and deoxypolynucleotides. *Nucleic Acids Res.*, **4**, 2655-2670.

Manderville, R. A., Ellena, J. F., & Hecht, S. M. (1995). Interaction of Zn(II).Bleomycin with $d(CGCTAGCG)_2$. A binding model based on NMR experiments and restrained molecular dynamics calculations. *J. Am. Chem. Soc.*, **117**, 7891-7903.

Maniatis, T., Fritsch, E. F., & Sambrook, J. (1982). Molecular Cloning. A Laboratory Manual. Cold Spring Harbor, N. Y., Cold Spring Harbor Laboratory.

Marini, J. C., Levene, S. D., Crothers, D. M., & Englund, P. T. (1982). Bent helical structure in kinetoplast DNA. *Proc. Natl. Acad. Sci. U.S.A.*, **79**, 7664-7668.

Mattes, W. B., Hartley, J. A., & Kohn, K. W. (1986a). DNA sequence selectivity of guanine-N7 alkylation by nitrogen mustards. *Nucleic Acids Res.*, **14**, 2971-2987.

Mattes, W. B., Hartley, J. A., & Kohn, K. W. (1986b). Mechanism of DNA strand breakage by piperidine at sites of N7-alkylguanines. *Biochim. Biophys. Acta*, **868**, 71-76.

Mattes, W. B., Hartley, J. A., Kohn, K. W., & Matheson, D. W. (1988). GC-rich regions in genomes as targets for DNA alkylation. *Carcinogenesis*, **9**, 2065-2072.

Maxam, A. M., & Gilbert, W. (1980). Sequencing end-labeled DNA with base-specific chemical cleavages. *Methods Enzymol.*, **65**, 499-560.

Mazzini, S., Musco, G., Ragg, E., & Penco, S. (1994). Binding modes of the distamycin analogue FCE-24517 to d(CGTATACG)$_2$. ^{1}H and ^{13}C sequence-specific assignments. *Magnetic Resonance in Chemistry*, **32**, 139-150.

McCarthy, J. G., Frederick, C. A., & Nicolas, A. (1993). A structural analysis of the bent kinetoplast DNA from *Crithidia fasciculata* by high resolution chemical probing. *Nucleic Acids Res.*, **21**, 3309-3317.

McCarthy, J. G., Williams, L. D., & Rich, A. (1990). Chemical reactivity of potassium permanganate and diethyl pyrocarbonate with B DNA: specific reactivity with short A-tracts. *Biochemistry*, **29**, 6071-6081.

Millard, J. T., Raucher, S., & Hopkins, P. B. (1990). Mechlorethamine cross-links deoxyguanosine residues at 5'-GNC sequences in duplex DNA fragments. *J. Am. Chem. Soc.*, **112**, 2459-2460.

Mitchell, M. A., Weiland, K. L., Aristoff, P. A., Johnson, P. D., & Dooley, T. P. (1993). Sequence-selective guanine reactivity by duocarmycin A. *Chem. Res. Toxicol.*, **6**, 421-424.

Montecucco, A., Fontana, M., Focher, F., Lestingi, M., Spadari, S., & Ciarrocchi, G. (1991). Specific inhibition of human DNA ligase adenylation by a distamycin derivative possessing antitumor activity. *Nucleic Acids Res.*, **19**, 1067-1072.

Montgomery, J. A. (1986). Design of chemotherapeutic agents. *Acc. Chem. Res.*, **19**, 293-300.

Morgan, A. R., Lee, J. S., Pulleybank, D. E., Murray, N. L., & Evans, D. H. (1979). Review: Ethidium fluorescence assays part 1. Physiochemical studies. *Nucleic Acids Res.*, **7**, 547-569.

Mrksich, M., & B., D. P. (1995). Recognition in the minor groove of DNA at 5'-(A.T)GCGC(A.T)-3' by a four ring tripeptide dimer. Reversal of the specificity of the natural product distamycin. *J. Am. Chem. Soc.*, **117**, 3325-3332.

Mrksich, M., & Dervan, P. B. (1993a). Antiparallel side-by-side heterodimer for sequence specific recognition in the minor groove of DNA by a distamycin/1-methylimidazole-2-carboxamide-netropsin pair. *J. Am. Chem. Soc.*, **115**, 2572-2576.

Mrksich, M., & Dervan, P. B. (1993b). Enhanced sequence specific recognition in the minor groove of DNA by covalent peptide dimers: Bis(pyridine-2-carboxamidonetropsin)$(CH_2)_{3-6}$. *J. Am. Chem. Soc.*, **115**, 9822-9899.

Mrksich, M., & Dervan, P. B. (1994). Design of a covalent peptide heterodimer for sequence-specific recognition in the minor groove of double-helical DNA. *J. Am. Chem. Soc.*, **117**, 3663-3664.

Mrksich, M., Parks, M. E., & Dervan, P. B. (1994). Hairpin peptide motif. A new class of oligopeptides for sequence-specific recognition in the minor groove of double-helical DNA. *J. Am. Chem. Soc.*, **116**, 7983-7988.

Mrksich, M., Wade, W. S., Dwyer, T. J., Geierstanger, B. H., Wemmer, D. E., & Dervan, P. B. (1992). Antiparallel side-by-side dimeric motif for sequence specific recognition in the minor groove of DNA by the designed peptide 1-methylimidazole-2-carboxamide netropsin. *Proc. Natl. Acad. Sci. U.S.A.*, **89**, 7586-7590.

Murray, V., Motyka, H., England, P. R., Wickham, G., Lee, H. H., Denny, W. A., & McFadyen, W. D. (1992). An investigation of the sequence-specific interaction of cis-diamminedichloroplatinum(II) and four analogues, including two acridine-tethered complexes, with DNA inside human cells. *Biochemistry*, **31**, 11812-11817.

Nadeau, J. G., & Crothers, D. M. (1989). Structural basis for DNA bending. *Proc. Acad. Natl. Sci. U.S.A.*, **86**, 2622-2626.

Natrajan, A., & Hecht, S. M. (1994). Bleomycins: Mechanism of polynucleotide recognition and oxidative degradation. In Molecular Aspects of Anticancer Drug-DNA Interactions. S. Neidle and M. Waring, eds. Basingstoke, Macmillan Press. 197-242.

Neidle, S. (1992). Minor-groove width and accessibility in B-DNA drug and protein complexes. *Febs. Lett.*, **298**, 97-99.

Neilson, P. E. (1991). Sequence-selective DNA recognition by synthetic ligands. *Bioconj. Chem.*, **2**, 1-12.

Nelson, H. C. M., Finch, J. T., Luisi, B. F., & Klug, A. (1987). The structure of an oligo(dA).oligo(dT) tract and its biological implications. *Nature,* **330**, 221-226.

Nicolaou, K. C., Smith, A. L., & Yue, E. W. (1993). Chemistry and biology of natural and designed enediynes. *Proc. Natl. Acad. Sci. U.S.A.*, **90**, 5881-5888.

O'Connor, P. M., & Kohn, K. W. (1990). Comparative pharmacokinetics of DNA lesion formation and removal following treatment of L1210 cells with nitrogen mustards. *Cancer Commun.*, **2**, 387-394.

O'Reilly, S. M., Newlands, E. S., Glaser, M. G., , & Stevens, M. F. (1993). Temozolomide: a new oral cytotoxic chemotherapeutic agent with promising activity against brain tumours. *Eu. J. Cancer,* **29A**, 940-942.

Ojwang, J. O., Grueneberg, D. A., & Loechler, E. L. (1989). Synthesis of a duplex oligonucleotide containing a nitrogen mustard interstrand DNA-DNA cross-link. *Cancer Res.*, **49**, 6529-37.

Olson, R. D., & Mushlin, P. S. (1990). Doxorubicin cardiotoxicity: analysis of prevailing hypotheses. *FASEB J.*, **4**, 3076-3086.

Osborne, M. R., Wilman, D. E. V., & Lawley, P. D. (1995). Alkylation of DNA by the nitrogen mustard bis(2-chloroethyl)methylamine. *Chem. Res. Toxicol.*, **8**, 316-320.

Owa, T., Haupt, A., Otsuka, M., Kobayashi, S., Tomoika, N., Itai, A., Ohno, M., Shiraki, T., Uesugi, M., Sugiura, Y., & Maeda, K. (1992). Man-designed

bleomycins: significance of the binding sites as enzyme models and of the stereochemistry of the linker moiety. *Tetrahedron,* **48**, 1193-1208.

Palmer, B. D., Wilson, W. R., Cliffe, S., & Denny, W. A. (1992). Hypoxia-selective antitumor agents. 5. Synthesis of water-soluble nitroaniline mustards with selective cytotoxicity for hypoxic mammalian cells. *J. Med. Chem.*, **35**, 3214-3222.

Panasci, L., Henderson, D., Torres-Garcia, S. J., Skalski, V., Caplan, S., & Hutchinson, M. (1988). Transport, metabolism, and DNA interaction of melphalan in lymphocytes from patients with chronic lymphocytic leukemia. *Cancer Res.*, **48**, 1972-1976.

Panthananickal, A., Hansch, C., A., L., & Quinn, F. R. (1978). Structure-activity relationships in antitumor aniline mustards. *J. Med. Chem.*, **21**, 16-26.

Parrick, J., & Porssa, M. (1993). Synthesis of a nitro oligo-*N*-methylimidazole carboxamide derivative: a radiosensitiser target to DNA. *Tett. Lett.*, **34**, 5011-5014.

Pegg, A. E. (1990). Mammalian O6-alkylguanine-DNA alkyltransferase: regulation and importance in response to alkylating carcinogenic and therapeutic agents. *Cancer Res.*, **50**, 6119-6129.

Pelton, J. G., & Wemmer, D. E. (1989). Structural characterization of a 2:1 distamycin A.d(CGCAAATTGGC) complex by two-dimensional NMR. *Proc. Natl. Acad. Sci. U.S.A.*, **86**, 5723-5727.

Pezzoni, G., Grandi, M., Biasoli, G., Capolongo, L., Ballinari, D., Giuliani, F. C., Barbieri, B., Pastori, A., Pesenti, E., & Mongelli, N. (1991). Biological profile of FCE 24517, a novel benzoyl mustard analogue of distamycin A. *Br. J. Cancer,* **64**, 1047-1050.

Pieper, R. O., & Erickson, L. C. (1990). DNA adenine adducts induced by nitrogen mustards and their role in transcription termination *in vitro*. *Carcinogenesis,* **11**, 1739-1746.

Pieper, R. O., Futscher, B. W., & Erickson, L. C. (1989). Transcription-terminating lesions induced by bifunctional alkylating agents *in vitro*. *Carcinogenesis*, **10**, 1307-14.

Ponti, M., Forrow, S. M., Souhami, R. L., D'Incalci, M., & Hartley, J. A. (1991). Measurement of the sequence specificity of covalent DNA modification by antineoplastic agents using Taq DNA polymerase. *Nucleic Acids Res.*, **19**, 2929-2933.

Portugal, J., & Waring, M. J. (1987). Hydroxyl radical footprinting of the sequence-selective binding of netropsin and distamycin to DNA. *FEB*, **225**, 195-200.

Powis, G. (1993). Pharmacological intervention with signal transduction. In New Approached in Cancer Pharmacology: Drug Design and Development. P. Workman, ed. Berlin, Springer-Verlag. 39-54.

Pratt, W. B., Ruddon, R. W., Ensminger, W. D., & Maybaum, J. (1994). The Anticancer Drugs. Oxford, Oxford University Press.

Priestman, T. J. (1989). Cancer Chemotherapy: an Introduction. London, Springer-Verlag.

Pullman, A., & Pullman, B. (1981). Molecular electrostatic potential of the nucleic acids. *Quart. Rev. Biophys.*, **14**, 289-380.

Ralph, R. K., Judd, W., Pommier, Y., & Kohn, K. W. (1994). DNA topoisomerases. In Molecular Aspects of Anticancer Drug-DNA Interactions. S. Neidle and M. Waring, eds. Basingstoke, Macmillan Press. 1-95.

Rao, K. E., Bathini, Y., & Lown, J. W. (1990). Synthesis of novel thiazole-containing DNA minor groove binding oligopeptides related to the antibiotic distamycin. *J. Org. Chem.*, **55**, 728-737.

Rao, K. E., Dasgupta, D., & Sasisekharan, V. (1988). Interaction of synthetic analogues of distamycin and netropsin with nucleic acids. Does curvature of ligand play a role in distamycin-DNA interactions? *Biochemistry*, **27**, 3018-3024.

Rao, K. E., Gosselin, G., Mrani, D., Perigaud, C., Imbach, J. L., Bailly, C., Henichart, J. P., Colson, P., Houssier, C., & Lown, J. W. (1994). Psoralen--lexitropsin hybrids: DNA sequence selectivity of photoinduced cross-linking from MPE footprinting and exonuclease III stop assay, and mode of binding from electric linear dichroism. *Anticancer Drug Des.*, **9**, 221-237.

Rao, K. E., Krowicki, K., Burckhardt, G., Zimmer, C., & Lown, J. W. (1991). Molecular recognition between oligopeptides and nucleic acids: DNA binding selectivity of a series of 1,2,4-triazole-containing lexitropsins. *Chem. Res. Toxicol.*, **4**, 241-252.

Rao, K. E., Shea, R. G., Yadagiri, B., & Lown, J. W. (1990). Molecular recognition between oligopeptides and nucleic acids: DNA sequence specificity and binding properties of thiazole-lexitropsins incorporating the concepts of base site acceptance and avoidance. *Anticancer Drug Des.*, **5**, 3-20.

Rao, K. E., Zimmerman, J., & Lown, J. W. (1991). Sequence-selective DNA binding by linked bis-*N*-methylpyrrole dipeptides: An analysis by MPE footprinting and force field calculations. *J. Org. Chem.*, **56**, 786-797.

Reed, E., & Kohn, K. W. (1990). Platinum analogues. In Cancer Chemotherapy: Principles and Practice. B. A. Chabner and J. M. Collins, eds. Philadelphia, J. B. Lippencott Company. 465-490.

Reynolds, V. L., Molineux, I. J., Kaplan, D. J., Swenson, D. H., & Hurley, L. H. (1985). Reaction of the antitumor antibiotic CC-1065 with DNA. Location of the site of thermally induced strand breakage and analysis of DNA sequence specificity. *Biochemistry*, **24**, 6228-6237.

Rink, S. M., & Hopkins, P. B. (1995). A mechlorethamine-induced DNA interstrand cross-link bends duplex DNA. *Biochemistry*, **34**, 1439-45.

Rink, S. M., Solomon, M. S., Taylor, M. J., Rajur, S. B., McLaughlin, L. W., & Hopkins, P. B. (1993). Covalent structure of a nitrogen mustard-induced DNA interstrand cross-link: an N7 to N7 linkage of deoxyguanosine residues at the duplex sequence 5'-d(GNC). *J. Am. Chem. Soc.*, **115**, 2551-2557.

Rosenberg, B., Van Camp, L., & Krigas, T. (1965). Inhibition of cell division in *Esherichia coli* by electrolysis products from a platinum electrode. *Nature,* **205**, 698-699.

Ross, W. E., Ewig, R. A., & Kohn, K. W. (1978). Differences between melphalan and nitrogen mustard in the formation and removal of DNA cross-links. *Cancer Res.*, **38**, 1502-6.

Sancar, A., & Sancar, G. B. (1988). DNA repair enzymes. *Ann. Rev. Biochem.*, **57**, 29-67.

Searle, M. S., & Embrey, K. J. (1990). Sequence-specific interaction of Hoechst 33258 with the minor groove of an adenine-tract DNA duplex studied in solution by ^{1}H NMR spectroscopy. *Nucleic Acids Res.*, **18**, 3753-3762.

Sessa, C., Pagani, O., Zurlo, M. G., de Jong, J., Hofmann, C., Lassus, M., Marrari, P., Strolin-Benedetti, M., & Cavalli, F. (1994). Phase I study of the novel distamycin derivative tallimustine (FCE 24517). *Ann. Oncol.*, **5**, 901-907.

Sigurdsson, S. T., & Hopkins, P. B. (1994). Synthesis and reactions with DNA of a family of DNA-DNA affinity cross-linking agents. *Tetrahedron,* **50**, 12065-12084.

Sigurdsson, S. T., Rink, S. M., & Hopkins, P. B. (1993). Affinity cross-linking of duplex DNA by a pyrrole-oligopeptide conjugate. *J. Am. Chem. Soc.*, **115**, 12633-12634.

Simon, S. M., & Schindler, M. (1994). Cell biological mechanisms of multidrug resistance in tumors. *Proc. Natl. Acad. Sci. U.S.A.*, **91**, 3497-3504.

Smellie, M., Kelland, L. R., Thurston, D. E., Souhami, R. L., & Hartley, J. A. (1994). Cellular pharmacology of novel C8-linked anthramycin-based sequence-selective DNA minor groove cross-linking agents. *Br. J. Cancer,* **70**, 48-53.

Spink, N., Brown, D. G., Skelly, J. V., & Neidle, S. (1994). Sequence-dependent effects in drug-DNA interaction: the crystal structure of Hoechst 33258 bound to the d(CGCAAATTTGCG)$_2$ duplex. *Nucleic Acids Res.*, **22**, 1607-1612.

Springer, C. J., & Niculescu-Duvaz, I. (1995). Antibody-directed enzyme prodrug therapy (ADEPT) with mustard prodrugs. *Anticancer Drug Des.*, **10**, 361-372.

Sprous, D., Zacharias, W., Wood, Z. A., & Harvey, S. C. (1995). Dehydrating agents sharply reduce curvature in DNAs containing A tracts. *Nucleic Acids Res.*, **23**, 1816-1821.

Stevens, M. F., Hickman, J. A., Langdon, S. P., Chubb, D., Vickers, L., Stone, R., Baig, G., Goddard, C., Gibson, N. W., Slack, J. A., Newton, C., Lunt, E., Fizames, C., & Lavalle, F. (1987). Antitumor activity and pharmacokinetics in mice of 8-carbamoyl-3-methyl-imidazo[5,1-d]-1,2,3,5-tetrazin-4(3H)-one (CCRG 81045; M & B 39831), a novel drug with potential as an alternative to dacarbazine. *Cancer Res.*, **47**, 5846-5852.

Stevens, M. F., Hickman, J. A., Stone, R., Gibson, N. W., Baig, G. U., Lunt, E., & Newton, C. G. (1984). Antitumor imidazotetrazines. 1. Synthesis and chemistry of 8-carbamoyl-3-(2-chloroethyl)imidazo[5,1-d]-1,2,3,5-tetrazin-4(3 H)-one , a novel broad-spectrum antitumor agent. *J. Med. Chem.*, **27**, 196-201.

Stevens, M. F., & Newlands, E. S. (1993). From triazines and triazenes to temozolomide. *Eur. J. Cancer*, **29A**, 1045-1047.

Sun, D., Lin, C. H., & Hurley, L. H. (1993a). A-tract and (+)-CC-1065-induced bending of DNA. Comparison of structural features using non-denaturing gel analysis, hydroxyl-radical footprinting, and high-field NMR. *Biochemistry*, **32**, 4487-4495.

Sun, D., Park, H. J., & Hurley, L. H. (1993b). Alkylation of guanine and cytosine in DNA by bizelesin. Evidence for a covalent immobilization leading to a proximity-driven alkylation of normally unreactive bases by a (+)-CC-1065 cross-linking compound. *Chem. Res. Toxicol.*, **6**, 889-894.

Sunters, A., Springer, C. J., Bagshawe, K. D., Souhami, R. L., & Hartley, J. A. (1992). The cytotoxicity, DNA crosslinking ability and DNA sequence selectivity of the aniline mustards melphalan, chlorambucil and 4-[bis(2-chloroethyl)amino] benzoic acid. *Biochem. Pharmacol.*, **44**, 59-64.

Takahara, P. M., Rosenzweig, A. C., Fredrick, C. A., & Lippard, S. J. (1995). Crystal structure of double-stranded DNA containing the major adduct of the anticancer drug cisplatin. *Nature*, **377**, 649-652.

Taylor, J. S., Schultz, P. G., & Dervan, P. B. (1984). DNA affinity cleaving: sequence specific cleavage of DNA by distamycin-EDTAFe(II) and EDTA-distamycinFe(II). *Tetrahedron*, **40**, 457-465.

Teng, S. P., Woodson, S. A., & Crothers, D. M. (1989). DNA sequence specificity of mitomycin cross-linking. *Biochemistry*, **28**, 3901-3907.

Tew, K. D. (1994). Glutathione-associated enzymes in anticancer drug resistance. *Cancer Res.*, **54**, 4313-20.

Thompson, A. S., & Hurley, L. H. (1995). Solution conformation of a bizelesin A-tract duplex adduct: DNA-DNA cross-linking of an A-tract straightens out bent DNA. *J. Mol. Biol.*, **252**, 86-101.

Thompson, A. S., Sun, D., & Hurley, L. H. (1995). Monoalkylation and cross-linking of DNA by cyclopropylpyrroloindoles entraps bent and straight forms of A-tracts. *J. Am. Chem. Soc.*, **117**, 2371-2372.

Tomasz, M. (1994). The mitomycins: Natural cross-linkers of DNA. In Molecular Aspects of Anticancer Drug-DNA Interactions. S. Neidle and M. Waring, eds. Basingstoke, MacMillan Press. 312-349.

Tomasz, M., Chowdary, D., Lipman, R., Shimotakahara, S., Veiro, D., Walker, V., & Verdine, G. L. (1986). Reaction of DNA with chemically or enzymatically activated mitomycin C: isolation and structure of the major covalent adduct. *Proc. Natl. Acad. Sci. U.S.A.*, **83**, 6702-6706.

Tomasz, M., Lipman, R., Chowdary, D., Pawlak, J., Verdine, G. L., & Nakanishi, K. (1987). Isolation and structure of a covalent cross-link adduct between mitomycin C and DNA. *Science*, **235**, 1204-1208.

Tong, W. P., Kirk, M. C., & Ludlum, D. B. (1982). Formation of the cross-link 1-[N3-deoxycytidyl),2-[N1-deoxyguanosinyl]ethane in DNA treated with *N,N'*-bis(2-chloroethyl)-N-nitrosourea. *Cancer Res.*, **42**, 3102-3105.

Treiber, D. K., Zhai, X., Jantzen, H. M., & Essigmann, J. M. (1994). Cisplatin-DNA adducts are molecular decoys for the ribosomal RNA transcription factor hUBF (human upstream binding factor). *Proc. Natl. Acad. Sci. U.S.A.*, **91**, 5672-5676.

Twentyman, P. R., & Luscombe, M. (1987). A study of some variables in a tetrazolium dye (MTT) based assay for cell growth and chemosensitivity. *Br. J. Cancer*, **56**, 279-285.

Van Dyke, M. W., Hertzberg, R. P., & Dervan, P. B. (1982). Map of distamycin, netropsin and actinomycin binding sites on heterogeneous DNA: DNA cleavage inhibition patterns with methidiumpropyl-EDTA Fe(II). *Proc. Natl. Acad. Sci. U.S.A.*, **79**, 5470-5474.

van Osdol, W. W., Myers, T. G., Paull, K. D., Kohn, K. W., & Weinstein, J. N. (1994). Use of the Kohonen self-organizing map to study the mechanisms of action of chemotherapeutic agents. *J. Natl. Cancer Inst.*, **86**, 1853-1859.

Wade, W. S., & Dervan, P. B. (1987). Alteration of the sequence specificity of distamycin on DNA by replacement of an N-methylpyrrolecarboxamide with pyridine-2-carboxamide. *J. Am. Chem. Soc.*, **109**, 1574-1575.

Wade, W. S., Mrksich, M., & Dervan, P. B. (1992). Design of peptides that bind in the minor groove of DNA at 5'-(A.T)G(A.T)C(A.T)-3' sequences by a dimeric side-by-side motif. *J. Am. Chem. Soc.*, **114**, 8783-8794.

Wade, W. S., Mrksich, M., & Dervan, P. B. (1993). Binding affinities of synthetic peptides, pyridine-2-carboxamidonetropsin and 1-methylimidazole-2-carboxamidonetropsin, that form 2:1 complexes in the minor groove of double-helical DNA. *Biochemistry*, **32**, 11385-9.

Walker, S. L., Andreotti, A. H., & Kahne, D. E. (1994). NMR characterization of calicheamicin γ bound to DNA. *Tetrahedron*, **50**, 1351-1360.

Wang, P., Bauer, G. B., Bennett, R. A., & Povirk, L. F. (1991). Thermolabile adenine adducts and A.T base pair substitutions induced by nitrogen mustard analogues in an SV40-based shuttle plasmid. *Biochemistry*, **30**, 11515-21.

Wang, P., Bauer, G. B., Kellogg, G. E., Abraham, D. J., & Povirk, L. F. (1994). Effect of distamycin on chlorambucil-induced mutagenesis in pZ189: evidence of a role for minor groove alkylation at adenine N-3. *Mutagenesis*, **9**, 133-139.

Wang, P., Bennett, R. A., & Povirk, L. F. (1990). Melphalan-induced mutagenesis in an SV40-based shuttle vector: predominance of A.T----T.A transversions. *Cancer Res.*, **50**, 7527-7531.

Wartell, R. M., Larson, J. E., & Wells, R. D. (1974). Netropsin. A specific probe for A-T regions of duplex deoxyribonucleic acid. *J. Biol. Chem.*, **249**, 6719-6731.

Watson, J. D., & Crick, F. H. C. (1953). A structure for deoxyribose nucleic acid. *Nature*, **171**, 737-738.

Weidner, M. F., Millard, J. T., & Hopkins, P. B. (1989). Determination at single-nucleotide resolution of the sequence-specificity of DNA interstrand cross-linking agents in DNA fragments. *J. Am. Chem. Soc.*, **111**, 9270-9272.

Weinstat, S. D., & Steeg, P. S. (1994). Angiogenesis and colonization in the tumor metastatic process: basic and applied advances. *Faseb J.*, **8**, 401-407.

Wickstrom, E. (1986). Oligodeoxynucleotide stability in subcellular extracts and culture media. *J. Biochem. Biophys. Methods*, **13**, 97-102.

Williamson, C. E., & Witten, B. (1967). Reaction mechanism of some aromatic nitrogen mustards. *Cancer Res.*, **27**, 33-38.

Wilman, D. E. V., & Connors, T. A. (1983). Molecular structure and antitumor activity of alkylating agents. In Molecular Aspects of Anti-cancer Drug Action. S. Neidle and M. J. Waring, eds. Weinheim, Verlag Chemie. 1, ed. 233-282.

Wilson, W. D. (1990). Reversible interactions of nucleic acids with small molecules. In Nucleic Acids in Chemistry and Biology. G. M. Blackburn and M. J. Gait, eds. Oxford, Oxford University Press. 295-336.

Wittman, M. D., Kadow, J. F., Langley, D. R., Vyas, D. M., Rose, W. C., Solomon, W., & Zein, N. (1995). The synthesis and biological activity of

enediyne minor groove binding hybrids. *Bioorg. Med. Chem. Lett.*, **5**, 1049-1052.

Wood, A. A., Nunn, C. M., Czarny, A., Boykin, D. W., & Neidle, S. (1995). Variability in DNA minor groove width recognised by ligand binding: the crystal structure of a bis-benzimidazole compound bound to the DNA duplex d(CGCGAATTCGCG)$_2$. *Nucleic Acids Res.*, **23**, 3678-3684.

Workman, P., Kaye, S. B., & Schwartsmann, G. (1992). Laboratory and phase I studies of new cancer drugs. *Cur.. Opin. Oncol.*, **4**, 1065-1072.

Wyatt, M. D., Garbiras, B. J., Haskell, M. K., Lee, M., Souhami, R. L., & Hartley, J. A. (1994a). Structure activity relationship of a series of nitrogen mustard and pyrrole containing minor groove binding agents related to distamycin. *Anticancer Drug Des.*, **9**, 511-525.

Wyatt, M. D., Garbiras, B. J., Lee, M., Forrow, S. M., & Hartley, J. A. (1994b). Synthesis and DNA binding properties of a series of N to C linked and imidazole-containing analogues of distamycin. *Bioorg. Med. Chem. Lett.*, **4**, 801-806.

Xie, G., Gupta, R., & Lown, J. W. (1995). Design, synthesis, DNA sequence preferential alkylation and biological evaluation of *N*-mustard derivatives of distamycin and netropsin analogues. *Anticancer Drug Des.*, **10**, 389-409.

Xie, G., Morgan, A. R., & Lown, J. W. (1993). Synthesis and DNA cleaving properties of hybrid molecules containing propargylic sulfones and minor groove binding lexitropsins. *Bioorg. Med. Chem. Lett.*, **3**, 1565-1570.

Yamamoto, Y., Cai, J., Nakamura, H., Sadayori, N., Asao, N., & Nemoto, H. (1995). Synthesis of netropsin and distamycin analogues bearing o-carborane and their DNA recognition. *J. Org. Chem.*, **60**, 3352-3357.

Youngquist, R. S., & Dervan, P. B. (1985). Sequence-specific recognition of B-DNA by oligo(*N*-methylpyrrolecarboxamide)s. *Proc. Natl. Acad. Sci. U.S.A.*, **82**, 2565-2569.

Youngquist, R. S., & Dervan, P. B. (1987). A synthetic peptide binds 16 base pairs of A.T double helical DNA. *J. Am. Chem. Soc.*, **109**, 7564-7566.

Zasedatelev, A. S., Gursky, G. V., Zimmer, C., & Thrum, H. (1974). Binding of netropsin to DNA and synthetic polynucleotides. *Mol. Biol. Rep.*, **1**, 337-342.

Zhang, Y., Chen, F. X., Mehta, P., & Gold, B. (1993). Groove- and sequence-selective alkylation of DNA by sulfonate esters tethered to lexitropsins. *Biochemistry*, **32**, 7954-7965.

Zimmer, C., Marck, C., Schneider, C., & Guschlbauer, W. (1979). Influence of nucleotide sequence on dA.dT-specific binding of netropsin to double stranded DNA. *Nucleic Acids Res.*, **6**, 2831-2837.

Zimmer, C., & Wahnert, U. (1986). Non-intercalating DNA-binding ligands: Specificity of the interaction and their use as tools in biophysical, biochemical and biological investigations of the genetic material. *Prog. Biophys. Molec. Biol.*, **47**, 31-112.

Zsido, T. J., Beerman, T. A., Meegan, R. L., Woynarowski, J. M., & Baker, R. M. (1992). Resistance of CHO cells expressing P-glycoprotein to cyclopropylpyrroloindole (CPI) alkylating agents. *Biochem Pharmacol*, **43**, 1817-22.

Zwelling, L. A., Michaels, S., Schwartz, H., Dobson, P. P., & Kohn, K. W. (1981). DNA cross-linking as an indicator of sensitivity and resistance of mouse L1210 leukemia to cis-diamminedichloroplatinum(II) and L-phenylalanine mustard. *Cancer Res.*, **41**, 640-9.